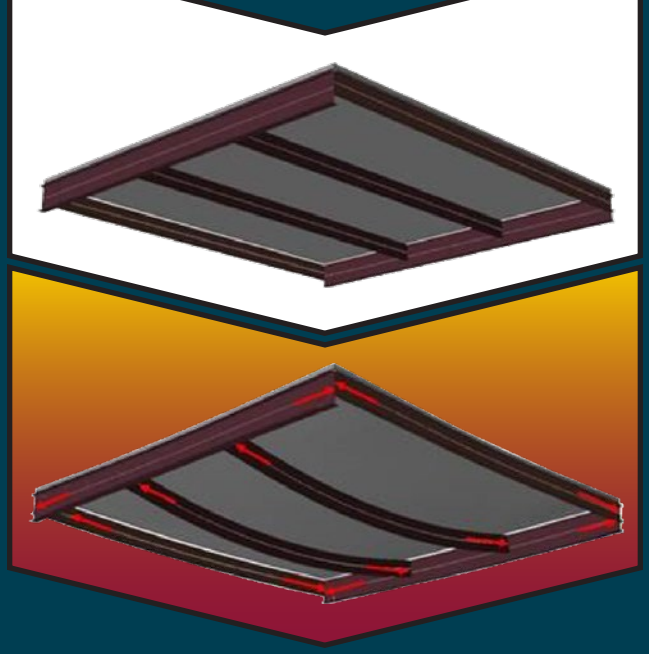

Performance-Based Structural Fire Design

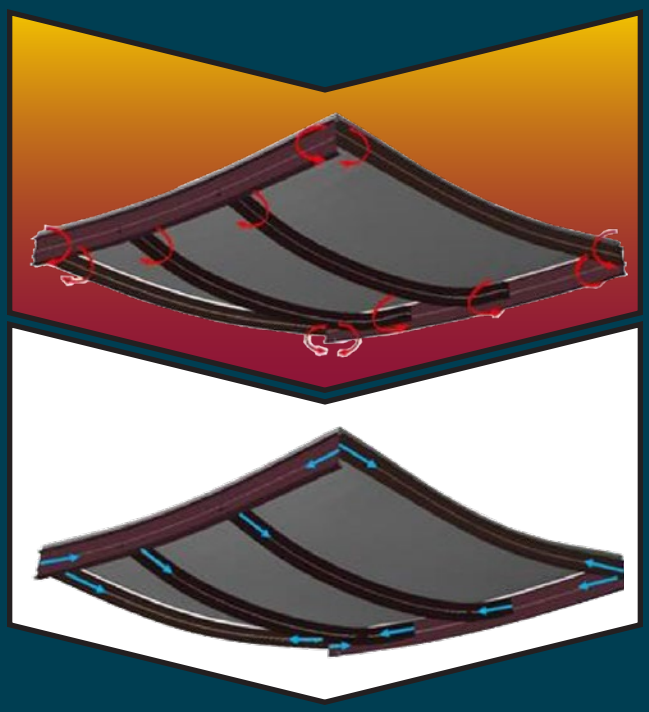

Exemplar Designs of Four Regionally Diverse Buildings using ASCE 7-16, Appendix E

ASCE

CHARLES PANKOW FOUNDATION

SEI ASCE STRUCTURAL ENGINEERING INSTITUTE

ASCE/SEI

Performance-Based Structural Fire Design

Exemplar Designs of Four Regionally Diverse Buildings using ASCE 7-16, Appendix E

PUBLISHED BY THE AMERICAN SOCIETY OF CIVIL ENGINEERS

Published by American Society of Civil Engineers
1801 Alexander Bell Drive
Reston, Virginia 20191-4382
www.asce.org/bookstore | ascelibrary.org

Errata: **Errata, if any, can be found at https://doi.org/10.1061/9780784482698.**

Library of Congress Cataloging-in-Publication Data on File

ISBN 978-0-7844-8269-8 (PDF)

Manufactured in the United States of America.

25 24 23 22 21 20 1 2 3 4 5

Disclaimer

The exemplar designs presented in this publication are intended to demonstrate the execution of a performance-based structural fire design (PBSFD) based on the present state of knowledge, laboratory and analytical research, and the engineering judgments of persons with substantial knowledge in the design and fire behavior of buildings. When properly implemented, PBSFD should provide design of buildings that are capable of fire performance equivalent or superior to that attainable by design in accordance with present prescriptive provisions. Performance-based structural fire design is a rapidly developing field and it is likely that knowledge gained in the future will suggest that some recommendations presented herein should be modified. Individual engineers and building officials implementing PBSFD must exercise their own independent judgments as to the suitability of these procedures for that purpose.

The Structural Engineering Institute (SEI), ASCE, the Charles Pankow Foundation, sponsors, participants and their firms or employees, and contributors offer no warranty, either expressed or implied, as to the suitability of the methods described in these exemplar designs for application to individual buildings or projects.

This exemplar procedural guidance was prepared through careful deliberations and review using current state of practice. Although further research is always ongoing and methodologies and criteria will evolve as more knowledge is gained in this area, this exemplar procedural guidance represents the best knowledge available at the time of publication.

Contents

PART II. Team Reports for Buildings 1–4

Executive Summary

The Structural Engineering Institute (SEI) of ASCE, with the support of the Charles Pankow Foundation (CPF), developed this project to explicitly demonstrate the proper execution and potential benefits of performance-based structural fire design (PBSFD) for structural fire protection as an alternative to the traditional prescriptive method. Specifically, PBSFD is an alternative method that allows for explicit evaluation of structural performance under realistic fire conditions. Therefore, PBSFD may be used to achieve broadly defined fire safety goals and objectives.

This project includes the analysis of four regionally diverse, protected, steel-framed building designs by design teams from four leading structural engineering firms: Simpson Gumpertz & Heger (SGH), Magnusson Klemencic Associates (MKA), Thornton Tomasetti (TT), and Walter P Moore (WPM). The design teams worked closely with a panel of academic advisors from four institutions: University at Buffalo, Oregon State University, Johns Hopkins University, and University College London (previously with University of Maryland). The design teams and academic advisors involved collectively shared a unique level of expertise and experience in the fire and structural design aspects, shared information freely, and worked in collegial partnership with the aim of advancing industry knowledge.

Each design team re-examined their existing building for three design scenarios that included varying levels of performance objectives and structural design freedom. The scope of each analysis included the characterization of uncontrolled fire exposure within building spaces, the associated thermal response of structural elements, and the resulting structural system response per the provisions of ASCE 7-16 *Minimum Design Loads and Associated Criteria for Buildings and Other Structures Appendix E Performance Based Design Procedures for Fire Effects on Structures* (Appendix E) (ASCE 2017) and based on the guidance contained in *Structural Fire Engineering, Manual of Practice 138* (ASCE 2018). Comprehensive structural analyses identified key structural system vulnerabilities under fire exposure to be addressed to achieve the required performance objectives specified in ASCE 7-16, Appendix E. In the context of the three design scenarios considered, each design team developed designs with rationally allocated protective insulation and modest structural enhancements, where necessary, to provide robust structural performance under defined fire conditions. By examining the three design scenarios, each design team demonstrated the value of structural engineering participation early in the building's fire design. Confirming fire performance is especially pertinent for buildings with high consequence of failure, such as high occupancy or critical buildings, or for structures with atypical framing or complex load paths. The results of the structural analyses and the necessary structural enhancements are unique to each individual building, and thus cannot be generalized across all buildings. Hence, structural engineering expertise is required on a project-by-project basis to achieve specific performance objectives using PBSFD.

Overall, these exemplar designs demonstrate the most significant benefit of PBSFD to new building project stakeholders — including building officials, fire marshals, or the appropriate Authority Having Jurisdiction (AHJ) for final approval — which is that the method provides an explicit process to confirm the structural system performance under fire exposure. Since PBSFD can consider both structural and applied fire protection design considerations, the method has the potential to impact multiple aspects of a project, including economics, for many building types.

This guidance is organized into two parts. Part I includes an overview of the methodology of PBSFD, as well as a description of this project's design procedures, followed by summaries of each Design Team's analyses, results, and conclusions. Appendix A to Part I includes the full Design Brief that the design teams followed. Part II includes each of the four design team reports, which further document and detail the evaluation of the design scenarios including analysis and design methods used.

Participants

The Structural Engineering Institute of ASCE acknowledges the work of the participants in this project. The participants include members from the four design teams, as well as the academic advisor.

INDUSTRY CHAMPIONS

The Simpson Gumpertz Heger (SGH) design team comprised the following contributors:

Kevin LaMalva, P.E., *Industry Champion, Principal Investigator*

Paul Cabasag, P.E.

Don Dusenberry, P.E.

Omer Erbay, Ph.D., P.E.

Qianru Guo, Ph.D., P.E.

Sean Hsieh

Keng-Wit Lim, Ph.D., P.E.

Adel Mashayekh, Ph.D.

Abhishek Master

Keith Palmer, Ph.D., P.E., S.E.

Chris Scangas

Georgios Tsampras, Ph.D.

Matt Yin, P.E.

The Magnusson Klemencic Associates (MKA) design team comprised the following contributors:

Ron Klemencic, P.E., S.E., Hon. AIA, *Industry Champion*

Robert Baxter, S.E.

Amy Garras, P.E.

Chris Lubke, S.E.

Mike Valley, S.E.

The Thornton Tomasetti (TT) design team comprised the following contributors:

Najib Abboud, Ph.D., P.E., *Industry Champion*
Zeynab Abbasi, Ph.D.
Ali Ashrafi, Ph.D., P.E., LEED AP
Pierre Ghisbain, Ph.D., P.E.
Jaimin Korat
Mostafa Mobasher, Ph.D.
Jenny Sideri, Ph.D., P.E.
Zhi Zhang, Ph.D.

The Walter P Moore (WPM) design team comprised the following contributors:

Lawrence G. Griffis, P.E., *Industry Champion*
Ozgur Atlayan, Ph.D., P.E.
Sridhar Baldava, P.E.
Samuel J. Baer
Addison L. Bliss
Viral B. Patel, P.E., S.E.

ACADEMIC ADVISORS

Negar Elhami-Khorasani, Ph.D.; University at Buffalo
Erica Fischer, Ph.D., P.E.; Oregon State University
Thomas Gernay, Ph.D.; Johns Hopkins University
Jose Torero, Ph.D.; University College of London (formerly University of Maryland)

CHARLES PANKOW FOUNDATION

Anne Ellis P.E., F.ACI., F.ASCE, Charles Pankow Foundation; Executive Director

STRUCTURAL ENGINEERING INSTITUTE OF ASCE TEAM

Laura Champion, P.E., F.ASCE, Structural Engineering Institute; Director
Jennifer Goupil, P.E., F.SEI, Structural Engineering Institute; Project Manager and Editor

Acknowledgments

The Structural Engineering Institute of ASCE prepared this exemplar guidance document with exclusive grant funding from the Charles Pankow Foundation.

The project would not have been possible without the financial support to the Charles Pankow Foundation from the following project sponsors:

- American Institute of Steel Construction,
- American Society of Civil Engineers Industry Leaders Council,
- ArcelorMittal, and
- MKA Foundation.

PART I
Performance-Based Structural Fire Design (PBSFD) Overview

Chapter 1. Introduction

The Structural Engineering Institute (SEI) of ASCE, with the support of the Charles Pankow Foundation (CPF) has pursued, as part of its vision, the advancement of performance-based design. Advancing the adoption of performance-based structural fire design (PBSFD) has the potential to provide explicitly defined levels of structural fire safety performance as well as deliver more efficient and economic building designs. Similar to other performance-based areas of structural engineering, use of a PBSFE requires stakeholder understanding and acceptance, and its level of benefit will vary from project to project.

Building codes generally allow for the use of alternative means and methods with the approval of the Authority Having Jurisdiction (AHJ), so that innovative methods or materials can be permitted. PBSFD is an alternative method that allows for explicit evaluation of structural performance under realistic fire conditions. PBSFD may be used to achieve broadly defined fire safety goals and objectives. The nationally adopted loading standard, ASCE 7-16 *Minimum Design Loads and Associated Criteria for Buildings and Other Structures*, Appendix E: Performance-Based Design Procedures for Fire Effects on Structures (ASCE 7-16, Appendix E) (ASCE 2017) provides a performance-based framework applicable to buildings and other structures as explicitly permitted by ASCE 7-16, Section 1.3.7, and permitted by the alternative means and methods provisions of building codes. ASCE 7-16, Appendix E, Section E.3 General Requirements, states that PBSFD procedures include two steps: evaluation of fire effects, and evaluation of the structural response with respect to explicitly defined performance objectives.

This project demonstrates the proper application and execution of PBSFD for four, existing, regionally diverse, anonymized building designs using the methodology specified in ASCE 7-16, Appendix E, and guidance contained within *Structural Fire Engineering,* Manual of Practice No. 138 (ASCE 2018). This project focuses on protected steel structures; concrete, masonry, and timber construction are not considered within the scope of this project. The four design teams that participated in this project used their own office procedures and design strategies, and this variation is reflected in the presentation of each design team's detailed analyses as provided in Part II.

1.1 BACKGROUND

Current prescriptive code requirements for structural fire protection, referred to as standard fire resistance design (SFRD), do not explicitly evaluate structural fire performance. In recent years, extensive research pertaining to the performance of structures at elevated temperatures can be leveraged by owners and other project stakeholders to efficiently address and potentially improve fire performance by using alternative methods, such as ASCE 7-16, Appendix E (ASCE/SEI 2016).

The PBSFD method is based on the application of engineering principles and physics-based modeling to achieve specified performance targets, in lieu of traditional prescriptive rules. Unlike prescriptive design, this method requires structural engineering analyses, and the added engineering effort can provide many worthwhile benefits. Currently, this method is not being widely adopted in practice in the United States. The factors hindering the adoption of PBSFD in the United States may include lack of understanding and participation by structural engineers, lack of trial designs demonstrating the potential benefits to owners and other stakeholders, and unfamiliarity with the

approach by building officials. This exemplar guidance is intended to increase understanding and acceptance of PBSFD among real-world project stakeholders, including structural engineers, architects, contractors, owners, and building officials.

1.2 PROJECT GOAL

The goal of this project is to advance the understanding and use of PBSFD within the building design and construction industry by demonstrating the engineering process and methodologies along with potential real project benefits. Notably, with possible modest structural enhancements, many structural systems can be designed to meet enhanced performance objectives under uncontrolled fire exposure, offering known and satisfactory structural performance, and potentially increased economy, as compared to the prescriptive approach.

1.3 PROJECT OBJECTIVES

To achieve the goal of this project as previously described, this project includes the following objectives:

- Demonstrate the proper execution of PBSFD in accordance with ASCE 7-16, Appendix E by using the approaches recommended in *Structural Fire Engineering,* MOP 138 (ASCE 2018).
- Provide exemplar procedural guidance for a set of buildings with regional representation.
- Explicitly illustrate the potential benefits of PBSFD through trial designs.
- Convey general cost implications of the trial designs, as well as discuss additional considerations such as carbon footprint impacts and aesthetics, where possible.

1.4 DESIGN SCENARIOS AND PERFORMANCE OBJECTIVES

To inform real project stakeholders on the highest impact implementation of PBSFD on real projects, each design team examined a series of hypothetical design scenarios ranging from a minimal level of structural design influence to a comprehensive level of structural design integration of *mandatory* and *discretionary* performance objectives, summarized as follows:

- **Design 0:** Prescriptive requirements for insulation according to the applicable building code.
    - o This is a nonengineered empirical indexing approach (which represents indeterminate performance).
- **Design 1:** Level of applied insulation needed to satisfy *mandatory* performance objectives, the *minimum* requirements of ASCE 7-16, Appendix E, Section 4.1 (see Section 2.3.1). This section states complete and safe occupant evacuation to a public way and ability of structural framing supporting refuge areas (if any such areas are present) to withstand fire burnout (see 2.3.2.1) without collapse.

- This is an engineered approach *without* the ability to modify the structural system (which represents minimum performance).

- **Design 2:** Level of applied insulation needed to satisfy the *discretionary* requirements of ASCE 7-16, Appendix E, Section 4.1, Section 2.3.2 to achieve fire burnout without any collapse of the structural system framing.

  - This is an engineered approach *without* the ability to modify the structural system (which represents optimum performance).

- **Design 3:** Level of applied insulation *and structural modifications* (if any) needed to achieve the *discretionary* requirements of fire burnout (same Section 2.3.2 requirement as Design 2) without any collapse of the structural system framing.

  - This is an engineered approach *with* the ability to modify the structural system (which represents optimum performance).

In practice, protective insulation may take the form of fibrous or cementitious spray-applied materials, gypsum board encasement, intumescent paint or epoxy spray-applied materials, and other protection types. The on-site spray application of protective insulation to structural members (*wet* construction trade) is commonly referred to as *fireproofing.*

Design 0 represents the traditional method of prescribing insulation for structural fire protection without any structural analysis. The acceptance metric for Design 0 is the prescriptive level of fire resistance required by the building code; there is no defined level of performance.

Design 1 represents a case in which only the minimum mandatory performance objectives are pursued, and the minimum level of performance is targeted.

Design 2 represents a case in which discretionary performance objectives (beyond the mandatory minimums) are pursued for an optimum level of performance.

The real-world cases of Designs 1 and 2 represent the scenarios in which a *structural fire engineer* is engaged late in the design process after the structural design has progressed to an extent in which significant changes are not possible—for example, during the construction documents (CD) phase of a real project.

Design 3 represents the case in which the structural fire engineer is involved in the structural design from the beginning—for example, during the schematic design (SD) phase of a real project—and discretionary (or beyond minimum) objectives are pursued for optimum performance. In this case, the structural fire engineer would be able to influence the structural design to achieve the desired level of performance when considering fire effects.

For Design 0, there are no modifications to the prescriptive design. For Designs 1 and 2, only the structural insulation can be modified to meet the minimum or discretionary performance objectives, respectively. For Design 3, structural design modifications can be made in addition to insulation modifications to meet discretionary performance objectives. In no cases can fire sprinkler systems be relied upon to meet the performance objectives, because completely uncontrolled

fire exposure must be assumed per ASCE 7-16, Appendix E, and *Structural Fire Engineering,* MOP 138.

The acceptance criteria for Designs 1, 2, and 3 is structural integrity as demonstrated by satisfying all applicable structural limit states and/or the explicit demonstration of satisfactory structural performance by other means (such as finite element simulations). In this context, the inherent ability of a structural system to withstand fire exposure may be considered in conjunction with the benefits of applied insulation. Unlike conventional structural engineering design, Designs 1, 2, and 3 may rely on load redistribution or nonconventional sources of load-carrying capacity, such as compressive–tensile membrane action.

1.5 APPROACH AND GENERAL REQUIREMENTS

The PBSFD methodologies include traditional structural engineering concepts for member and connection strength evaluation given the applied load, as well as consideration of fire effects such as restrained thermal expansion. As explained in *Structural Fire Engineering,* MOP 138, Chapter 2, and in accordance with the fundamental philosophy used to design structures, PBSFD explicitly evaluates demand and capacity of structural systems under fire exposure (ASCE 2018). Therefore, in addition to identifying the performance objectives as stated in Section 1.4, compliance with ASCE 7-16, Appendix E, Section E.3 requires the proper determination of demands due to fire effects as well as an evaluation of the capacity of the structural system to endure such effects. Specifically stated in Section E.5, the evaluation of fire effects must include quantifying the fuel load, identifying structural design fires, and determining the temperature histories of structural members and connections. Specifically stated in Section E.6, the evaluation of capacity must consider the response of the structural system through the heating and subsequent cooling phases of the structural design fires.

For Designs 1 through 3, each design team used the generalized analysis process illustrated in Figure 1-1. This analysis approach is deterministic, as described in ASCE 7-16, Appendix E.

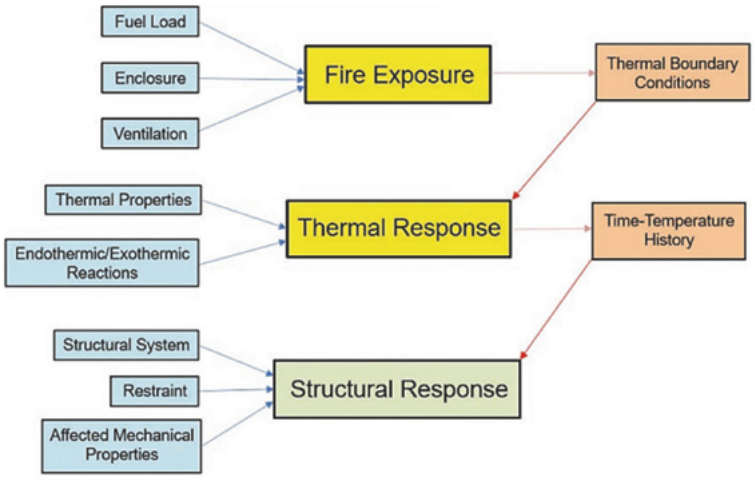

Figure 1-1. Performance-based structural fire engineering analysis process.
Source: Structural Fire Engineering, MOP 138 (ASCE 2018).

Because PBSFD is deterministic, each design was required to consider multiple fire scenarios that influence the given structure. Once the fire exposure is determined, heat transfer calculations are conducted to derive the thermal responses of the given structure, which are represented as structural temperature–time histories. Finally, structural analyses are conducted based on the thermal response. Chapter 2 includes many specific details of this analysis process including the overview and explanation of the stakeholder collaboration tool referred to as the Design Brief.

1.6 DESIGN TEAMS

The design teams for this project are shown in Table 1-1. The panel of expert academic advisors counseled the design teams on certain technical aspects during the design phase and collectively reviewed the final technical work product of each team, including their detailed calculations, which are not entirely reproduced in this report. As stated in the Design Brief (see Chapter 2), the original plan was for one academic advisor to be assigned to each design team. However, it was later decided that a collective technical review process would be more comprehensive, given the variety of expertise represented by the collective academic advisors.

Table 1-1. Design Teams.

Team Designation	Design Team Name; Industry Champion	Academic Advisors
Team 1	Simpson Gumpertz & Heger (SGH); Kevin LaMalva	Negar Elhami-Khorasani, *University at Buffalo* Erica Fischer, *Oregon State University* Thomas Gernay, *Johns Hopkins University* Jose Torero, *University College London (formerly University of Maryland)*
Team 2	Magnusson Klemencic Associates (MKA); Ron Klemencic	
Team 3	Thornton Tomasetti (TT); Najib Abboud	
Team 4	Walter P Moore (WPM); Larry Griffis	

1.7 PROJECT BUILDINGS

Four existing buildings, anonymized, have been selected to provide a range of geographic locations, building sizes, and uses (see Table 1-2). All four buildings are steel-framed structures with composite floors with applied fire protection required for all primary and secondary members according to prescriptive code requirements. Moment frame lateral systems were not considered for this project because of their relatively uncommon use in practice as compared to braced frames.

1.7.1 Building 1

Building 1 is a previously completed Risk Category II real project, which was built in the early 2000s and located in the Boston metropolitan area. The building has six stories, approximately

Table 1-2. Comparison of Exemplary Design Project Buildings.

Team/ Building Designation	Height	Occupancy	Geographic Location	Risk Category	Lateral System	Controlling Design Load	Required Fire Rating on Framing
Team 1 Building 1	Low-rise (6 stories)	Office	East	RC II	Braced	Wind	1 h = all framing and roof
Team 2 Building 2	Mid-rise (12 stories)	Healthcare	West	RC IV	Braced (BRB)	Seismic	2 h = all framing; 1 h = roof
Team 3 Building 3	High-rise (50 stories)	Office/ Residential	Midwest	RC III	Concrete Core	Wind	3 h = primary; 2 h = secondary; 1-1/2 h = roof
Team 4 Building 4	Low-rise (6 stories)	Office	South	RC II	Braced	Wind	2 h = all framing; 1 h = roof

24,000 sq. ft per floor, and is used primarily for office space on all levels (occupancy Group B). Given a reduction granted for buildings over 70 ft, the construction type of the building according to the applicable building code prescriptively requires all steel framing (including roof construction) to have 1 h fire resistance. The building has a braced-frame, lateral-force-resisting system that is primarily controlled by design wind loads.

1.7.2 Building 2

Building 2 is a previously completed Risk Category IV real project, which was built in the late 2000s and located in the state of Washington. The building has 12 stories, approximately 50,000 sq. ft per floor and is used primarily as a healthcare center/hospital. The construction type of the building per the applicable building code prescriptively requires all steel framing to have 2 h fire resistance, except the roof is permitted to have a 1 h fire resistance rating. The building has a buckling-restrained braced (BRB) lateral-force-resisting system that is primarily controlled by design seismic loads.

1.7.3 Building 3

Building 3 is based on a previously completed Risk Category III real project, which was built in the mid-2010s and located in the Midwest. The building has 50 stories, approximately 20,000 sq. ft per floor, and is used for office space on the lower levels (occupancy Group B) and residential space on the upper levels (occupancy Group R). The building frame is of steel construction at the lower 30 floors, transferring to concrete framing at upper floors through a series of steel transfer trusses. The construction type of the building per the applicable building code prescriptively requires the primary and secondary members to have a 3 h and 2 h fire resistance rating, respectively, except the roof is permitted to have a 1-1/2 h fire resistance rating. The office levels have perimeter steel columns and utilize a reinforced concrete core as lateral-force-resisting system that is primarily controlled by design wind loads.

1.7.4 Building 4

Building 4 is a previously completed Risk Category II real project, which was built in the late 2000s and located in the state of Florida. The building has six stories, approximately 30,000 sq. ft per floor, and is used primarily for office space on all levels (occupancy Group B). The construction type of the building per the applicable building code prescriptively requires all the steel framing to have a 2 h fire resistance rating, except the roof is permitted to have a 1 h fire resistance rating. The building has a braced frame lateral-force-resisting system that is primarily controlled by design wind loads.

1.8 POTENTIAL REAL PROJECT IMPACTS

PBSFD has the potential to impact multiple aspects of a real building project. Although these potential project impacts are beyond the scope of this exemplar guidance, it is important to note that these impacts vary by region and building type and should be studied independently to determine project-by-project benefits to stakeholders.

Traditionally, structural engineers conduct their designs to optimize steel tonnage and erection costs. Once completed, applied fire protection is typically specified for structural members in a generalized (*blanketed*) fashion, for example, specific thickness to all primary and secondary framing. Because PBSFD can consider both structural and applied fire protection design considerations, this method has the potential to reduce construction costs and benefit other real project aspects such as those related to schedule, embodied carbon, architectural flexibility, aesthetics, and life cycle.

1.9 LIMITATIONS

The exemplar guidance contained herein intends to demonstrate the present state-of-knowledge for this emerging field. Laboratory and analytical research identified in other literature and the engineering judgment of persons with knowledge in PBSFD are reflected in the analyses and designs that were examined and does not necessarily demonstrate a complete design and submittal to AHJ for approval. The authors have endeavored to develop this exemplar guidance to be applicable to the PBSFD of representative buildings, given present industry knowledge and practice limitations realizing the limitations that exist and where further research is needed. However, no guidance can anticipate every structure to which it may be applied, nor can it anticipate advances in the state-of-knowledge-and-practice. The authors do not intend to preclude the application of alternative techniques or approaches when performing a PBSFD. PBSFD is a rapidly developing field, and it is likely that knowledge gained in the future will suggest that some guidance presented herein should be modified. Individual engineers, building officials, and project stakeholders implementing PBSFD must exercise their own independent judgment as to the suitability of these recommendations for that purpose.

Chapter 2. Project Design Procedures

As described in Chapter 1, the PBSFD approach includes the establishment of performance objectives as well as determination of the appropriate structural design fires. Given this project's goals as stated in Chapter 1, the design teams discussed and agreed upon several design parameters for the analysis and design of their buildings. These agreed-upon aspects of this exemplar design project are documented in the collaboration tool referred to as the Design Brief.

2.1 DESIGN BRIEF

This project included the development of a design brief. This stakeholder collaboration tool was developed to document the agreed upon aspects of the PBSFD for this project. The purpose of a design brief is to outline the actual project goals, identify applicable tools to be used by the teams (such as industry references and software), and reach agreement on specific analysis and design considerations pertaining to the definition of fuel load and structural design fires, characterization of fire effects, and structural analysis procedures. Establishment of this type of document enables real project stakeholders, including the Authority Having Jurisdiction (AHJ), to understand and agree upon the approach at the onset of the project.

For added insight into how this project was defined, the final document that was used by the design teams is included in Appendix A: Project Design Brief. This is also an example of what actual project stakeholders would need to define and receive approval from the AHJ prior to starting on a PBSFD for a specific project.

Relevant sections of the final Design Brief are included here for discussion purposes; see Appendix A for the complete document.

2.2 INDUSTRY TOOLS AND DEFINITIONS

Within any design brief, it is important to specify which industry-endorsed standards and software the design team will use. This document clarifies the approach for the new project stakeholders and specifically for the (AHJ), who must agree on these aspects of the proposed design. For this project, key definitions that are specific to the methodologies of PBSFD are reproduced in Section 2.2.3 for clarity.

2.2.1 Industry References

The analyses described for this project have been conducted entirely in conformance with the only industry consensus standard for PBSFD that is developed in the United States as follows:

- ASCE 7-16 *Minimum Design Loads and Associated Criteria for Buildings and Other Structures* (ASCE 2017)
    - o Appendix E: Performance-Based Design Procedures for Fire Effects on Structures

The analyses and design also referenced aspects of the following at the discretion of each design team:

- *Structural Fire Engineering*, (MOP) 138 (ASCE 2018)
- AISC 360 *Specification for Structural Steel Buildings* (AISC 2016) Appendix 4: Structural Design for Fire Conditions
- EN 1991-1-2: *Eurocode 1: Actions on Structures; Part 1-2: Actions on Structures Exposed to Fire* (CEN 2001).
- EN 1992-1-2: *Eurocode 2: Design of Concrete Structures – Part 1-2: General Rules – Structural Fire Design* (CEN 2004).
- EN 1993-1-2: *Eurocode 3: Design of Steel Structures – Part 1-2: General Rules. Structural Fire Design* (CEN 2005a).
- EN 1994-1-2: *Eurocode 4: Design of Composite Steel and Concrete Structures – Part 1-2: General Rules. Structural Fire Design* (CEN 2005b).
- SFPE S.01 *Standard on Calculating Fire Exposure to Structures* (SFPE 2010).
- SFPE S.02 *Standard on Calculation Methods to Predict the Thermal Performance of Structural and Fire Resistive Assemblies* (SFPE 2015).

2.2.2 Industry Software

Software is used for the different aspects of analysis for PBSFD, including building evacuation and fire exposure analyses, as well as thermal and structural response evaluation. The design teams used the following software in their analyses; see Part II: Team Reports in Chapters 7 through 10 for specifics for each team and building.

For evacuation analysis (see Appendix A: Project Design Brief, Section 6.1):

- *Pathfinder* (Thunderhead Engineering Consultants, Inc. 2016).

For fire exposure analysis (see Appendix A: Project Design Brief, Section 7.2.3):

- *Fire Dynamics Simulator* (NIST 2000).

For thermal response analysis (see Appendix A: Project Design Brief, Section 7.3):

- Abaqus (Dassault Systèmes Simulia Corp. n.d.)
- SAFIR (University of Liège and Johns Hopkins University 2017)

For structural response analysis (see Appendix A: Project Design Brief, Section 9.2).

- Abaqus (Dassault Systèmes Simulia Corp.)
- SAFIR (University of Liège and Johns Hopkins University 2017)
- MACS+ (ArcelorMittal)
- SPM (Heavy Engineering Research Association (HERA) / University of Auckland)

2.2.3 Definitions

Definitions of key terminology that are helpful to understand for this project are taken from *Structural Fire Engineering*, (MOP) 138 (ASCE 2018), Chapter 1, except those indicated by **, which are taken from ASCE 7-16, Appendix E.

Active Fire Protection System: A fire protection system designed to sense, control, or suppress fire, which requires activation by sensing fire byproducts (e.g., hot gases). An automatic fire sprinkler system is an example of an active fire protection system.

Available Safe Egress Time (ASET): The available time for building occupants to evacuate or reach a place of safety prior to the onset of untenable conditions or inadequate structural performance. Evaluation of tenable conditions is addressed separately from PBSFD.

Building Refuge Area: Any location within a building that is designed to safely shelter occupants during a fire event, when immediate evacuation may not be safe or possible.

Burnout: Extinguishment of fire because of the consumption of fuel load.

Coefficient of Thermal Expansion: Measure of the amount that an element's size changes with temperature. Common units for the coefficient of thermal expansion are mm/mm/K.

Conductive Heat Transfer: Transfer of heat through a solid body, such as a concrete wall, owing to a spatial thermal gradient often measured in kilowatts per square meter (kW/m^2).

Convective Heat Transfer: Transfer of heat because of bulk motion of a fluid to a solid surface, such as hot gases moving along a concrete wall; often measured in kilowatts per square meter (kW/m^2).

Density: Mass of a material per unit volume. Common units for density are kilograms per cubic meter (kg/m^3).

Enclosed Compartment: A room with intersecting ceiling, floor, and wall surfaces that may have openings.

Fire Effects: Thermal and structural response caused by fire exposure and subsequent cooling.

Fire Exposure: The extent to which materials, products, or assemblies are subjected to the conditions created by fire.

Fire Model: A physical or mathematical representation of the dynamics of burning and associated processes.

Fire Scenario: A description or set of conditions that defines the development of fire, such as ventilation area and compartment geometry, and the distribution of fuel load in the compartment or building area of interest.

Flashover: A rapid transition in a compartment fire from localized burning to burning of all combustible materials in a compartment. Flashover can only occur in an enclosed compartment with sufficient fuel and ventilation, where the ceiling can trap hot gases that lead to radiant heating of all fuels to the point of combustion.

Fuel Load:** The total quantity of combustible contents within a building, space, or area expressed either as total energy or equivalent mass.

Heat Release Rate: The rate at which the combustion reactions of a fire produce heat; commonly measured in megawatts (MW).

Heat Transfer: The exchange of thermal energy caused by a temperature difference.

Intumescent Coatings: Paint or coating applied in layers as passive fire protection. When exposed to heat, intumescent coatings char and swell, increasing the coating volume and thickness and decreasing its density and thermal conductivity to create an insulating effect.

Localized Fire: A fire that burns combustibles at a given location and would heat a structure locally. Localized burning can occur in open exposures, large spaces, areas with high ceilings, or other similar locations.

Openings: Doors, windows, or penetrations into a compartment that provide a path for ventilation to a fire.

Performance Based Structural Fire Design (PBSFD):** The explicit design of structural members and connections to satisfy performance objectives for structural design fires.

Radiative Heat Transfer: Transfer of heat through electromagnetic waves; often measured in kilowatts per square meter (kW/m^2).

Required Safe Egress Time (RSET): The required time from fire ignition to the time when building occupants have evacuated or reached a place of safety.

Specific Heat: Measure of the amount of energy required to raise the temperature of a unit of mass a unit of temperature; often measured in joules per kilogram-kelvin [J/(kg-K)].

Spray-Applied Fire Resistive Material (SFRM): A passive fire protection material intended for direct application to structural building members. The intent of this material is to increase the fire resistance of building members primarily through its insulating characteristics.

Standard Fire Resistance Design (SFRD): The selection of qualified fire resistive assemblies to meet code requirements for structural fire resistance (also known as prescriptive-based design).

Structural Design Fire: An uncontrolled fire that has the potential to affect the integrity and stability of a structure that is used for the design and evaluation of the structure.

Thermal Boundary Condition: The temperature and/or heat flux to which an assembly or the structure is subjected during or after fire exposure based on the radiative and convective heating/cooling conditions at exposed surfaces.

Thermal Conductivity: Measure of a material's ability to conduct heat. Common units for thermal conductivity are watts per meter-kelvin W/(m-K).

Thermal Response:** The temperature distribution of members and connections when exposed to thermal boundary conditions.

Thermal Restraint:** A condition in which thermal expansion or contraction of structural members is resisted by forces external to the members. The level of restraint depends on the adjacent framing and connection details.

2.3 PERFORMANCE OBJECTIVES

The exemplar designs considered the mandatory and discretionary performance objectives as described in Section 1.4.

Design 0 does not have any explicit performance expectations. The performance expectations for Designs 1, 2, and 3 are described in the following sections.

2.3.1 Mandatory Performance Objectives

ASCE 7-16, Section E.4.1, requires that the structural system remains stable, with a continuous load path to the extent necessary to confirm occupant life safety during fire exposure. Hence, the performance of the structural system under structural design fires shall allow for building occupants to safely exit the building to a public way (such as public roadway). Specifically, structural support of building egress routes shall be maintained for a period necessary to confirm that occupants can evacuate safely and completely. Also, parts of the structural system that support areas where occupants are expected to take refuge during a fire should be maintained through full fire burnout (such as heating and cooling phase of the fire).

Design 1 was conducted to satisfy these minimum requirements only.

2.3.1.1 Occupant Egress Considerations

Building codes limit egress travel distances to exits (such as stairways), but generally do not limit the total evacuation time. As the vertical remoteness of occupants from the point of discharge to

a public way is increased, the time required to evacuate the building increases. Unlike SFRD, PBSFD explicitly evaluates the consequences of increased occupant evacuation times, and the reliance on building refuge areas.

To demonstrate the adequacy of occupant egress routes, an *ASET versus RSET* analysis is conducted for each building. The Available Safe Egress Time (ASET) is based on the endurance of the structural system to fire exposure. The Required Safe Egress Time (RSET) is the time it would take occupants to travel safely to refuge areas within the building or exit the building to a public way. The ASET value shall be greater than the RSET value. Structural endurance through fire burnout would satisfy this requirement. For the high-rise structure of Building 3, the impact of phased evacuation is considered.

2.3.2 Discretionary Performance Objectives

ASCE 7-16, Section E.4.2, states that any project-specific performance objectives required by project stakeholders must be met.

Designs 2 and 3 are conducted to satisfy the mandatory minimum requirements described in Section 2.3.1, as well as to provide for the discretionary, project-specific performance objective of fire burnout without any structural collapse (optimum performance).

2.3.2.1 Burnout Design

Design for full fire burnout represents ideal performance during an uncontrolled fire exposure. In this case, no collapses are expected to occur. Accordingly, only the replacement of select damaged structural components — rather than complete demolition of the building — would be expected following an uncontrolled fire event.

2.4 ANALYSIS

The exemplar designs include analysis procedures to determine the demands that are required to evaluate the performance objectives of Designs 1, 2, and 3, described in Section 2.3. Demand considerations include determining the fire loads (calculated from the design fuel load and the resulting structural design fire) and structural fire effects.

When evaluating structural performance when fire effects are present, both structural hand calculations and simulation of structural response can be used. Notable fire effects include restrained thermal expansion and temperature-dependent material properties.

Chapter 3. Summary of Analyses

In accordance with the process described in Section 2.4, the following subsections collectively summarize the analyses conducted for the four existing project buildings; see Section 1.7 for descriptions of the buildings. For more complete descriptions of each Design Team Analysis, see Part II: Team Reports.

3.1 FIRE EXPOSURE

Fire exposure is defined as the extent to which materials, products, or assemblies are subjected to the conditions created by fire. The fire exposure is evaluated by development of the fire time–temperature history, which represents the structural design fire, and it is used to evaluate the thermal response of the structure. To determine the fire time–temperature history of the structural design fire, the compartmentalization, ventilation, and design fuel load need to be determined.

For this project, the steps are described in conjunction with the requirements of ASCE 7-16, Appendix E, which necessitates the consideration of uncontrolled fire conditions within building spaces — referred to as the *structural design fire*. According to Appendix E, once the structural design fires were determined, the thermal response of the structure was evaluated, as described in Section 3.2.

As a first step for determining the structural design fires, each design team considered a series of conceivable ventilation and compartmentation conditions to account for differing or uncertain environmental aspects of the building spaces — referred to as *structural design fire scenarios*. For instance, window breakage or building plan openness can provide ventilation to a fire. In general, lower ventilation extends the duration of an uncontrolled fire, and it can reduce the fire intensity via oxygen deprivation — where fire intensity is defined as the rate of heat energy released. On the contrary, higher ventilation conditions can increase the intensity of a fire, but at the same time, it can also allow for hot gases to escape, which lowers the temperatures. In addition to ventilation, the compartmentation from the layout of interior walls can contain heat from a fire and raise temperatures.

Once the ventilation and compartmentation conditions are considered, each design team determined an appropriate level of combustibles within the building spaces — referred to as the *design fuel load*. Combustibles that reside in building spaces represent potential energy that can be liberated by ignition and quantified as a fire heat-release-rate. Accordingly, higher fuel loads generally lengthen the duration of fire exposure. The design team elected to use the Eurocode 1, Annex E (which is an acceptable alternative to the NFPA 557 when approved by the AHJ), to calculate an appropriate distributed design fuel load for each structural design fire scenario. This reference provides characteristic distributed fuel loading values (such as the amount of potential energy per unit floor area) based on the building occupancy type. Although the Eurocode, Annex E provides fuel load risk increase/reduction factors related to the presence or absence of conditions that usually mitigate fire exposure, such as fire detection systems, this project's goal of evaluating an uncontrolled fire meant that the risk reduction factors were not used. In addition, some of the design teams studied a series of elevated design fuel loads to test the general fragility of

the structural design; this is analogous to considering earthquake design parameters that are in excess of the typical design earthquake levels.

Uncontrolled fire exposure may or may not be influenced by the compartment boundaries, so this needs to be evaluated for each building specifically. For each building, the defined space will primarily determine the fire type as either an *enclosure fire* or a *localized fire*, which is based on the likelihood of flashover occurring. Hand calculations were used to determine which type to consider. Flashover happens in an enclosed compartment when all combustibles are burning at the same time because of the containment of heat levels causing simultaneous ignition. SFPE S.01 (SFPE 2010) was used to calculate the heat release rate that would be required to cause flashover within a given building space, which was then compared to the anticipated peak heat release rate based on the occupancy type, per Eurocode 1, Annex E. If the peak heat release rate of the compartment combustibles exceeds that required for flashover, an enclosure fire should be considered. Otherwise, a localized fire may be considered. For most of the buildings studied, the design teams only considered enclosure fires because most building spaces were conducive to this fire type. However, Design Team 3 used field modeling to analyze a localized fire exposure, in addition to an enclosure fire, for a specific structural design fire scenario.

For the derivation of enclosure fire temperature histories, each design team used the parametric equations contained in Eurocode 1, Annex A. These parametric equations are a function of the compartmentation (including the thermal properties of boundaries), ventilation characteristics, and the design fuel load. This was considered as the most convenient method to derive multiple fire time–temperature histories; however, it is important to note that other fire exposure calculation methods — such as zone modeling — would be expected to produce similar results. In fact, Design Team 1 used field modeling and computational fluid dynamics to study the impact of roof heat vents on the fire time–temperature histories of enclosure fire scenarios.

3.2 THERMAL RESPONSE

Based on the fire time–temperature histories derived (and described in Section 3.1) and material thermal properties (as described in Appendix A: Project Design Brief, Section 7.3.2), each design team conducted heat transfer calculations to characterize the thermal response of structural systems, which are presented as structural time–temperature histories.

For these heat transfer calculations, the design teams used a few different approaches. Most design teams used the hand calculation approach from AISC 360, Appendix 4 to derive structural time-temperature histories of protected and unprotected steel members, accounting for the heated perimeter of each member — for example, considering the top flange of a beam to be shielded from direct fire exposure because of contact with slab/deck above. As a supplement to this approach, Design Team 1 conducted two-dimensional finite difference calculations to derive the structural temperature distribution histories through concrete slabs. Alternatively, the other design teams conducted two-dimensional finite element heat transfer analyses to derive spatial temperature distribution histories for complete steel/concrete structural assemblies.

Unlike the consideration of fire exposure within building spaces, the associated thermal response of a structural system is far less uncertain. Hence, although varying modeling approaches can be used, these do not necessarily affect the certainty of the output. Therefore, multiple iterations and

variations of these calculations were not necessary to develop the structural time–temperature histories.

3.3 STRUCTURAL RESPONSE

Based on the structural time–temperature histories derived (and described in Section 3.2), each design team conducted a new structural analyses to determine the adequacy of its design and to determine the extent of insulation and/or structural enhancements that were necessary to meet the performance objectives for each design case (such as Designs 1, 2, and 3, as described in Section 1.5). Except for highly compartmentalized spaces, the structural time–temperature histories derived by each design team are relatively similar. However, the structural system of each building is unique, which is not necessarily considered by traditional prescriptive design. Hence, analysis of structural response is by far the most critical aspect of the entire PBSFD process.

For this project, the majority of the analytical work conducted by each design team was dedicated to understanding the influence of high temperatures on the structural systems — referred to as *fire effects* — and the ability of the structural systems to accommodate these effects safely — referred to as *fire robustness*. Whereas a variety of design professionals, including structural engineers, may be capable of conducting the fire exposure and thermal response analyses (as described in Sections 3.1 and 3.2), structural engineers are uniquely capable of conducting structural response analyses.

ASCE 7-16, Section E.6.3, requires that the structural load combination for extraordinary events contained in ASCE 7-16, Section 2.5.2.1 be used for PBSFD analyses as follows:

$$1.2D + A_k + 0.5L + 0.2S \tag{3-1}$$

where

D = Dead load,
A_k = Load or load effect resulting from extraordinary event A,
L = Live load, and
S = Snow load.

The fire load effect term contained in the load combination above includes forces induced into a member or component (such as axial force, shear force, bending moment, and/or torque) because of restrained thermal expansion/contraction during fire exposure. The design dead, live, and snow loads should be derived from the applicable building code or directly from the construction documents of the given building.

Each design team evaluated the demands on the structural systems under fire exposure considering the following fire effects:

- Applied mechanical loads, per the required load combination for an extraordinary event,
- Thermal expansion and contraction of structural members during the heating and cooling phases of fire exposure,

- Induced forces and moments at structural connections because of restrained thermal expansion or contraction,
- Deflection and deformation of structural members resulting from the loss of strength and stiffness at elevated temperatures,
- Rotations at connections because of large member deflections,
- Local buckling of structural members resulting from induced forces or moments and large deflections,
- Concrete slab crushing and tensile strain or rupture of reinforcement bars or mesh,
- Metal decking delamination from concrete, and
- Effect of nonuniform heating through cross sections, such as differential expansion.

Each design team evaluated the capacity of the structural systems under fire exposure considering the following aspects of fire robustness:

- Temperature-dependent stress–strain behavior of steel and concrete,
- Ductility of structural connections and slab reinforcement,
- Influence of structural continuity, load redistribution, and alternative sources of load-carrying capacity, such as compressive tensile membrane action,
- Ability of the metal decking to prevent concrete spalling,
- Ability of the structural system to remain stable and prevent collapse if local failures occur,
- Influence of PBSFD structural enhancements on the performance of the structural system to other required design loads, such as seismic loading, and
- Integrity of floor continuity to prevent vertical fire spread.

The design teams conducted structural analyses using a variety of structural design tools including the following:

- Hand calculations per AISC 360, Appendix 4,
- Specialized structural fire engineering (SFE) software [SAFIR (Franssen and Gernay 2017), MACS+ (Vassart et al. n.d.), and Slab Panel Method (SPM) software (HERA)], and
- Generalized finite-element analysis (FEA) software [Abaqus (Dassault Systems n.d.)].

Based on analyses of structural demands and capacities under fire exposure, most of the design teams identified certain structural vulnerabilities inherent in the nominal structural designs that

needed to be addressed with greater levels of structural insulation, or structural enhancements, or both to achieve this project's specified performance objectives. As an alternative to adding structural insulation as a strategy to decrease the steel temperatures, Design Team 1 opted for the installation of passive heat vents or skylights at the roof levels. For some of these design scenarios, increasing the level of structural insulation (to the extents that have been qualified for its ability to stay in place reliably) did not appreciably improve the level of structural fire robustness, and therefore, did not meet this project's specified performance objectives. Also, Design Team 2 intentionally reduced the level of insulation to alleviate member strains.

In summary, the collective types of structural enhancements used by the design teams to meet the performance objectives are shown in Table 3.1.

Overall, the Design Teams were able to create robust designs that provide the required level of performance under uncontrolled fire conditions. Also, it was generally found that in-situ fire effects (those in place within actual building construction) are significantly more important to the structural response than the temperature of structural members alone. Last, the results of the structural analyses and the necessary structural enhancements are unique to each individual building, and thus cannot be generalized across all buildings in a prescriptive manner. Hence, structural engineering expertise is required on a project-by-project basis to achieve performance goals using PBSFD.

Table 3-1. Proposed Structural Enhancements and Potential Benefits.

Proposed Structural Enhancement	**Potential Benefit[a]**
Increase the density of concrete slab mesh reinforcement	Provides enhanced strength to resist bidirectional tension during the heating phase of fire.
Increase the size of concrete slab reinforcement bars	Provides enhanced strength to resist bidirectional tension during the heating phase of fire
Lower the positioning of the mesh reinforcement within concrete slabs	Provides enhanced flexural strength by increasing the effective slab depth to compensate for metal deck strength loss during the heating phase of fire; and Provides slab edge stability for full-developed tensile-compressive membrane action during the heating and cooling phases of fire.
Modify mesh reinforcement detailing at slab edges	Provides slab edge stability for full-developed tensile-compressive membrane action during the heating and cooling phases of fire
Increase lapping of mesh reinforcement within concrete slabs	Provides continuous slab tensile strength for full-developed tensile-compressive membrane action during the heating and cooling phases of fire
Increase the bolt hole edge distance of structural connections	Provides enhanced strength to resist induced tension on connections during the cooling phase of fire

Table 3-1. Proposed Structural Enhancements and Potential Benefits (con't).

Proposed Structural Enhancement	Potential Benefit[a]
Increase the number of bolts in structural connections*b*	Provides enhanced strength to resist compressive thrust on connections during the heating phase of fire and induced tension on connections during the cooling phase of fire
Modify bolt pattern of structural connections	Provides enhanced strength to resist compressive thrust on connections during the heating phase of fire and induced tension on connections during the cooling phase of fire
Add slotted holes to structural connections[b]	Provides allowance for connections to accommodate expansion or contraction of the beam as a result of heating, cooling, and loss of stiffness and strength, without inducing axial loads in the connections, thereby reducing the connection demands.
Increase thickness of shear tab connections*b*	Provides enhanced strength to resist compressive thrust on connections during the heating phase of fire and induced tension on connections during the cooling phase of fire
Modify structural connections from shear tab type to double angle type	Provides enhanced ductility for connections to experience rotation during the heating phase of fire without connection fracture
Reorient perimeter columns (strong axis orthogonal to the building perimeter)	Provides enhanced flexural strength to resist lateral loading induced by the expansion of floors during the heating phase of fire
Modify corner steel columns from W-shapes to HSS-shapes	Provides enhanced flexural strength to resist bidirectional lateral loading induced by the expansion of floors during the heating phase of fire
Increase primary member sizes for girders and/or boundary beams	Provides enhanced flexural strength for full-developed tensile-compressive membrane action during the heating phase of fire
Add metal deck rib reinforcement	Provides enhanced flexural strength by increasing the effective slab depth to compensate for metal deck strength loss during the heating phase of fire

[a] Ongoing research may change these findings over time.

[b] Proposed enhancements still require testing validation to prove their effectiveness.

Chapter 4. Design Summary and Discussion of Results

4.1 OVERVIEW

The design summary includes the design team results for each of the design scenarios with respect to the specified performance objectives. The discussion includes how each design team compared the findings from each analysis and includes considered aspects such as volume of material or cost comparisons, if made by the design team.

4.2 BUILDINGS 1−4

Each team has stated its own design summary and discussion in the separate sections following.

4.2.1 Building 1: Design Summary and Discussion

The design summary and discussion that follow were developed by Simpson Gumpertz & Heger for Building 1, which is a Risk Category II, 6-story office building located in the Boston metro area that was governed by wind design. The construction type of the building per the applicable building code prescriptively requires all steel framing (including roof construction) to have 1 h fire resistance. Motivation for Design 3 is discussed in Section 4.2.1.2 and the complete design team report is included in Chapter 7.

4.2.1.1 Summary of Designs

Table 4-1 summarizes the design results for Building 1. The nominal design of Building 1 specified UL Design No. D908 to meet the code requirement for 1 h fire resistance–rated floors. This floor listing, along with many others (e.g., UL Designs D920, D923, D925, D929m, D931, D940, D943, and D949), does not require slab deck rib reinforcement. As discussed in Part II, Chapter 7, Section 7.6.3, the lack of positive moment reinforcement in the slab contributes to the infeasibility of Design 1 and Design 2. Granted, the selection of a fire resistance–rated assembly that requires

Table 4-1. Building 1 Design Summary.

Design Scenario	Structural Enhancements Allowed?	Reduction of Insulation Scope?	Satisfied Mandatory Performance Objectives?	Satisfied Discretionary Performance Objectives: Allows for Full Fire Burnout (Optimum Performance)?
0	No	No	Unknown*	Unknown*
1	No	No	No	No
2	No	No	No	No
3	Yes	Yes	Yes	Yes

* Prescriptive method does not include or require any appreciable structural analyses.

metal deck rib reinforcement could make these designs achievable. However, such a design decision would constitute a structural modification/upgrade, which is not permitted by Design 1 and Design 2.

Design 3 satisfies the discretionary performance objectives and provides robust and reliable structural fire protection by demonstrating optimum (full fire burnout) performance by modestly adjusting the nominal structural design and rationally allocating insulation as follows:

- Nearly all secondary members are left unprotected,
- All roof members are left unprotected,
- Slab mesh is enhanced from 6x6-D2.9×2.9 to 4×4-D5.4×5.4,
- Slab mesh top cover is increased from 3/4 in. to 1-5/8 in.,
- Slab mesh at slab edges is detailed for proper anchorage,
- Primary member web bolt hole clear distance is increased from 1-1/2 in. to 1-3/4 in.,
- Number of bolts for the boundary beam connections is increased from three to four,
- Perimeter columns are reoriented (strong axis orthogonal to the building perimeter), and
- Perimeter corner columns are changed from W-shapes to HSS sections and their connections are further enhanced from that as described.

Figure 4-1 illustrates the Design 3 distribution of structural insulation for a typical floor level of Building 1 that includes a lower roof section. Also, Figure 4-2 illustrates the required enhancement of typical floor boundary beam connections. Lastly, Figure 4-3 illustrates the required slab mesh placement and edge details. At the lower/upper roof levels, the installation of passive heat vents/skylights are used to dramatically reduce the temperature demands on the roof structures (as opposed to reliance on structural insulation) and maintain structural stability under fire exposure. Figure 4-4 depicts the computational fluid dynamics (CFD) modeling used for this confirmation.

The combination of rationally allocated structural insulation and the structural enhancements mentioned above allow for floor bays to form self-equilibrated and stable compressive/tensile membranes at large deflections resulting from uncontrolled fire exposure. Figure 4-5 provides a conceptual illustration of this force equilibration, and Figure 4-6 shows a structural modeling result confirming this behavior for Design 3. For the structural temperature histories plotted in Figure 4-7 resulting from fire exposure, Figure 4-8 plots the evolution of the floor system's capacity compared to the constant applied loading. This demonstrates how the reinforced slab actually strengthens as the level of deflection increases, which effectively compensates for the unprotected infill floor beams' rapid loss of strength (becoming almost negligible at peak heating). Also, the critical reinforcement mesh is highly insulated from fire exposure because of its embedment within the concrete slab. This stabilizing mechanism is analogous to pushing down on the center hub of a horizontally oriented bicycle wheel in which the spoke resists the applied loading in tension and the rim in compression.

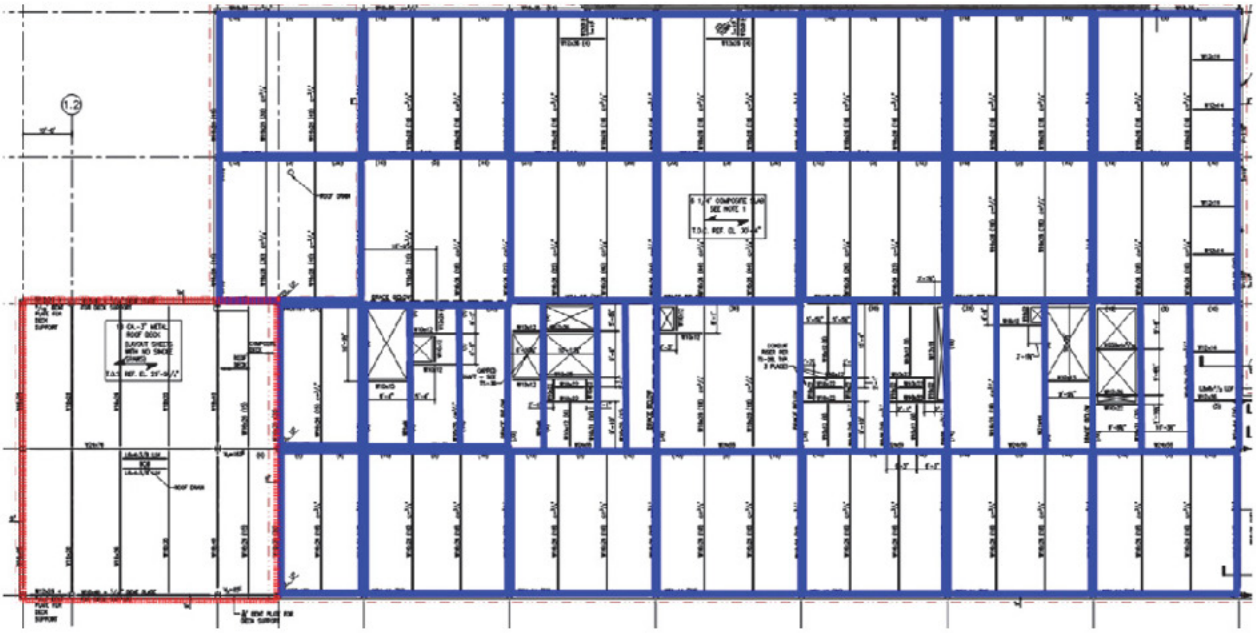

Figure 4-1. Design 3 structural insulation distribution.

Source: Courtesy of Simpson Gumpertz & Heger (2019).

Note: Insulation is shown in blue; roof area is designated in red.

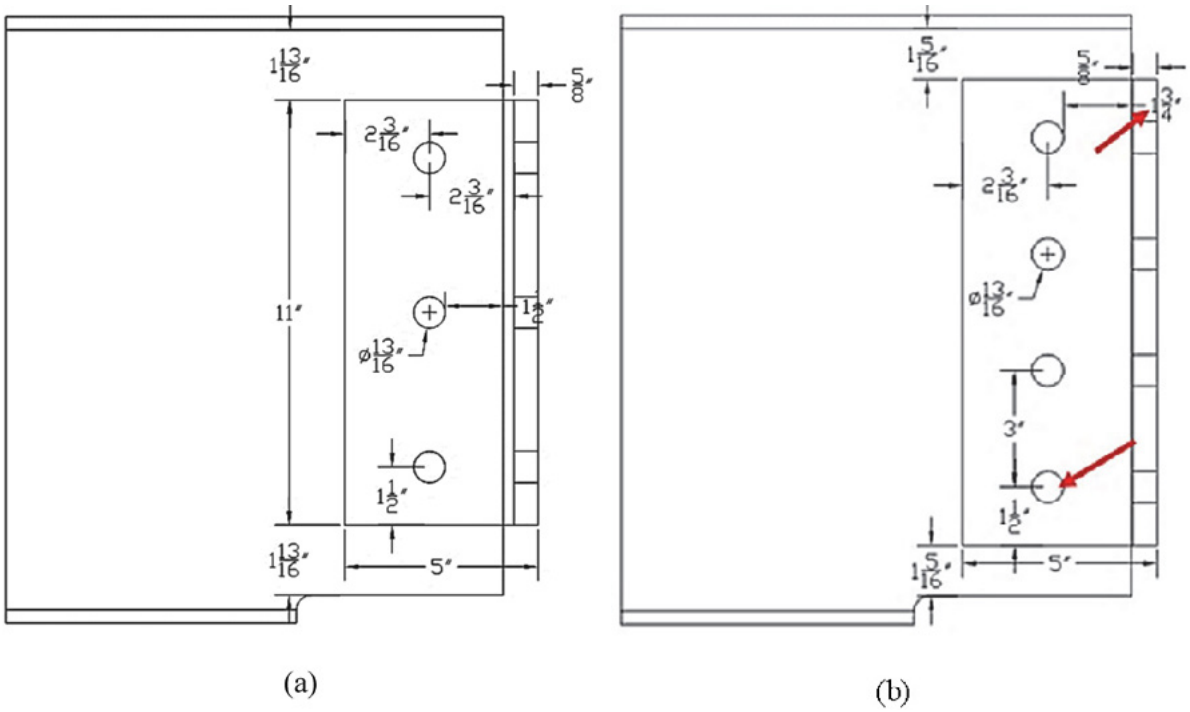

Figure 4-2. Typical boundary beam connection: (a) nominal, and (b) enhanced.

Source: Courtesy of Simpson Gumpertz & Heger (2019).

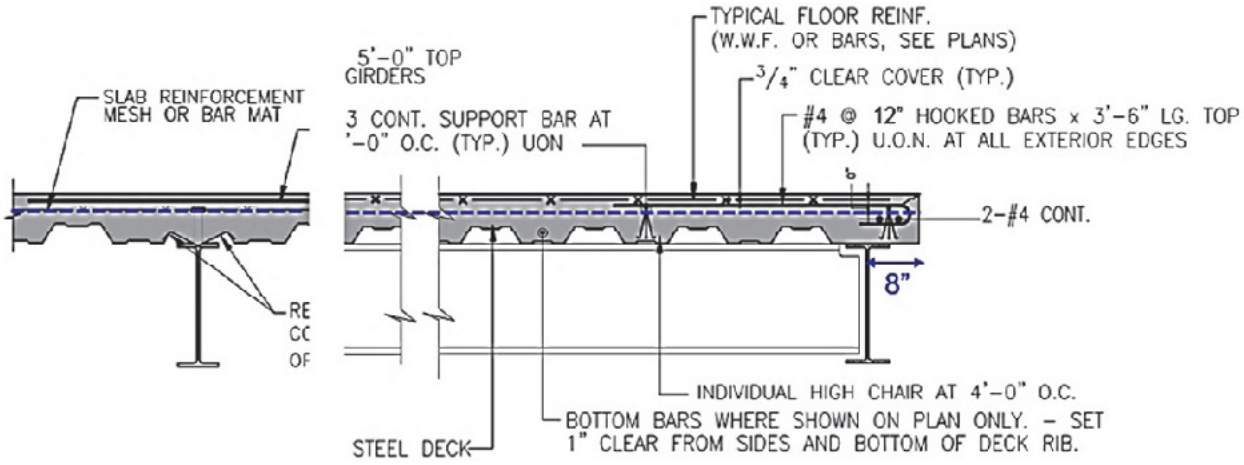

Figure 4-3. Slab mesh placement and edge details.

Source: Courtesy of Simpson Gumpertz & Heger (2019).
Note: Mesh is shown in blue.

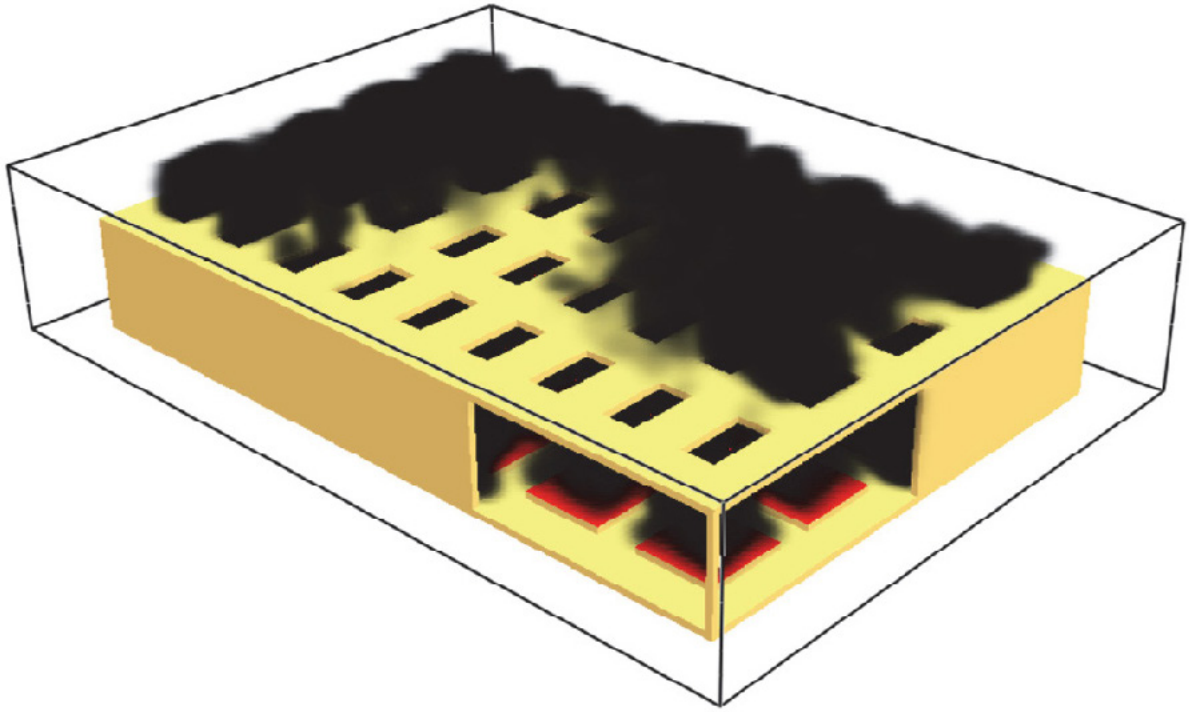

Figure 4-4. Roof heat venting performance (CFD model).

Source: Courtesy of Simpson Gumpertz & Heger (2019), and NIST Fire Dynamics Simulator (FDS) Software ©2019.

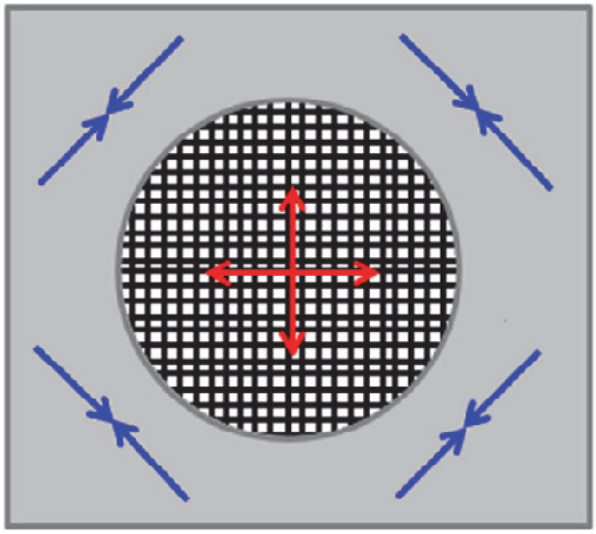

Figure 4-5. Floor slab stabilized compressive/tensile membrane action (center zone mesh revealed within concrete).

Source: Courtesy of Simpson Gumpertz & Heger (2019)

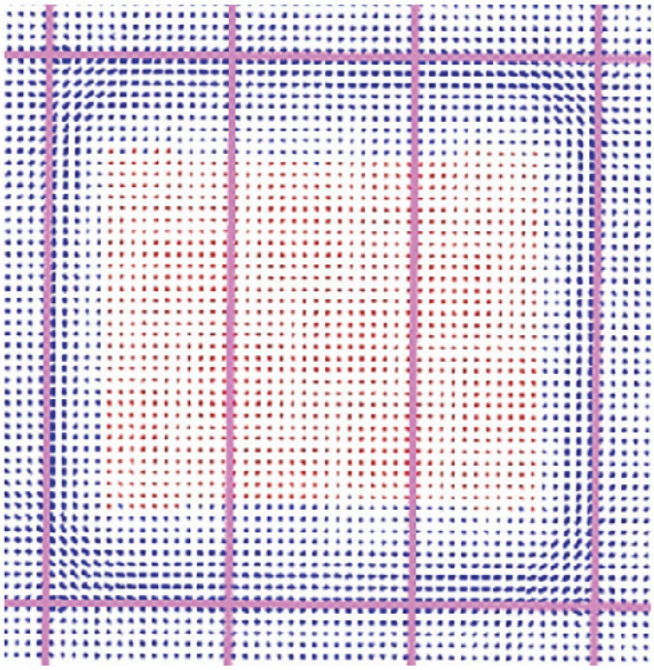

Figure 4-6. Floor slab principal membrane forces.

Source: Courtesy of Simpson Gumpertz & Heger (2019), and SAFIR Software ©2017.
Note: Red represents tension; blue represents compression.

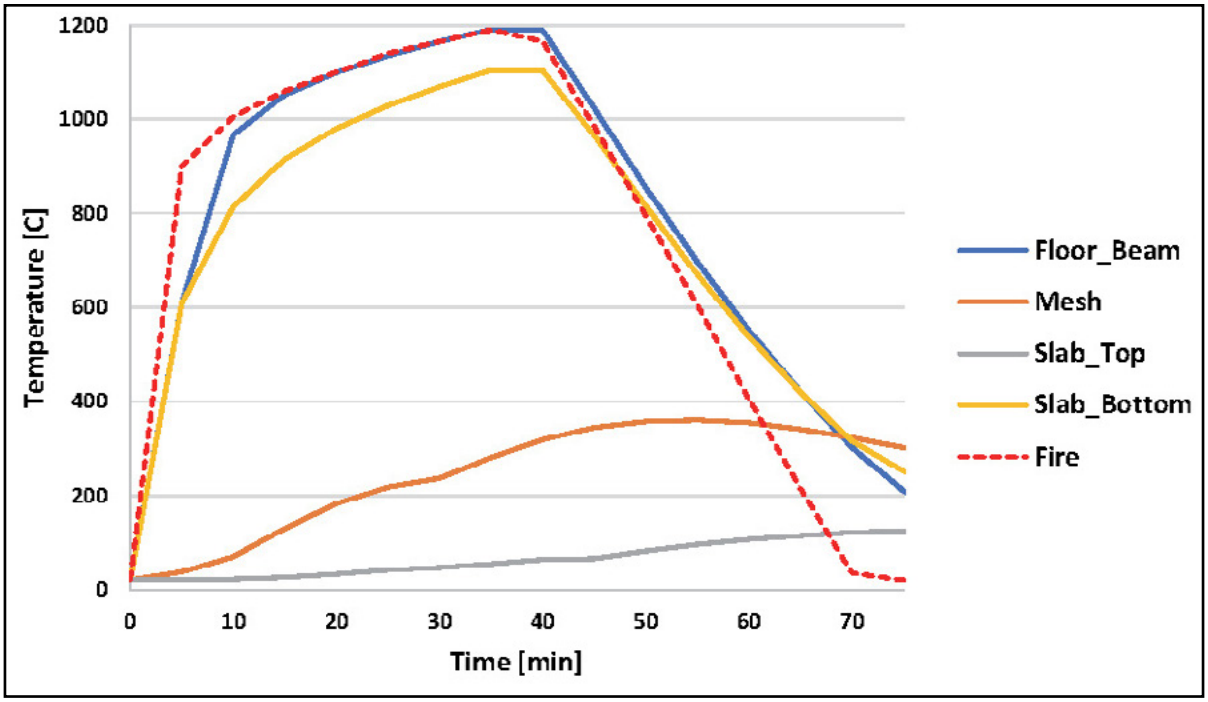

Figure 4-7. Structural temperature histories during fire exposure.
Source: Courtesy of Simpson Gumpertz & Heger (2019).

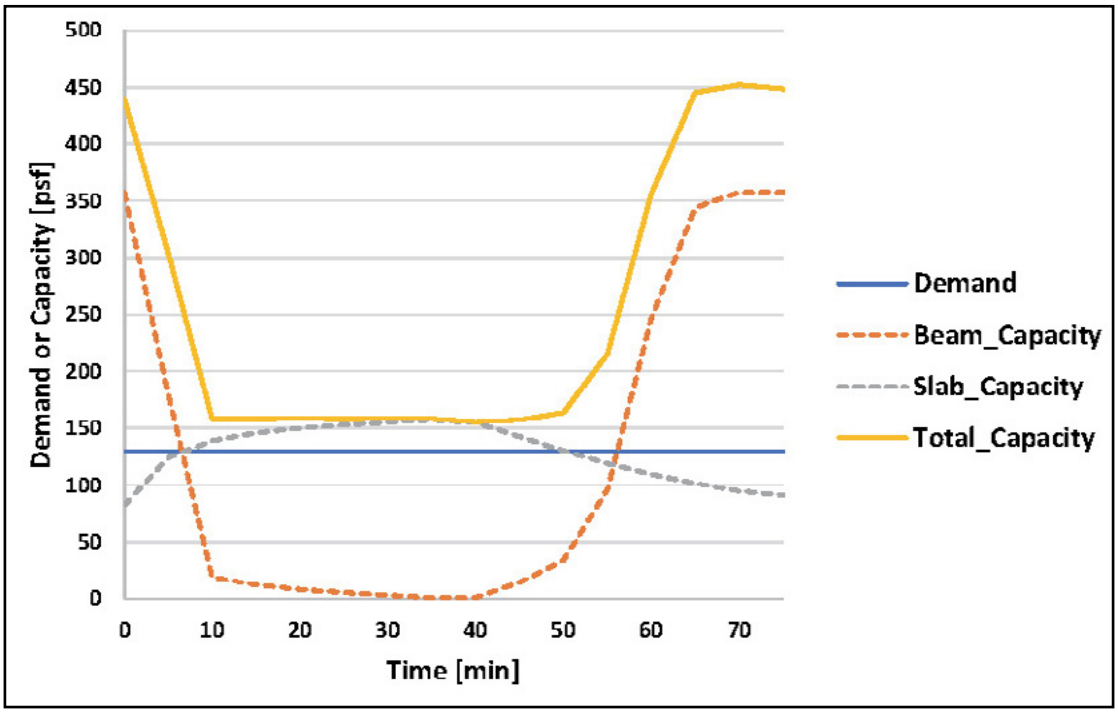

Figure 4-8. Floor demand/capacity history during fire exposure.
Source: Courtesy of Simpson Gumpertz & Heger (2019).

The analytically demonstrated fire robustness of Design 3 is corroborated by examining a similar floor assembly that was physically tested under a similar fire exposure intensity (as compared to the *above-design* fuel load with low ventilation case) that performed comparably with similar deflection histories (Vassart et al. 2012). Although any fire-exposed floors would undergo significant permanent deformation, experience from the Cardington Fire Tests (Lamont 2001) and the Broadgate fire (SCI 1991) demonstrate that such floors could be replaced, and the building put back into service. Hence, Design 3 could also be compliant with additional performance goals for resiliency, which are beyond the scope of this project.

4.2.1.2 Potential Design Impacts

For Design 3, PBSFD is harnessed to holistically synergize structural and applied fire protection designs with a specific aim toward accelerating the overall construction process of Building 1. Specifically, Design 3 defines an applied fire protection distribution and performance specification (as discussed in Section 7.7) which effectively eliminates the need for on-site spray fireproofing to the floor undersides of the building as described in 7.7.1. Aside from the potential to reduce construction costs, this approach could also potentially improve other related aspects including carbon footprint, aesthetics, quality control, site safety, and life-cycle maintenance as described in Section 7.7.2.

4.2.2 Building 2: Design Summary and Discussion

The following design summary and discussion were developed by Magnusson Klemencic Associates for Building 2, which is a Risk Category IV, 12-story healthcare/hospital building located in Washington State that was governed by seismic design. The construction type of the building per the applicable building code prescriptively requires all steel framing to have 2 h fire resistance, except the roof is permitted to have a 1 h fire resistance rating. The complete design team report is included in Chapter 8.

4.2.2.1 Summary of Designs

Design 0

The structure as considered was able to maintain integrity for a duration of approximately 3.5 h when exposed to the controlling full-burnout fire scenario, S1C (see Chapter 8 for scenario descriptions). Beyond this duration, the demand/capacity ratio of one of the infill beams evaluated using the bare steel section properties exceeds 1.0. The relative slab deflection between infill beams begins to exceed the L/20 limit (170 mm) at approximately 3.5 h.

Design 1

The structure was not evaluated for Design 1 because the building occupancy is an in-patient hospital, and safe egress of the occupants is not possible.

Design 2

For Design 2 — where only changes to the level of applied insulation is permitted — the SFRM is removed from the underside of the slab, and S1D is the controlling full-burnout fire scenario. In addition to increasing temperatures in the slab, removing slab SFRM changes the parameters for the fire time-temperature curve, resulting in a lower peak gas temperature and a longer duration. In contrast to Design 0, slab temperatures in Design 2 increased much more rapidly in the heating phase than the beam and girder temperatures. Large tensile forces, which exceeded connection capacity, developed in the girder-to-interior-column connections because of girder-line axial continuity. This tensile force is developed through differential self-strain of the beam and slab, which is resolved as a force couple in the rigidly linked slab and beam elements. It is reasonable to assume this force has been amplified because stud slip is not accounted for in the model, but more sophisticated modeling is needed to confirm these assumptions.

To mitigate the effect of differential slab and beam strain in this simplified modeling approach, the thickness of SFRM applied to the girders was reduced to decrease the temperature differential. Connection axial load decreased but was still more than the available capacity. Connection rotations of more than 0.08 radians were observed before the connection axial load could be reduced below its capacity. Further refinement of stud–slip and connection modeling would be needed to confirm the viability of the connections for Design 2. The columns, beams, and slab were sufficient to resist the fire effects for Design 2.

Given the low infill beam demand/capacity ratios with full SFRM, the SFRM thickness was reduced to 20 mm. Considering the slabs, beams, girders, and columns, the amount of SFRM provided in Design 2 was reduced by 40% from Design 0. A summary of the SFRM thickness is provided in Table 4-3.

Design 3

The Design 3 scenario permitted changes to level of insulation as well as structural enhancements. For this scenario, the objective was to remove fireproofing from infill elements by making structural enhancements to slab reinforcement and provide additional capacity for the slab to support the gravity load with membrane action of the slab. The slab panel method [SPM (Clifton 2006)] shows that the reinforcement in the slab needs to be upgraded to allow for the SFRM to be removed from the infill beams. Two levels of enhanced reinforcement were evaluated as summarized in Table 4-2. The Design 0 slab reinforcement is shown for reference. Reinforcement

Table 4-2. Design 3 Slab Reinforcement Enhancement.

Design Scheme	0	3A	3B
Top Reinforcement	#3 @ 450 mm	W2.9 @ 150 mm	#3 @ 450 mm
Transverse Reinforcement	#3 @ 450 mm	W2.9 @ 150 mm	#3 @ 450 mm
Bottom Reinforcement	–	#3 @ 300 mm	#3 @ 300 mm
Total Reinforcement Area	320 mm^2/m^2	490 mm^2/m^2	550 mm^2/m^2
Total Reinforcement Weight	24 N/m^2	37 N/m^2	42 N/m^2
Mid-Bay Deflection	–	440 mm	350 mm

schemes 3A and 3B are both structurally viable. Scenario 3B meets an L/20 deflection limit for the full duration of the fire. The reinforcement weights in Table 4-2 do not include additional quantity for lap splices.

Without changing the modeling assumptions, the W21 girder to column connections needed to be enhanced from a 6-bolt shear tab connection to an 8-bolt shear tab connection in a 2 × 4 pattern to accommodate the axial loads induced in the girder connections. Similarly, the W16 girder to column connections needed to be enhanced from a 6-bolt shear tab connection (2 × 3) to an 8-bolt (2 × 4) shear tab connection. Alternatively, the connections could be changed to 3-bolt and 4-bolt double angle connections at the W16 and W21 girders, respectively. More refined modeling of the nonlinear connection properties may show better girder connection performance by relieving some of the axial forces transferred through the end connections.

Although the infill beam end connections become overstressed when exposed to the elevated temperatures of the beam, the weak axis shear capacity of the slab can support the full vertical reaction along each girder line.

Consideration was given to reduction in SRFM thickness along the girders to minimize the axial forces transmitted through the connection. A nominal reduction in the axial force is realized, but not enough to significantly change the connection requirements.

Considering the slabs, beams, girders, and columns, the amount of SFRM provided in Design 3 was reduced by 60% from Design 0. A summary of SFRM thicknesses for the three design scenarios can be found in Table 4-3. The beam and girder groupings for SFRM thickness iterations are defined in Figure 4-9.

Table 4-3. SFRM Thickness Summary.

Design Case	Design 0	Design 2	Design 3
Slab (mm)	10	0	0
W21 Girder (mm)	27	27	27
W16 Girder (mm)	27	12	27
Perimeter Beam (mm)	27	20	27
Infill Beam (mm)	27	20	0
Column (mm)	43	43	43

To illustrate the relative SRFM quantity applied to each element, the total SFRM applied to the bay is calculated and divided by the total bay area. As shown in Figure 4-10, for Design 0 the largest volumes of SFRM are associated with the slab and the beams.

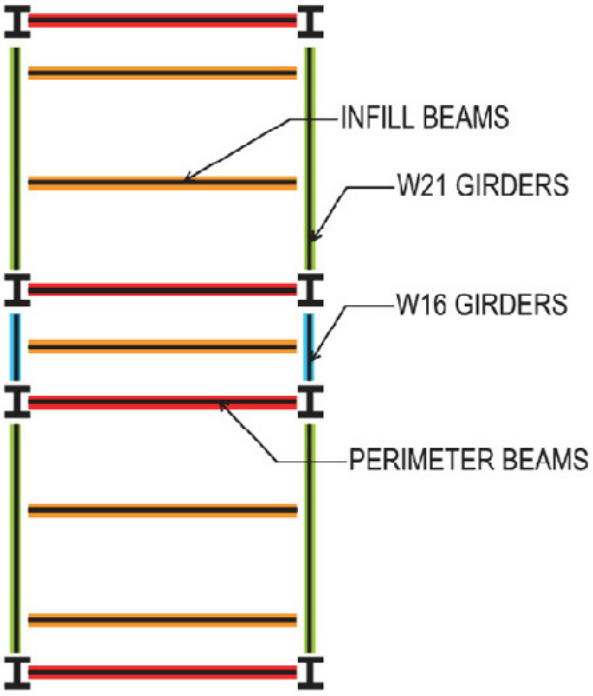

Figure 4-9. Beam categories for SFRM thickness.
Source: Courtesy of Magnusson Klemencic Associates (2019).

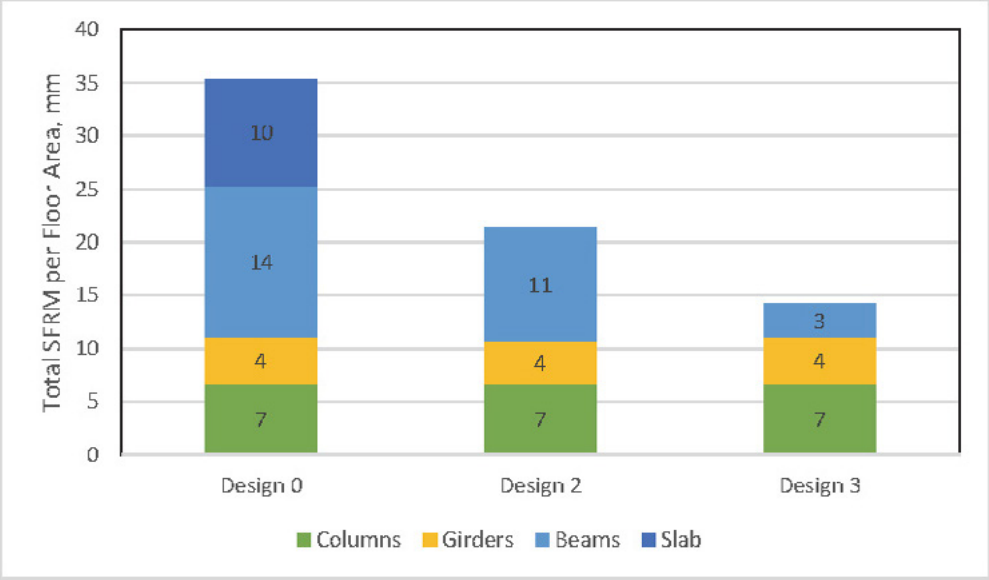

Figure 4-10. Beam categories for SFRM thickness iteration.
Source: Courtesy of Magnusson Klemencic Associates (2019).

4.2.2.2 Discussion of Results

Thermal Analysis Comparison

Lumped-mass calculations were performed in accordance with Eurocode 4, Part 1.2, Section 4.3.4.2.2 for composite beam temperatures and compared to the temperature histories using finite-element heat transfer. AISC does not provide guidance for lumped-mass (LM) modelling of composite members in its fire provisions. In the scenarios considered, the LM model predicted a peak temperature 5% to 20% higher than the finite element analysis model (FEM). Based on these results, the LM model as proposed by Eurocode provides a reasonable and conservative approximation of expected temperatures. A comparison of top flange, web, and bottom flange temperatures for a W21x44 beam subjected to the gas temperatures in Scenario 1-D is shown in Figure 4-11.

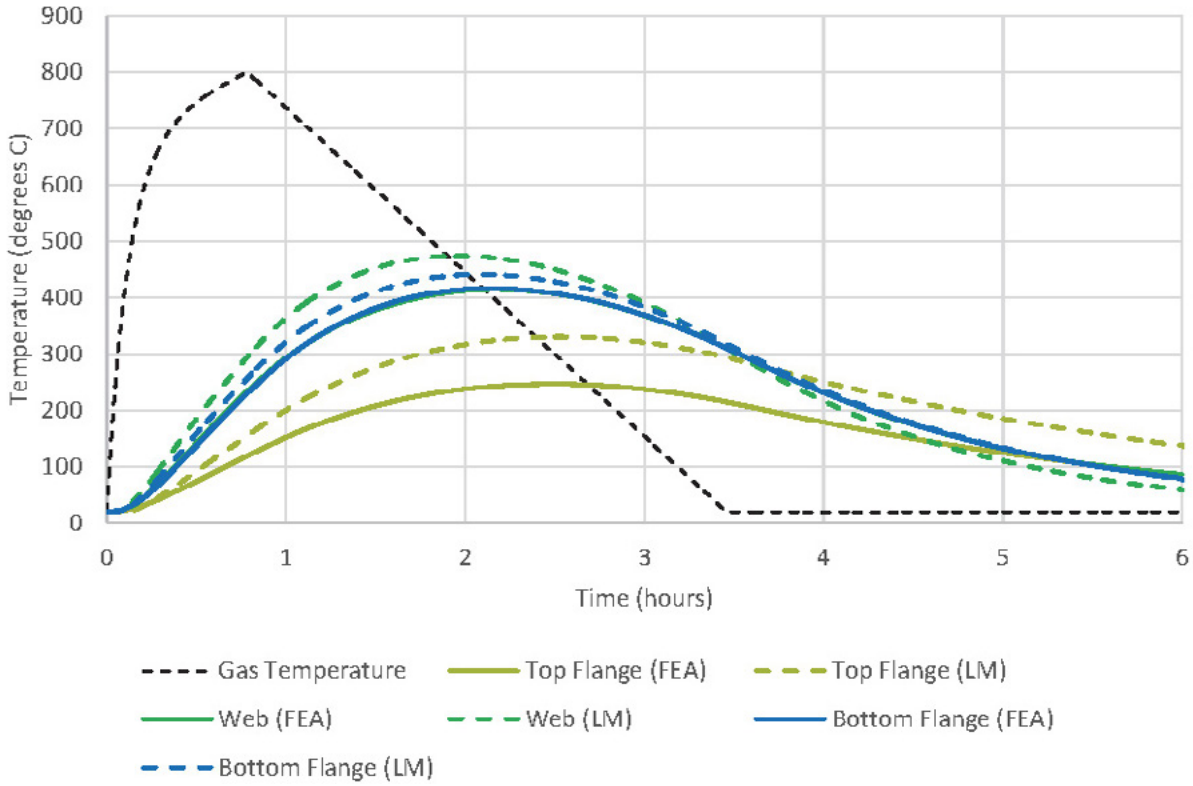

Figure 4-11. Scenario S1-D, W21 × 44 composite beam temperature values using FEM and LM model of Eurocode 4, Part 1.2, Section 4.3.4.2.2.

Source: Courtesy of Magnusson Klemencic Associates (2019).

As shown in Figure 4-12, column temperatures determined through FEM were compared to the LM calculation guidelines in the AISC Appendix 4.2.2 commentary. As with the composite beam LM calculation, the peak temperature prediction was conservative when compared with FEM but within 20%. LM calculations are a useful alternative when finite element methods are unavailable.

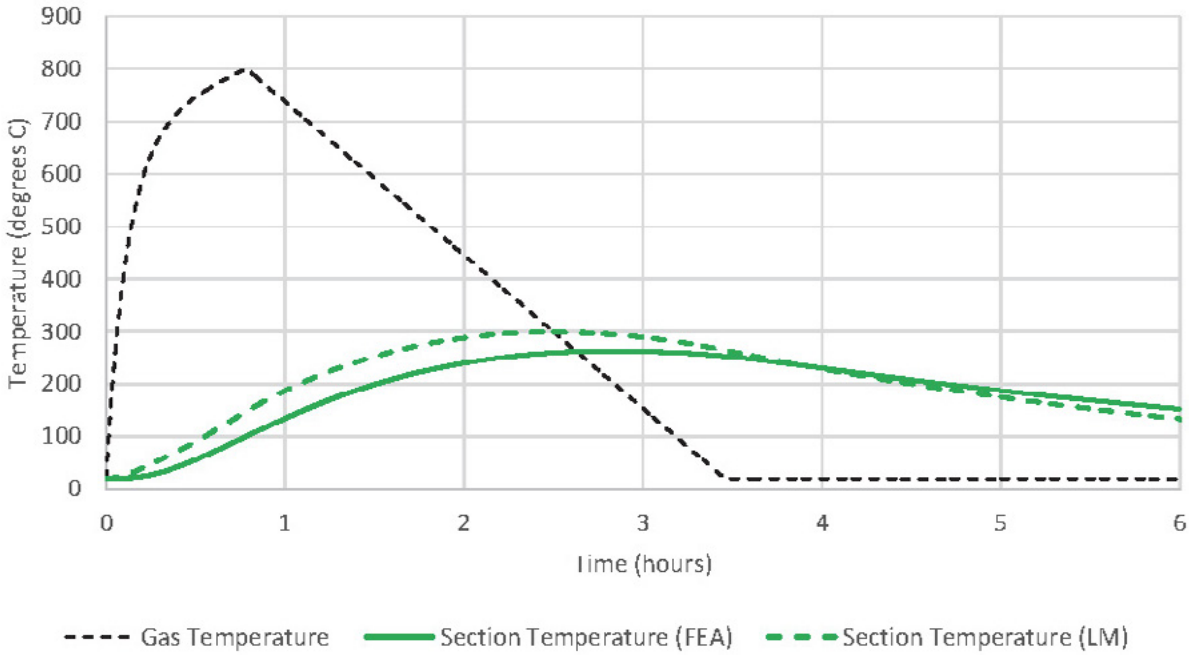

Figure 4-12: Scenario S1-D, W14 × 74 column temperature values using FEM and LM calculations of AISC Appendix 4.2.2 commentary.

Source: Courtesy of Magnusson Klemencic Associates (2019).

Beam and Girder End Constraints

The three-dimensional model considered beam end conditions with and without strong axis flexural continuity. With consideration of flexural continuity, very large moments are developed at connections to columns. The magnitudes of the moments are not compatible with the simple shear connections that are provided at the beam-to-column connections. Therefore, as a lower-bound solution for the floor system's load-carrying capacity, the member end connections were idealized without flexural continuity. The member end rotations were then compared to the connection rotations that have been validated through testing (Choe et al. 2019) to confirm that they have sufficient deformation compatibility to accommodate the expected rotations of the beam ends. This is a similar approach to the justification of connections of members that are not part of the seismic force-resisting system as discussed in the commentary of AISC 341, Section D3. For shear tab connections, the maximum shear tab rotation can be determined based on the available end offset distance, *g*, as shown in Figure 4-13 (Astaneh-Asl 2005).

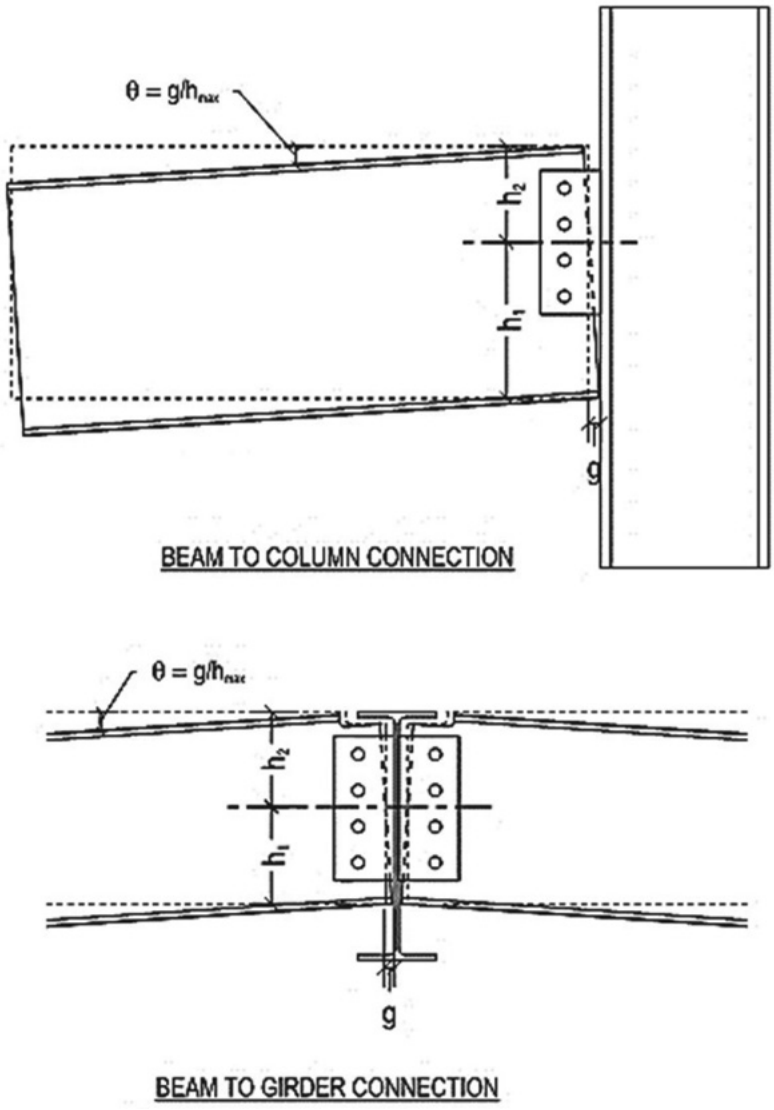

Figure 4-13: Rotation of shear tab connection.

Source: Courtesy of Magnusson Klemencic Associates (2019).

Slab Modeling

It has been observed in fire events that at elevated temperatures, the steel deck debonds from the underside of composite slabs (Lim 2003, Li et al. 2017) and is no longer capable of acting as positive flexural reinforcement for the slab. As a result of early deck debonding, it is common practice to model only the concrete topping slab (Gernay et al. 2020) and ignore the participation of the metal deck and concrete in the flutes. When only the concrete topping slab is considered in the analysis of Building 2, gravity deflections are vastly overpredicted before temperature loads are applied. If a slab profile is modeled that represents both the thin and thick portions of the composite slab and includes metal deck stiffness in the gravity loading step, the slab can span to the secondary beams without relying on membrane action for gravity loads, and the associated large

displacements are mitigated. There is significantly more negative bending capacity at the beam lines because the effective depth of the section extends down from the topping reinforcement to the bottom of the deck flutes.

Because the slab reinforcement from the original design, which includes reinforcement placed low in the deck flutes, is more robust than traditional slab-on-deck welded-wire-fabric reinforcement placed above the deck flutes, the design team did additional analyses to appropriately examine and account for the capacity of the original slab, especially the deck rib reinforcement. Modeling of the thin and thick portions of the slab also allows for reinforcement to be analytically placed low in the deck flutes to be appropriately leveraged for maximizing the load carrying capacity of a slab panel.

Figure 4-14 shows the geometric options considered for the slab profile. The alternating strips of thick and thin elements in Option (d) were found to produce the best longitudinal behavior while limiting error in in the weak axis. This option was favored over Option (c), where similar deflection results were seen, because the smaller quantity of shell elements reduces runtime and composite section cut results are easier to post-process. Option (b), where a truss element is added below the slab with area equal to the flute area, was rejected because there was not an easy way to include the contribution of the metal deck without adding another element, which was found to be important in predicting initial deflection. Gravity-step deflections for a one-bay test model of the floor system using each slab geometry option can be seen in Figure 4-15.

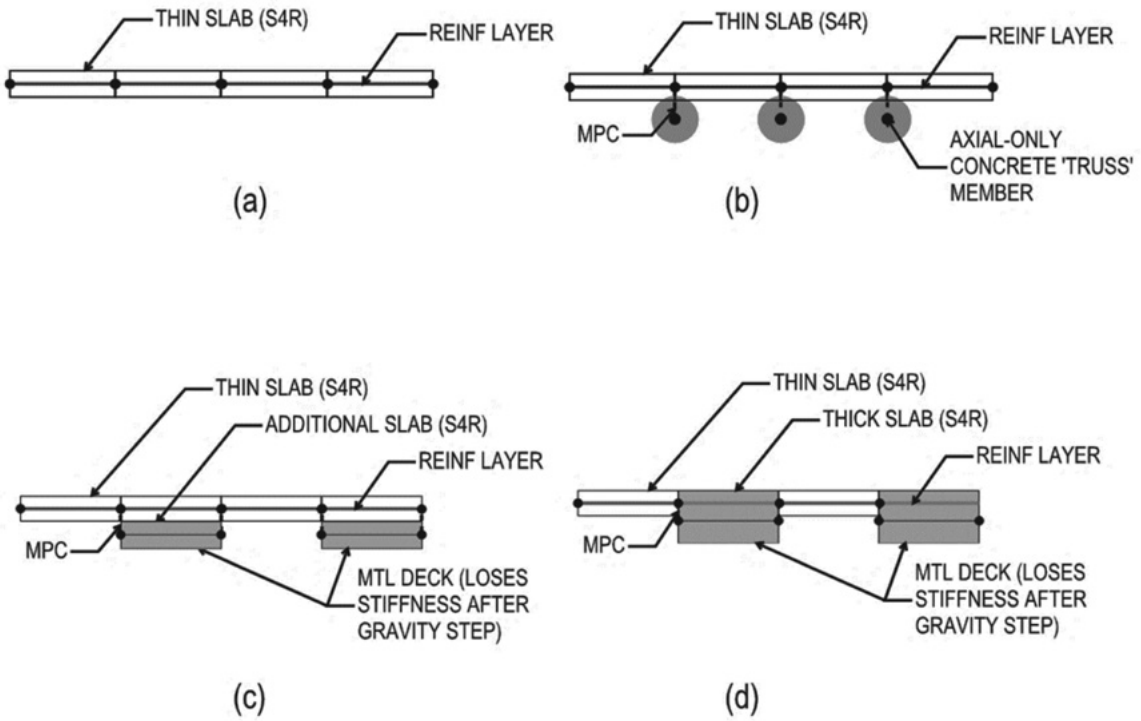

Figure 4-14: Slab geometry options: (a) Topping-only, (b) Topping with truss elements rigidly connected, (c) Topping with additional flute elements rigidly connected, (d) Alternating thick-thin elements with rigid connection.

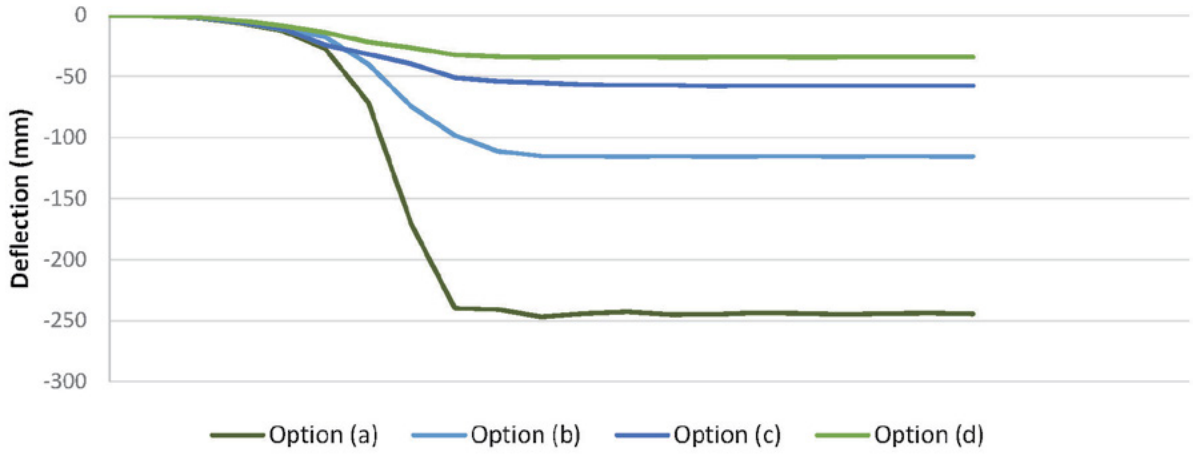

Figure 4-15: Comparison of deflections over the gravity step for slab geometry options: (a) Topping-only, (b) Topping with truss elements rigidly connected, (c) Topping with additional flute elements rigidly connected, (d) Alternating thick-thin elements with rigid connection.

4.2.2.2.4 Slab Panel Methodology

The slab panel method (SPM) as described in the literature (Clifton 2006) was used to develop preliminary designs to be verified with the three-dimensional model. Limitations were imposed on the panel deflections to target the maximum allowable rotations of the beam and girder connections. The SPM provides a reasonable prediction of the system behavior in comparison with three-dimensional analysis. Given that only two secondary beams occur within the slab panel under consideration, and SPM relies on a reasonably distributed reinforcement assumption, the beams were not assumed to contribute to the strength of the slab panel.

4.2.2.2.5 Column Design

The exterior columns experience significant shear and bending moments associated with the growth of the floor subjected to a fire event as shown in Figure 4-16. To maintain the global stability, the columns need to be able to accommodate the thermal expansion of the building.

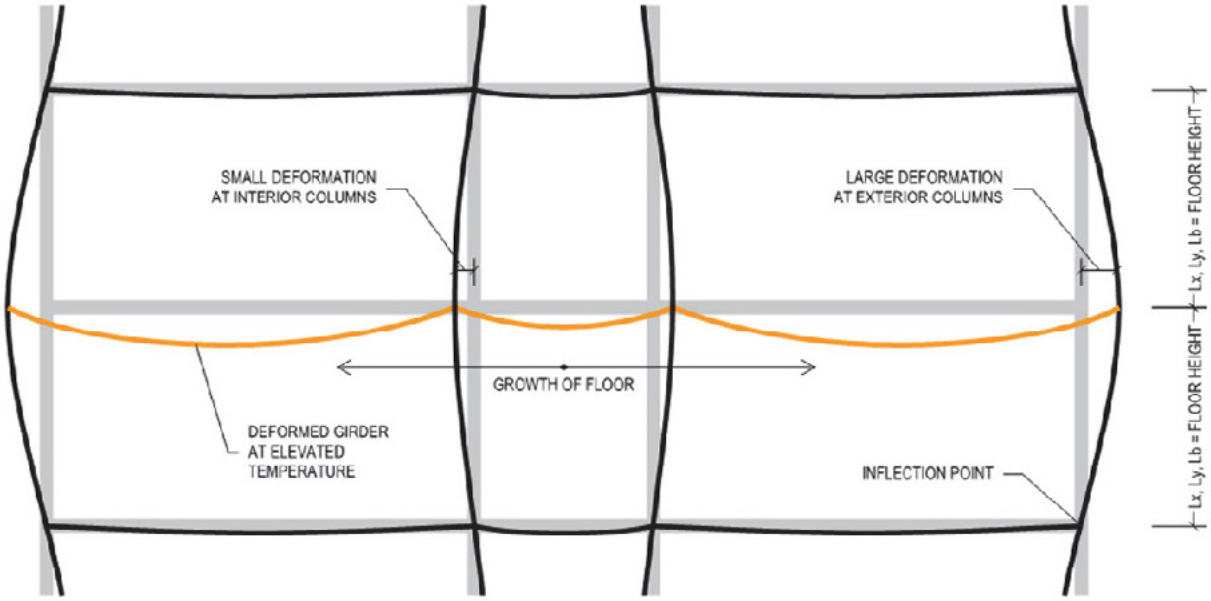

Figure 4-16. Exterior column bending.

Source: Courtesy of Magnusson Klemencic Associates (2019).

Given that Building 2 has been designed to the provisions of seismic design category D, the column splices have the shear capacity to develop the plastic moment capacity of the columns in accordance with AISC 341 for columns that are not part of the seismic force-resisting system. This precludes a shear failure at columns under a fire event.

The columns were designed to support gravity loads assuming the unbraced length between floors. Therefore, gravity load-carrying capacity is maintained, as long as flexural hinges can develop at the top and bottom of the columns. Axial capacity is maintained because there is a load path to support the resulting lateral loads and the columns do not buckle laterally or in torsion prior to the development of the plastic moment.

Flexural members that are unbraced along their length in single curvature can assume $Cb = 1.67$. For rolled shapes, when the slenderness ratio of the column, L/r, is less than 130, the lateral torsional buckling capacity will exceed the plastic moment capacity. Higher values of Cb and the resulting L/r can be justified for columns in double curvature provided there is enough stiffness to restrain the column rotation at the floors above and below. Because the location of the inflection point is dependent on the stiffness of the beams and connections at adjacent floors and the floor-to-floor heights, it is simple and conservative to assume $Cb = 1.67$ for the column design.

4.2.2.2.6 Composite Beam Section Capacity

AISC 360, Appendix 4.2.4d (d) addresses composite beam design for flexure in a fire event. Using the AISC method, capacities are either determined using AISC 360, Chapter I with reduced yield stresses consistent with temperature variation or using the nominal flexural capacity at ambient temperature multiplied by a retention factor, $r(T)$, to account for losses resulting from reduced strength and stiffness.

The results presented for Building 2 use reduced material properties. A comparison of the approaches for the Design 0 case are presented in Figure 4-17, with thick lines indicating the use of retention factors and thin lines representing reductions to material properties.

The retention factor approach consistently underpredicts capacity, compared with the material property modification approach. This is intuitive because it is a simplification of several variables and was developed to be a lower bound on observed behavior.

The retention factor approach implies a baseline moment capacity calculation that can be used at each step in the temperature history. This is only valid if significant net tensile and compressive forces in the composite section are not observed. According to AISC 360, Appendix 4.2.4d(f), combined flexure and axial force must be considered where it occurs. Tensile and compressive forces vary throughout the temperature history because of changes in the steel and concrete temperature differential, so the moment capacity is also variable based on the axial–flexural interaction. Because the capacity for combined forces must be calculated at each time step, it is straightforward to also include the variation in material properties directly. The retention factor approach predicts a lower capacity and does not provide a significant benefit in reducing computation complexity.

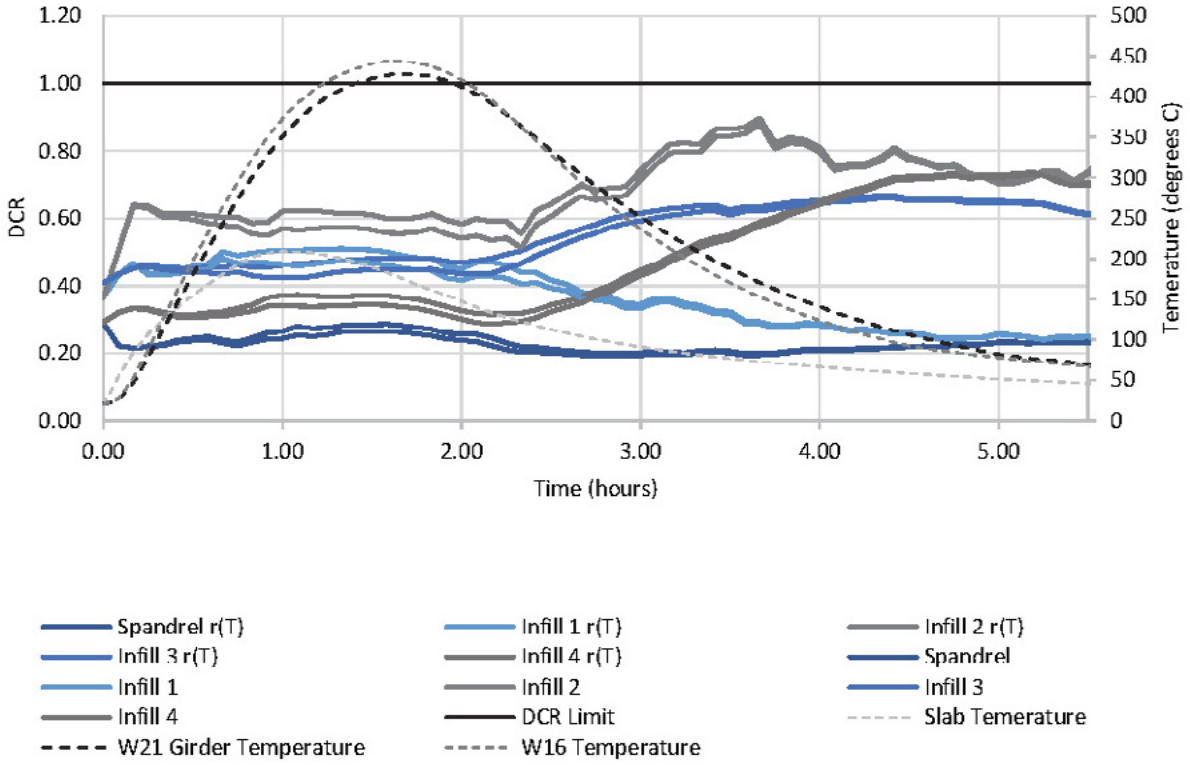

Figure 4-17. Design 0 demand/capacity ratios at beam midspans, composite sections. Comparison of retention factor, *r(T)*, to reduction in material properties.

Source: Courtesy of Magnusson Klemencic Associates (2019).

4.2.3 Building 3: Design Summary and Discussion

The following design summary and discussion was developed by Thornton Tomasetti for Building 3, which is a Risk Category III, 50-story mixed use building located in the Midwest that was governed by wind design. The building frame is of steel construction at the lower 30 floors, transferring to concrete framing at upper floors through a series of steel transfer trusses. The construction type of the building per the applicable building code prescriptively requires the primary and secondary members to have a 3 h and 2 h fire resistance rating, respectively, except the roof is permitted to have a 1-1/2 h fire resistance rating. The complete design team report is included in Chapter 9.

4.2.3.1 Summary of Designs

For Design 1, the performance objective regarding occupant egress requires providing enough time for the occupants to travel safely to refuge areas within the building or exit the building to a public way. Full evacuation for this high-rise building may require hours, practically making this requirement into designing for full burnout. Depending on the specifics of a design, a similar building that relies on refuge in place strategies could provide for a shorter survival duration for the typical floor framing. Such an approach would not be acceptable for the transfer trusses in any situation, because their failure would affect the refuge floors as well. For this exemplar design project, it was decided that Design 1 is not applicable to either design location of this existing building.

Design 2 consists of providing full burnout capacity by only adjusting the fireproofing of the building, and Design 3 consists of providing full burnout capacity by adjusting both the structure and the fireproofing. Design 2 was not possible for the typical bay because the connection demands could not be accommodated by only adjusting fireproofing without modifying the connections. Design 3 was developed for the typical bay and Designs 2 and 3 are similar for the transfer trusses. Two compartment fire scenarios are considered for design checks for each of the typical bay or transfer trusses: A fire with a more severe impact (Scenarios 2A and 3A; see Chapter 9 for scenario descriptions) representing a design with lower ventilation and higher fuel content, and a fire with more moderate impact (Scenarios 2B and 3B) representing a design with more ventilation and more standard fuel content.

Typical Bay

For the typical floor framing, beam behavior was checked through capturing steel plasticity and buckling explicitly in the model and checking concrete forces against capacity, accounting for thermal changes in properties of steel and concrete. The beams remained capable of carrying the loads with fireproofing reduced to 2 h rating for Fire Scenario 2A, and 1 h rating for Fire Scenario 2B. However, connection demands were large enough that connections would have to be changed, even when beam fireproofing was increased to the maximum fireproofing thickness for beams with any classification per UL N743 (2-15/16 in.). Therefore, Design 2 is not achievable.

For Design 3, connections have been changed by providing slots that can accommodate the movements resulting from the structural response to fire. The bolts and slots are covered with premade laths that will be under the fireproofing such that any movement does not affect the fireproofing next to the bolts. If a small unprotected area of the connection is exposed when a

beam is pulling away from the connection, the connection capacity is evaluated considering the temperature effects. Connections for primary members are designed as slip critical at ambient temperatures and provide adequate bracing forces for the columns. In a fire, the bolts can slide to relieve large thermal forces, but the connection has adequate capacity in other limit states, so they do not govern. The columns are checked to be able to carry their loads when deformed as a result of the thermal expansion. The option of providing increased connection capacity was not selected, as it required substantial strengthening of the connections and sometimes the columns. For secondary interior beams framing into spandrels, the connections are designed with slots and finger-tight bolts to accommodate the movement because of structural response to fire and to prevent imposition of large weak axis bending and torsional loads on spandrels. Given that the connections are essential to the structural integrity in fire, additional fireproofing has been provided locally to beam connections to limit the reduction of their capacities, particularly of the bolts, during fire. The additional fireproofing covers the connection plus an additional 3 ft for Fire Scenario 2A and 1 ft for Fire Scenario 2B.

Overall, the fireproofing for all the beams was lowered to what would be equivalent to a prescriptive 2 h rating for Fire Scenario 2A, and 1 h rating for Fire Scenario 2B. Additional fireproofing at connections offset some of these reductions, resulting in a total fireproofing change in the beams of +7% in Fire Scenario 2A and -41% in Fire Scenario 2B.

The floor system at this typical office location is comprised of 3.25 in. light-weight concrete with 4 ksi strength on 20-gauge 3-in.-deep metal deck, with 6x6-W2.9/W2.9 welded wire mesh reinforcement placed 3/4 in. below the slab surface and lapped 6 in. The metal deck is unprotected in Design 0 and it will be kept as such in Design 2 and Design 3. The wire mesh was relied on to develop catenary action in the direction of the metal deck during fire, as the exposed metal deck would rapidly lose capacity during a fire. In the more severe fire scenario 3A, equilibrium was reached with a slab deflection of 11.1 in. This deflection is acceptable, considering the other large deflections experienced by the floor steel framing during a fire. The deflection was 9.2 in. in Fire Scenario 3B. For Design 2, the floor system works with catenary action. At the building perimeter, the behavior relies on catenary reaction being developed within the approximately 2 ft cantilever slab past the spandrel. Design 3 improves the certainty of the outcome of this behavior by specifying that the wire mesh be lowered by 1.25 in. at the slab edges to engage the studs. Increasing the wire mesh lap splice to 12 in. can further increase the floor capacity and lower its deflection during fire by half.

The steel column sizes vary from W14x99 to built-up columns heavier than W14x730. High enough reserve capacity was found to be able to reduce the fireproofing by 38%. There is no need for adjustment to the structural design (Table 4-4).

Transfer Trusses

For the transfer trusses, Design 2 involves changes to the fireproofing to achieve burnout capacity. Because the response of the transfer trusses to fire can affect all the upper supported floors, Design 2 was provided with several options, all of which satisfy the performance criteria, but with different extent of impacts on the upper floors. The design team would select one of these designs based on the building owner's preferences. For Design 3, the design team has the option of modifying the structure to achieve the same performance. The failure mode in the trusses is buckling of structural members, and the solution could be a combination of providing additional strength,

Table 4-4. Summary of Typical Bay Framing for Design Scenarios.

Design scenario	Fire scenarios considered	Beam fireproofing thickness	Column fireproofing thickness	Shear tab connection
0	n/a	Primary: 1-3/8 in. (3 h) Secondary: 7/8 in. (2 h)	Varies (3 h)	t=1/4 in., (4) 3/4 in. A-325 bolts
1	n/a	n/a	n/a	n/a
2	1 + 2A	n/a	n/a	n/a (no acceptable design without modifying connections)
	1 + 2B	n/a	n/a	n/a (no acceptable design without modifying connections)
3	1 + 2A	7/8 in. (2 h)	Varies (1 and 2 h)	Primary interior beams and spandrel beams: t=3/8 in., (6) 1 in. A-490 slip critical bolts with slotted holes, more fireproofing Secondary interior beams: t=3/8 in., (4) 7/8 in. A-490 finger-tight bolts with slotted holes, more fireproofing
	1 + 2B	½ in. (1 h)	Varies (1 h)	Primary interior beams and spandrel beams: t=3/8 in., (6) 1 in. A-490 slip critical bolts with slotted holes, more fireproofing Secondary interior beams: t=3/8 in., (4) 7/8 in. A-490 finger-tight bolts with slotted holes, more fireproofing

or additional fireproofing. Providing additional fireproofing locally has limited additional cost and is the most straightforward solution. Unlike typical areas in a structure, the alternative solution of creating alternative load paths is not reasonable for the transfer trusses, which are main structural features of the building. Hence, Design 3 is the same as Design 2.

Truss connections are proportioned to carry the design forces. Based on the reduction in bolt capacity by 37% at maximum truss temperature of 464 °C, the reduced gravity load demand in truss axial forces of at least 15% for fire load combination, and the fact that bolts are designed with a resistance factor of 0.75, the actual connection capacities will remain adequate, and no additional fireproofing was required. However, additional local fireproofing at critical connections may be added at minimal cost (Table 4-5).

4.2.3.2 Discussion of Results

This study on a high-rise building highlighted the significant impact of the design choices on the performance of the building and the role of performance-based design in ensuring that the performance

Table 4-5. Summary of Transfer Trusses for Design Scenarios.

Design Scenario	Fire Scenarios considered	Allowable damage	Inner trusses fireproofing	Perimeter truss fireproofing
0	n/a	n/a	3 h	3 h
1	Performance objectives not applicable to high-rise			
2	3A	Cosmetic damages above, initiation of limited buckling in some truss members	1 h	3 h
2	3A	Minimal	Increase fireproofing compared to Design 0 as needed	
2	3B	Minimal damages above, initiation of limited buckling in some truss members	1 h	1 h
2	3B	Minimal	2 h	2 h
3	Similar to Design 2; structural upgrade not cost-effective versus fireproofing for transfer trusses			

goals presumed in a prescriptive design are actually achieved. Analysis showed that, at least in some cases, there might not be a realistic acceptable design without changes to the design of the structure. However, with structural fire engineering incorporated into the design from early stages, it is possible to both increase the integrity of a building in fire and reduce the fireproofing.

As shown in Section 9.2 starting with fuels loads, it was shown how different regulatory environments can have a meaningful impact on the fire load considered for design of the building. It was also shown in Section 9.3 how information regarding openings in the façade, as well as from the interior layout of the building, can have a profound impact on the fire loads. Increasingly, the different features of a façade including its window sizes are part of a parametric study at the beginning looking at the holistic impact on the building performance including lighting, energy usage, and aesthetics. If quantified, the effect on fire performance can also be added to the mix of factors being considered. Similarly, many new high-rise designs start with anchor tenants with long-term leases and a clear general understanding of the type of interior layout. While the designer needs to be conservative within the range of uncertainty of design parameters, such layout information can be incorporated into the design when appropriate.

One of the most important findings of the study was that the prescriptive design, which are calibrated to a very specific and different set of criteria do not meet the mandatory requirements and cannot be fully capable of providing the presumed life safety goals and could not be fully remedied by only adjusting fireproofing; see discussion of Design 2 in Section 9.1. This finding highlights the importance of PBSFD. Although this is currently not a code requirement, being able to quantify this effect can allow owners and developers to make decisions when they want to increase the certainty of the outcome of their building design, especially for high occupancy or critical buildings.

It is also noteworthy that performance-based design does not necessarily mean more expensive design. Indeed, if both modifications to the structure and fireproofing are permitted, a building could benefit both from increased fire safety and reduced material costs. In addition, the better

fire performance of a building may be leveraged for other real project impacts such as reducing the insurance premiums on the building, possibly providing additional benefit.

Finally, this design showed a reduction of up to 42% in the quantity of fireproofing in the moderate fire scenario and a slight increase of 4% in the severe fire scenario. These impacts to the fire protection could have beneficial real project impacts, as described in Section 1.8.

4.2.4 Building 4: Design Summary and Discussion

The design summary and discussion below was developed by Walter P Moore for Building 4, which is a Risk Category II, 6-story office building located in Florida that was governed by wind design. The construction type of the building per the applicable building code prescriptively requires all the steel framing to have a 2 h fire resistance rating, except the roof is permitted to have a 1 h fire resistance rating. The complete Design Team report is included in Chapter 10.

4.2.4.1 Summary of Designs

Design 1 requires 1/4 in. thick SFRM on all central and peripheral beams/girders, and Design 2 requires 1/2 in. and 3/4 in. thick SFRM on central and peripheral beams respectively under baseline fires (Cases 1, 2, and 3; see Chapter 10 for descriptions). For Design 3, about 40% of the beams can be left unprotected (see Figure 4-18). Slab wire-mesh reinforcement is increased from 0.058 in2/ft to 0.162 in2/ft and repositioned at 1.75 in. from the surface. The SFRM of the peripheral beams can be reduced to 1 in. According to findings in Section 10.5.3, column SFRM thicknesses can be reduced from 1-1/8 in. to 7/8 in. for Designs 1, 2, and 3. There is no need to make changes in the connections in any of the designs under the baseline fire cases; baseline fires are defined in Section 10.2.

Table 4-6 summarizes the slab wire mesh reinforcement and position, central beam, boundary beam/girder and column SFRM thicknesses used for all designs under all fire cases.

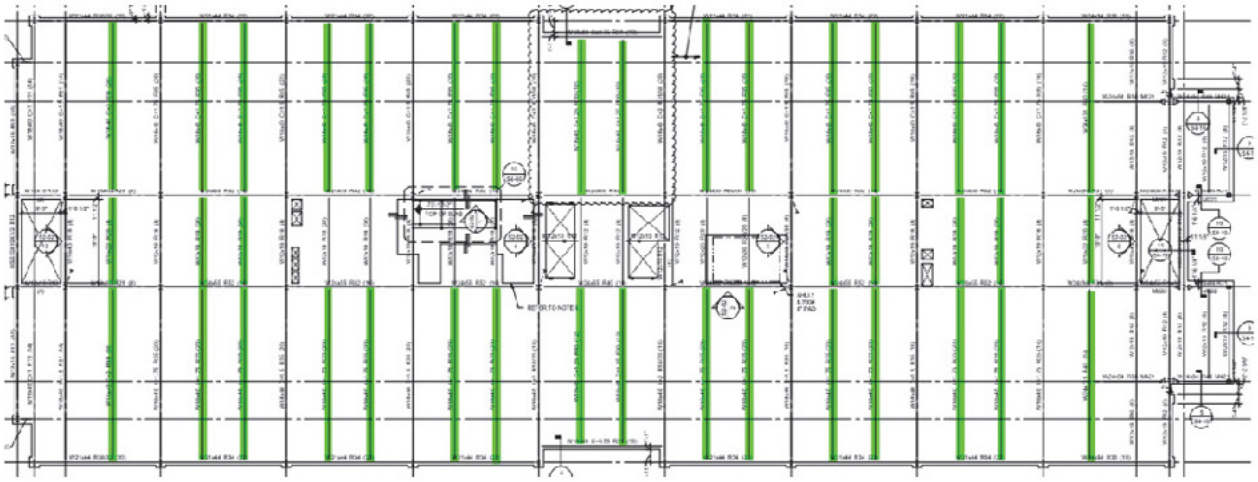

Figure 4-18. Typical floor with unprotected beams highlighted.
Source: Courtesy of Walter P Moore (2019).

Table 4-6. Summary of Results for All Designs and All Fire Cases.

Fire Case	Parameter	Design 0[b]	Design 1	Design 2	Design 3
1	Central Beam SFRM (in.)	1-1/16	None; 1/4	1/4	None
	Wire Mesh (in2/ft)	0.058	0.058	0.058	0.120
	Mesh clear cover (in.)	0.75	0.75	0.75	1.75
	Boundary Beam / Girder SFRM (in.)	1-1/16	3/4; 1/4	1/4	3/4
	Column SFRM (in.)	1-1/8	11/16	11/16	11/16
2	Central Beam SFRM (in.)	1-1/16	1/4	1/4	None
	Wire Mesh (in2/ft)	0.058	0.058	0.058	0.120
	Mesh clear cover (in.)	0.75	0.75	0.75	1.75
	Boundary Beam / Girder SFRM (in.)	1-1/16	1/4	1/4	3/4
	Column SFRM (in.)	1-1/8	11/16	11/16	11/16
3	Central Beam SFRM (in.)	1-1/16	1/4	1/2	None
	Wire Mesh (in2/ft)	0.058	0.058	0.058	0.162
	Mesh clear cover (in.)	0.75	0.75	0.75	1.75
	Boundary Beam / Girder SFRM (in.)	1-1/16	1/4	3/4	1
	Column SFRM (in.)	1-1/8	7/8	7/8	7/8
4	Central Beam SFRM (in.)	1-1/16	1/4	1/4	None
	Wire Mesh (in2/ft)	0.058	0.058	0.058	0.120
	Mesh clear cover (in.)	0.75	0.75	0.75	1.75
	Boundary Beam / Girder SFRM (in.)	1-1/16	1/4	1/4	3/4
	Column SFRM (in.)	1-1/8	11/16	11/16	11/16
5	Central Beam SFRM (in.)	1-1/16	1/4	1/4	None
	Wire Mesh (in2/ft)	0.058	0.058	0.058	0.162
	Mesh clear cover (in.)	0.75	0.75	0.75	1.75
	Boundary Beam / Girder SFRM (in.)	1-1/16	1/4	1/2	3/4
	Column SFRM (in.)	1-1/8	11/16	11/16	11/16
6	Central Beam SFRM (in.)	1-1/16	1/4	3/4	None
	Wire Mesh (in2/ft)	0.058	0.058	0.058	0.240
	Mesh clear cover (in.)	0.75	0.75	0.75	1.75
	Boundary Beam / Girder SFRM (in.)	1-1/16	1/4	1	1-1/16
	Column SFRM (in.)	1- 1/8	7/8	7/8	7/8
7	Central Beam SFRM (in.)	1-1/16	1/4	1/4	None
	Wire Mesh (in2/ft)	0.058	0.058	0.058	0.162
	Mesh clear cover (in.)	0.75	0.75	0.75	1.75
	Boundary Beam / Girder SFRM (in.)	1-1/16	1/4	1/2	3/4
	Column SFRM (in.)	1-1/8	11/16	11/16	11/16
8	Central Beam SFRM (in.)	1-1/16	1/4	1/2	None
	Wire Mesh (in2/ft)	0.058	0.058	0.058	0.200
	Mesh clear cover (in.)	0.75	0.75	0.75	1.75
	Boundary Beam / Girder SFRM (in.)	1-1/16	1/4	3/4	1-1/16
	Column SFRM (in.)	1-1/8	7/8	7/8	7/8
9	Central Beam SFRM (in.)	1-1/16	1/4	1	None; None[a]; ½
	Wire Mesh (in^2/ft)	0.058	0.058	0.058	0.360; 0.240[a]; 0.120
	Mesh clear cover (in.)	0.75	0.75	0.75	2.50; 1.75[a]; 2.50
	Boundary Beam / Girder SFRM (in.)	1-1/16	1/4	1	1-1/16; 1[a]; 1 1/16
	Column SFRM (in.)	1-1/8	1-1/8 (ext) 7/8 (int)	1-1/8 (ext) 7/8 (int)	1-1/8 (ext) 7/8 (int)

a Boundary beam sizes are increased to W21x44 from W18x40 for this design.

b Design 0 is the nonengineered prescriptive design for insulation.

4.2.4.2 Discussion of Results

PBSFD was implemented on a 6-story braced frame building in Florida. Under prescriptive code requirements, this building required a 2 h fire rating for the primary structural frame because of slightly exceeding the International Building Code (IBC) height limits of Type IIA construction that allows for a 1 h fire rating. The occupancy of the building is open office, with typical floor plans. One fire compartment with the largest possible area on the plan was selected, and nine fire scenario cases were generated using different fire load densities, ventilation assumptions, and active fire-fighting measure assumptions to have a robust design; See Table 10-1 for the nine fire scenarios.

The main design strategy for Design 3 was to take advantage of the enhanced load carrying capacity of the reinforced concrete composite slab through tensile membrane action (TMA) by removing the fire protection from the central beams and adjusting the amount and the position of the slab reinforcement and, if necessary, increasing the boundary beam sizes. The performance goal was to allow localized damage, as long as the overall stability of the building is maintained, and this is achievable by utilizing tensile membrane action in the slab.

The position of the reinforcement within the slab is important in TMA. Typical designs only use slab reinforcement close to the surface for cracking control. For Design 3, slab reinforcement position was lowered from 0.75 in. to 1.75 in. from the surface and then the reinforcement amount was increased until the stability was achieved following the design strategy explained in the previous sections. Although lowering the reinforcement within the slab increases the lever arm for bending resistance, depending on the fire case, lowered reinforcement also faces higher temperatures that can affect the response and the stability of the slab. Placing the reinforcement at about half the depth of the slab above the flutes worked well for this study in terms of preventing high temperatures and increasing the bending resistance. ACI-318 crack control checks, which are based on reinforcement spacing and yield stress, are also considered while repositioning the reinforcement within the slab.

For baseline fire (Cases 1 to 3), the design was governed by the ventilation-controlled fire, Case 3. Full fire burnout stability was achieved when the wire mesh reinforcement was increased from 0.058 in2/ft to 0.162 in2/ft, leaving the central beams unprotected. When all nine fire cases are considered, the slab reinforcement needs to be increased to 0.360 in2/ft because of governing long duration ventilation-controlled fire, Case 9. The maximum required slab reinforcement of the other eight cases is 0.24 in2/ft. The failure mechanism of Case 9 was the yielding of the boundary beams, which leads to excessive deflections and prevents the use of TMA. When the boundary beam sizes are increased from W18x40 to W21x44, the slab reinforcement could be reduced to 0.24 in2/ft for Case 9 as well. Note that the other failure mechanism for the rectangular bay of this study was the yielding of the slab reinforcement in the longer span, which occurs because of concrete fracture across the shorter span.

For baseline fire cases (1 to 3), peripheral beam and all column SFRM thicknesses could be reduced to 1 in. and 7/8 in., respectively. The small reduction of the peripheral beams was the result of the high utilization ratios of the boundary beams of the studied bay. Thinner insulation on the boundary beams could be achieved if the boundary beams had been stiffened up by changing their sizes. This was not done except for fire Case 9. The utilization ratios of the columns were relatively lower than the beams for the existing design and thus more reduction could be made

on the column insulation for most of the fire cases. When all nine fire cases are considered, the governing fire Case 9 resulted in 1in. thick SFRM on the peripheral beams and 1-1/8 in. SFRM on exterior columns and 7/8 in. SFRM on interior columns.

Most of the beam-to-girder or beam-to-column connections of this existing building are double angle connections. These connections were converted to shear tab connections to be able to use them with the component method and evaluated at high temperatures. Connection shear and axial force time histories obtained from SAFIR were compared against the capacity curves created with component method using Strand7. There was no need to make any changes on the existing connections.

Table 4-7 shows the reduction in SFRM thicknesses (in percent) of Designs 1, 2, and 3, compared to the prescriptive Design 0. Fire scenarios are grouped as *baseline fire* (80% fractile fire load density with EC reduction for only sprinklers), Alternative 1: *high density* (95% fractile fire load density with sprinkler reductions), and Alternative 2: *no EC reduction* (80% fractile fire load density with no reductions per EC). There is reduction on SFRM for all engineered designs. Note that there are 40 central beams that are left unprotected for Design 3. This stands for about 40% of the total lengths of the beams of the floor. Peripheral beam SFRM thicknesses could not be reduced significantly for long duration fires of Design 2 and Design 3 because of high utilization (low stiffness) of the boundary beams.

Table 4-8 includes a volumetric SFRM comparison of the nonengineered prescriptive Design 0 and engineered Designs 1, 2, and 3. Tabulated SFRM volumes are per story. When the total SFRM volumes are compared, there is about 64% reduction (71.7 cu yd to 26.0 cu yd) in Design 1, which only satisfies the minimum performance objective of RSET stability. Design 2 results in about 35% reduction (71.7 cu yd to 46.4 cu yd) under *baseline fire*, 17% reduction (71.7 cu yd to 59.2 cu yd) under Alternative 1 *high density* fire scenarios and only 7% reduction (71.7 cu yd to 66.6 cu yd) for the last Alternative 2 *no EC reduction* fire scenarios. The reason for the low reduction with Design 2 for the alternative severe scenarios is the low amount of slab reinforcement and its high position within the slab. Note that Design 0 prescriptive design center bay node displacements already reach 19 in. (~ 48 cm) and 23 in. (~ 60 cm) under fire scenario Cases 6

Table 4-7. SFRM Reduction Comparisons.

	Reduction of SFRM for Design 1			Reduction of SFRM for Design 2			Reduction of SFRM for Design 3		
Fire scenario	**Central beams**	**Peripheral beams**	**Columns**	**Central beams**	**Peripheral beams**	**Columns**	**Central beams**	**Peripheral beams**	**Columns**
Baseline fire (Cases 1 to 3)	76%	76%	22%	53%	29%	22%	100%	6%	22%
Alternative - 1 High density (Cases 4 to 6)	76%	76%	22%	29%	6%	22%	100%	0%	22%
Alternative - 2 No EC reduction (Cases 7 to 9)	76%	76%	9%	6%	6%	9%	100%	6%	9%

and 9, respectively. Because structural modifications are not permissible for Design 2, it was not possible to reduce the SFRM volume further with the existing slab condition. Design 3, which requires full fire burnout optimum performance like Design 2, allowed more reduction (~ 35% under all fire scenarios) compared to Design 2 because insulation optimization is much easier with the ability of modifying the structural system. Thus, it is important for the structural engineer to become involved early in the design stage for better optimization.

Table 4-8. SFRM Comparisons by Volume.

	Total beam SFRM (cu yd) for all designs				Total column SFRM (cu yd) for all designs				Total SFRM (cu yd) for all designs			
Fire scenario	**0**	**1**	**2**	**3**	**0**	**1**	**2**	**3**	**0**	**1**	**2**	**3**
Baseline fire (Cases 1 to 3)	53.5	12.2	32.6	31.5	18.3	13.8	13.8	13.8	71.7	26.0	46.4	45.4
Alternative 1 High density (Cases 4 to 6)	53.5	12.2	45.4	33.6	18.3	13.8	13.8	13.8	71.7	26.0	59.2	47.4
Alternative 2 No EC reduction (Cases 7 to 9)	53.5	12.2	50.2	31.5	18.3	13.8	16.4	16.4	71.7	26.0	66.6	47.9

Table 4-9 summarizes the changes in structural quantities for Design 3 for all fire scenario groups. Quantities are provided in terms of the total weight per floor and per unit area.

Table 4-9. Summary of Increases in Structural Member Quantities.

	Increase in quantity for Design 3		
Fire scenario	**Slab reinforcement**	**Beam sizes**	**Connections**
Baseline fire (Cases 1 to 3)	+ 10.9 tons (0.75 psf)	None	None
Alternative 1 High density (Cases 4 to 6)	+19.2 tons (1.32 psf)	None	None
Alternative 2 No EC reduction (Cases 7 to 9)	+19.2 tons (1.32 psf)	+ 1.95 tons (0.13 psf)	None

Chapter 5. Conclusions

5.1 OVERVIEW

The four exemplar designs all share similar findings. First, it was found that some robust structures at ambient temperatures may not necessarily be robust under fire conditions examined in this project. Specifically, several of the exemplar designs demonstrated that the specified performance objectives could not be achieved by the code-prescribed levels of protective insulation, which are calibrated to a very specific and different set of criteria nor by increasing these levels of insulation absent structural enhancements. On the other hand, for some buildings, especially those in higher risk categories or in geographic locations with higher demands, the robust ambient temperature design was able to meet desired fire performance objectives with minimal modifications. Second, it was commonly found that the combination of rationally allocated protective insulation and targeted structural enhancements could provide structural designs that are capable of withstanding full fire burnout without collapse (optimum performance).

5.2 BUILDINGS 1–4

While each design team was able to achieve optimum performance for their buildings, each team used a solution unique to that structure and scenario, thus highlighting the unique role of the structural engineer in PBSFD. Furthermore, the four design teams that participated in this project used their own office procedures and design strategies, and this variation is reflected in the presentation of each team's detailed analyses as provided in Part II. In addition to the common findings stated in Section 5.1, each design team provided their own detailed conclusions in the following sections.

5.2.1 Building 1

Simpson Gumpertz & Heger analyzed a previously completed, 6-story, Risk Category II office building located on the East Coast to compare the safety and practical implications (including economics) of applying prescriptive (SFRD) and PBSFD approaches. The following conclusions were derived based on analysis of this specific building, and do not necessarily apply to all buildings or circumstances:

- PBSFD revealed key structural system vulnerabilities under fire exposure, which would not have been revealed if SFRD was employed.

- Thermal restraint dominates the behavior of the structural system (which cannot be addressed with insulation alone), with degradation of stiffness and strength a secondary factor (typically addressed with insulation) (LaMalva et al. 2020).

- Structural restraint of thermal expansion is predominately deleterious to structural system performance under fire exposure.

- Modest structural upgrades per PBSFD analysis dramatically increased the level of structural fire safety.

- Increasing the level of structural insulation (absent structural enhancements) does not appreciably improve the level of structural fire safety.

- PBSFD has the potential to significantly improve and enhance new project economics, carbon footprint, aesthetics, quality control, and site safety conditions when harnessed with performance-specified off-site applied thin-film (paint) intumescent protection.

- The potential economic benefit of PBSFD increases as the level of new project speculation and construction complexity increases.

- Potential cost savings provided by PBSFD may outweigh the cost of modest structural enhancements required and the increased material cost for intumescent may be offset and possibly advantaged as compared to traditional fireproofing.

- PBSFD burnout design may be justified, regardless of economics, because it confirms adequate structural system performance under fire exposure, especially for buildings with a high consequence of failure.

- PBSFD requires structural engineering competency (SFPE 2018).

5.2.2 Building 2

Magnusson Klemencic Associates analyzed the structural integrity of the Risk Category IV Building 2, which was originally designed for West Coast loads. The structural behavior was evaluated using PBSFD and derived the following conclusions:

- Prescriptive fireproofing in Design 0 showed good performance when subjected to a fire exposure considering full burnout.

- Structural response to fire exposure is highly dependent on the restraint imposed on the structural system. The strength and stiffness reductions to concrete and steel mechanical properties are not significant contributors to the structural response. Removing prescriptive-based SFRM from the underside of composite slabs is achievable with minimal changes to the structural design if the thermal strains can be balanced with the beam thermal strains. This may require modifications to the SRFM thicknesses on beams and girders.

- Design process for improving performance by balancing fireproofing thicknesses is iterative because of the many nonlinear and interdependent parameters defining the thermal and structural behavior of the system.

- Slab panel method accurately represented membrane action from added slab reinforcement in Design 3.

- Relying on slab reinforcement for membrane action is an effective method to improve the structural response to fire exposure because it is insulated by concrete and is typically already included in the floor assembly.

- For each of the design options presented, the girder to column connections are the limiting factor. More refined connection modeling may show better performance by reducing stiffness and allowing slip at bolts, but greatly increases the model complexity.

- Minor upgrades to the slab reinforcement and girder to column connections can result in significant reductions to the volume of SFRM required in a conventionally framed steel building and allow the owner and engineer to establish performance objectives that are absent from traditional prescriptive methods.

5.2.3 Building 3

Thornton Tomasetti's design team analysis of Building 3 — a Risk Category III, high-rise located in the Midwest — identified that prescriptive, code compliant design might not adequately provide the presumed level of structural safety or adequately limit the extent of damage. The large range of building performances obtained when considering the full design space for the same building highlights the limitation of a prescriptive approach in providing a solution that is specific to a real project and meets the appropriate performance goals. The design team also identified many circumstances in which PBSFD can reduce the fireproofing needs of a structure while achieving the required safety goals. Being a rational design approach that explicitly studies the parameters of the design space and adjusts them based on their impact, PBSFD enables better robustness and performance by allowing for more optimal allocation of resources for the same cost, or enables better economy for the same robustness and performance. With Building 3, this was achieved through easily implemented modifications of connections, as well as reduction of fireproofing in beams and columns, while increasing fireproofing on beam connections in some scenarios. In addition, PBSFD helps quantify the expected behavior of buildings in fire, allowing for informed decisions and reliable performance.

Within the context of PBSFD, our analysis also showed that being able to adjust the fireproofing alone has its limitations and cannot always result in a satisfactory result, even when it can improve the performance compared to the prescriptive design. Only the incorporation of modifications to structural design in addition to fireproofing provides the designer with all the tools required to achieve performance goals for the buildings considering their specific features. Fortunately, this approach can frequently improve both safety and potentially the economy of a design.

5.2.4 Building 4

Walter P Moore analyzed Building 4, which is a 6-story, Risk Category II building. The building is 87 ft tall and has a 2 h fire-resistance rating because of barely exceeding the IBC height limit (87 ft versus 85 ft). The sensitivity of the southernly located structure was studied with various uncontrolled fire scenarios to have a robust design.

Current prescriptive practice in the United States only considers component level safety and does not provide insight on the structural system behavior. Structural integrity is maintained in engineered approach by understanding the system behavior and failure mechanisms through structural analyses. It is ideal to set the performance criteria based on stakeholder and design objectives at an early stage of the design process to give the structural design engineer more flexibility on possible economical and efficient solutions.

Significant reduction (~ 64%) in the fire insulation of the beams and columns could be achieved under Design 1, where only a minimum code-mandated performance objective of structural stability up to RSET time was considered. The savings for Design 2, which requires full fire burnout optimum performance without structural modifications, depends on the fire hazard scenario considered. The reduction of SFRM changes from 35% to 17% to 7% from the baseline fire to more conservative Alternative 1 and 2 fire scenarios.

It was shown that about 40% of the beams in the composite floor system can be left unprotected with the development of membrane action in the slab and the total SFRM volume used on beams and columns could be reduced about 35% under all fire scenario groups for Design 3. This can potentially lead to substantial material and labor savings. The payback of leaving the central beams unprotected is the additional slab reinforcement and other potential peripheral beam and connection adjustments, which are required to utilize the tensile membrane action in the composite slab. As both Design 2 and Design 3 have the same performance objectives, the cost study determines the best economical solution.

Typical prescriptive design for fire does not consider structural response or capacity and thus has indeterminate margin of safety. PBSFD increases the understanding of levels of safety and understanding of the structural behavior. Real fire scenarios and structural responses to those fires are evaluated explicitly through PBSFD. The real project goals and stakeholder design objectives need to be set at an early stage of the design to have more efficient and economical design process.

Chapter 6. Recommendations

This project has demonstrated the proper execution and benefits of PBSFD for four regionally diverse building designs with the goal to increase understanding among real project stakeholders on how to adopt and harness such an approach. Overall, the adoption of PBSFD within the AEC industry can improve building performance while potentially delivering more efficient and economic building designs.

To increase the adoption of PBSFD by real project stakeholders on building designs that would benefit, the following steps will need to be taken across the United States:

- Project stakeholders will need to be made aware of the applicability, potential benefits, and opportunities that exist with a PBSFD approach.

- Building authorities will need to understand the process and require the participation of a structural engineer if a performance-based approach to structural fire protection is proposed, as stipulated in Appendix E of ASCE 7-16, *Minimum Design Loads and Associated Criteria for Buildings and Other Structures*.

- Structural engineers will need to become competent in PBSFD methodologies, as well as in structural fire protection design, in order to effectively harness PBSFD on projects that could benefit from this approach.

- Project team conducting PBSFD shall have the required competencies to characterize the fire/thermal effects, conduct heat transfer analysis within the structure, and determine the structural impact of thermal stresses and changes in material properties at high temperatures (Maluk et al. 2017, Jönsson 2019).

- Manufacturers of protective structural insulation (especially thin-film intumescent) will need to conduct testing to develop the necessary data to properly respond to PBSFD performance specifications. This is important because the requirements for protective insulation for PBSFD differs from that for SFRD, which relies on fire resistance qualification (Lucherini and Maluk 2019). Similarly, additional information and testing by manufacturers of fireproofing and the research community regarding the performance and integrity of fireproofing at connections subject to plasticity or other movement will be helpful, because connections are not part of the prescriptive testing procedure.

References

ACI (American Concrete Institute). 2014. *Building code requirements for structural concrete*, ACI 318. Farmington Hills, MI: American Concrete Institute.

AISC (American Institute of Steel Construction). 2016a. *Seismic provisions for structural steel buildings* AISC 341. Chicago: American Institute of Steel Construction.

AISC. 2016b. *Specification for structural steel buildings*, AISC 360. Chicago: American Institute of Steel Construction.

ASCE. 2018. *Structural fire engineering*, Manual of Practice No. 138. Reston, VA: ASCE.

Ansys, Inc. n.d. ANSYS software. Canonsburg, PA: Ansys, Inc.

ASCE. 2017. *Minimum design loads and associated criteria for buildings and other structures*, ASCE 7-16, Reston, VA: ASCE.

Astaneh-Asl, A. 2005. "Design of shear tab connections for gravity and seismic loads." *Steel Tips: Structural Steel Educational Council*. June. Accessed August 21, 2019. http://www.steeltips.org/steeltips/tip_details.php?id=90

Buildings Magazine. 2011. *Economics/Cost Model*. May. Accessed August 5, 2020. http://global.ctbuh.org/resources/papers/download/2013-overview-of-the-benefits-of-structural-fire-engineering.pdf

CEN (European Committee for Standardization). 2001. EN 1991-1-2 *Eurocode 1: Basis of Design and Actions on Structures, Part 1.2: Actions on Structures. Actions on Structures Exposed to Fire*. Brussels: CEN.

CEN. 2004. EN 1992-1-2. *Eurocode 2: Design of Concrete Structures. Part 1-2: General Rules. Structural Fire Design*. Brussels: CEN.

CEN. 2005a. EN 1993-1-2 *Eurocode 3: Design of Steel Structures. Part 1-2: General Rules. Structural Fire Design*. Brussels: CEN.

CEN. 2005b. EN 1994-1-2 *Eurocode 4: Design of Steel Structures. Part 1-2: General Rules. Structural Fire Design*. Brussels: CEN.

Clifton, G. C. 2006. *Design of composite steel floor systems for severe fires*. HERA Report R4-131. Manukau City, Auckland, NZ: New Zealand Heavy Engineering Research Association.

Choe, L. Y., S. Ramesh, M. S. Hoehler, M. S. Seif, M. F. Bundy, J. Reilly, et al. (2019). "Compartment fire experiments on long-span composite beams with simple shear connections Part 2: Test results," *Tech Note, TN 2055*. Gaithersburg, MD: NIST.

Dassault Systèmes Simulia Corp. n.d. Abaqus software. Johnston, RI: Dessault Systèmes Simulia Corp.

Davison, J. B., I. W. Burgess, R. J. Plank, H. Yu, and Y. Hu. 2010. “Ductility of simple steel connections in fire.” In *Proc., SDSS’ Rio 2010: International Colloquium Stability and Ductility of Steel Structures*. Rio de Janeiro: Federal University of Rio de Janeiro, 441−448.

Easen, N. 2017. “Construction: An industry ripe for tech disruption.” *Raconteur*, June 13. Accessed August 22, 2019. https://www.raconteur.net/business-innovation/construction-an-industry-ripe-for-tech-disruption

Fischer, E., and A. Varma. 2015. “Sustainability and structural fire engineering,” In *Proc., Structures Congress*. Portland, OR: ASCE.

Fischer, E. C., J. Gambatese, and A. B. Shephard. 2019. “A holistic approach to the resilience of steel-frame construction in fire,” *Pract. Period. Struct. Des. Const*. 24(4).

Franssen, J.-M., and T. Gernay. 2017. “Modeling structures in fire with SAFIR®: Theoretical background and capabilities.” *J. Struct. Fire Eng.* 8 (3): 300−323.

Garlock M., and S. Quiel. 2008. “Plastic axial load and moment interaction curves for fire exposed steel sections with thermal gradients.” *J. Struct. Eng.* 134 (6): 874–880.

Gernay, T., and N. E. Khorasani. 2020. Recommendations for performance-based fire design of composite steel buildings using computational analysis. *J. Construc. Steel Res.*166, 105906.

Helwig, T. A., and Yura, J. A. 1999. “Torsional bracing of columns.” *J. Struct. Eng.* 125 (5): 547−555.

HERA (Heavy Engineering Research Association) 2012. *SPM - Slab panel method of fire emergency design,* version 3.1.1. Manukau, Auckland, NZ: HERA.

ICC (International Code Council) 2018. *International building code*. Washington, DC: International Code Council.

Jönsson, J. 2019. “Are you a competent practitioner?” *SFPE Europe*. Q1 (13). Accessed August 21, 2019. https://www.sfpe.org/page/Issue13Feature1

Khorasani, N, M. Garlock, and P. Gardoni. 2014. “Fire load: Survey data, recent standards, and probabilistic models for office buildings.” *Eng. Struct.* 58 (January): 152−165.

Kirby, B. R. 1998. *The behaviour of a multi-storey steel framed building subject to fire attack− Experimental data*. Moorgate, Rotherham, UK: British Steel Swinden Technology Centre.

LaMalva, K. J., L. Bisby, J. Gales, T. Gernay, E. Hantouche, C. Jones, et al. 2020. “Rectification of restrained vs. unrestrained,” *Fire Mat. J.*

LaMalva, K. J., T. McAllister, and L. Bisby. 2018. "Restrained vs. unrestrained: Within the context of new industry guidance," *Structure*. September. Accessed August 22, 2019. https://www.structuremag.org/?p=13699

Lamont, S. 2001. "The behaviour of multi-storey composite steel framed structures in response to compartment fires," Ph.D. diss., Univ. of Edinburgh.

Li, G. Q., N. Zhang, and J. Jiang. (2017). Experimental investigation on thermal and mechanical behaviour of composite floors exposed to standard fire. *Fire Safety J.* 89: 63−76.

Lim, L. 2003. "Membrane action in fire exposed concrete floor," Ph.D. diss., Univ. of Canterbury, Christchurch, NZ.

Lucherini, A., and C. Maluk. 2019. "Intumescent coatings used for the fire-safe design of steel structures: A review." *J. Construct. Steel Res.* 162 (November): 105712.

Maluk, C., M. Woodrow, and J. L. Torero. 2017. "The potential of integrating fire safety in modern building design." *Fire Safety J.* 88: 104−112.

Newman, L., J. Dowling, and W. Simms. 2005. *Structural fire design: Off-site applied thin film intumescent coatings.* Berkshire, UK: Steel Construction Institute.

NIST (National Institute of Standards and Technology). 2000. *Fire dynamics simulator*. Gaithersburg, MD: NIST.

SCI (Steel Construction Institute). 1991. *Structural fire engineering: Investigation of the Broadgate phase 8 fire. Ascot, UK*. Berkshire, UK: Steel Construction Institute.

SFPE (Society of Fire Protection Engineers). 2010. *Standard on calculating fire exposure to structures*, SFPE S.01. Gaithersburg, MD: Society of Fire Protection Engineers.

SFPE. 2015. *Standard on calculation methods to predict the thermal performance of structural and fire resistive assemblies*, SFPE S.02. Gaithersburg, MD: Society of Fire Protection Engineers.

SFPE. 2016. *SFPE handbook of fire protection engineering*, 5th ed. Gaithersburg, MD: Society of Fire Protection Engineers.

SFPE. 2018. *Recommended minimum technical core competencies for the practice of fire protection engineering*. Gaithersburg, MD: Society of Fire Protection Engineers.

Thunderhead Engineering Consultants, Inc. 2016. *Pathfinder: Agent based evacuation simulation*. Manhattan, KS: Thunderhead Engineering Consultants, Inc.

University of Sheffield. 2008. *EPSRC Project EP/C510984/1: Robustness of joints in fire, 2005−2008*. Accessed August 21, 2019. https://fire-research.group.shef.ac.uk/downloads.html

Vassart, O., C. Bailey, M. Hawes, A. Nadjai, W. Simms, B. Zhao, et al. 2012. “Large-scale fire test of unprotected cellular beam acting in membrane action.” In *Proc., Institution of Civil Engineers (ICE)−Structures and Buildings*. 165 (7): 327−334.

Vassart, O., M. Hawes, A. Nadjai, W. Simms, B. Zhao, and J.-M. Franssen. 2010. *Fire resistance of long cellular beam made of rolled profiles (FICEB)*. Luxembourg: Research Fund for Coal and Steel, European Commission.

Vassart, O., B. Zhao, R. Hamerlink, B. Hauke, J. de la Quintana, I. Talvik, et al. n.d. *MACS+ − Membrane action of composite structures in case of fire*. Accessed August 22, 2019. https://constructalia.arcelormittal.com/en/news_center/articles/macs_membrane_action_of_composite_structures_in_case_of_fire

Wald F., P. Kallerová, R. Chlouba, Z. Sokol, and M. Strejček. 2010. *Fire test on an administrative building in Mokrsko*. Prague: Czech Technical Univ.

Appendix: Project Design Brief

Contents

1. Introduction

The Structural Engineering Institute (SEI) of ASCE with the support of the Charles Pankow Foundation (CPF) is pursuing, as part of its Vision, the advancement of performance-based design. Advancing the adoption of performance-based structural fire engineering (SFE) within the AEC industry will benefit public safety while delivering more efficient and economic building designs. This project seeks to demonstrate the proper execution and benefits of SFE for real building designs. This project focuses on protected steel structures; concrete and timber construction are not considered within the scope.

1.1 Background

Current prescriptive code requirements, referred to as standard fire resistance design (SFRD), for structural fire protection often result in designs that have inconsistent — and arguably unknown — safety levels, and this 100 yr old paradigm also often stifles innovation in the design of buildings. In recent years, extensive research pertaining to the performance of structures at elevated temperatures has laid the foundation for a legitimized alternative method, as sanctioned by the provisions of ASCE 7-16.

The SFE method requires a dramatically higher level of engineering rigor as compared to prescriptive design, but it can provide many worthwhile benefits; this method is based on the application of engineering principles and physics-based modeling in lieu of prescriptive/archaic rules. Yet, this method is not being widely adopted in practice in the United States. The factors hindering the adoption of SFE in the United States include the lack of understanding and participation by structural engineers, the lack of trial designs demonstrating the potential benefits to stakeholders, and the unfamiliarity with the approach by building officials.

1.2 Project Goal

The goal of this project is to advance the adoption of SFE within the AEC industry. With specific design confirmation and possible modest structural enhancements, structural systems can be engineered to satisfactorily endure uncontrolled fire exposure, while also potentially providing enhanced design freedom and economy as compared to a SFRD approach. The results should also benefit the public by enabling development of more innovative designs with improved safety/performance.

1.3 Project Objectives

To achieve the goal described previously, the project has the following objectives:

- Demonstrate the proper execution of SFE designs in accordance with ASCE 7-16, Appendix E.
- Provide exemplar procedural guidance for a set of buildings with regional representation.
- Explicitly illustrate the benefits of this integrated approach to fire safety through trial designs.
- Estimate cost implications of the trials designs, including aesthetic, maintenance, and carbon footprint impacts.

1.4 Project Teams

The teams for this project are shown in Table 1.

Table 1. Project Teams

Designation	Designer	Peer Reviewer
Team 1	Kevin LaMalva, Simpson Gumpertz & Heger (SGH)	Negar Elhami-Khorasani, University of Buffalo (UB)
Team 2	Ron Klemencic, Magnusson Klemencic Associates (MKA)	Erica Fischer, Oregon State University (OSU)
Team 3	Najib Abboud, Thornton Tomasetti (TT)	Thomas Gernay, Johns Hopkins University (JHU)
Team 4	Larry Griffis, Walter P Moore (WPM)	Jose Torero, University of Maryland (UMD)

1.5 Scope of Work

Each of the four project teams will complete the following structural fire protection designs for an existing (anonymous) building:

- Design 0: Prescriptive requirements for insulation.
  - o *Nonengineered empirical indexing approach (indeterminate performance).*
- Design 1: Optimize insulation to satisfy the minimum requirements of ASCE 7-16 (allowance for complete and safe occupant evacuation to a public way and ability of structural framing supporting refuge areas (if any such areas are present) to withstand fire burnout without collapse).
  - o *Engineered approach without the ability to modify the structural system (minimum performance).*
- Design 2: Optimize insulation to achieve fire burnout without any collapse of the structural system framing.
  - o *Engineered approach without the ability to modify the structural system (optimum performance).*
- Design 3: Optimize insulation and structural modifications (if any) to achieve fire burnout without any collapse of the structural system framing.
  - o *Engineered approach with the ability to modify the structural system (optimum performance).*

Design 0 is the century-old norm of prescribing insulation for structural fire protection, which excludes any structural analysis. The acceptance metric for Design 0 is the level of fire resistance, which is an artifact of standard fire testing and its failure criteria.

Designs 1 and 2 represent a case in which the structural fire engineer is engaged late in the design process in which the structural design is essentially crystallized. Design 1 represents a case in which no discretionary performance objectives are enacted by the project stakeholders, and the minimum level of performance is deemed as adequate. Design 2 represents a case in which discretionary performance objectives are enacted to an extent to which optimum performance is required. Design 3 represents the ideal case in which the structural fire engineer is involved in the structural design and optimum performance is sought. Optimum performance is the demonstration of full fire burnout and cooling without collapse of the structural system framing, and it does not necessarily provide assurance of post-fire-event functionality of the structure (e.g., residual stiffness/capacity for reoccupation that can be influenced by the method (water/air)/rate of cooling).

The acceptance metric for Designs 1, 2, and 3 is structural integrity as demonstrated by satisfactory fulfillment of all applicable structural limit states and/or simulation of satisfactory structural performance. In this context, the inherent ability of a structural system to endure fire exposure may be considered in conjunction with the benefits of applied insulation. Unlike conventional structural engineering design, Designs 1, 2, and 3 may rely on load redistribution and/or nonconventional sources of load-carrying capacity (e.g., tensile membrane action), which generally have not been utilized in U.S. practice to date.

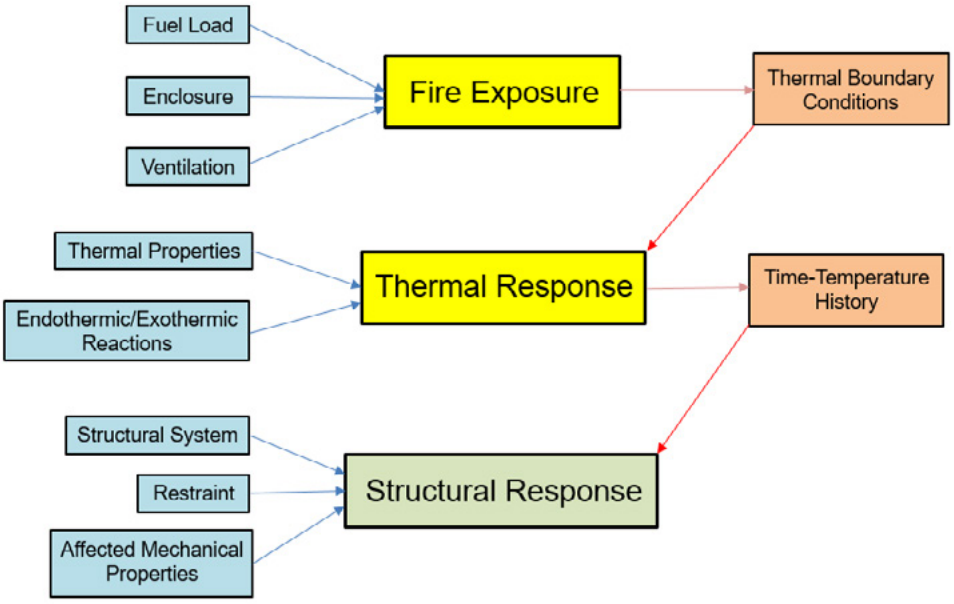

Figure 1. SFE Design Process.
Source: Structural Fire Engineering, MOP 138 (2018).

Designs 1, 2, and 3 shall account for temperature-dependent material properties, boundary conditions, and thermally induced failure modes and shall evaluate structural stability, strength, deformation, and load path continuity. Figure 1 illustrates the sequentially coupled deterministic design process (note: thermal reactions of insulation shall be implicitly represented per Section 7.3.2.3).

2. Host Structural Systems

Four existing (anonymous) buildings have been selected to provide a range of geographic location, project size and use as shown in Table 2. All four buildings are steel-framed structures with composite floors, and insulation (*fireproofing*) prescriptively required for all primary and secondary members per SFRD.

Table 2. Existing Buildings to Study.

Designation	Team	Height	Occupancy	Lateral* System	Location	Risk Category
Building 1	Team 1	Low-rise (6 stories)	Office	Braced	East	RC II
Building 2	Team 2	Midrise (12 stories)	Healthcare	Braced (BRB)	West	RC IV
Building 3	Team 3	High-rise (45 stories)	Office/ Residential	Concrete Core	Midwest	RC III
Building 4	Team 4	Low-rise (6 stories)	Office	Braced	South	RC II

* Note: Moment frames not considered due to their relatively uncommon use in practice as compared to braced frames.

2.1 Building 1

Building 1 is a previously completed structural design project from SGH, which was built in the early 2000s and located in the Boston Metro area. The building has six stories, approximately 24,000 sq ft per floor and is used primarily for office space on all levels (occupancy Group B). Given a reduction granted for buildings over 70 ft, the construction type of the building per the applicable building code prescriptively requires all steel framing (including roof construction) to have 1 h fire resistance. The building has a braced-frame lateral-force-resisting system that is primarily controlled by design wind loads.

2.2 Building 2

Building 2 is a previously completed structural design project from MKA, which was built in the late 2000s and located in the state of Washington. The building has twelve stories, approximately 50,000 sq ft per floor and is used primarily as a healthcare center/hospital. The construction type of the building per the applicable building code prescriptively requires all steel framing to have 2 h fire resistance, except the roof is permitted to have a 1 h fire resistance rating. The building has

a buckling-restrained braced (BRB) lateral-force-resisting system that is primarily controlled by design seismic loads.

2.3 Building 3

Building 3 is a previously completed structural design project from TT, which was built in the mid-2010s and located in the Chicago metropolitan area. The building has 45 stories, approximately 20,000 sq ft per floor, and is used for office space on the lower levels (occupancy Group B) and residential space on the upper levels (occupancy Group R). A floor near the midheight of the building is a transfer floor with steel trusses. The construction type of the building per the applicable building code prescriptively requires the primary and secondary members to have a 3 h and 2 h fire resistance rating, respectively, except the roof is permitted to have a 1-1/2 h fire resistance rating. The building has perimeter steel columns and utilizes a reinforced concrete core for its lateral-force-resisting system that is primarily controlled by design wind loads.

2.4 Building 4

Building 4 is a previously completed structural design project from WPM, which was built in the late 2000s and located in the state of Florida. The building has six stories, approximately 30,000 sq ft per floor and is used primarily for office space on all levels (occupancy Group B). The construction type of the building per the applicable building code prescriptively requires all of the steel framing to have a 2 h fire resistance rating, except the roof is permitted to have a 1 h fire resistance rating. The building has a braced frame lateral-force-resisting system that is primarily controlled by design wind loads.

3. Industry References

The analyses shall be conducted entirely in conformance with the only US industry consensus standard for SFE as follows:

- *Minimum Design Loads and Associated Criteria for Buildings and Other Structures,* ASCE 7-16 (2017) [i]
    - *Appendix E: Performance-Based Design Procedures for Fire Effects on Structures*

The analyses shall utilize aspects of the following industry guides at the discretion of each design team:

- *Structural Fire Engineering*, MOP 138 (2018) [ii]
- *Specification for Structural Steel Buildings*, AISC 360 (2016) [iii]
    - *Appendix 4: Structural Design for Fire Conditions*
- Eurocode 1 – Actions on Structures; Part 1-2 – Actions on Structures Exposed to Fire[iv]
    - *Provisions in conflict with ASCE 7-16, Appendix E will not be used.*

- Eurocode 2 – Design of Concrete Structures – Part 1-2: General Rules – Structural Fire Design[v]
    - *Provisions in conflict with ASCE 7-16, Appendix E will not be used.*
- Eurocode 3 – Design of Steel Structures – Part 1-2: General Rules – Structural Fire Design [vi]
    - *Provisions in conflict with ASCE 7-16, Appendix E will not be used.*
- *Standard on Calculating Fire Exposure to Structures*, SFPE S.01 (2010) [vii]
- *Standard on Calculation Methods to Predict the Thermal Performance of Structural and Fire Resistive Assemblies,* SFPE S.02 (2015) [viii]

4. Industry Software

The analyses may utilize the following industry software at the discretion of each design team:

- Evacuation Analysis (Section 6.1).
    - *Pathfinder* (Thunderhead Engineering*).*
- Fire Exposure Analysis (Section 7.2.3).
    - *Fire Dynamics Simulator* (National Institute of Standards and Technology).
- Thermal Response Analysis (Section 7.3).
    - *Abaqus* (Dassault Systems)
    - *SAFIR* (Liege University)
    - *Ansys* (Ansys, Inc.)
- Structural Response Analysis (Section 9.2).
    - *Abaqus* (Dassault Systems)
    - *SAFIR* (Liege University)
    - *Ansys* (Ansys, Inc.)

5. Performance Objectives

Design 0 does not have any explicit/known performance expectations. The performance expectations for Designs 1, 2, and 3 are described as follows.

5.1 Mandatory Performance Objectives

ASCE 7-16, Section E.4.1 requires that the structural system remains stable, with a continuous load path to the extent necessary to ensure occupant life safety during fire exposure. Hence, the performance of the structural system under structural design fires shall allow for building occupants to safely exit the building to a public way (e.g., public roadway). Specifically, structural support of building egress routes shall be maintained for a period of time necessary to ensure that occupants can evacuate safely and completely. Also, parts of the structural system that support areas where occupants are expected to take refuge during a fire shall be maintained through full fire burnout (i.e., heating and cooling phase of the fire).

Design 1 will be conducted to satisfy these minimum requirements only.

5.2 Discretionary Performance Objectives

ASCE 7-16, Section E.4.2 states that project-specific performance objectives may be required by project stakeholders.

Designs 2 and 3 will be conducted to satisfy the minimum requirements described in Section 5.1, as well as provide for fire burnout without any collapse (optimum performance).

6. Occupant Life Safety (Evacuation/Refuge)

Building codes limit egress travel distances to exits (e.g., stairways), but generally do not limit the total evacuation time. As the vertical remoteness of occupants from the point of discharge to a public way (e.g., a public street) is increased, the time required to evacuate the building will increase. Unlike SFRD, SFE explicitly evaluates the consequences of increased occupant evacuation times, and the reliance on building refuge areas.

To demonstrate the adequacy of occupant egress routes, an “ASET versus RSET” analysis will be conducted for each building. The Available Safe Egress Time (ASET) will be determined by analyzing the endurance of the structural system to fire exposure (see Section 9). The Required Safe Egress Time (RSET) will be determined by analyzing the time it would take occupants to travel safely to refuge areas within the building or exit the building to a public way. The ASET value shall be greater than the RSET value. Structural endurance through fire burnout would satisfy this requirement.

6.1 Required Safe Egress Time (RSET)

For each building, the RSET will be estimated using hand calculations (e.g., per the SFPE Handbook[ix]) and/or advanced computer-based models that simulate human behaviors. In either case, occupant premovement time (i.e., alarm awareness and movement initiation) should be included in the total evacuation time. The effects of occupant queuing will be conservatively accounted for. Also, egress time delays resulting from phased evacuation (e.g., as occurring in a high-rise buildings) should be accounted for. Lastly, it will be assumed that mobile and mobility- impaired occupants would utilize stairways and accessible elevators, respectively, for evacuation to a public way during a fire event.

6.2 Areas of Refuge

Exit stairways and other building spaces that serve mobile and mobility-impaired occupants will not be considered as refuge areas. Designated spaces in which occupants, including assisted-mobility occupants (e.g., hospital patients), are expected to remain in place during a fire event should be considered as refuge areas.

7. Nominal Fire Load (Structural Temperature Histories)

Uncontrolled fire within an engineered building is an extraordinary event that can have severe consequences. Fire sprinkler systems significantly reduce the probability of this occurrence, but these systems are in general, not effective against very large fires.[x] Accordingly, inherent and applied structural fire protection is intended to serve as a secondary safety measure (in sprinkler-protected buildings) in the rare case that a fire becomes uncontrolled; otherwise, it serves no purpose. Hence, the nominal fire load (i.e., the temperature field of the structure at a given point in time) will be evaluated assuming there exists no manual or automatic intervention to the fire growth (i.e., uncontrolled fire).

7.1 Design Fuel Load

The nominal fuel load is the total expected quantity of combustible contents within a building area. For enclosure-type fire exposures (Section 7.2.1), a design distributed fuel load (MJ/m^2) may be used. For localized-type fire exposures (Section 7.2.2), a design local fuel load (MJ) may be used.

The occupancy-based method in the Eurocode 1 may be used to determine the design fuel load. This method treats the nominal fuel load as a variable parameter with a Gumbel distribution and an 80% upper confidence interval. Further, the design fuel load is a function of the nominal fuel load and specific risk factors per Eurocode 1, Annex E. Notably, a risk factor must be calculated, which accounts for the presence or absence of active fire protection measures. It should be noted that the growth of each structural design fire scenario may not consider manual or active measures per Section 7 (such as enforcing an artificial cap on the fire's heat release rate due to sprinkler control is not permitted). Alternatively, the design fuel load may be based on specific fuel load survey data and/or dedicated studies according to the discretion of each design team.

7.2 Structural Design Fires

Structural design fires should be classified as either enclosure-type or localized-type based upon the likelihood of flashover occurring. First, the peak heat release rate should be determined based on the occupancy type per Eurocode 1. Second, the heat release rate required for a given building space to support flashover should be calculated using the hand calculation method in SFPE S.01. If the peak heat release rate exceeds that required for flashover, an enclosure fire should be considered (Section 7.2.1). Otherwise, a localized fire may be considered (Section 7.2.2).

Explicit consideration of traveling fire scenarios is not required but may be conducted at the discretion of each project team. In general, consideration of an enclosure-type fire within a given building space instead of a traveling-type fire is conservative. Appendix A provides further commentary on traveling-type fires.

7.2.1 Enclosure Fire Exposure

The time–temperature history of a ventilation-controlled enclosure-type fire exposure is a function of the following parameters:

- Distributed fuel load (MJ/m^2)
- Total area of enclosure boundaries (m^2)
- Total area of ventilation openings (m^2)
- Height of ventilation openings (weighted average) (m)
- Density of enclosure boundaries (kg/m^3)
- Thermal conductivity of enclosure boundaries (W/mK)
- Specific heat of enclosure boundaries (J/kgK)

Hand calculation methods in Eurocode 1 and/or SFPE S.01 may be used to calculate the time–temperature histories of enclosure fires. Further commentary on each of the two approaches is provided in Appendix B. Ambient thermal properties may be used for the enclosure boundaries per Eurocode 1 recommendations. Ventilation openings should include all doors, windows, or penetrations into a compartment that provide a path for ventilation to a fire. Window breakage and door conditions (open/closed) are difficult to predict and variable. Hence, a few different ventilation scenarios should be considered (e.g., all open/broken, all closed/intact, and partially closed/broken). In general, the fire duration is more important than the peak temperature in terms of its effect on the structural system.

7.2.2 Localized Fire Exposure

Hand calculation methods in SFPE S.01 may be used to calculate the time-temperature histories of localized fires. Also, flame height hand calculations should be conducted to confirm whether flame impingement on the structure is anticipated.

7.2.3 Fire Simulation

If necessary, computational fluid dynamics (CFD) simulation(s) may be conducted to determine time–temperature histories for structural design fire scenarios. In this case, any mechanical ventilation of heat must be neglected; however, the presence of passive-type natural ventilation (e.g., roof-mounted vents operated by fusible links) may be considered.

7.2.4 Fire Exposure Extent

If a given floor of a building has no fire-rated boundaries, fire exposure across the entire extent of the floor should be considered as a structural design fire scenario. Otherwise, the extent of the floor encompassed by fire-rated boundaries and building extents may be considered. If the given building has fire-rated floors and noncombustible exterior wall systems, consideration of fire on

multiple floors is not required. Otherwise, the possibility for multiple-floor fire involvement may be considered. Appendix C provides additional commentary on fire exposure extent.

7.3 Thermal Response

For each structural design fire scenario, the temperature field history of the structural system should be calculated based upon the fire exposure time–temperature history (Section 7.2), surface thermal conditions (Section 7.3.1), and material thermal properties (Section 7.3.2).

For structural hand calculations (Section 9.1), only the maximum temperature reached (by the given structural member or component) needs to be considered. For simulation of structural response (Section 9.2), the temperature field history should be considered.

7.3.1 Heat Transfer Calculations

The uniform temperature field history of individual steel members (beams, girders, and columns) may be determined using the lumped-mass hand calculation method per AISC 360, Appendix 4. For simulation of structural response (Section 9.2), nonuniform temperature distributions should be considered.

If required, finite element heat transfer analyses may be used to determine the temperature field histories of structural members and components. SFPE S.02 provides guidance on such analyses. Notably, such analyses should consider the three modes of heat transfer: conduction, convection, and radiation. Also, the convective heat transfer coefficient from fire exposure may be taken as 35 W/m^{2}K per Eurocode 1.

7.3.2 Thermal Material Properties

Relevant thermal material properties of steel, concrete, and insulation should be considered, including density, thermal conductivity, and specific heat. Also, the emissivity of each material should be considered as a radiative surface condition in conjunction with the Stefan-Boltzmann constant of 5.67×10^{-8} W/(m^{2}K^4) and absolute zero of –273.15 °C.

7.3.2.1 Steel

The density of steel may be taken as a constant 490 lb/cu ft. Also, the emissivity may be conservatively taken as a constant 0.7 per Eurocode 3.

The temperature-dependent thermal conductivity of steel may follow the Eurocode 3 recommendations as follows.[xi]

$$k_s = \begin{cases} 54 - 3.33 \times 10^{-2} T & \text{for } 20\ \text{C} \le T \le 800\ \text{C} \\ 27.3 & \text{for } 800\ \text{C} < T \le 1200\ \text{C} \end{cases}$$

The temperature-dependent specific heat of steel may also follow the Eurocode 3 recommendations as follows.

$$c_s = \begin{cases} 425 + 7.73 \times 10^{-1}T - 1.69 \times 10^{-3}T^2 + 2.22 \times 10^{-6}T^3 & \text{for } 20\text{ C} \le T \le 600\text{ C} \\ 666 + 13002/(738 - T) & \text{for } 600\text{ C} < T \le 735\text{ C} \\ 545 + 17820/(T - 731) & \text{for } 735\text{ C} < T \le 900\text{ C} \\ 650 & \text{for } 900\text{ C} < T \le 1200\text{ C} \end{cases}$$

7.3.2.2 Concrete

The emissivity of concrete may be taken as a constant 0.7 per Eurocode 2.

The temperature-dependent density of normal-weight and lightweight concrete may follow the Eurocode 2 recommendations as follows (based on the density at ambient in kg/m^3).[xii]

$$\begin{cases} \rho_{c,20} & \text{for } 20\text{ C} \le T \le 115\text{ C} \\ \rho_{c,20}[1 - 0.02(T - 115)/85] & \text{for } 115\text{ C} < T \le 200\text{ C} \\ \rho_{c,20}[0.98 - 0.03(T - 200)/200] & \text{for } 200\text{ C} < T \le 400\text{ C} \\ \rho_{c,20}[0.95 - 0.07(T - 400)/800] & \text{for } 400\text{ C} < T \le 1200\text{ C} \end{cases}$$

The temperature-dependent thermal conductivity of normal-weight and lightweight concrete may follow the Eurocode 2 recommendations as follows.

$$k_c = 2 - 0.2451(T/100) + 0.0107(T/100)^2 \text{ (normal weight)}$$

$$k_c = \begin{cases} 1 - (T/1600) & \text{for } 20\text{ C} \le T \le 800\text{ C} \\ 0.5 & \text{for } 800\text{ C} < T \le 1200\text{ C} \end{cases} \text{ (lightweight)}$$

The temperature-dependent specific heat of normal-weight concrete may follow the Eurocode 2 recommendations as follows.

$$c_c = \begin{cases} 900 & \text{for } 20\text{ C} \le T \le 100\text{ C} \\ 900 + (T - 100) & \text{for } 100\text{ C} < T \le 200\text{ C} \\ 1000 + \dfrac{T - 200}{2} & \text{for } 200\text{ C} < T \le 400\text{ C} \\ 1100 & \text{for } 400\text{ C} < T \le 1200\text{ C} \end{cases}$$

The specific heat of lightweight concrete may be taken as a constant 840 J/kg-K per Eurocode 2 recommendations.

7.3.2.3 Insulation

For consistency, the thermal properties of protective insulation shall be taken as the generic temperature-independent values shown in Table 3. These constant values are referenced in the literature as reasonable design values.[xiii] Furthermore, these values may be referenced as part of a prospective performance specification for each building design. Additional commentary on this subject is contained in Appendix D.

Table 3. Insulation Thermal Properties.

Density [kg/m^3]	Thermal Conductivity [W/m*K]	Specific Heat [J/kg*K]	Emissivity
300	0.12	1,200	0.9

For cost estimation purposes, all protective insulation for Buildings 1 and 4 (low rise) will be assumed to be spray-applied fire resistance material (SFRM) due to its common use and application for interior ordinary environments. For Building 2 (height between 75 and 420 ft), all insulation will be assumed to be SFRM with a minimum 430 psf bond strength per International Building Code[xiv] (IBC) requirements. For Building 3 (height over 420 ft), all insulation will be assumed to be SFRM with a minimum 1,000 psf bond strength per IBC requirements. Cost estimates will also account for SFRM testing/inspections and ongoing maintenance, as well as the impact on the building's carbon footprint (e.g., accounting for potential future carbon taxes). Also, aesthetic considerations will be evaluated on a qualitative basis.

Independent of access to (or existence of) manufacturers' SFRM mechanical integrity data, standard fire testing qualification may be assumed to provide reasonable assurance that all the insulation will stay in place (i.e., maintain proper adhesion/cohesion) under fire exposure and structural deformations.

For floor construction, it is common for the concrete slab to provide sufficient thickness to justify the selection of a UL listing that precludes the application of SFRM to the underside of the steel deck. However, roof construction typically needs the application of SFRM to the steel deck if the roof is required to be fire resistance rated.

For floor construction, the thickness of insulation on beams and girders shall be assumed as in accordance with UL Design No. D925 (as summarized in Table 4), which is a relatively generalized SFRM specification (e.g., multiple qualified SFRM product types) that would not require a debatable *restrained versus unrestrained* judgment for this application.xv

Table 4. Insulation Thickness (Floor Beams and Girders).

Fire Resistance Rating	SFRM Thickness
1 h	1/2 in.
2 h	1-1/16 in.
3 h	1-9/16 in.

For roof construction, the thickness of insulation on beams, girders, and the underside of the roof deck shall be assumed as in accordance with UL Design No. D739 (as summarized in Table 5), which is also a relatively generalized SFRM specification that would not require *restrained versus. unrestrained* judgment for this application.

Table 5. Insulation Thickness (Roof Beams, Girders, and Deck).

Fire Resistance Rating	SFRM Thickness (Beams/Girders)	SFRM Thickness (Deck Underside)
1 h	3/4 in.	3/8 in.
1-1/2 h	7/8 in.	3/8 in.
2 h	1 in.	3/8 in.
3 h	1-9/16 in.	11/16 in.

The thickness of insulation on columns shall be in accordance with UL Design No. X701 (as summarized in Table 6), which is a relatively generalized SFRM specification.

Table 6. Insulation Thickness (Columns).

Fire Resistance Rating	SFRM Thickness
1 h	11/16 in.
2 h	1-1/8 in.
3 h	1-11/16 in.

UL Designs No. D925, No. D739, and No. X701 are shown in their entirety in Appendix E (within this document). The analyses shall consider the uniform nominally specified thickness values shown in Tables 4, 5, and 6, thereby neglecting any possible in situ variability of thickness or damage. Also, half flange nonuniform thickness schemes permitted by floor/roof assembly listings will not be considered.

8. Structural Fire Effects

Heating of structural systems from fire exposure causes thermal load effects that are not contemplated in conventional structural engineering design. These load effects shall be considered and evaluated in the analyses.

8.1 Fire Load Effect

ASCE 7-16, Section E.6.3 requires that the structural load combination for extraordinary events contained in ASCE 7-16, Section 2.5.2.2 be used for SFE analyses as follows.

$$1.2D + A + 0.5L + 0.2S$$

where

D = Dead Load,
A = Load effect resulting from extraordinary event,
L = Live Load, and
S = Snow Load.

The fire load effect term contained in the load combination above includes forces induced into a member or component (i.e., axial force, shear force, bending moment, and/or torque) due to restrained thermal expansion/contraction during fire exposure. The design dead, live, and snow loads should be derived from the applicable building code, or directly from the construction documents of the given building. Because the relation between the nominal fire load (i.e., temperature of the structure at a given time) and the resulting fire-load effect is usually nonlinear, the load factor can only be applied to the fire load effect itself and not the nominal fire load. Conveniently, the fire load effect factor specified in ASCE 7-16 is unity, so there is no procedural impact.

The potential for thermal expansion of members to induce additional forces (i.e., the load effect resulting from the extraordinary event) shall be accounted for. Also, nominal lateral stability of the structural system shall be confirmed by applying 0.2% of the gravity loading at each framing level.

For analysis of restrained thermal expansion, the thermal expansion coefficient of materials may be taken in accordance with AISC 360 recommendations as shown in Table 7. Use of the temperature-dependent thermal expansion coefficient of materials from Eurocode 2 and Eurocode 3 is also acceptable.

Table 7. Thermal Expansion Coefficient.

Material	Thermal Expansion Coefficient [/ °C]
Steel	0.0000140
Normal-Weight Concrete	0.0000180
Lightweight Concrete	0.0000079

8.2 Structural Capacity

For structural hand calculations (Section 9.1) and simulation of structural response (Section 9.2), the Poisson's ratio of a given material may be considered temperature-independent and equal to the nominal ambient value.

8.2.1 Structural Steel

For structural hand calculations (Section 9.1), AISC 360, Appendix 4 provides temperature-dependent nominal strength parameters for structural steel, which are compatible with conventional strength reduction factors contained in this standard.

For simulation of structural response (Section 9.2), Eurocode 3 equations may be used to represent the temperature-dependent uniaxial stress-strain curves of structural steel as shown in Figure 2.

The Eurocode 3 model implicitly accounts for thermal creep and is permitted for steel heating rates of 2 °C/min and faster. Slower heating rates are not anticipated for this application; however, Appendix F provides guidance for explicitly representing thermal creep of structural steel if necessary.

Strain Range	Stress σ	Tangent Modulus
$\varepsilon \le \varepsilon_{p,T}$	εE_T	E_T
$\varepsilon_{p,T} < \varepsilon < \varepsilon_{y,T}$	$F_{p,T} - c + (b/a)\sqrt{a^2 - (\varepsilon_{y,T} - \varepsilon)^2}$	$\dfrac{b(\varepsilon_{y,T} - \varepsilon)}{a\sqrt{a^2 - (\varepsilon_{y,T} - \varepsilon)^2}}$
$\varepsilon_{y,T} \le \varepsilon \le \varepsilon_{t,T}$	$F_{y,T}$	0
$\varepsilon_{t,T} < \varepsilon < \varepsilon_{u,T}$	$F_{y,T}\left[1 - \dfrac{(\varepsilon - \varepsilon_{t,T})}{(\varepsilon_{u,T} - \varepsilon_{t,T})}\right]$	--
$\varepsilon = \varepsilon_{u,T}$	0	--
Parameters	$\varepsilon_{p,T} = \dfrac{F_{p,T}}{E_T};\ \varepsilon_{y,T} = 0.02;\ \varepsilon_{t,T} = 0.15;\ \varepsilon_{u,T} = 0.20$	
Functions	$a^2 = (\varepsilon_{y,T} - \varepsilon_{p,T})\left(\varepsilon_{y,T} - \varepsilon_{p,T} + c/E_T\right)$ $b^2 = c(\varepsilon_{y,T} - \varepsilon_{p,T})E_T + c^2$ $c = \dfrac{(F_{y,T} - F_{p,T})^2}{(\varepsilon_{y,T} - \varepsilon_{p,T})E_T - 2(F_{y,T} - F_{p,T})}$	
Definitions of terms	E_T: elastic modulus at temperature T $F_{y,T}$: effective yield strength at temperature T $F_{p,T}$: proportional limit at temperature T $\varepsilon_{y,T}$: strain at yield at temperature T $\varepsilon_{p,T}$: strain at proportional limit at temperature T $\varepsilon_{t,T}$: limit strain for yield strength at temperature T $\varepsilon_{u,T}$: ultimate strain at temperature T	

Figure 2. Structural Steel Temperature-Dependent Stress–Strain Model.

8.2.2 Steel Bolts

For structural hand calculations (Section 9.1), AISC 360, Appendix 4 provides temperature-dependent nominal strength parameters for Group A and B high-strength steel bolts, which are compatible with conventional strength reduction factors contained in this standard.

Section 9.2.1 discusses the representation of steel bolts when conducting simulation of structural response.

8.2.3 Steel Reinforcement

For structural hand calculations (Section 9.1), temperature-dependent retention factors for composite floors in flexure in conjunction with equations in AISC 360, Chapter I account for steel

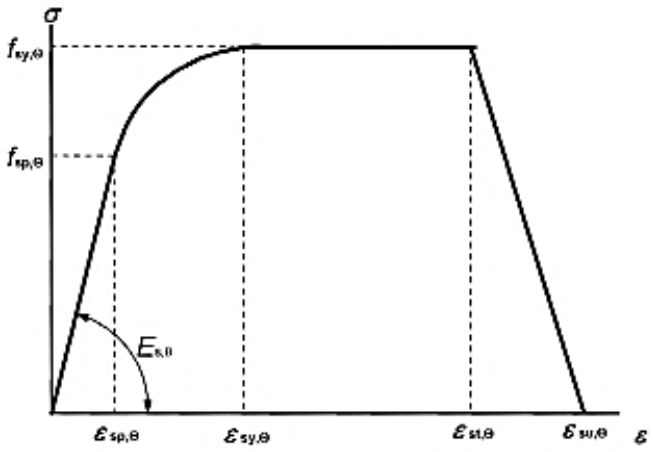

Range	Stress $\sigma(\theta)$	Tangent modulus
$\varepsilon_{sp,\theta}$	$\varepsilon E_{s,\theta}$	$E_{s,\theta}$
$\varepsilon_{sp,\theta} \le \varepsilon \le \varepsilon_{sy,\theta}$	$f_{sp,\theta} - c + (b/a)[a^2 - (\varepsilon_{sy,\theta} - \varepsilon)^2]^{0.5}$	$\frac{b(\varepsilon_{sy,\theta} - \varepsilon)}{a\left[a^2 - \left(\varepsilon - \varepsilon_{sy,\theta}\right)^2\right]^{0.5}}$
$\varepsilon_{sy,\theta} \le \varepsilon \le \varepsilon_{st,\theta}$	$f_{sy,\theta}$	0
$\varepsilon_{st,\theta} \le \varepsilon \le \varepsilon_{su,\theta}$	$f_{sy,\theta}[1-(\varepsilon - \varepsilon_{st,\theta})/(\varepsilon_{su,\theta} - \varepsilon_{st,\theta})]$	-
$\varepsilon = \varepsilon_{su,\theta}$	0,00	-
Parameter *)	$\varepsilon_{sp,\theta} = f_{sp,\theta} / E_{s,\theta}$ $\varepsilon_{sy,\theta} = 0{,}02$ $\varepsilon_{st,\theta} = 0{,}15$ $\varepsilon_{su,\theta} = 0{,}20$ Class A reinforcement: $\varepsilon_{st,\theta} = 0{,}05$ $\varepsilon_{su,\theta} = 0{,}10$	
Functions	$a^2 = (\varepsilon_{sy,\theta} - \varepsilon_{sp,\theta})(\varepsilon_{sy,\theta} - \varepsilon_{sp,\theta} + c/E_{s,\theta})$ $b^2 = c\,(\varepsilon_{sy,\theta} - \varepsilon_{sp,\theta})\,E_{s,\theta} + c^2$ $c = \frac{(f_{sy,\theta} - f_{sp,\theta})^2}{(\varepsilon_{sy,\theta} - \varepsilon_{sp,\theta})E_{s,\theta} - 2(f_{sy,\theta} - f_{sp,\theta})}$	

Figure 3. Steel Reinforcement Temperature-Dependent Stress−Strain Model (Equations).

reinforcement (Section 8.2.5). Otherwise, AISC 360, Appendix 4 temperature-dependent nominal strength parameters for structural steel may be used for analysis of steel reinforcement.

For simulation of structural response (Section 9.2), Eurocode 2 equations for Class N carbon steel reinforcement (Class N broadly covers Class A, B, C steel reinforcement types) should be used to represent the temperature-dependent uniaxial stress–strain behavior of slab reinforcement as shown in Figure 3.

Explicit representation of thermal creep of steel reinforcement is not required. Previous research has shown that thermal creep is not very critical in reinforcing bars, because the bars typically would not reach a temperature at which creep is significant and because constant long-term loading conditions are not a typical loading scenario for reinforcing bars.[xvi] However, Appendix F provides guidance for explicitly representing thermal creep of structural reinforcement if necessary.

Table 8. Steel Reinforcement Temperature-Dependent Stress-Strain Model (Parameter Values).

Steel Temperature θ[°C]	$f_{sy,\theta} / f_{yk}$ hot rolled	$f_{sy,\theta} / f_{yk}$ cold worked	$f_{sp,\theta} / f_{yk}$ hot rolled	$f_{sp,\theta} / f_{yk}$ cold worked	$E_{s,\theta} / E_s$ hot rolled	$E_{s,\theta} / E_s$ cold worked
1	2	3	4	5	6	7
20	1,00	1,00	1,00	1,00	1,00	1,00
100	1,00	1,00	1,00	0,96	1,00	1,00
200	1,00	1,00	0,81	0,92	0,90	0,87
300	1,00	1,00	0,61	0,81	0,80	0,72
400	1,00	0,94	0,42	0,63	0,70	0,56
500	0,78	0,67	0,36	0,44	0,60	0,40
600	0,47	0,40	0,18	0,26	0,31	0,24
700	0,23	0,12	0,07	0,08	0,13	0,08
800	0,11	0,11	0,05	0,06	0,09	0,06
900	0,06	0,08	0,04	0,05	0,07	0,05
1000	0,04	0,05	0,02	0,03	0,04	0,03
1100	0,02	0,03	0,01	0,02	0,02	0,02
1200	0,00	0,00	0,00	0,00	0,00	0,00

8.2.4 Steel Welds

For structural hand calculations (Section 9.1), the strength of complete-penetration welds may be taken as equal to the weaker part of the joining parts (i.e., failure is not governed by the weld). The strength of any partial-penetration welds and fillet welds should be determined in accordance with Eurocode 3, which include temperature-dependent strength retention factors.

For simulation of structural response (Section 9.2), welds may be evaluated outside of the model (Section 9.2.1). For fillet welds, the force/moment at the weld location may be compared to the temperature-dependent strength per Eurocode 3.

8.2.5 Composite Floors

For structural hand calculations (Section 9.1), AISC 360, Appendix 4 provides temperature-dependent retention factors for composite floors in flexure, which are used in conjunction with design equations in AISC 360, Chapter I.

For simulation of structural response (Section 9.2), the Eurocode 2 equation shown in Figure A4 may be used to represent the temperature-dependent multiaxial stress–strain curves of normal-strength concrete (normal weight or lightweight). The equation shown in Figure 4 assumes siliceous aggregate, and Eurocode 2 may be consulted for other aggregates.

$$\sigma(\theta) = \frac{3\varepsilon f_{c,\theta}}{\varepsilon_{c1,\theta}\left(2 + \left(\frac{\varepsilon}{\varepsilon_{c1,\theta}}\right)^3\right)}, \quad for\ \varepsilon \le \varepsilon_{c1,\theta}$$

Figure 4. Concrete Temperature-Dependent Compressive Stress–Strain Model (Equation).

Table 9. Concrete Temperature-Dependent Compressive Stress–Strain Model (Parameter Values).

Temperature, θ (°C)	$\frac{f_{c,\theta}}{f_{ck}}$	$\varepsilon_{c1,\theta}$	$\varepsilon_{cu1,\theta}$
20	1.00	0.0025	0.0200
100	1.00	0.004	0.0225
200	0.95	0.0055	0.0250
300	0.85	0.0070	0.0275
400	0.75	0.0100	0.0300
500	0.60	0.0150	0.0325
600	0.45	0.0250	0.0350
700	0.30	0.0250	0.0375
800	0.15	0.0250	0.0400
900	0.08	0.0250	0.0425
1000	0.04	0.0250	0.0450
1100	0.01	0.0250	0.0475
1200	0.00	–	–

The Eurocode 2 model shown above implicitly considers concrete transient creep, which is sufficient for analysis of composite floor systems. For concrete applications in which an implicit consideration of transient creep strain is deemed as unconservative (e.g., concrete columns), explicit consideration of transient creep should be employed as discussed in Appendix G.

Due to the containment provided by the metal deck, concrete spalling is not anticipated and may be neglected for the analyses. Also, perfect bond between the concrete and steel reinforcement (i.e., no bond-slip) may be assumed. Even over a length that prospectively includes several cracks in the tension zone of the slab, the average strain in both the reinforcement and the concrete may be approximated as equal.

For simulation of structural response, shear stud connectivity between the steel members and concrete slab may be considered ideally rigid if the floor was designed for 80% or greater composite action at ambient as justified in the literature.[xvi]i For less than 80% composite action, Appendix H provides guidance for representing the temperature-dependent force-slip behavior of individual shear studs if necessary.

9. Structural Analyses

Both structural hand calculations (Section 9.1) and simulation of structural response (see Section 9.2) shall account for restrained thermal expansion and temperature-dependent material properties.

9.1 DCR Calculations

If used, Demand-to-Capacity (DCR) hand calculations may be conducted in accordance with AISC 360, Appendix 4, which is assumed to provide enough conservatism for complex behaviors

to be neglected (e.g., nonuniform column heating in conjunction with lateral loading from connecting girder expansion). Accordingly, ambient strength reduction factors in conjunction with temperature-dependent material strength retention factors should be used to determine DCR ratios for all applicable limit states.

9.1.1 Simulation of Structural Response

Simulation of structural response may be conducted to demonstrate satisfactory structural performance when DCR calculations are not appropriate or not used and when they are inconclusive (i.e., DCR ≥ 1.0). In this case, load redistribution to underutilized members (e.g., bracing members) may be relied on.

Simulation of structural response should include geometric nonlinearity (large deflection theory) and nonlinear temperature-dependent material behavior, which would adequately capture any global buckling modes (without the need for sophisticated Riks analyses). Explicit or implicit finite element analysis techniques may be employed for simulations. If an explicit solver is used, artificial dynamic effects should be minimized to a negligible level by limiting the mechanical loading rate. If an implicit solver is used, parasitic strain energy should be minimized to a negligible level in the case that viscous damping is introduced to assist with model convergence.

Framing members may be represented by beam-type elements with a torsional/warping degree of freedom. Specified beam camber may be neglected. The concrete slab may be represented by shell-type elements with multiple integration points through its represented thickness. The associated steel reinforcement may be represented as part of these shell-elements using a layered rebar technique.

9.1.2 Connection Representation

Shear-tab and double-angle connections may be modeled as ideally pinned, and moment-type connections may be modeled as ideally fixed. Other connection types (e.g., truss gusset connections) may be represented at the discretion of each design team.

When connections are considered in an ideal sense as previously discussed, a separate evaluation of the connections should be conducted. The evaluation may be conducted using structural capacity equations and material strength retention factors from AISC 360 and/or Eurocode 3. Also, the forces acting on connections may be extracted from a model and/or conservatively derived from first principles. Where slab reinforcement is discontinuous, inadequately lapped at the connection region, or absent, or its capacity is exceeded, the contribution of the slab to moment resistance at a connection should be neglected during the heating phase. During the cooling phase, resistance to thermal contraction may be evaluated based on the ambient-temperature capacity of steel connections and slab reinforcement.

As an alternative to the approach as described previously, steel connections may be explicitly evaluated by representing each as an array of nonlinear springs in series/parallel. In this case, the connections would be qualified based on their ability to support the forces developed in a model. Specifically, springs acting in the plane of the connecting beam should have nonlinear behavior assigned, and a gap element should represent any contact between the beam lower flange and the connecting girder/column during the heating phase. The stiffness of springs in other degrees

of freedom should be considered as ideally rigid. Appendix I provides guidance for representing the nonlinear behavior of shear tab connections.

For either of the approaches described previously, the thermal creep of steel bolts need not be explicitly considered. Nonetheless, Appendix F provides commentary on the explicit representation of the thermal creep of steel bolts if necessary.

9.1.3 Concrete Slab Profile

Due to the metal decking geometry (flutes/troughs), the concrete thickness is variable in a periodic fashion. For simulation of structural response, only the top concrete (constant) thickness (i.e., above the deck flutes) should be considered. Otherwise, the variability of the slab thickness may be accounted for explicitly at the discretion of each design team. The thermal and structural performance of the metal decking itself may be neglected, because it would likely delaminate from the concrete in the early stages of a fire. However, the metal decking may be relied upon to provide lateral restraint to floor beams.

9.1.4 Concrete Slab Continuity

In general, reinforcement continuity across a given floor is beneficial to its performance under fire exposure. If reinforcement continuity is not provided over girder framing (and if the tension strength of the concrete is exceeded), the degree of freedom for bending moment should be released within the concrete slab shell elements, along the lines of girder framing. This can be accomplished by specifying discontinuous (coincident) nodes within the shell element mesh. When reinforcement continuity is provided, the strength of this reinforcement should be analyzed in conjunction with steel connections for their ability to resist the bending moment demand. If the reinforcement (and concrete) is expected to fail, the degree of freedom for bending moment should be released as described above.

9.1.5 Egress Pathway Levelness

Deflections of L/20 or less may be assumed to provide a satisfactory walking surface for mobile and mobility-impaired occupants to safely traverse during a fire event despite visible deformations. Floor deflections in excess of this limit should be considered as nontraversable by building occupants.[xvii]i

APPENDIX A: TRAVELING-TYPE FIRES

A traveling-type fire is characterized by the spread of fire from combustible to combustible across an open space that does not burn simultaneously throughout the entire compartment. CFD simulation may be used to study traveling-type fires explicitly. However, such an approach should specify discrete heat release rate (HRR) histories (individual “burners”) (e.g., Figure 5) and not rely on simulation of flame spread. Otherwise, pattern-type heated boundary studies may be used to evaluate traveling-type fires (see Appendix C).

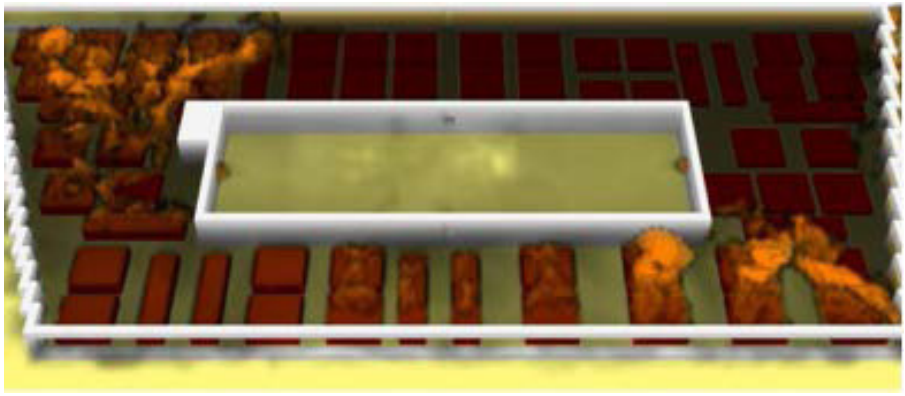

Figure 5. Explicit Simulation of a Traveling Fire.[xix]
Source: Courtesy of Simpson Gumpertz & Heger (2019).

APPENDIX B: ENCLOSURE FIRE CALCULATION METHODS

Eurocode 1, Annex A provides parametric equations to calculate the time–temperature history of an enclosure fire, which includes input for all of the parameters listed in Section 7.2.1. In general, the calculation method contained in Eurocode 1, Annex A provides a strong correlation with actual fire curves, but may not envelope all possible scenarios.[xx] Annex A equations in general apply to enclosure areas up to 500 m^2 (approximately 72 ft by 72 ft). However, applying these equations to areas exceeding 500 m^2 may be regarded as conservative.[xxi]

As an alternative to Eurocode 1, SFPE S.01 provides two methods to calculate the time-temperature history of an enclosure fire. First, the temperature may be assumed as a constant 1,200 °C for the calculated fire duration. Alternatively, the Refined Tanaka Method equations may be used to calculate the time–temperature history. In general, the SFPE S.01 calculation methods provide a relatively weak correlation to actual fires curves. Also, the equations result in very conservative time–temperature histories, which have an extremely low probability of exceedance.[xxii]

Both the Eurocode 1 and SFPE S.01 methods account for all of the parameters mentioned in Section 7.2.1 (either implicitly or explicitly).

APPENDIX C: FIRE EXPOSURE EXTENT

In all cases, the extent of heating should be reasonable and conservative. Currently, an industry consensus on the selection of structural design fire scenarios does not exist and remains within the purview and judgment of the designer. In Europe, it is common to consider fire involving only one compartment on one floor. However, there exists contemporary commentary that is more conservative on the matter within SFPE S.01, which should be adopted herein. SFPE S.01 recommends considering that portion of a floor that is bounded by exterior walls and/or by fire-rated boundaries. It is well known that standard furnace testing does not provide an adequate measure of in situ structural performance.[xxiii] However, standard furnace testing of fire barriers (vertical and horizontal) does provide a reasonable measure of in situ flame resistance performance. It may be

assumed that fire barrier walls are not adversely affected by structural deformations, which is not characterized by standard fire testing (furnace boundaries remain static).

The fire exposure extent does not necessarily dictate the scope of the analysis. For instance, a single structural bay may be analyzed under heating with varying patterns/timing of heating to adjacent boundaries (e.g., all surrounding bays are heated). This approach would potentially provide an understanding of structural response under a variety of possible structural design fire scenarios (including traveling-type fires). Such an approach is analogous to the consideration of varying live-load patterns on a continuous beam system.

APPENDIX D: SFRM THERMAL PROPERTIES

Applied fire protection products (e.g., SFRM) are qualified based on standard fire testing. Although these tests provide a fire resistance rating, they do not provide any further information (e.g., thermal property data) and have no direct quantitative relationship to the thermal performance of the given product.

The thermal properties of SFRM can vary significantly from one particular product type to another, and data for these properties are usually only characterized by the manufacturer, and if so, such data is almost always deemed as proprietary to the manufacturer. In the rare cases otherwise, a Non-Disclosure Agreement (NDA) generally is necessary to acquire the information, which is not suitable to this project. Particularly, the temperature-dependent specific heat of SFRM is difficult to quantify.[xxiv]

APPENDIX E: REFERENCED UL LISTINGS

This section intentionally left blank.

APPENDIX F: EXPLICIT REPRESENTATION OF STEEL THERMAL CREEP

In steel, creep is highly affected by the type of steel, applied stress, temperature, and duration of loading. There are two types of creep models: explicit and implicit. Section 8.2.1 describes an implicit representation, which consists of creep strains being incorporated within the stress–strain definition of the material. Implicit inclusion of creep into stress–strain curves results in a change in the stress-strain curve for structural steels at temperatures greater than 400 °C.

Explicit creep models are calculation intensive and consist of the inclusion of creep strains into the strain profile of the member section. Typically, this is implemented by calculating a strain profile at the instance when the internal forces in the cross section are at equilibrium with the applied forces.

The time-hardening power law, which modifies the nominal Eurocode 3 stress–strain response (Figure 2) as a function of uniaxial equivalent deviatoric stress, time and temperature may be used to explicitly represent the thermal creep of structural steel. Figure 6 specifies the power law

function and temperature-dependent inputs,[xxv] where t is time and q is the uniaxial equivalent deviatoric stress, and the parameters A, B, and C are the temperature-dependent constants.

$$\varepsilon_{cr} = At^B\sigma^C$$

$$A = \frac{1}{100}\begin{bmatrix} 10^{-(6.10+0.00573T)} & \text{for } T < 500^oC \\ 10^{-(13.25-0.00851T)} & \text{for } T > 500^oC \end{bmatrix}$$

$$B = -1.1 + 0.0035T$$

$$C = 2.1 + 0.0064T$$

Figure 6. Structural Steel Creep Model

The Harmathy creep model[xxvi] may be used to explicitly represent the thermal creep of steel reinforcement.

The thermal creep of steel bolts may be explicitly represented using a time-hardening power law model as follows.[xxvii]

$$\dot{\varepsilon}^{cr} = Aq^n t^m$$

$$A = \frac{C_1 e^{\frac{-C_2}{T}}}{C_3 + 1}$$

The temperature-dependent constants C_1, C_2, C_3, and C_4 are listed in Table 10. The Equivalent Stress Order, n, corresponds to C_2, and the Time Order, m, corresponds to $C_3 + 1$.

Table 10. Bolt Creep Constants.

	Constants for Creep Model at Temperature:			
Constant	**450 °C**	**500 °C**	**550 °C**	**Generic Value**
C_1	0.000199	3.27×10^{-7}	2.41×10^{-7}	1.8×10^{-8}
C_2	0.2224	0.8548	0.8214	0.923853
C_3	–0.9287	–0.7800	–0.5172	–0.36659
C_4	246.5064	2.3651	9.4610	–13.8052

APPENDIX G: EXPLICIT REPRESENTATION OF CONCRETE TRANSIENT CREEP

Transient creep strain is a specific, stress-temperature path dependent, irrecoverable strain that develops in concrete at elevated temperature. This strain develops under first-time heating of concrete under stress. It is a function of the stress-temperature history in the material and is arguably the result of transformations in the cementitious matrix during first heating under applied stress. Transient creep is essentially dependent of temperature, and not of time. It is also essentially independent of type of concrete, moisture, and thermal expansion of concrete. Analytically, it is defined as the difference in strain between concrete heated under load and concrete loaded at elevated temperature.

As a comparatively large strain component, it is widely agreed that transient creep strain needs to be included in any structural analysis of heated concrete. Two different types of material models exist to include transient creep strain, namely implicit models and explicit models. Implicit models, such as the Eurocode concrete model described in Section 8.2.5, have their stress–strain relationship calibrated on transient tests where transient creep strain developed, but they do not evaluate the contribution of transient creep in the total strain.

The Explicit Transient Creep (ETC) modelx[xviii] may be employed to explicitly account for transient creep strain. The model was designed as a new formulation of the Eurocode concrete model that contains an explicit term for transient creep. The ETC model separately evaluates the free thermal strain, the instantaneous stress-related strain, and the transient creep strain. The instantaneous stress–strain relationship considered in the ETC model agrees with experimental data obtained by steady-state tests. The transient creep–strain relationship depends linearly on the stress level and nonlinearly on the temperature and agrees with experimental data and other models found in the literature. Furthermore, as the Eurocode model was based on transient tests, the ETC model is calibrated to return the same total strain as the Eurocode model for a material subjected to a transient test situation (first-time heating under constant stress).

SAFIR is a nonlinear finite-element software for modeling structures in fire. The ETC model is implemented by default in SAFIR. General-purpose FEA programs typically do not have a predefined high-temperature material model with explicit transient creep; however, it is possible to program such a model in many cases. For instance, when using the finite-element software Abaqus, the Drucker-Prager (DP) plasticity model coupled with a creep user subroutine and the use of CSS8 8-noded brick shell elements within a visco analysis would allow for the explicit representation of concrete transient creep. This approach has been recently proposed in the literature.[xxix] If this approach is used, the following parameters should be input for the DP plasticity model:

- Angle of Friction: 37° (not less than 30° and also not less than dilation angle).
- Dilation Angle: 31° (not less than 30°).
- Flow Stress Ratio: 1 (values not equal to 1 are not allowed in the concrete model coupled with creep).
- Flow Potential Eccentricity: 0.1 (recommended by most literature).

Drucker Prager Hardening as shown in Table 11 for calcareous concrete (the first column has been normalized; it has to be multiplied by the compressive strength at ambient temperature).

Table 11. Drucker Prager Hardening Parameters for Calcareous Concrete.

Yield Stress/fc,k	Abs. Plastic Strain	Temperature °C
0.1327	0.0000000	20
0.2620	0.0000058	20
0.3846	0.0000192	20
0.4979	0.0000443	20
0.6000	0.0000833	20
0.6897	0.0001379	20
0.7664	0.0002086	20
0.8304	0.0002953	20
0.8824	0.0003971	20
0.9231	0.0005128	20
0.9538	0.0006411	20
0.9756	0.0007805	20
0.9898	0.0009294	20
0.9976	0.0010863	20
1.0000	0.0012500	20
0.0050	0.0199938	20
0.1327	0.0000000	100
0.2620	0.0000070	100
0.3846	0.0000231	100
0.4979	0.0000531	100
0.6000	0.0001000	100
0.6897	0.0001655	100
0.7664	0.0002504	100
0.8304	0.0003543	100
0.8824	0.0004765	100
0.9231	0.0006154	100
0.9538	0.0007694	100
0.9756	0.0009366	100
0.9898	0.0011152	100
0.9976	0.0013036	100
1.0000	0.0015000	100
0.0050	0.0214925	100
0.1288	0.0000000	200
0.2541	0.0000089	200
0.3731	0.0000292	200
0.4830	0.0000673	200

Table 11. Drucker Prager Hardening Parameters for Calcareous Concrete (con't).

Yield Stress/fc,k	Abs. Plastic Strain	Temperature °C
0.5820	0.0001267	200
0.6690	0.0002097	200
0.7434	0.0003171	200
0.8055	0.0004488	200
0.8559	0.0006035	200
0.8954	0.0007795	200
0.9251	0.0009745	200
0.9463	0.0011863	200
0.9602	0.0014126	200
0.9677	0.0016512	200
0.9700	0.0019000	200
0.0049	0.0232905	200
0.1208	0.0000000	300
0.2384	0.0000116	300
0.3500	0.0000385	300
0.4531	0.0000885	300
0.5460	0.0001667	300
0.6276	0.0002759	300
0.6974	0.0004173	300
0.7557	0.0005905	300
0.8029	0.0007941	300
0.8400	0.0010256	300
0.8679	0.0012823	300
0.8878	0.0015610	300
0.9008	0.0018587	300
0.9078	0.0021726	300
0.9100	0.0025000	300
0.0046	0.0254875	300
0.1128	0.0000000	400
0.2227	0.0000147	400
0.3269	0.0000485	400
0.4232	0.0001115	400
0.5100	0.0002100	400
0.5862	0.0003476	400
0.6515	0.0005258	400
0.7059	0.0007441	400

Yield Stress/fc,k	Abs. Plastic Strain	Temperature °C
0.7500	0.0010006	400
0.7846	0.0012923	400
0.8107	0.0016157	400
0.8293	0.0019668	400
0.8414	0.0023420	400
0.8480	0.0027375	400
0.8500	0.0031500	400
0.0043	0.0262843	400
0.0982	0.0000000	500
0.1939	0.0000203	500
0.2846	0.0000669	500
0.3685	0.0001540	500
0.4440	0.0002900	500
0.5103	0.0004800	500
0.5672	0.0007261	500
0.6145	0.0010275	500
0.6529	0.0013818	500
0.6831	0.0017846	500
0.7058	0.0022312	500
0.7220	0.0027161	500
0.7325	0.0032342	500
0.7382	0.0037803	500
0.7400	0.0043500	500
0.0037	0.0262783	500
0.0796	0.0000000	600
0.1572	0.0000296	600
0.2308	0.0000977	600
0.2988	0.0002248	600
0.3600	0.0004233	600
0.4138	0.0007007	600
0.4599	0.0010599	600
0.4983	0.0015000	600
0.5294	0.0020171	600
0.5538	0.0026051	600
0.5723	0.0032570	600
0.5854	0.0039649	600
0.5939	0.0047211	600

Yield Stress/fc,k	Abs. Plastic Strain	Temperature °C
0.5986	0.0055184	600
0.6000	0.0063500	600
0.0030	0.0226683	600
0.0571	0.0000000	700
0.1127	0.0000310	700
0.1654	0.0001023	700
0.2141	0.0002355	700
0.2580	0.0004433	700
0.2966	0.0007338	700
0.3296	0.0011100	700
0.3571	0.0015708	700
0.3794	0.0021124	700
0.3969	0.0027282	700
0.4101	0.0034108	700
0.4195	0.0041522	700
0.4256	0.0049442	700
0.4290	0.0057791	700
0.4300	0.0066500	700
0.0022	0.0257668	700
0.0358	0.0000000	800
0.0707	0.0000326	800
0.1038	0.0001077	800
0.1344	0.0002479	800
0.1620	0.0004667	800
0.1862	0.0007724	800
0.2069	0.0011684	800
0.2242	0.0016535	800
0.2382	0.0022235	800
0.2492	0.0028718	800
0.2575	0.0035904	800
0.2634	0.0043707	800
0.2673	0.0052044	800
0.2694	0.0060833	800
0.2700	0.0070000	800
0.0014	0.0289650	800
0.0199	0.0000000	900
0.0393	0.0000349	900

Yield Stress/fc,k	Abs. Plastic Strain	Temperature °C
0.0577	0.0001154	900
0.0747	0.0002656	900
0.0900	0.0005000	900
0.1034	0.0008276	900
0.1150	0.0012518	900
0.1246	0.0017716	900
0.1324	0.0023824	900
0.1385	0.0030769	900
0.1431	0.0038468	900
0.1463	0.0046829	900
0.1485	0.0055761	900
0.1496	0.0065178	900
0.1500	0.0075000	900
0.0008	0.0324625	900
0.0080	0.0000000	1,000
0.0157	0.0000349	1,000
0.0231	0.0001154	1,000
0.0299	0.0002656	1,000
0.0360	0.0005000	1,000
0.0414	0.0008276	1,000
0.0460	0.0012518	1,000
0.0498	0.0017716	1,000
0.0529	0.0023824	1,000
0.0554	0.0030769	1,000
0.0572	0.0038468	1,000
0.0585	0.0046829	1,000
0.0594	0.0055761	1,000
0.0599	0.0065178	1,000
0.0600	0.0075000	1,000
0.0003	0.0349625	1,000
0.0027	0.0000000	1,100
0.0052	0.0000349	1,100
0.0052	0.0000349	1,100
0.0077	0.0001154	1,100
0.0100	0.0002656	1,100
0.0120	0.0005000	1,100
0.0138	0.0008276	1,100

Yield Stress/fc,k	Abs. Plastic Strain	Temperature °C
0.0153	0.0012518	1,100
0.0166	0.0017716	1,100
0.0176	0.0023824	1,100
0.0185	0.0030769	1,100
0.0191	0.0038468	1,100
0.0195	0.0046829	1,100
0.0198	0.0055761	1,100
0.0200	0.0065178	1,100
0.0200	0.0075000	1,100
0.0001	0.0374625	1,100
0.0001	0.0000000	1,200
0.0001	1.0000000	1,200

In conjunction with the DP plasticity model, the user creep subroutine may be programed as shown in Figure 7.

APPENDIX H: SHEAR STUD REPRESENTATION

When modeling shear studs explicitly, the shear force–slip characteristics of each stud should be characterized. The force–slip relationship is generally obtained using push-out tests. A set of push-out tests at ambient and high temperatures has been conducted to determine the force-slip relationship for shear stud behavior.[xxx] Based on data derived from this testing, the temperature-dependent force-slip behavior of individual shear studs may be represented as shown in Figure 8. The stiffness of shear studs in all other directions may be assumed as ideally rigid. Also, the temperature of shear studs may be assumed to be 80% of the steel-beam top-flange temperature.[xxxi]

APPENDIX I: CONNECTION COMPONENT METHOD

The component method idealizes a structural steel connection into an assembly of nonlinear springs (and a gap-type element) that each represent a specific aspect of the connection as shown in Figure 9 for a shear tab connection. This method provides an accurate characterization of a connection with less computational cost than a comparable solid-type-element representation with explicit contact definitions. Using this method, the force–rotation relationship of a given connection may be represented up to ultimate failure.

The primary components of a shear tab connection include plate and beam web bearing, bolt shear, and friction of the plate surfaces. The nonlinear stiffness of each connection aspect are derived based on the works of Sarraj (2007),[xxxiii] Yu et al. (2009a[xxxiv] and 2009b[xxxv]), Agarwal (2011),[xxxvi] and Taib (2012).[xxxvii] As an example, Figure 10 provides temperature-dependent nonlinear spring definitions based on a specific set of input dimensions/properties given in Table 12. Details of this connection can be found in Sarraj (2007), with further discussions in Agarwal (2011).

```
      SUBROUTINE CREEP(DECRA,DESWA,STATEV,SERD,EC,ESW,P,QTILD,
     1 TEMP,DTEMP,PREDEF,DPRED,TIME,DTIME,CMNAME,LEXIMP,LEND,
     2 COORDS,NSTATV,NOEL,NPT,LAYER,KSPT,KSTEP,KINC)

      INCLUDE 'ABA_PARAM.INC'
      CHARACTER*80 CMNAME
      REAL fck,PHI, TT, PHI1, PHI0
      DIMENSION DECRA(5),DESWA(5),STATEV(*),PREDEF(*),DPRED(*),
     1 TIME(2),COORDS(*),EC(2),ESW(2),TT(13),PHI(13)


c TT is temperature [°F], keep unit consistent with analysis
      TT=[68,212,392,572,752,932,1112,1292,1472,1652,1832,2012,2192]

c PHI is the value of transient creep function at different temperatures;
c calcareous concrete (see Table 1)
      PHI=[0.0000,0.0010,0.00172,0.0022,0.00431,0.00856,0.02056,0.02713,
     1 0.04074,0.06667,0.16667,0.5,0.5]
c siliceous concrete
c     PHI=[0.0000,0.0010,0.00175,0.00235,0.00489,0.01056,0.02741,0.03889,
c     1 0.07333,0.125,0.25,1,1]

c concrete compressive strength at room temperature [ksi]
      fck=4.35114;

      DECRA(1)=0;
      DECRA(5)=0;

      DO  I = 1, 12, 1
      IF ((TEMP.GE.TT(I)).AND. (TEMP.LE.TT(I+1))) THEN
      EXIT;
      ENDIF
      ENDDO
      PHI1=PHI(I)+(PHI(I+1)-PHI(I))/(TT(I+1)-TT(I))*(TEMP-TT(I));

      DO  I = 1, 12, 1
      IF (((TEMP-DTEMP).GE.TT(I)).AND. ((TEMP-DTEMP).LE.TT(I+1))) THEN
      EXIT;
      ENDIF
      ENDDO
      PHI0=PHI(I)+(PHI(I+1)-PHI(I))/(TT(I+1)-TT(I))*((TEMP-DTEMP)-TT(I));



      IF ((QTILD .GE. 0) .AND. (DTEMP .GE. 0)) THEN
            DECRA(1)=(PHI1-PHI0)*QTILD/fck;
            IF(LFXTMP.EQ.1) THEN
            DECRA(5)=(PHI1-PHI0)/fck;
            ENDIF
      ELSE
              DECRA(1)=0;
              DECRA(5)=0;
      ENDIF
      RETURN
      END
```

Figure 7. User Creep Subroutine.

Source: Courtesy of Simpson Gumpertz & Heger (2019)

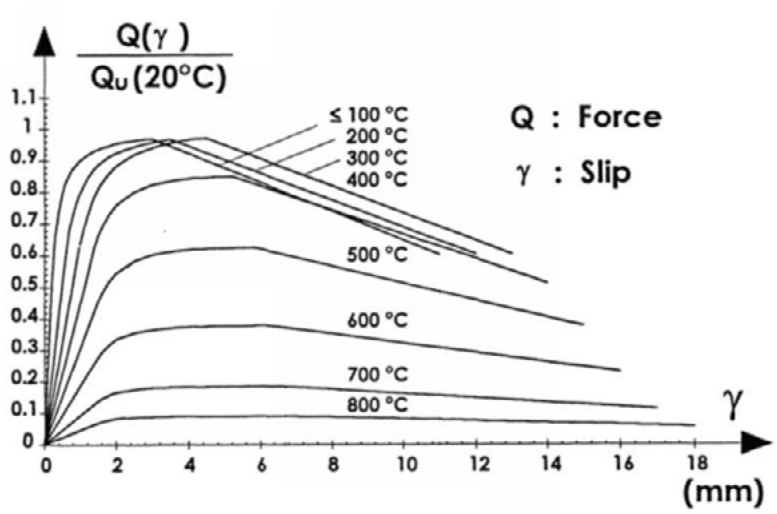

Figure 8. Shear Stud Force–Slip Relationship.[xxxii]

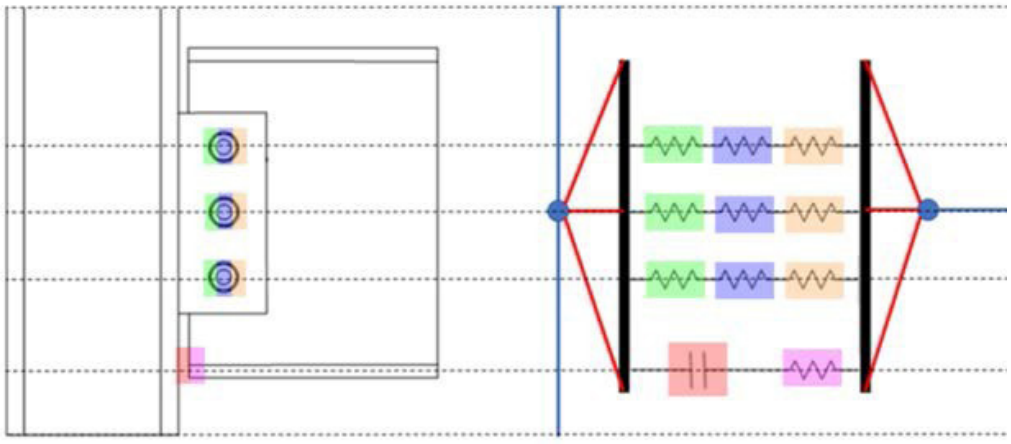

Figure 9. Component Method
(Illustration of Spring Assembly for Shear Tab Connection).
Source: Courtesy of Simpson Gumpertz & Heger (2019).

Table 12. Shear Tab Sample Input Values.

Input	Description	Unit	Plate	Beam	Bolt
E	Modulus of elasticity	N/mm^2	200,000	200,000	200,000
F_y	Yield strength	N/mm^2	248	248	635
F_u	Tensile strength	N/mm^2	400	400	827
v	Poisson ratio	–	0.3	0.3	–
e_2	End distance	mm	38.1	34.65	–
t	Thickness	mm	9.525	7.62	–
d	Bolt diameter	mm	–	–	19
dd	Bolt hole clearance	mm	–	–	1.6

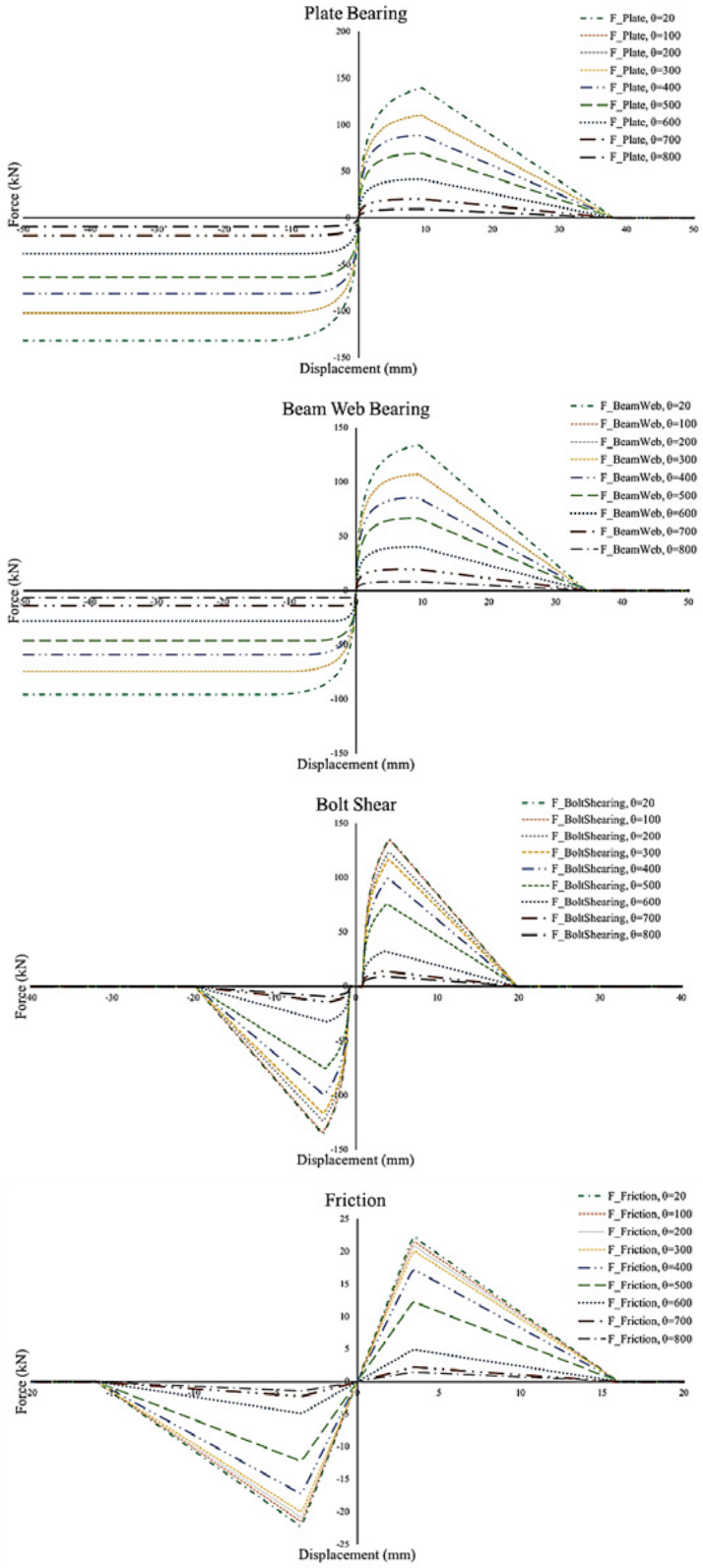

Figure 10. Nonlinear Spring Definitions (Sample Shear Tab Connection).

ENDNOTES

[i] ASCE. 2017. *Minimum design loads and associated criteria for buildings and other structures*, ASCE 7-16. Reston, VA: ASCE.

[ii] LaMalva, K. J. 2018. *Structural fire engineering*, MOP 138. Reston, VA: ASCE.

[iii] AISC *Specification for structural steel buildings* AISC 360. 2016.

[iv] Eurocode 1 − Basis of design and actions on structures, Part 1-2: Actions on structures – Actions on structures exposed to fire, *EN 1991-1-2*, 2001.

[v] Eurocode 2 − Design of concrete structures – Part 1-2: General rules – Structural fire design, *EN 1992-1-2*, 2004.

[vi] Eurocode 3 − Design of Steel Structures. Part 1-2: General rules. Structural fire design. *EN 1993-1-2*, 2006.

[vii] *Standard on calculating fire exposure to structures,* SFPE S.01, 2010.

[viii] *Standard on calculation methods to predict the thermal performance of structural and fire resistive assemblies*, SFPE S.02, 2015.

[ix] Proulx, G. 2002. "The movement of people: The evacuation timing." *SFPE handbook of fire protection engineering*, 3rd Ed. Gaithersburg, MD: SFPE.

[x] Ahrens, M. 2017. *U.S. experience with sprinklers*. Quincy, MA: NFPA.

[xi] Eurocode 3 − Design of steel structures, Part 1-2: Structural fire design, *EN 1993-1-2*, 2010.

[xii] Eurocode 2 − Design of concrete structures, Part 1-2: Structural fire design, *EN 1992-1-2*, 2005.

[xiii] Buchanan, A. and A. Abu, *Structural design for fire safety*, 2nd Ed. Hoboken, NJ: Wiley.

[xiv] International Code Council. 2018. *International building code*.

[xv] LaMalva, K. J., T. McAllister, and L. Bisby. 2018. "Restrained vs. unrestrained: Within the context of new industry guidance." *Structure* magazine, September.

[xvi] A. Y. Elghazouli, K. A. Cashell, and B. A. Izzuddin. 2009. "Experimental evaluation of the mechanical properties of steel reinforcement at elevated temperature." *Fire Safety J.* 44 (6): 909–919.

[xvii] Selden, K., "Structural behavior and design of composite beams subjected to fire." Ph.D. diss., Purdue University, West Lafayette, IN, 2014.

[xviii] LaMalva, K. J. 2018. *Structural fire engineering*, MOP 138. Reston, VA: ASCE.

[xix] LaMalva, K. J. 2018. *Structural fire engineering*, MOP 138. Reston, VA: ASCE.

[xx] Hughes Associates. 2006. *Summary of comparisons of test methods*. Bethesda, MD. SFPE.

[xxi] Kirby, B., et al. 1999. "Natural fires in large scale compartments," *Int. J. Eng. Perf.* 1 (2): 43–58.

[xxii] Hughes Associates. 2006. *Summary of comparisons of test methods*. Bethesda, MD. SFPE.

[xxiii] Law, M., "Designing fire safety for steel – Recent work." ASCE Spring Convention, Reston, VA, 1981.

[xxiv] Carino, N., et al. 2005. "Passive fire protection, federal building and fire safety investigation of the World Trade Center disaster." *NIST NCSTAR 1-6A*. Gaithersburg, MD: NIST.

[xxv] Fields, B. A., and R. J. Fields. 1988. “Elevated temperature deformation of structural steel.” *NISTIR 88-3899*. Gaithersburg, MD: NIST, 124.

[xxvi] Harmathy, T. 1967. “A comprehensive creep model.” *J. Basic Eng.* 89 (3): 496–502.

[xxvii] Norton, F. H. 1929. *Creep of steel at high temperatures.* New York: McGraw-Hill.

[xxviii] Gernay, T., and J. M. Franssen. 2012. “A formulation of the Eurocode 2 concrete model at elevated temperature that includes an explicit term for transient creep.” *Fire Safety J.* 51 (1–9).

[xxix] Alogla, S., and V. K. R. Kodur. 2018. “Quantifying transient creep effects on fire response of reinforced concrete columns.” *Eng. Struct.* 174, 885–895.

[xxx] Zhao, B., and J. Kruppa. 1997. “Fire resistance of composite slabs with profiled steel sheet and of composite steel concrete beams, Part 2: Composite beams.” *Final report EUR 16822*, ISSN 1018-5593.

[xxxi] Dara, S. 2015. “Behavior of the shear studs in composite beams at elevated temperatures,” Ph.D. diss., University of Texas, Austin, TX.

[xxxii] Zhao, B., and J. Kruppa. 1997. “Fire resistance of composite slabs with profiled steel sheet and of composite steel concrete beams, Part 2: Composite beams.” *Final report EUR 16822*, ISSN 1018-5593.

[xxxiii] Sarraj, M. “The behaviour of steel fin-plate connections in fire,” Ph.D. thesis, University of Sheffield, Sheffield, South Yorkshire, UK, 2007.

[xxxiv] Yu, H., I. W. Burgess, J. B. Davison, and R. J. Plank. 2009a. “Experimental investigation of the behaviour of fin plate connections in fire.” *J. Construct. Steel Res*. 65, 723–736.

[xxxv] Yu, H., I. W. Burgess, J. B. Davison, and R. J. Plank. 2009b. “Tying capacity of web cleat connections in fire, Part 2: Development of component-based model.” *Eng. Struct.* 31, 697-708.

[xxxvi] Agarwal, A. “Stability behavior of steel building structures in fire condition,” Ph.D. diss., Purdue University, West Lafayette, IN, 2011.

[xxxvii] Taib, M. “The performance of steel framed structures with fin-plate connections in fire,” Ph.D. diss., University of Sheffield, Sheffield, South Yorkshire, UK, 2012.

PART II
Team Reports for Buildings 1−4

Chapter 7. Building 1: Detailed Analysis Description, Simpson Gumpertz & Heger (SGH)

Participants

The Structural Engineering Institute of ASCE acknowledges the work of the participants in this project.

Industry Champions

The Simpson Gumpertz & Heger (SGH) design team comprised the following contributors:

Kevin LaMalva, P.E., *Industry Champion, Principal Investigator*

Paul Cabasag, P.E.

Don Dusenberry, P.E.

Omer Erbay, Ph.D., P.E.

Qianru Guo, Ph.D., P.E.

Sean Hsieh

Keng-Wit Lim, Ph.D., P.E.

Adel Mashayekh, Ph.D.

Abhishek Master

Keith Palmer, Ph.D., P.E., S.E.

Chris Scangas

Georgios Tsampras, Ph.D.

Matt Yin, P.E.

BUILDING 1

Building 1 is a previously completed structural design project from SGH, which was built in the early 2000s and is located in the Boston metro area. The building has six stories, approximately 23,000 sq. ft per floor, and is used primarily for open office space on all levels (occupancy Group B). Given a reduction granted for buildings over 70 ft tall, the construction type of the building according to the applicable building code prescriptively requires all steel framing (including roof construction) to have 1 h fire resistance. Traditional spray-applied insulation (fireproofing) is nominally used to provide the required level of fire resistance. The building has a braced-frame, lateral-force-resisting system that is primarily controlled by design wind loads. Figure 7-1 is a typical floor framing plan for the building.

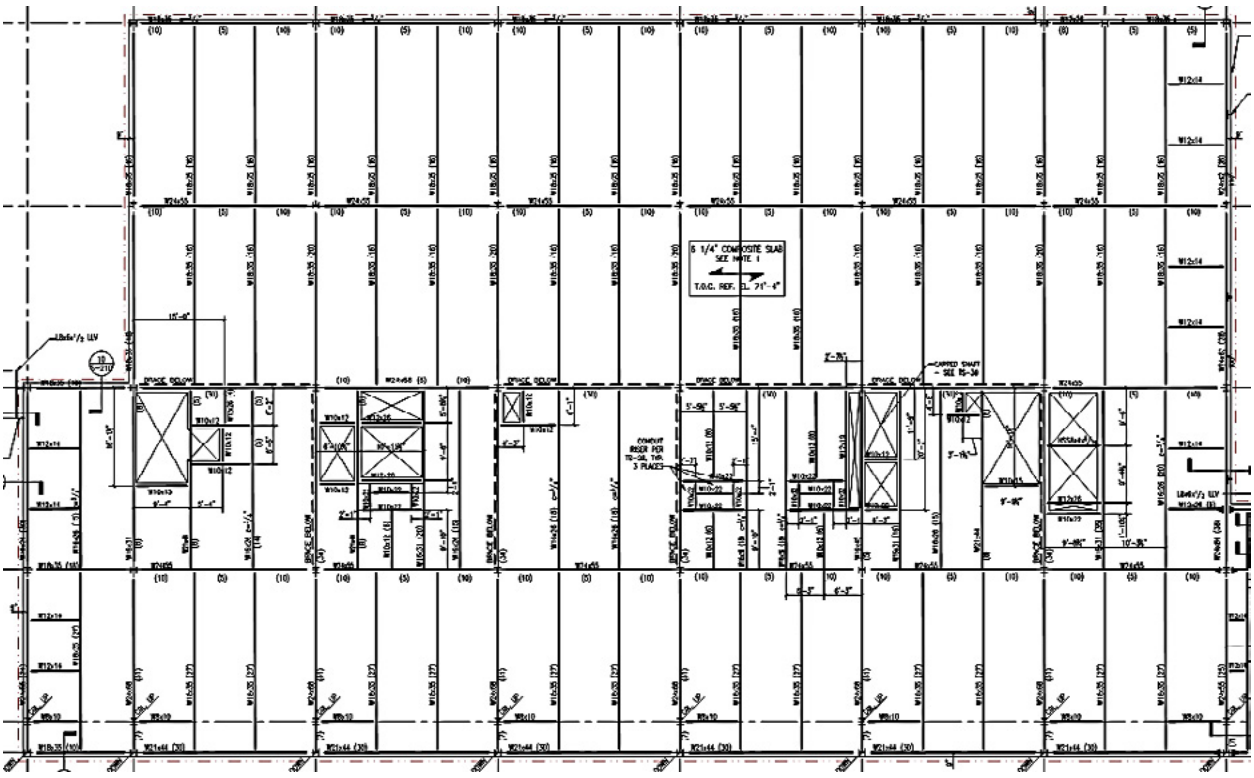

Figure 7-1. Typical floor framing plan.

Source: Courtesy of Simpson Gumpertz & Heger (2019).

The design team consulted with the Structural Engineer of Record for this building to properly interpret the details and drawings. Characteristic 30 ft × 30 ft structural floor bays of the building are constituted as follows:

- 3-1/4 in. lightweight concrete slab (4,000 psi compressive strength) on 3 in. metal deck (Figure 7-2)
    - o ASTM A497 6x6-D2.9x2.9 welded wire fabric (Class B) 3/4 in. from top of slab,
    - o #4 rebar (5 ft length) spaced 12 in. on center placed over all girders, and
    - o No deck rib reinforcement.
- W16x26 infill beams and boundary beams (beam size varies),
- W24x55 girders (girder size varies),
- Beam–girder connections that are welded-bolted shear tabs, and
- Beam/girder–column connections that are bolted-bolted double angle connections (Figures 7-3 and 7-4).

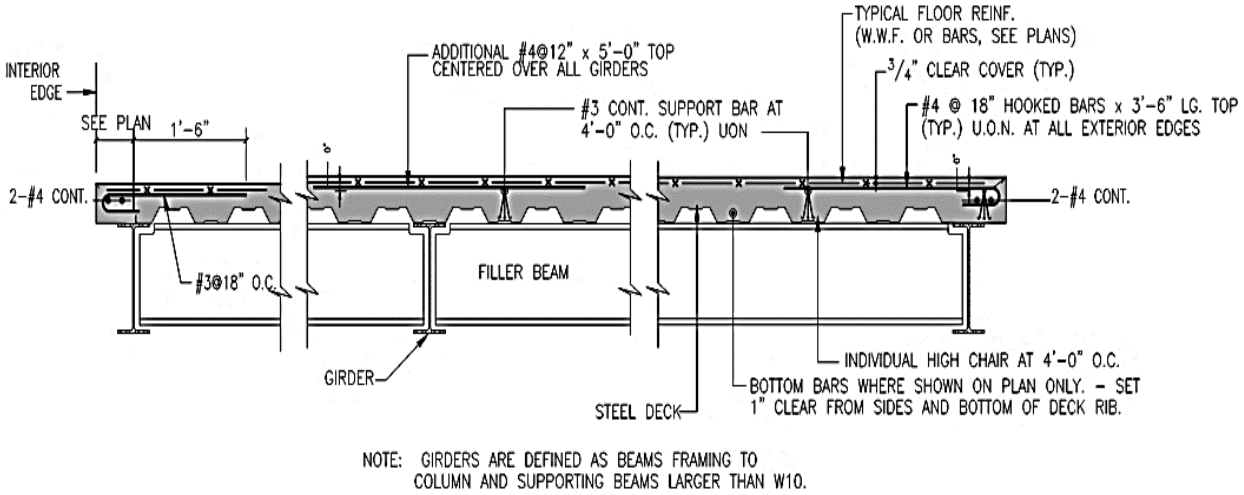

Figure 7-2. Typical floor slab-deck configuration.

Source: Courtesy of Simpson Gumpertz & Heger (2019).

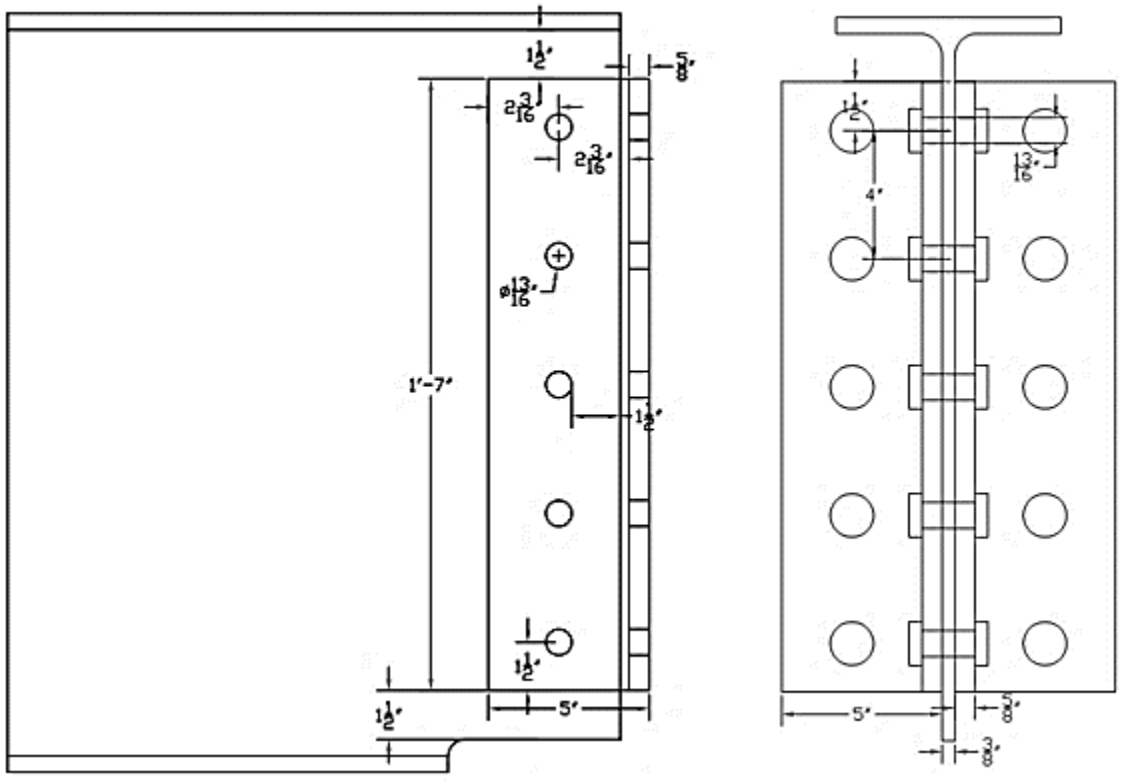

Figure 7-3. Typical girder–column connection.

Source: Courtesy of Simpson Gumpertz & Heger (2019).

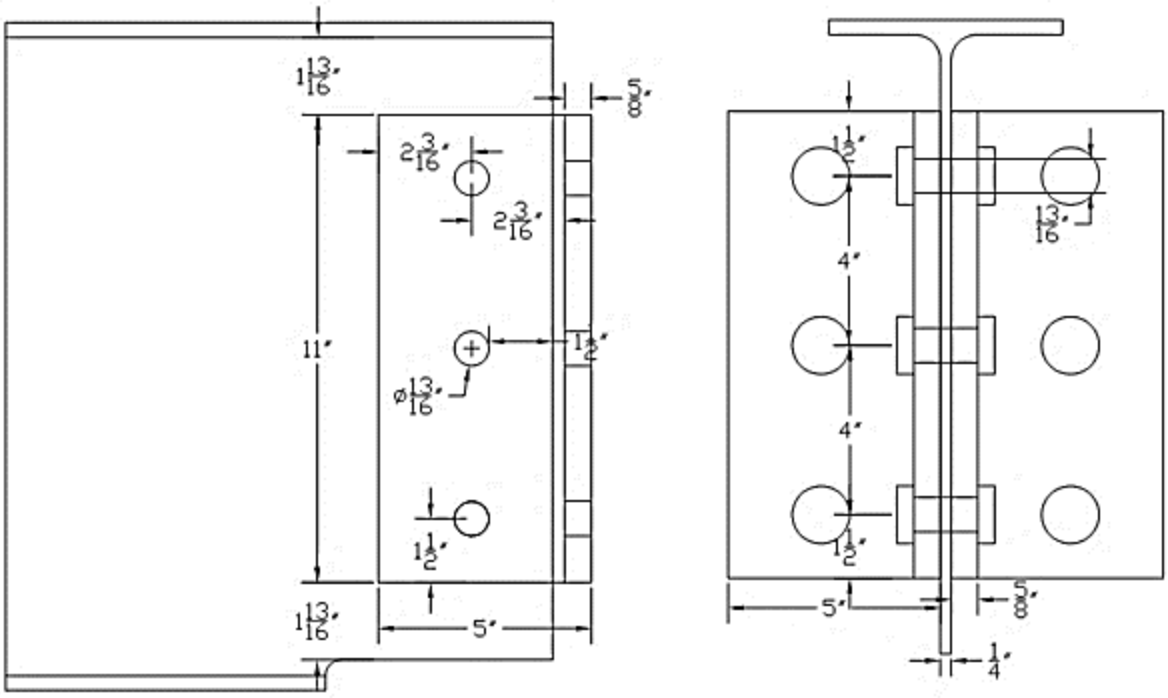

Figure 7-4. Typical boundary beam–column connection.
Source: Courtesy of Simpson Gumpertz & Heger (2019).

The characteristic unfactored design floor and roof loading are as follows:

- Floor Dead loads:
  - Slab: 51 psf,
  - Superimposed: 8 psf, and
  - Beams/girders: self-weight.
- Floor Live load: 100 psf
- Roof Dead loads:
  - Deck: 3 psf,
  - Superimposed: 16 psf, and
  - Beams/girders: self-weight.
- Roof Snow load: 30 psf

7.1 DESIGN STRATEGY

The overall design strategy for each design scenario (as described in Section 1.4) is as follows:

- Design 0 (prescriptive):
  - Code-prescribed insulation as summarized in Design Brief Tables 7-4 to 7-6 (no analysis required).
- Design 1 (performance-based; minimum performance; no structural modifications):
  - Start with code-prescribed insulation and increase/decrease as necessary.
- Design 2 (performance-based; optimum performance; no structural modifications):
  - Start with code-prescribed insulation and increase/decrease as necessary.
- Design 3 (performance-based; optimum performance; structural modifications allowed):
  - Facilitate the transition of floors from one-way bending-dominant behavior to two-way compressive tensile membrane behavior to achieve reliable/robust stability at high temperatures.
  - Target insulation to the primary beam members, beam–column connections, and columns to properly support the floors under high deflections (secondary beams are left unprotected).
  - Start with the nominally specified slab mesh and enhance as necessary.
  - Start with the nominally specified beam–column connections and enhance as necessary.

7.2 REQUIRED SAFE EGRESS TIME

As it pertains to Design 1 (as discussed in Section 7.1), the total evacuation time of the building was estimated to be 25 min, which includes a 10 min allowance for occupant premovement (i.e., alarm recognition, decision to act, and gathering/assisting others) plus a 15 min movement time for all occupants to reach a public way outside the building. The premovement time allowance was determined based on examination of human behavior data (e.g., interviews with persons subjected to a fire evacuation) contained in the *SFPE Handbook* (SFPE 2016). Also, the people movement simulation software (Pathfinder) (Thunderhead Engineering Consultants 2016) was used to determine the movement time, including the important effects of occupant queuing as shown in Figures 7-5 and 7-6.

Figure 7-5. People movement simulation (start of evacuation).
Source: Courtesy of Simpson Gumpertz & Heger (2019)
and Thunderhead Pathfinder Software ©2019.

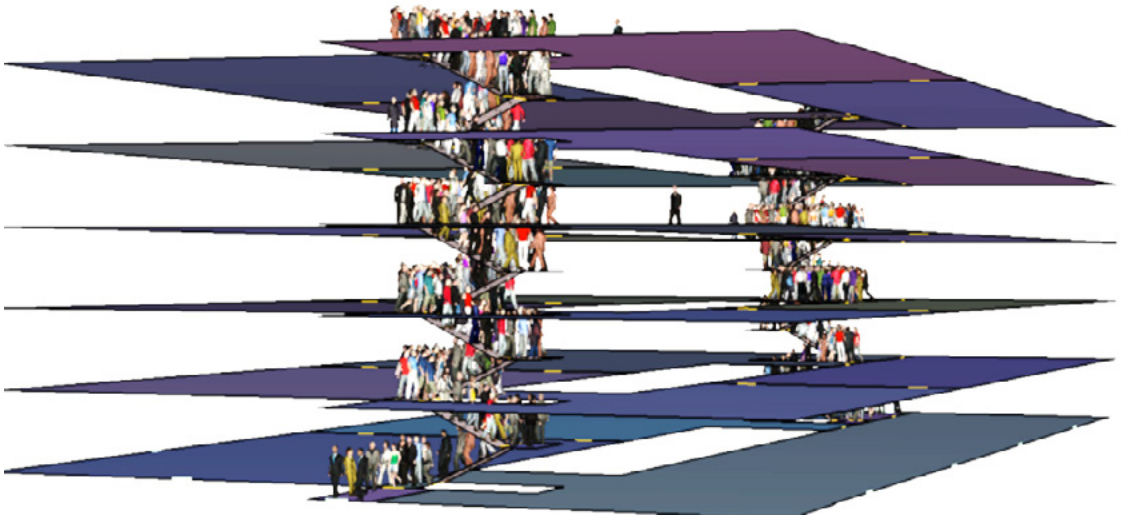

Figure 7-6. People movement simulation (queuing at exit stairways).
Source: Courtesy of Simpson Gumpertz & Heger (2019),
and Thunderhead Pathfinder Software ©2019.

7.3 DESIGN FUEL LOAD

The design fuel load was calculated to be 374 MJ/m^2 per Eurocode 1 (CEN 2001). This magnitude of fuel load was calculated, neglecting all permitted risk reduction factors, except those pertaining to the presence of a fire sprinkler system in the building, which is reasonably considered. The following fuel loads in excess of the design fuel load were also considered to demonstrate a reliable/robust solution:

- *Above-design* fuel load: 613 MJ/m^2
    - Neglects the risk reduction factor for a fire sprinkler system.

- *Ultra-design* fuel load: 912 MJ/m^2

    - Neglects the risk reduction factor for a fire sprinkler system and considers the 98% fractile nominal fuel load (Khorasani et al. 2014).

    - Almost equal to the fuel load used in the Cardington fire tests that produced the most intense exposure of the test series (Kirby 1998).

- *3X-design* fuel load: 1,122 MJ/m^2

    - Three times the design fuel load, representing a nearly inconceivable condition for this building occupancy type.

7.4 STRUCTURAL DESIGN FIRES

As discussed in Section 3.1, enclosure fires are primarily governed by fuel load, compartment geometry, and ventilation openings. In general, lower ventilation extends the duration of the fire, and higher fuel load increases the maximum temperatures reached in a compartment (which a given level of ventilation can support). The final arrangement of interior walls may not be known during PBSFD and/or may change over time. Also, individual windows may or may not break during fire exposure. To account for these uncertainties and randomness and to demonstrate a reliable/robust solution, a series of structural design fires with multiple conceivable compartment geometries and ventilation levels were considered. Ventilation may be conveyed to the outside environment via window breakage or to remote areas of a given floor plan that are not simultaneously on fire. In total six structural design fire scenarios were considered, which have high, moderate, and low levels of ventilation for this building. For instance, Figure 7-7 illustrates the two low ventilation cases that have no exterior glass breakage during the fire exposure. In these illustrations, the extent of fire exposure is highlighted, along with the extent of ventilation openings.

As discussed in Section 3.1, localized fires may occur in large spaces in which the compartment has little to no influence on the fire severity. To determine whether localized structural design fire scenarios (in addition to the enclosure-type structural design fire scenarios described previously) need to be considered, the required fire heat release rates to cause flashover within the characteristic building spaces were calculated and compared to the anticipated fire heat release rates. These calculations demonstrate that only enclosure-type fire exposure scenarios need to be considered.

Considering the six structural design fire scenarios and the varying levels of fuel load (discussed in Section 7.3), 11 structural design fire time–temperature histories were derived using Eurocode parametric equations as discussed in Section 3.1, and are illustrated in Figure 7-8. The wall lining factor used for these calculations represents gypsum walls and lightweight concrete floors/ceilings. Other fire exposure calculation methods could be similarly employed, such as zone modeling (as discussed in EC1, Annex D.1 and D.2) or field modeling (as employed selectively herein and discussed subsequently).

Considering the *above-design* fuel load with low ventilation case, the impact of adding passively activated combination heat vents/skylights (each independently activated via a fusible link when a temperature of 74 °C (165 °F) is reached) at the roof levels (including the small lower roof portion of the building at Level 3) was analyzed using the computational fluid dynamics (CFD) software

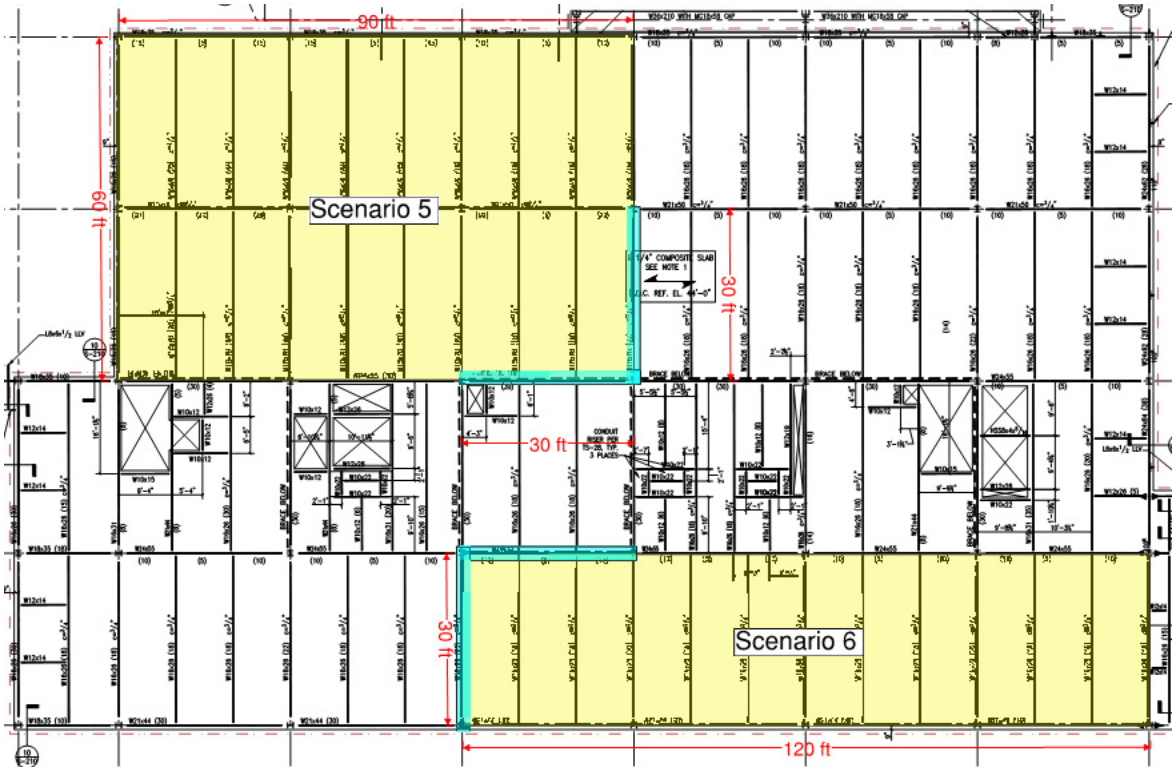

Figure 7-7. Structural design fire scenarios (low ventilation).

Source: Courtesy of Simpson Gumpertz & Heger (2019).

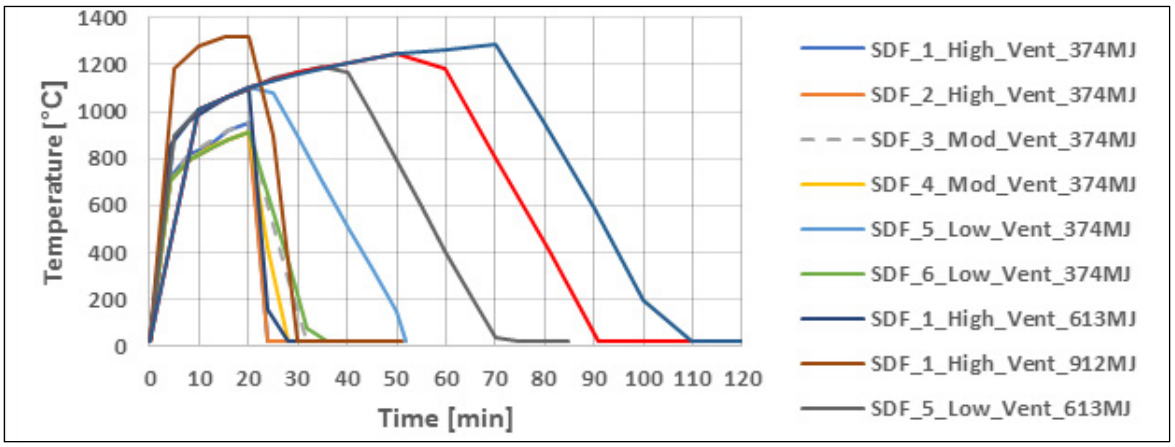

Figure 7-8. Structural design fire temperature histories.

Source: Courtesy of Simpson Gumpertz & Heger (2019).

Fire Dynamics Simulator (FDS) (NIST 2000). For both the nominal and vented scenarios, a heat release rate per unit floor area of 250 kW/m^2 was considered according to Eurocode 1 for office occupancies. It is observed that the maximum gas temperatures for the simulated nominal scenario (i.e., no roof vents) are approximately 200 °C lower than that predicted using the Eurocode 1 parametric equations, which demonstrates the conservatism of the Eurocode 1 approach, as relied on extensively herein. As shown in Figures 7-9 and 7-10, adding roof vents reduces the maximum upper gas temperature by approximately 55% to 450 °C.

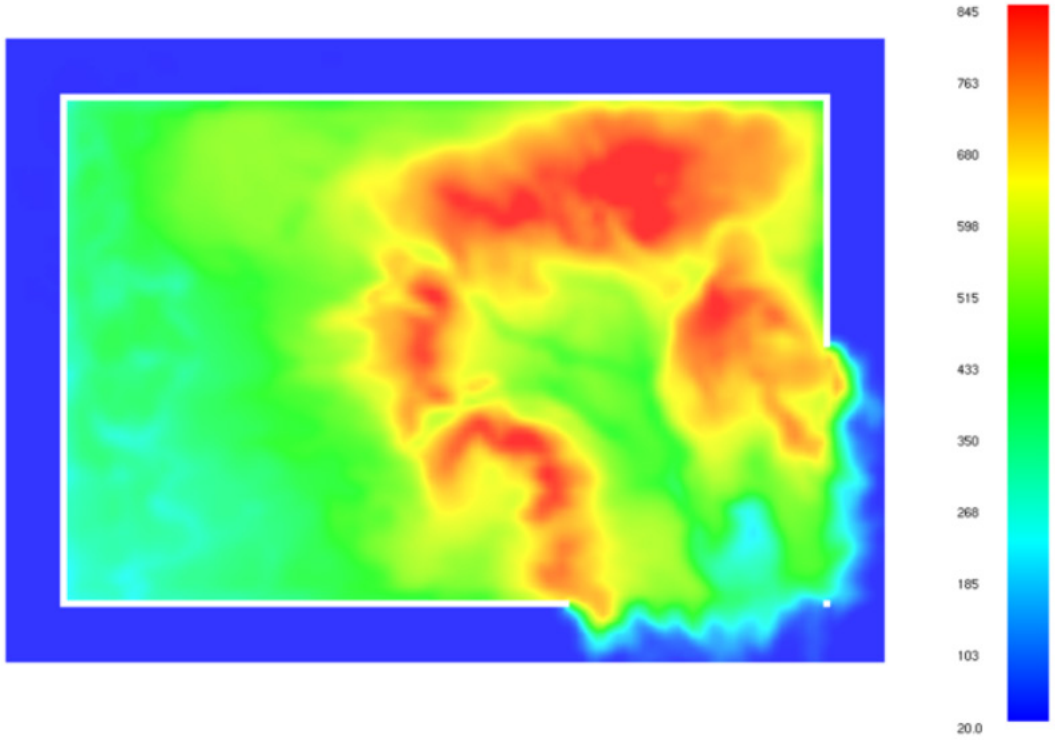

(a)

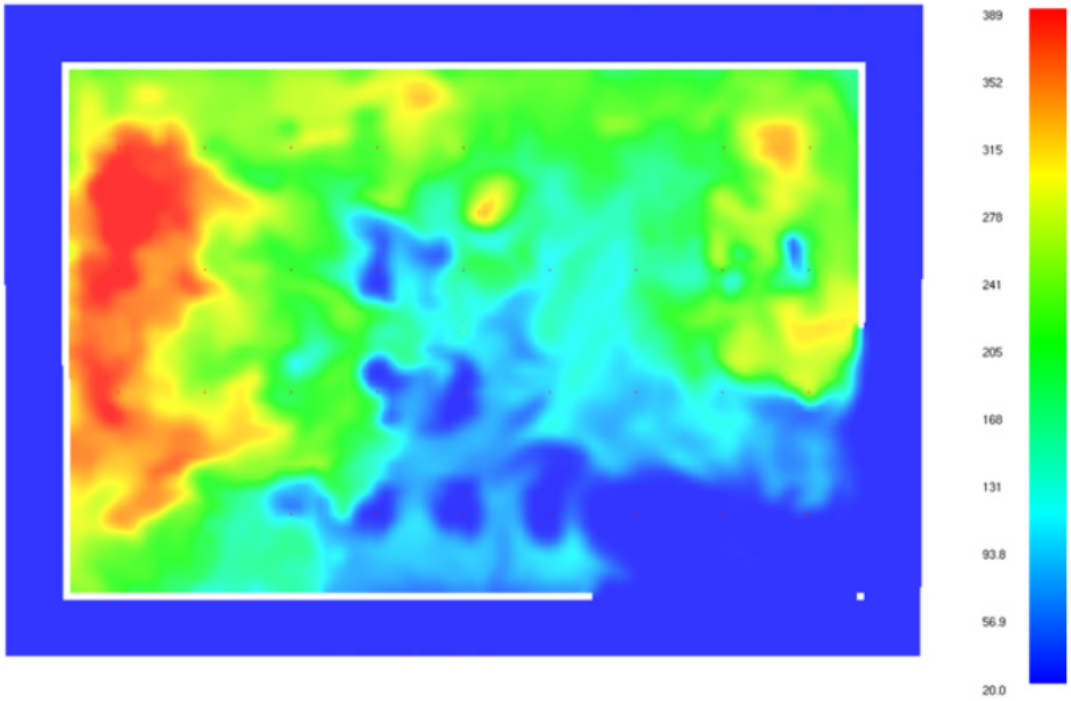

(b)

Figure 7-9. Gas temperature contours at roof level: (a) no vents, and (b) with vents.
Source: Courtesy of Simpson Gumpertz & Heger (2019, and NIST FDS Software ©2019.
Note: Values are in °C.

(a)

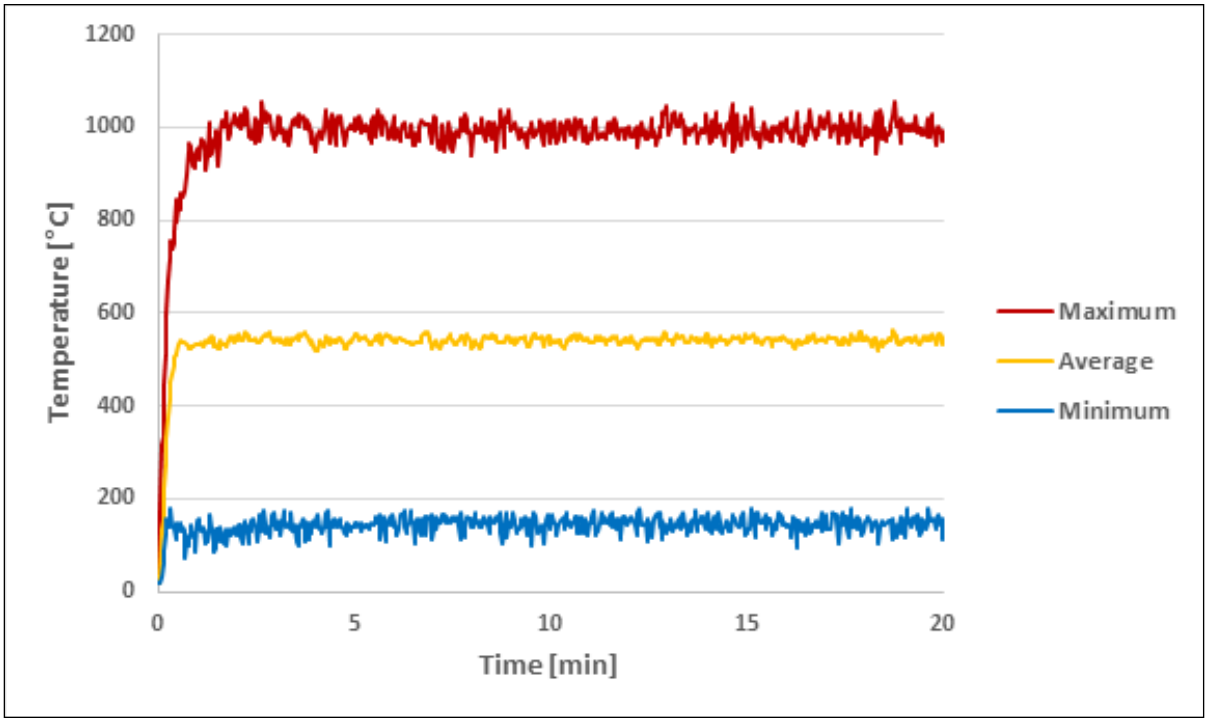

(b)

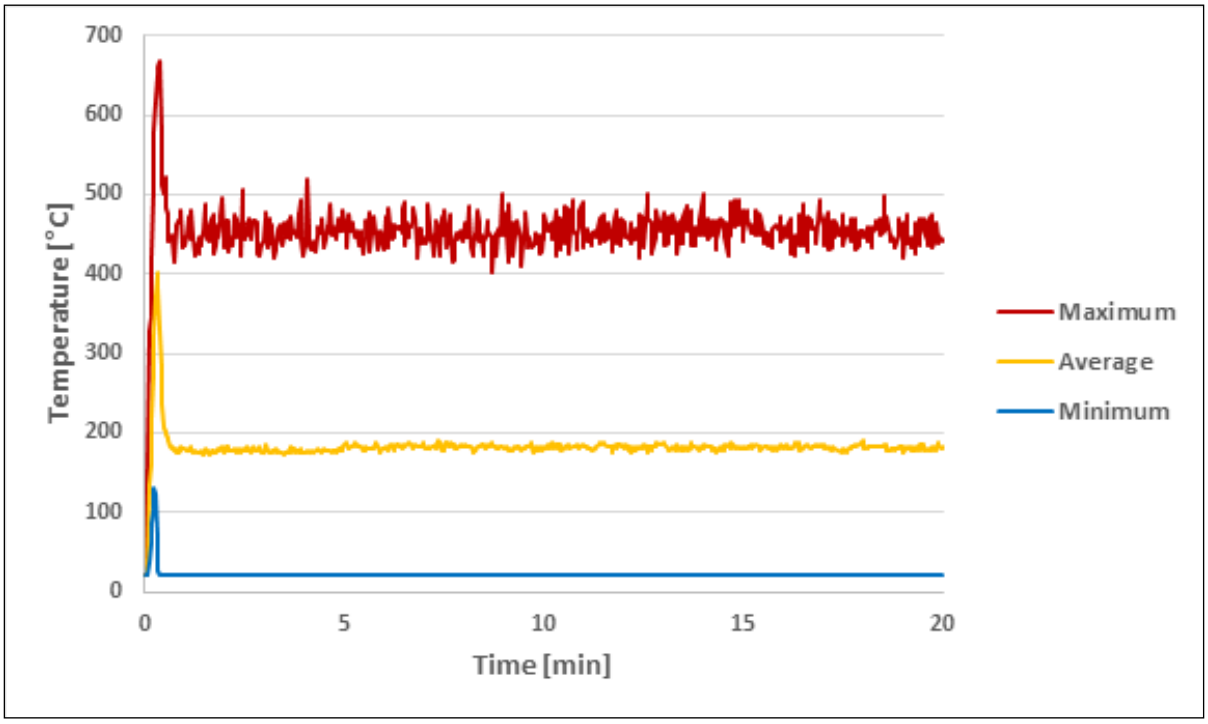

Figure 7-10. Gas temperature histories at roof level: (a) no vents, and (b) with vents.
Source: Courtesy of Simpson Gumpertz & Heger (2019).

7.5 STRUCTURAL TEMPERATURE HISTORIES

Based on the structural design fire time–temperature histories described in Section 7.4, temperature-dependent material thermal properties according to Eurocode 4 (CEN 2005b), and convective heat transfer coefficients (fire-exposed and unexposed surfaces) according to Eurocode 1 and SFPE S.02, the time–temperature histories of the protected and unprotected steel beams, girders, and columns were calculated using a lumped-capacitance approach according to Eurocode 4 and AISC 360. The nonuniform temperature distribution history through the slab (including the mesh) was calculated using a two-dimensional finite difference approach, which accounts for the shadowing effect of the deck ribs.

For Designs 1 and 2, Figure 7-11 plots the structural temperature histories for the *above-design* fuel load with low ventilation case, considering the nominal 1/2 in. insulation thickness applied to all floor members. For Design 3, Figure 7-12 plots the structural temperature histories for the *above-design* fuel load with low ventilation case, considering unprotected infill members, 3/4 in. thick insulation on the periphery members, and the mesh relocated to the midthickness of the top slab portion (e.g., 1-5/8 in. from the top of slab). Temperature histories of beam/girder–column connections are based on their relative weight-to-heated perimeter ratios (connections have higher thermal mass and heat up more slowly than the corresponding framing members), neglecting any beneficial column heat sink effects. Figure 7-13 illustrates the temperature histories of representative columns on various levels of the building with the nominal insulation thickness (11/16 in.) applied for the *above-design* fuel load with low ventilation fire case.

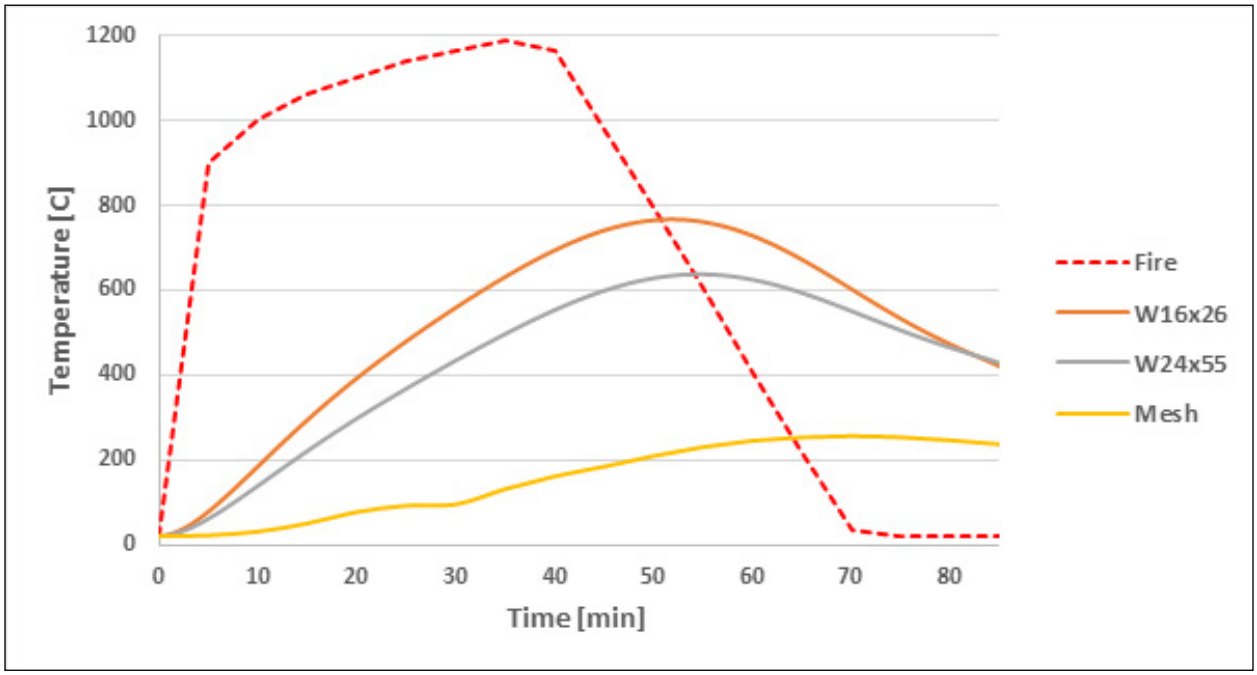

Figure 7-11. Floor system temperature histories (prescriptive case).
Source: Courtesy of Simpson Gumpertz & Heger (2019).

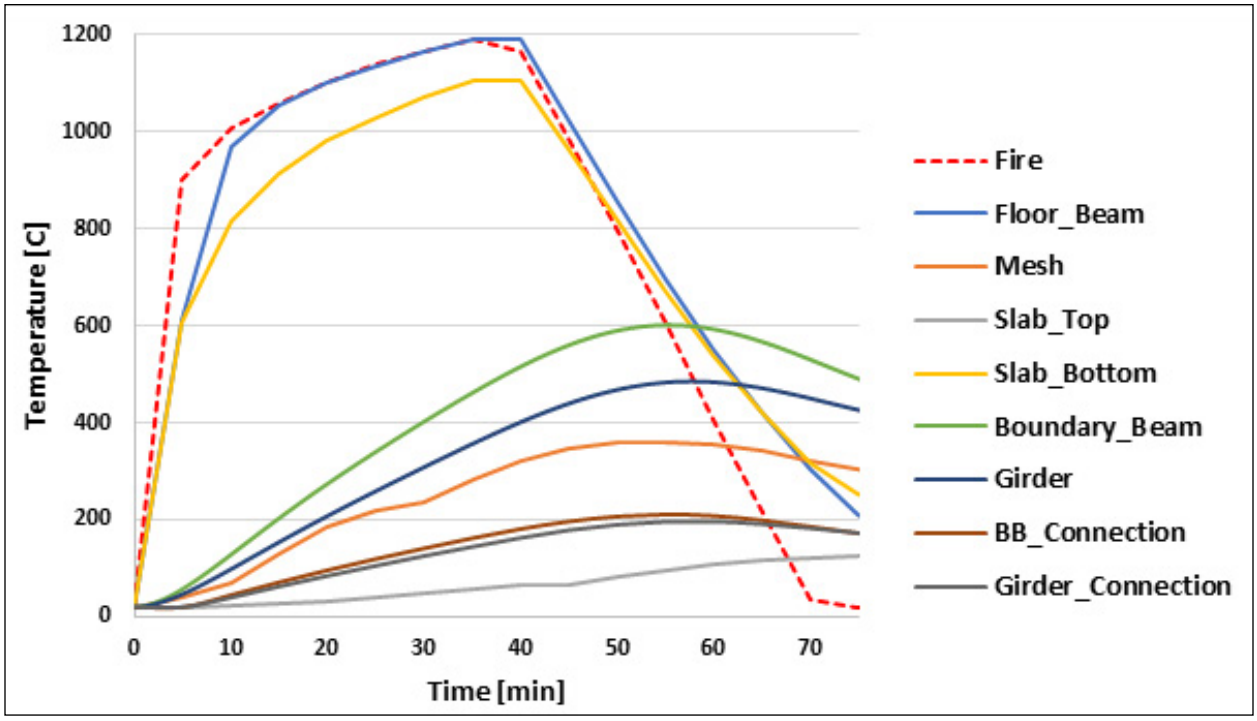

Figure 7-12. Floor system temperature histories (Design 3).
Source: Courtesy of Simpson Gumpertz & Heger (2019).

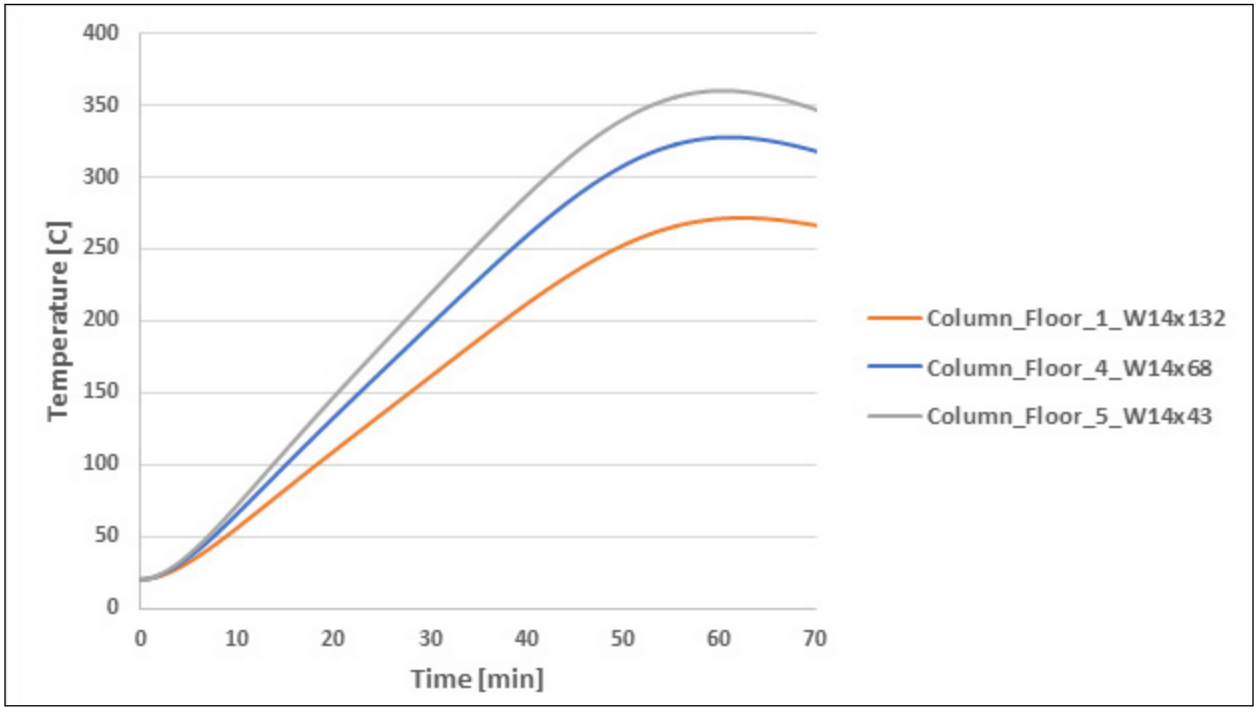

Figure 7-13. Protected column temperature histories.
Source: Courtesy of Simpson Gumpertz & Heger (2019).

7.6 STRUCTURAL ANALYSES

Structural analyses conducted herein include the following general aspects according to Design Brief Section 8:

- Nonlinear/temperature-dependent material mechanical behavior,
- Temperature-dependent material thermal expansion, and
- Geometric nonlinearity (large deflection theory).

7.6.1 Design Assumptions

For Designs 1, 2 and 3, the following general assumptions were made:

- Thermal expansion/contraction of periphery members (i.e., boundary beams and girders) is horizontally restrained at column locations (conservative for the beam/girder–column connections because this would maximize the thrust and contraction forces). However, the axial stiffness of the connections is represented as discussed in Section 7.6.3.
- Periphery member ends are pinned (conservative because this would maximize member deflections and the rotation at beam/girder–column member connections).
- All slab edges are discontinuous (conservative because this neglects the potential for load redistribution to contiguous bays by means of slab/mesh reinforcement continuity). Slab edges that are restrained ideally in-plane and due to explicit representation of contiguous bays (i.e., fire exposing an interior bay, an edge bay, and a corner bay) were also analyzed for sensitivity purposes.
- Only the slab portion above the deck (i.e., the top slab) contributes to the load carrying capacity (conservative because this neglects the anisotropic slab section properties and the metal deck which becomes ineffective quickly under fire exposure).
- Metal decking prevents spalling of the concrete slab.

7.6.2 Software

Collectively, the following software was used to conduct the structural analyses discussed herein:

- MACS+ (Membrane Action of Composite Structures in Case of Fire) (Vassart et al. n.d.) — Algebraic solver for single bays at elevated temperatures that solves slab yield line capacity with enhancements resulting from membrane action at large deflections.
- SPM (Slab Panel Method of Fire Emergency Design) (HERA 2012) — Algebraic solver for single or multiple bays at elevated temperatures that solves slab yield line capacity with enhancements resulting from membrane action at large deflections (alternative formulation/empirical references as compared to MACS+).

- SAFIR (Structural Analysis for Fire) (Franssen and Gernay 2017) — Special purpose finite-element solver including representation of concrete transient creep strain and robust substepping algorithms for convergence at damaged concrete states.

7.6.3 Structural Floors

For Designs 1 and 2, the structural floor becomes unstable approximately 12 min into the structural design fire with design fuel load and low ventilation. Because the metal deck would delaminate from the slab early in the fire [about 5 min is expected due to the direct heating exposure and early steam release from the heated slab (Lim 2003)], its strength contribution was neglected as discussed in Section 7.6.1. Consequently, the slab spanning between infill members is not able to maintain its load-carrying capacity beyond 12 min of exposure. Specifically, unstable plastic hinges form in the slab, and the mesh is not strong enough to resist the applied loading as a catenary. Moreover, catenary action may not even be activated because the slab is not specifically detailed for this condition (e.g., the mesh is not located below the heads of perimeter shear studs for proper anchoring, as discussed in Section 7.6.4) and there may not be a self-equilibrating support present at the ends (e.g., the slab might not be able to form a compression ring, as discussed in this section). Aside from loss of load-carrying capacity between infill members, the formation of plastic hinges in the slab could allow for flame/heat passage to the floor above. Figure 7-14 illustrates the deflection of the structural floor at the onset of slab mesh fracture (approximately 12 min). Hand calculations were also conducted to corroborate this simulated behavior, and an independent numerical analysis was performed by an academic advisor member supporting the results. This failure mode highlights possible differences between in situ and furnace test loading conditions as discussed in Section 4.2.1.1. Notwithstanding the behavior of the slab, the girder/boundary beam–column connections would not be sufficient for this case as discussed in Section 7.6.5.

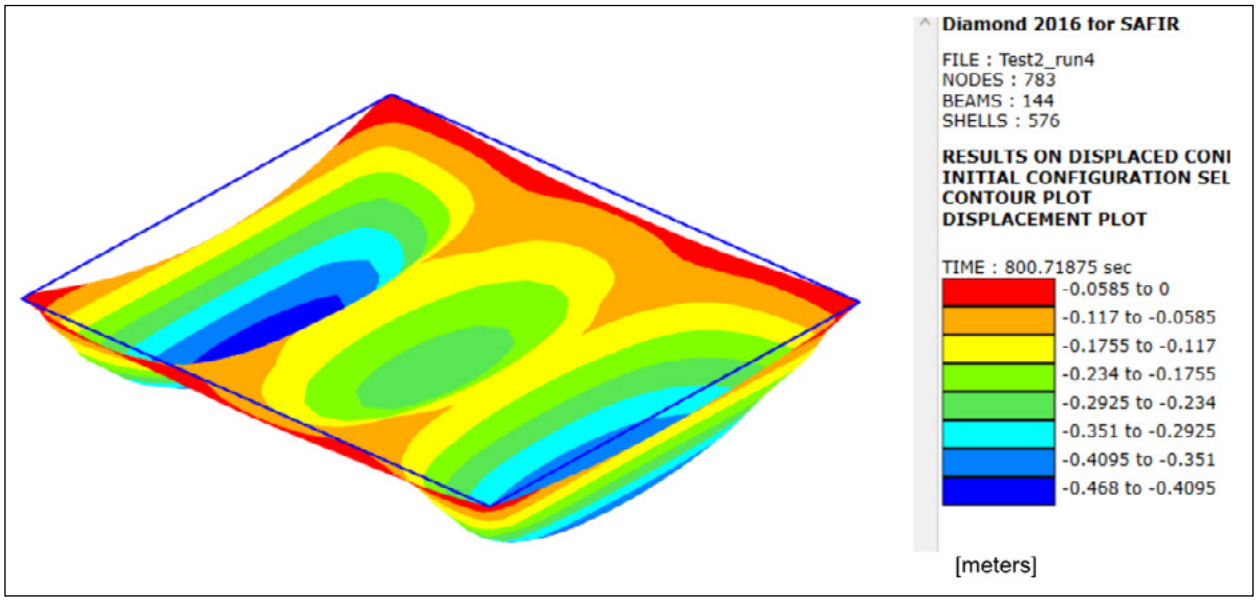

Figure 7-14. Deflection contour after 12 min. of fire exposure (prescriptive case).
Source: Courtesy of Simpson Gumpertz & Heger (2019), and SAFIR Software ©2019.

Designs 1 and 2 only allow for modifications to the structural insulation. Increasing the insulation (to thicknesses that have been qualified for their mechanical integrity performance) on the beams and girders would not appreciably improve the overall performance of the structural floor in this case because the controlling connection demands occur at relatively low temperatures (as discussed in Section 7.6.5). For instance, a 3 in. thickness of insulation on girders would be required to limit their temperature to 150 °C, approximately below which axial forces on connections would not pose an issue. For comparison, the insulation thickness required for a 3 h fire resistance rating is only 1-9/16 in. Also, adding insulation to the deck underside would not reliably prevent slab instability, because the level of thickness needed for reliable deck delamination prevention (for positive moment resistance) would pose a mechanical integrity concern as characterized in SFPE S.02 (i.e., cohesion/adhesion of a very thick layer of insulation suspended below the deck faces). Even if mechanical integrity were not a concern, the addition of such insulation would be expected to only marginally delay the onset of instability given the low thermal tolerance of the deck.

Design 3 has the freedom to implement structural enhancements and/or insulation. To allow for the slab to perform adequately as a two-way compressive tensile membrane under fire exposure, its mesh reinforcement is upgraded from 6x6-D2.9x2.9 to 4x4-D5.4x5.4. The mesh is relocated from 3/4 in. from the top of the slab to the center of the top slab (1-5/8 in. from the top of the slab), which is permitted and would not compromise its slab crack control intent according to ACI 318 (ACI 2014), Section 10.6.4. Increasing the mesh density increases its tensile strength and lowering it within the slab profile enhances its membrane performance. Granted, lowering the mesh within the slab increases its heating slightly under fire exposure, which is accounted for in the thermal analyses described in Section 7.5. The insulation thickness on the periphery members is slightly increased from 1/2 in. to 3/4 in., and the insulation on the infill members is completely removed.

With the structural enhancements and insulation distribution described, structural analyses conducted using MACS+ and SPM demonstrate that the floor system would reliably/robustly endure a myriad of increasingly intense fire exposures. Specifically, it is demonstrated that the floor system would survive full burnout for the *design*, *above-design*, and *ultra-design* fuel load cases with all conceivable compartment ventilations considered, as summarized in Table 7-1. For instance, Figure 7-16 plots the evolution of the floor system's capacity compared to its constant applied mechanical loading (demand) for the structural temperature histories plotted in Figure 7-15 (Case 10 as shown in Table 7-1). This demonstrates how the reinforced slab actually strengthens as the level of deflection increases, which effectively compensates for the unprotected infill floor beams' rapid loss of strength (becoming almost negligible at peak heating). Also, the critical reinforcement mesh is highly insulated from fire exposure as a result of its embedment within the concrete slab. This stabilizing mechanism is analogous to pushing down on the center hub of a horizontally oriented bicycle wheel in which the spoke resists the applied loading in tension and the rim in compression.

To corroborate that the protected periphery members maintain adequate strength during fire exposure, hand calculations per AISC 360 were conducted for confirmation. Also, a variety of structural bay configurations present in the building were analyzed under the *above-design* fuel load with low ventilation case to confirm that the results can be applied to the majority of the floor framing, as summarized in Table 7-2.

Table 7-1. Typical Floor System Structural Analyses Summary.

Case	1	2	3	4	5	6	7	8	9	10	11	12
Bay Width (ft)	30	30	30	30	30	30	30	30	30	30	30	30
Bay Length (ft)	30	30	30	30	30	30	30	30	30	30	30	30
Slab Mesh Designation	6x6-D2.9x2.9	4x4-D5.4x5.4	4x4-D5.4x5.4	4x4-D5.4x5.4	4x4-D5.4x5.4	4x4-D5.4x5.4	4x4-D5.4x5.4	4x4-D5.4x5.4	4x4-D5.4x5.4	4x4-D5.4x5.4	4x4-D5.4x5.4	4x4-D5.4x5.4
Slab Mesh Density ($in^2/ft.$)	0.058	0.162	0.162	0.162	0.162	0.162	0.162	0.162	0.162	0.162	0.162	0.162
Slab Mesh Bar Size (mm)	5.0	6.7	6.7	6.7	6.7	6.7	6.7	6.7	6.7	6.7	6.7	6.7
Mesh Top Offset (in.)	0.75	1.625	1.625	1.625	1.625	1.625	1.625	1.625	1.625	1.625	1.625	1.625
Infill Beam % Composite Action	50%	50%	50%	50%	50%	50%	50%	50%	50%	50%	50%	50%
Perimeter Beam % Composite Action	50%	50%	50%	50%	50%	50%	50%	50%	50%	50%	50%	50%
Fuel Load Scenario	Design Basis (80% Fractile)	Design Basis (80% Fractile)	Design Basis (80% Fractile)	Design Basis (80% Fractile)	Design Basis (80% Fractile)	Design Basis (80% Fractile)	Design Basis (80% Fractile)	No Sprinkler Reduc-tion (80%) Fractile)	No Sprinkler Reduc-tion (98%) Fractile)	No Sprinkler Reduc-tion (98%) Fractile)	No Sprinkler Reduc-tion (98%) Fractile)	3x Design Basis
Fuel Load (MJ/m^2)	374	374	374	374	374	374	374	613	912	613	912	1122
Structural Design Fire Scenario	1	1	2	3	4	5	6	1	1	5	5	5
Ventilation Level	High	High	High	Moderate	Moderate	Low	Low	High	High	Low	Low	Low
Compartment Width (m)	27.4	27.4	36.6	27.4	36.6	27.4	36.6	27.4	27.4	27.4	27.4	27.4
Compartment Length (m)	18.3	18.3	9.1	18.3	9.1	18.3	9.1	18.3	18.3	18.3	18.3	18.3

Table 7-1. Typical Floor System Structural Analyses Summary (con't).

Compartment Height (m)	3	3	3	3	3	3	3	3	3	3	3	3
Opening Height (m)	3	3	3	3	3	3	3	3	3	3	3	3
Opening Length (m)	45.7	45.7	45.7	27.4	24.4	18.3	18.3	45.7	45.7	18.3	18.3	18.3
Combustion Factor	1	1	1	1	1	1	1	1	1	1	1	1
Glazing Breakage Fraction	1	1	1	1	1	1	1	1	1	1	1	1
Compartment Surface Area (m^2)	1277	1277	940	1277	940	1277	940	1277	1277	1277	1277	1277
Ventilation Fraction of Walls	18%	18%	18%	11%	10%	8%	8%	18%	18%	8%	8%	8%
Opening Factor (m(1/2))	0.19	0.19	0.25	0.11	0.13	0.07	0.10	0.19	0.19	0.07	0.07	0.07
Fire Growth Rate	Medium	Medium	Medium	Medium	Medium	Medium	Medium	Medium	Medium	Medium	Medium	Medium
Loading (psf)	129.5	129.5	129.5	129.5	129.5	129.5	129.5	129.5	129.5	129.5	129.5	129.5
Failure Time (min)	12	N/A	N/A	N/A	N/A	N/A	N/A	N/A	N/A	N/A	N/A	70
Controlling DCR	1.94	0.81	0.81	0.81	0.81	0.82	0.81	0.82	0.83	0.83	0.97	1.19
Boundary Beam Critical Temperature (°C)	N/A	617	620	617	620	603	620	613	603	597	595	N/A
Girder Critical Temperature (°C)	N/A	752	752	752	752	752	752	752	752	752	750	N/A

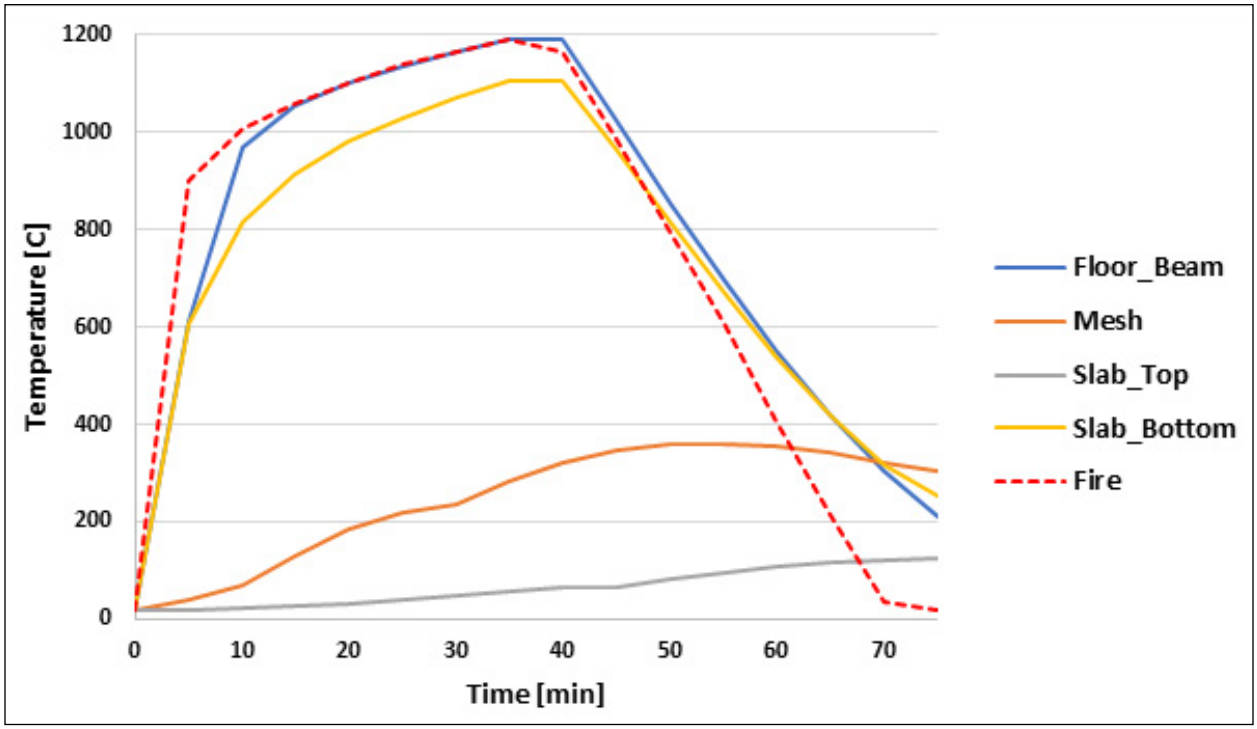

Figure 7-15. Structural temperature histories during fire exposure (Case 10).
Source: Courtesy of Simpson Gumpertz & Heger (2019).

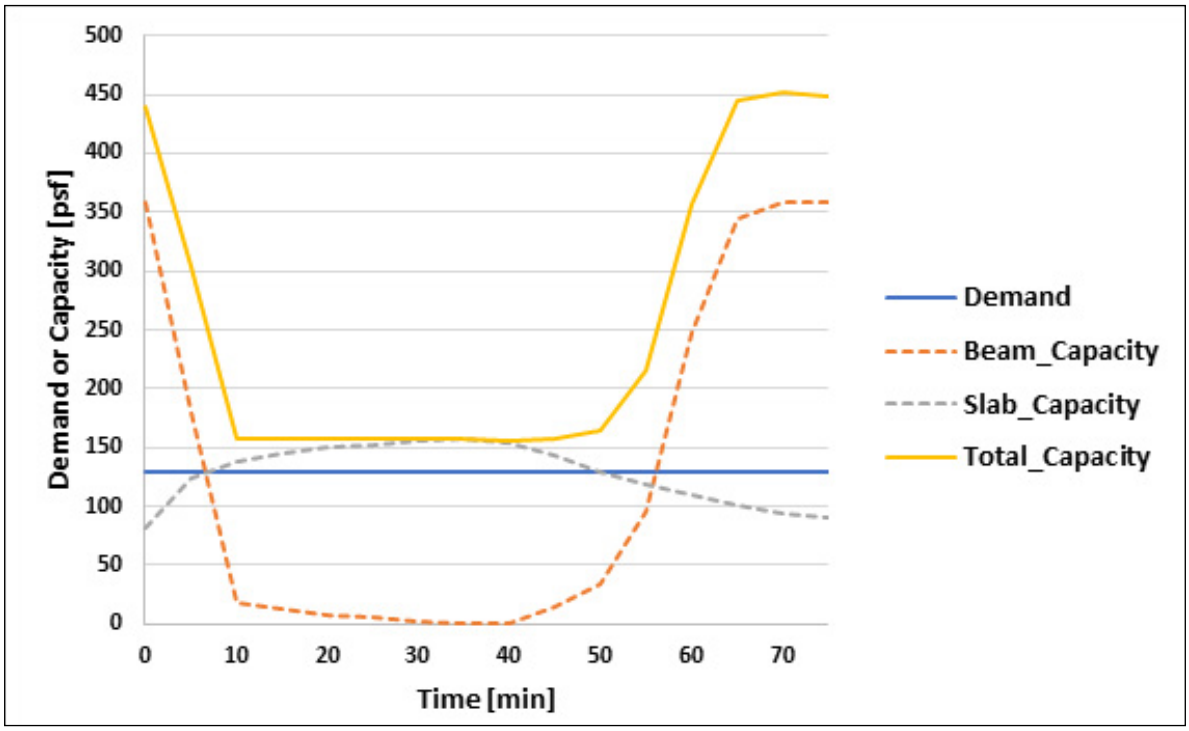

Figure 7-16. Floor demand/capacity history during fire exposure (Case 10).
Source: Courtesy of Simpson Gumpertz & Heger (2019).

Table 7-2. Atypical Floor Systems Analyzed.

Config-uration	Bay Width	Bay Length	Infill Beams	Bound-ary Beam 1	Bound-ary Beam 2	Girder 1	Girder 2	Controlling Periphery Member Temperature
Base	30 ft	30 ft	W16x26	W16x26	W16x26	W24x55	W24x55	597 °C
2	30 ft	30 ft	W16x26	W16x26	W16x26	W24x55	W18x35	597 °C
3	30 ft	30 ft	W16x26	W16x26	W18x35	W24x55	W18x35	597 °C
4	30 ft	30 ft	W16x26	W16x26	W16x26	W21x50	W18x35	597 °C
5	30 ft	30 ft	W16x26	W16x26	W16x26	W21x44	W24x55	597 °C
6	30 ft	30 ft	W16x26	W16x26	W24x62	W21x50	W24x55	597 °C
7	30 ft	30 ft	W18x35	W18x35	W18x35	W18x35	W24x55	656 °C
8	30 ft	30 ft	W18x35	W18x35	W18x35	W24x55	W24x55	656 °C
9	30 ft	30 ft	W18x35	W18x35	W18x35	W21x44	W24x55	656 °C
10	30 ft	30 ft	W18x35	W24x68	W24x68	W21x44	W24x55	700 °C
11	30 ft	30 ft	W18x35	W18x35	W24x62	W24x55	W24x55	656 °C
12	30 ft	30 ft	W16x26	W16x26	W24x62	W18x35	W21x50	597 °C
13	30 ft	30 ft	W18x35	W18x35	W24x62	W18x35	W24x55	656 °C
14	30 ft	18 ft	W16x26 (1)	W18x35	W16x31	W40x167	W40x183	695 °C
15	30 ft	18 ft	W16x26 (1)	W18x35	W16x26	W33x130	W40x183	677 °C
16	30 ft	18 ft	W16x26 (1)	W16x26	W16x31	W18x35	W18x35	677 °C
17	30 ft	18 ft	W16x26 (1)	W16x26	W16x26	W18x35	W18x35	677 °C
18	30 ft	18 ft	W18x35 (1)	W18x35	W18x35	W18x35	W18x35	725 °C
19	30 ft	18 ft	W18x35 (1)	W24x55	W24x68	W18x35	W18x35	809 °C

Even considering inconceivably low ventilation cases (as low as approximately 300 sq. ft of total ventilation area from the fire zone) for the *above-design* fuel load, the floor system still survives full burnout, and survives at least 130 min when the absolute lower bound ventilation opening factor of 0.02 is considered. Also, the floor system would survive approximately 70 min under the 3X-design fuel load case with low ventilation, which upholds the minimum performance expectation (as discussed in Section 2.3.1) under a nearly inconceivable fuel load level. Overall, the variety of conditions in which the floor system performs adequately demonstrates the reliability/robustness of the enhanced floor design, which was not possible to achieve for Designs 1 and 2.

To corroborate the Design 3 structural analyses conducted using MACS+/SPM and to extract connection force histories (see Section 7.6.5), SAFIR was used to simulate a single structural bay for the *above-design* fuel load with low ventilation case for a 4 h time frame to capture the entirety of the cooling phase (Figure 7-17). In this model, the periphery members are pin-released, using the software's *SAME* function to ensure that they undergo the maximum possible deflection, which is conservative. In addition, the axial stiffness of the girder/boundary beam–column connections are represented in the model using the software's *RELAX* function. Hand calculations were conducted to determine the axial stiffness of the girder/boundary beam–column connections, and these values were conservatively taken at ambient, which would produce the highest level of restraint.

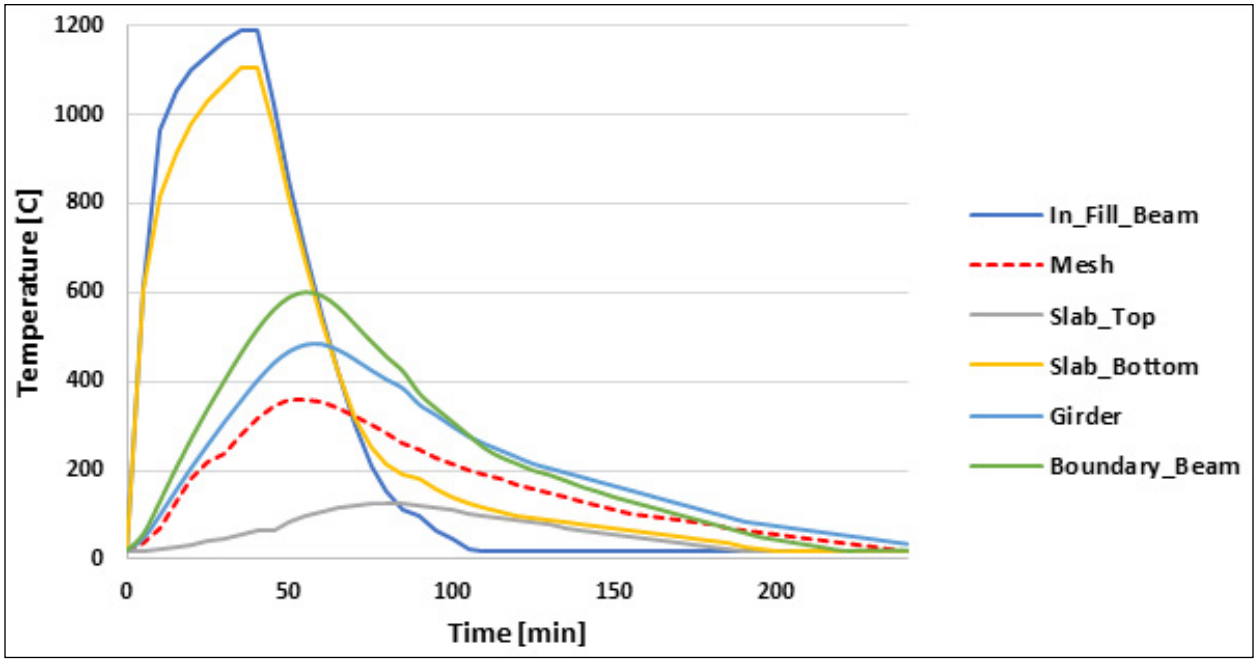

Figure 7-17. Structural temperature histories (Case 10 extended to 4 h).
Source: Courtesy of Simpson Gumpertz & Heger (2019).

The single-bay SAFIR model survives full burnout without any instability (including any mesh yielding), which corroborates the previous results. Figure 7-18 plots the deflection histories of the floor members. Figures 7-19 and 7-20 illustrate the evolution of the floor slab deflection and principal membrane forces as it heats and cools, respectively. A case in which 25% of the floor loading from adjacent bays (also under fire exposure) is shed to the single (modeled) bay (approximately 1 kip/ft added to the periphery members) was simulated, and no floor failure was observed. This case would also account for any cladding load at the edges of the building (approximately 0.2 kip/ft). Also, the floor system was simulated without thermal expansion represented to confirm that stable tensile membrane action could form without restraint effects (i.e., owing to deflection compatibility alone).

To corroborate the performance of the single-bay SAFIR model, multi-bay scenarios were considered. As an upper bound restraint condition, in-plane rigid restraints were applied to the full periphery of the slab (single-bay model), and no floor failure were observed. Also, explicit representation of various slab restraint conditions was simulated with a nine-bay SAFIR model with fire exposing an interior bay, an edge bay, and a corner bay as illustrated in Figure 7-21. Figure 7-22 shows floor member deflections for the interior bay fire condition. As expected, these simulated conditions demonstrate no floor failure, as shown in Figures 7-23 through 7-31.

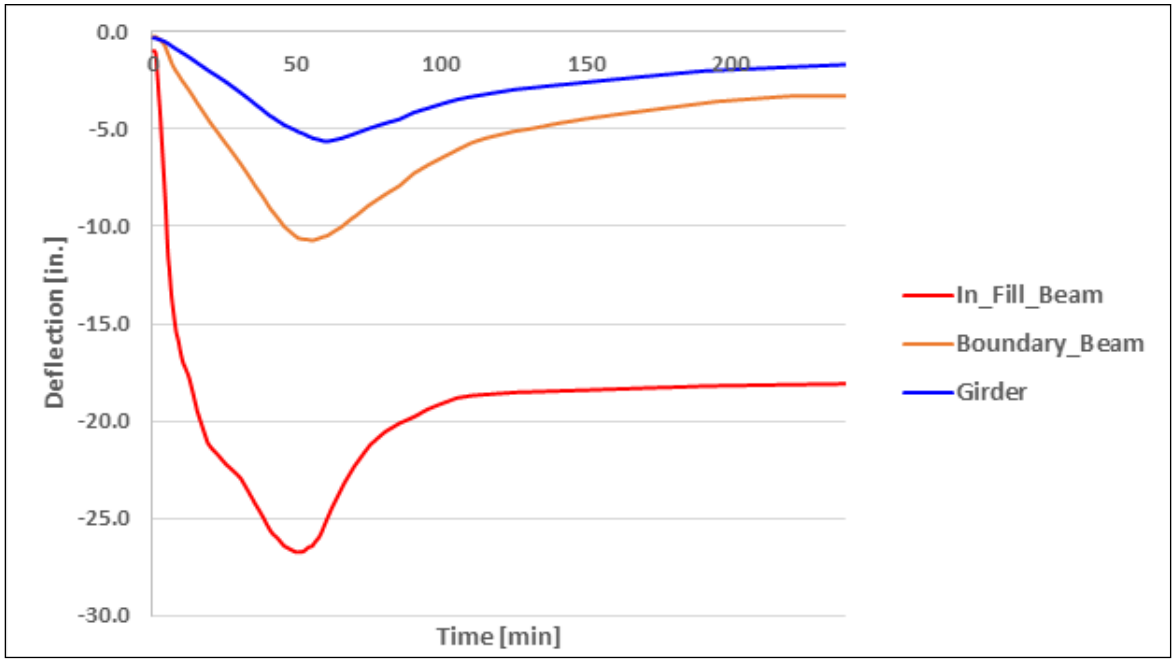

Figure 7-18. Floor member deflection histories (Case 10).
Source: Courtesy of Simpson Gumpertz & Heger (2019).

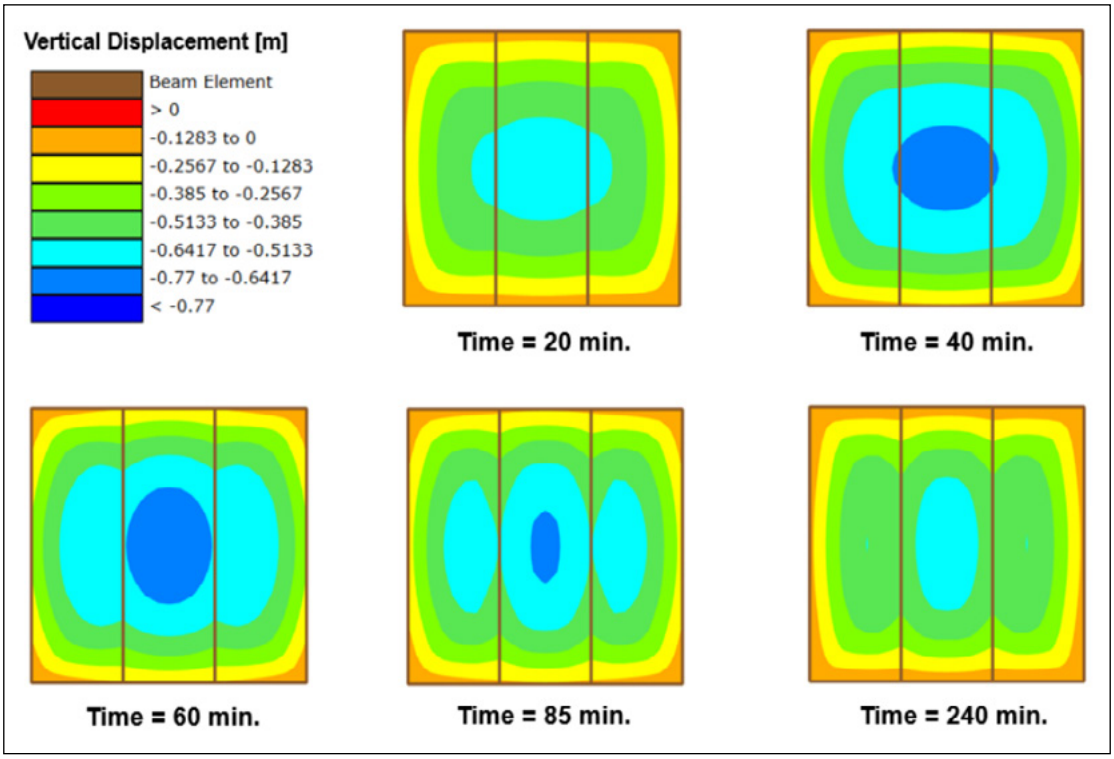

Figure 7-19. Floor slab deflection (Case 10).
Source: Courtesy of Simpson Gumpertz & Heger (2019), and SAFIR Software ©2019.

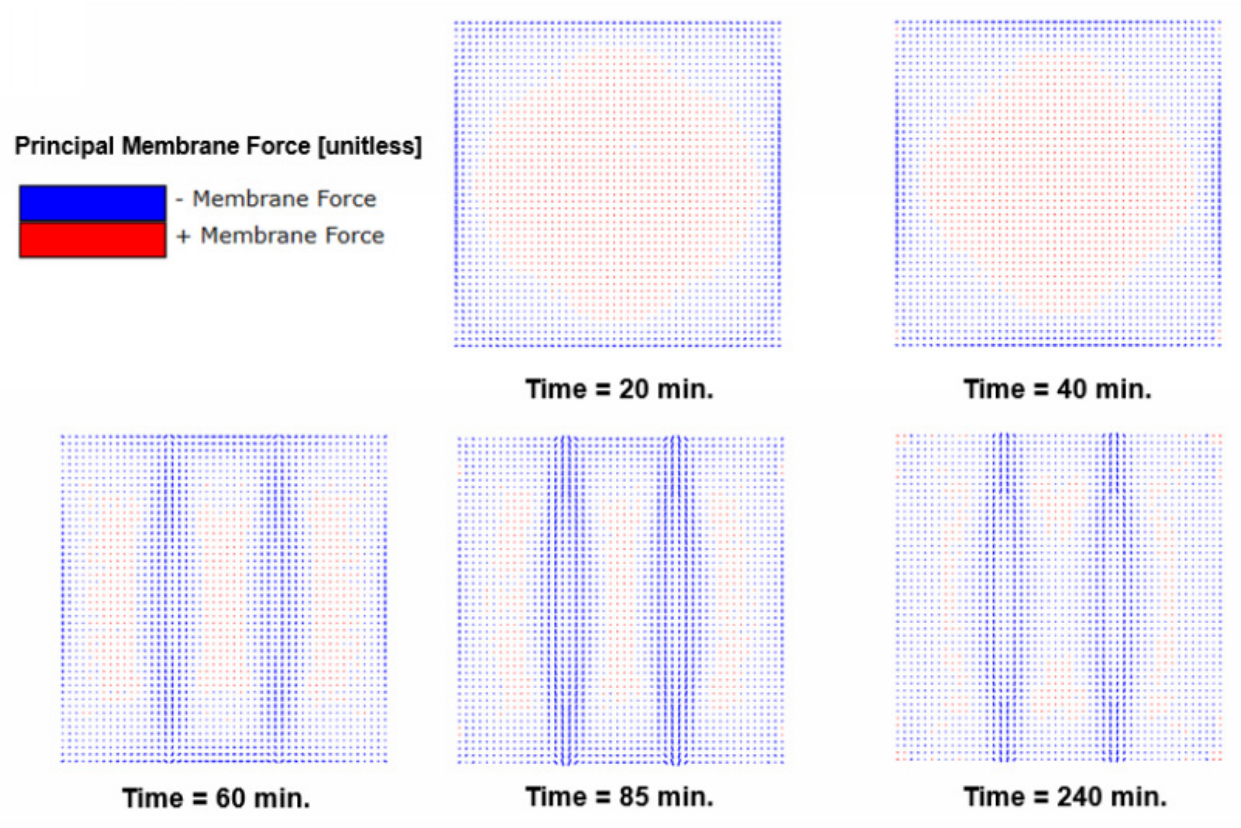

Figure 7-20. Floor slab principal membrane forces (Case 10).
Source: Courtesy of Simpson Gumpertz & Heger (2019), and SAFIR Software ©2019.

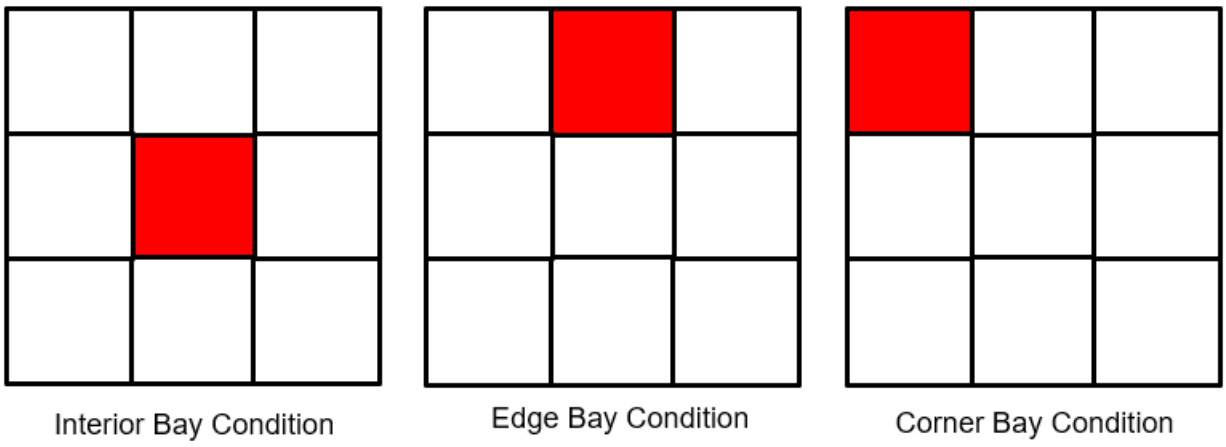

Figure 7.21. Fire locations (sensitivity studies of floor bay restraint).
Source: Courtesy of Simpson Gumpertz & Heger (2019).

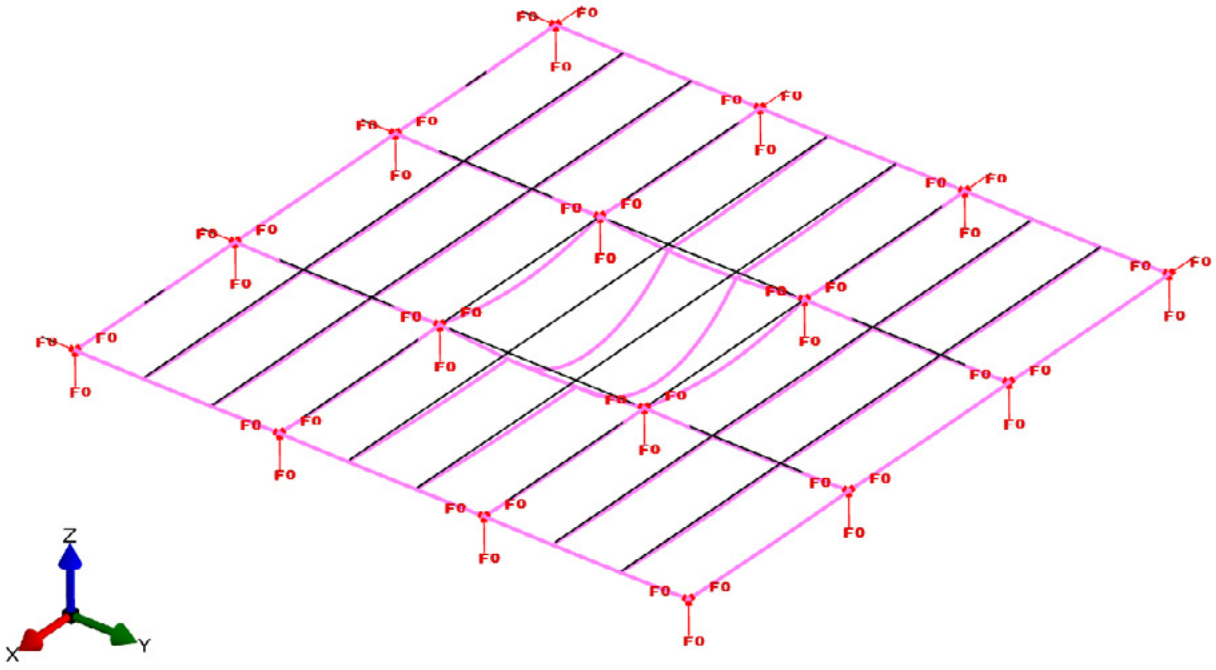

Figure 7-22. Floor member deflection for interior bay fire condition.
Source: Courtesy of Simpson Gumpertz & Heger (2019), and SAFIR Software ©2019.

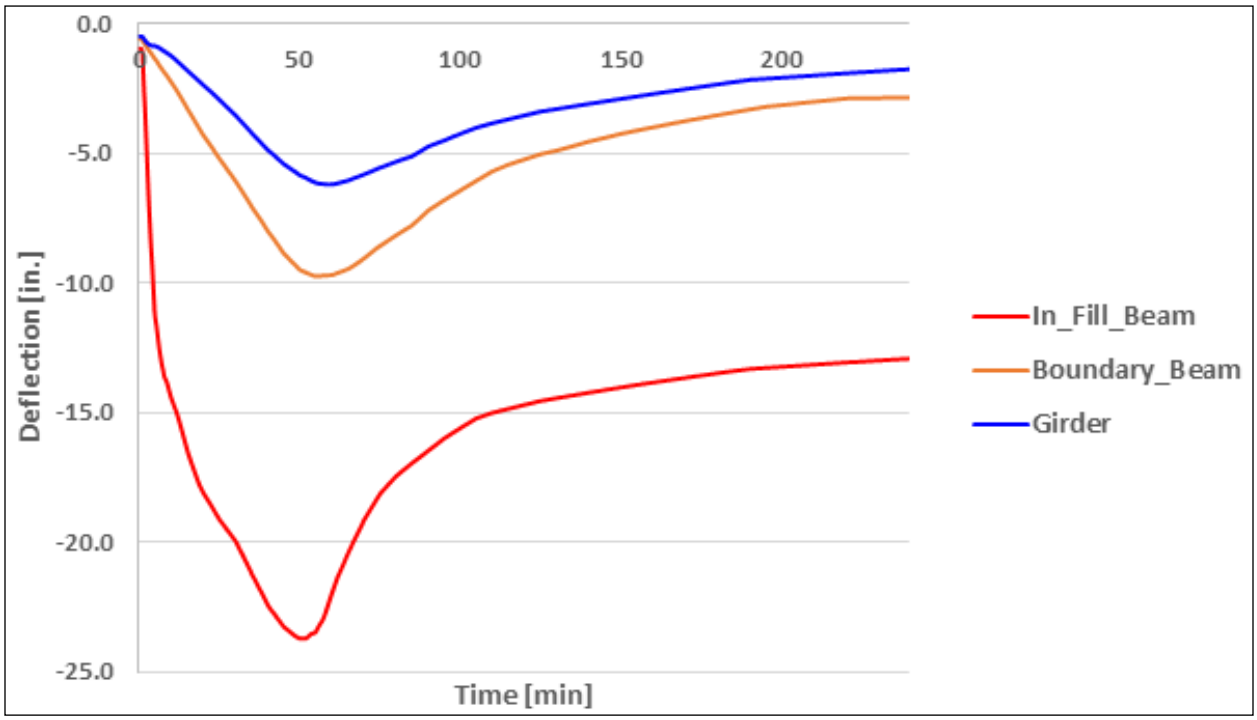

Figure 7-23. Floor member deflection histories (Case 10) (interior bay fire).
Source: Courtesy of Simpson Gumpertz & Heger (2019).

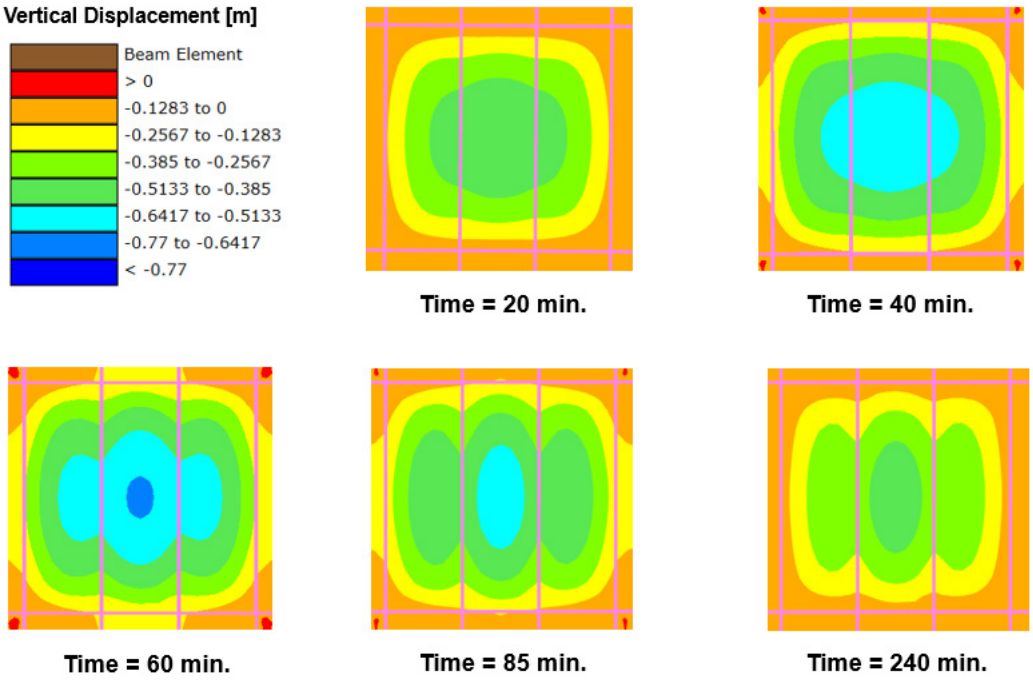

Figure 7-24. Floor slab deflection (Case 10) (interior bay fire).

Source: Courtesy of Simpson Gumpertz & Heger (2019), and SAFIR Software ©2019.

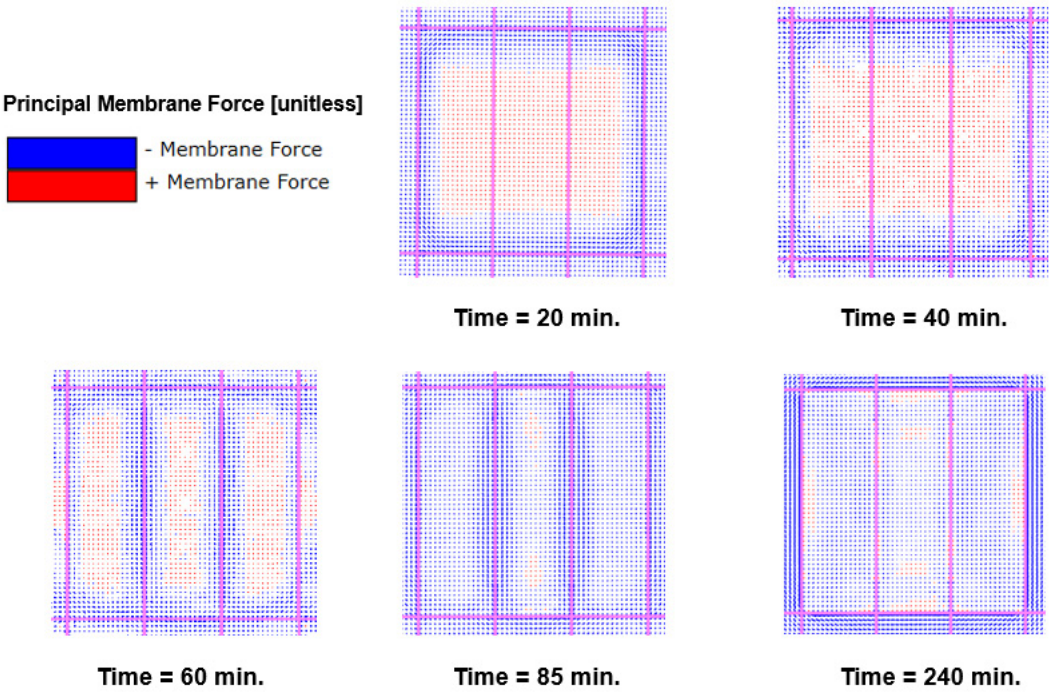

Figure 7-25. Floor slab principal membrane forces (Case 10) (interior bay fire).

Source: Courtesy of Simpson Gumpertz & Heger (2019), and SAFIR Software ©2019.

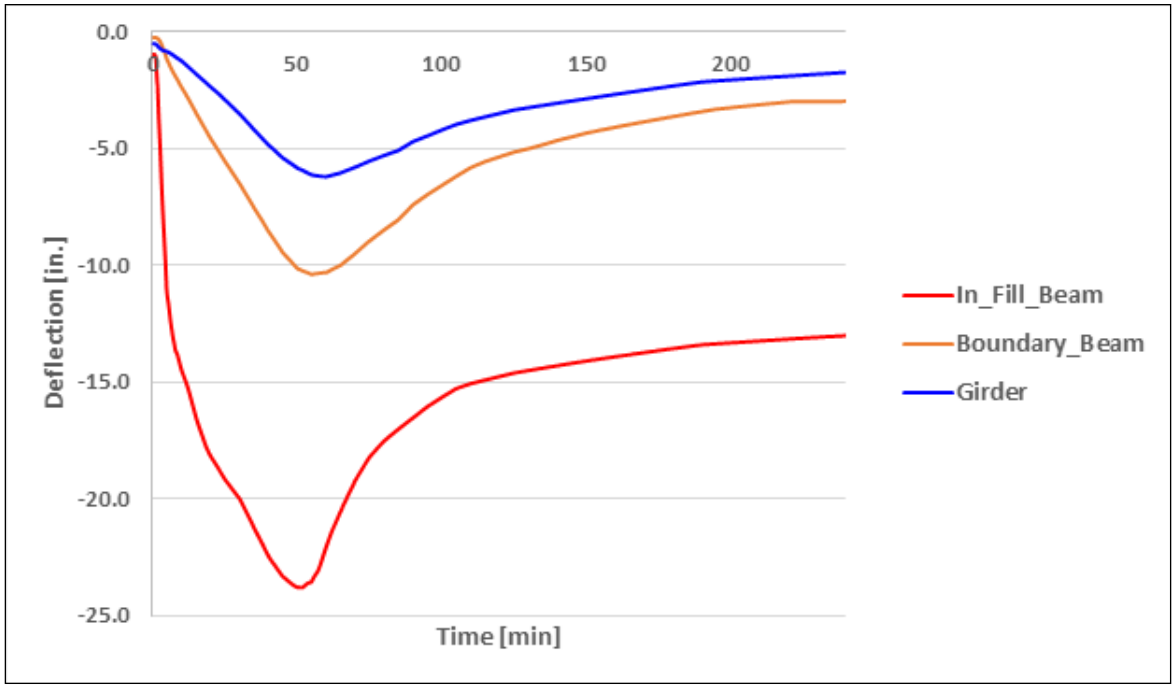

Figure 7-26. Floor member deflection histories (Case 10) (edge bay fire).
Source: Courtesy of Simpson Gumpertz & Heger (2019).

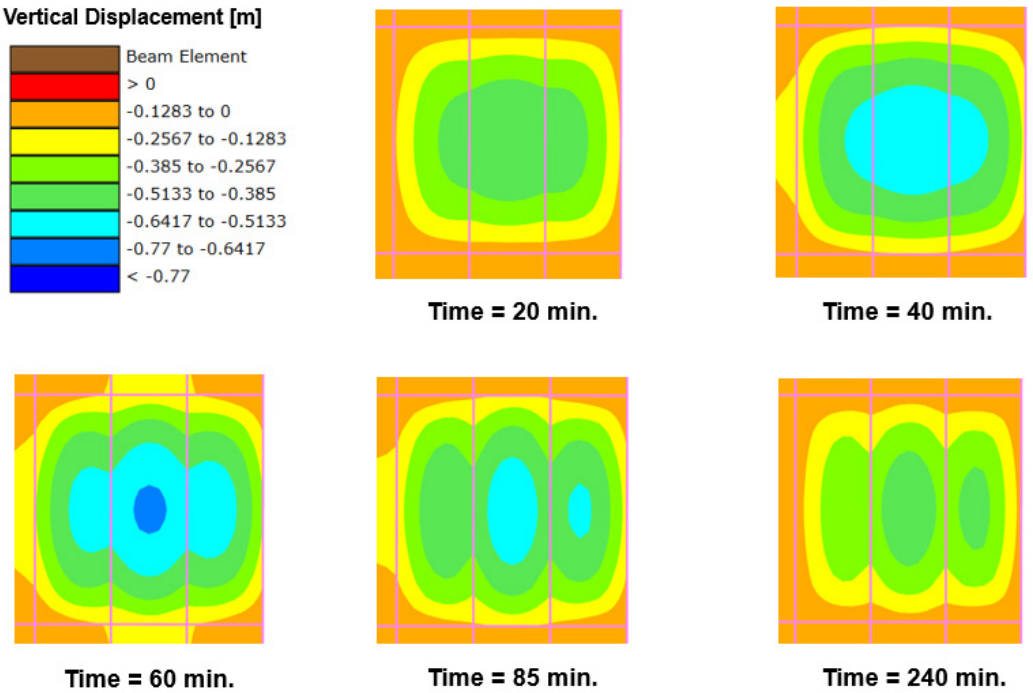

Figure 7-27. Floor slab deflection (Case 10) (edge bay fire).
Source: Courtesy of Simpson Gumpertz & Heger (2019), and SAFIR Software ©2019.

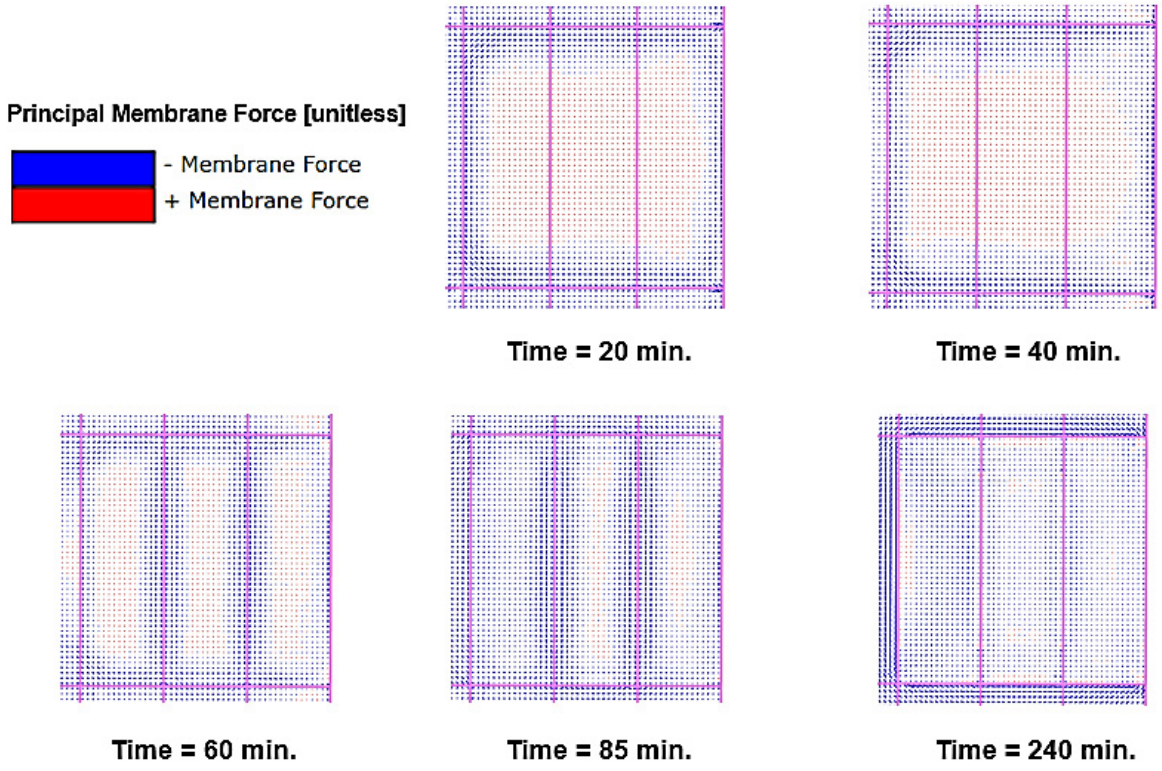

Figure 7-28. Floor slab principal membrane forces (Case 10) (edge bay fire).
Source: Courtesy of Simpson Gumpertz & Heger (2019), and SAFIR Software ©2019.

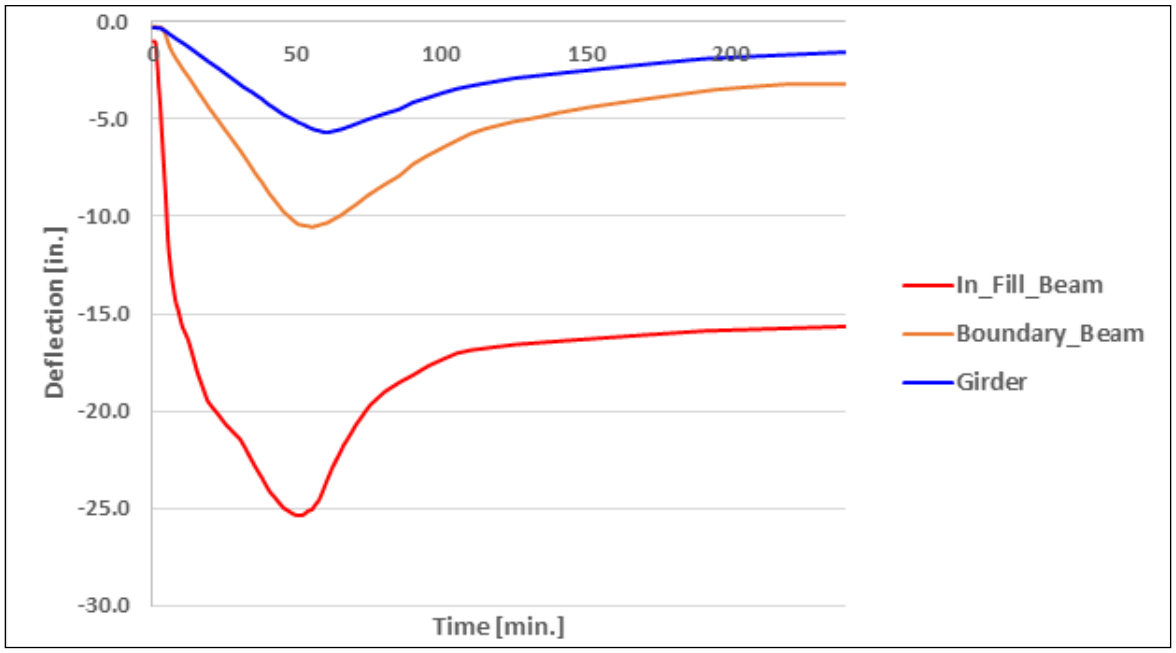

Figure 7-29. Floor member deflection histories (Case 10) (corner bay fire).
Source: Courtesy of Simpson Gumpertz & Heger (2019).

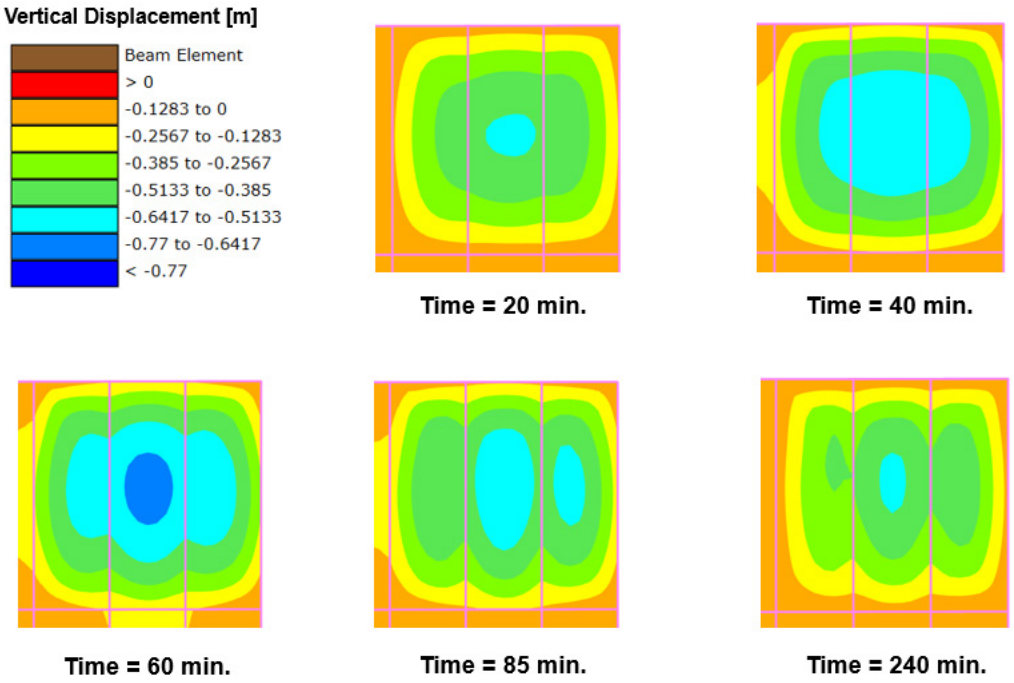

Figure 7-30. Floor slab deflection (Case 10) (corner bay fire).

Source: Courtesy of Simpson Gumpertz & Heger (2019), and SAFIR Software ©2019.

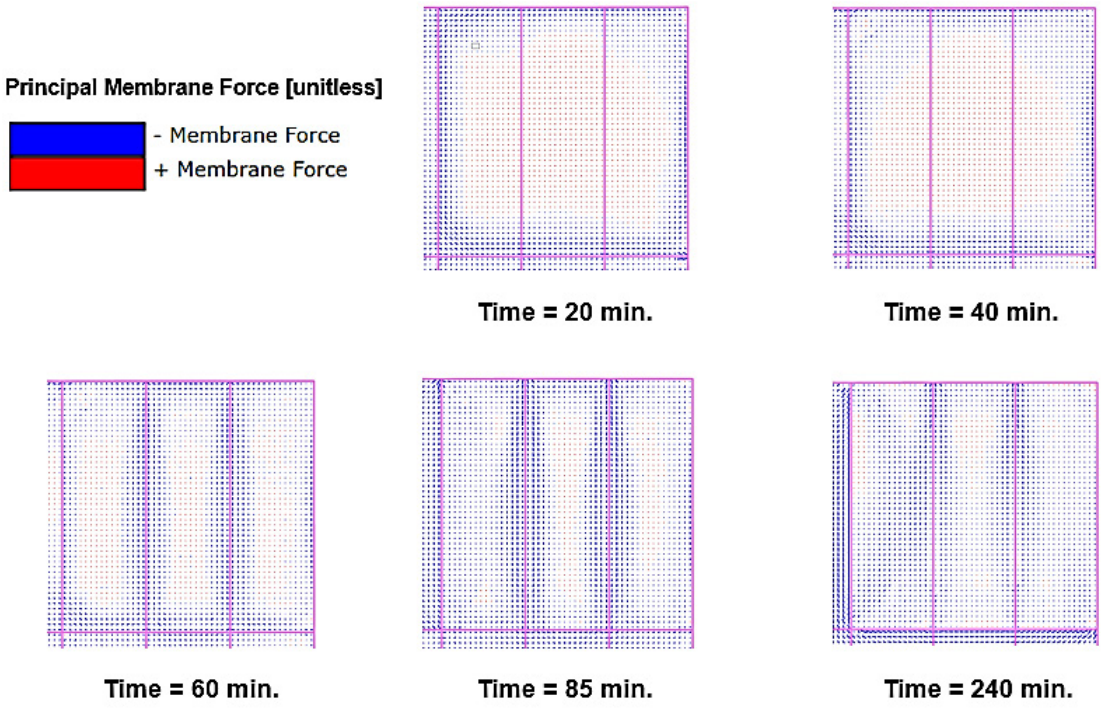

Figure 7-31. Floor slab principal membrane forces (Case 10) (corner bay fire).

Source: Courtesy of Simpson Gumpertz & Heger (2019), and SAFIR Software ©2019.

7.6.4 Slab Mesh Detailing

In addition to increasing the slab mesh reinforcement from 6x6-D2.9x2.9 to 4x4-D5.4x5.4, the mesh must be properly lapped and anchored to the composite girders/boundary beams at the outside edges of the building (spandrel beams) to prevent the slab from being pulled off the supports as witnessed by physical testing without such detailing (Wald et al. 2010). Based on industry recommendations (Vassart et al. 2010) and on provisions ACI 318, Sections 25.4.6 and 25.4.7, the 4x4-D5.4x5.4 mesh must be lapped and extended at spandrel beams a minimum of 8 in., which can be readily accommodated given that slab edges up to 12 in. are common for this type of construction. The extended mesh ends must be lapped with #4 hook bars that are placed 12 in on center and are commonly present within edge trim extensions of metal deck, to prevent longitudinal splitting of the slab. Specifically, this detailing would allow for the tensile capacity of the mesh to become fully developed prior to the onset of longitudinal splitting. Based on the positioning of the mesh at the half-depth of the top slab, this reinforcement would be positioned below the head of the shear studs as required for proper anchoring. The required mesh detailing is illustrated in Figure 7-32. Overall, this mesh detailing would reliably maintain the seating of the slab on the periphery support members under fire exposure.

7.6.5 Floor Member Connections

Figures 7-3 and 7-4 illustrate the nominal design of the girder/boundary beam–column connections. Hand calculations were conducted to estimate the axial thrust/contraction force demands on these critical connections considering beam curvature axial softening and composite section stiffness. The unrealistically high estimates provided by this simplified approach demonstrate the need to capture time-dependent behavior under fire exposure in this respect. Notably, competing effects of restrained thermal expansion and deflection curvature need to be more accurately captured, and the axial stiffness of the connections should be considered. The simplified calculations do not capture these key force-alleviating aspects. Accordingly, Figures 7-33 through 7-36 illustrate the axial and shear force histories at the girder/boundary beam–column connections as derived from the SAFIR single-bay model described in Section 7.6.3 , which were used for the connection designs.

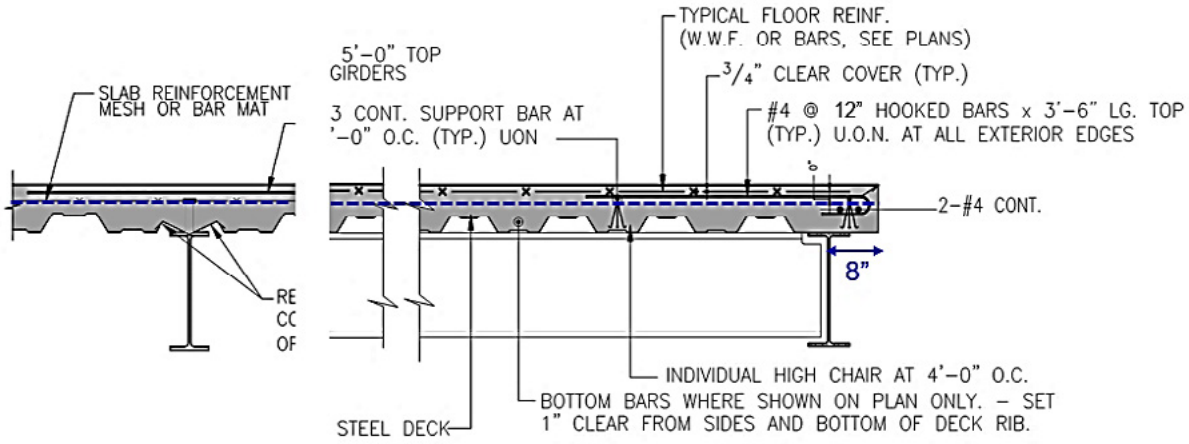

Figure 7-32. Slab mesh placement and edge anchoring.

Source: Courtesy of Simpson Gumpertz & Heger (2019).
Note: Mesh is shown in blue.

As illustrated in Figure 7-12, the protected girder/boundary beam-–column connections do not exceed approximately 200 °C during fire exposure. Hence, the degradation of connection material properties owing to heating does not need to be considered according to AISC 360, Appendix 4, Section 4d. Granted, the controlling connection demands occur very early in the fire (initial compressive thrust) and hours after the fire burns out (contractive tension). Accordingly, connection strength checks were conducted that demonstrate that the nominal design of the beam/girder–column connections is sufficient, except that the boundary beam and girder web bolt hole clear distance must be .modestly increased from 1-1/2 in. to 1-3/4 in., and the number of bolts for the boundary beam connections must be increased from three to four. Section 7.8 provides representative connection strength check calculations. Figures 7-37 and 7-38 illustrate the enhanced design of the girder/boundary beam–column connections.

As derived from the SAFIR single-bay model described in Section 7.6.3, the maximum girder-column and boundary beam–column connection rotation is 2.6 degrees and 4.8 degrees, respectively. Relevant test results of steel bolted–bolted double angle connections at elevated temperatures (SFER 2008) demonstrate that steel double angle connections (with three bolts) can generally handle up to approximately 18 degrees at 20 °C, 10 degrees at 450 °C, and 15 degrees at 650 °C without fracturing (ductile deformation only). Because of the relatively small rotation values observed in relation to these applicable test results (and contemplating the fact that the four-bolt and five-bolt design configurations would allow less rotation), the connection designs are judged as adequate in this respect. Notably, added connection prying resulting from bottom flange-to-column contact under rotation is not expected to occur because the girder–column and boundary beam–column connections have coped bottom flanges.

The infill beam–girder connections (shear tab connections) are not critical for Design 3 because the slab is designed to behave as a stable two-way membrane. Also, these members are composite and would remain suspended if these connections were to fail during fire exposure as observed during the Cardington Fire Tests (Lamont 2001). Granted, the punching shear strength of the slab was checked under a condition in which the infill beam–girder connections failed. Lastly, the infill beams are not relied on to laterally brace the girders because they are composite and compact, and the deformation/failure of these connections would serve as structural *fuses* to prevent excessive out-of-plane loads on critical periphery members and their connections to columns. As described in Section 4.2.1.1, a similar physical test result demonstrated the stability of the floor when the infill beams have lost nearly all their strength (i.e., the bottom flanges have laterally buckled).

The nine-bay SAFIR model was used to analyze unique restraint conditions with fire exposing an interior bay, an edge bay, and a corner bay. As shown in Figures 7-39 through 7-44, the connection axial demands vary from the baseline design condition and are summarized in Table 7-3. In general, the presence of contiguous bays allows for beneficial load redistribution and lower connection demands. However, it is observed that corner column connections have slightly increased demands, which requires that these connections be further enhanced. Lastly, the rotations at girder/boundary beam–column connections do not appreciably change as compared to the baseline design condition.

Table 7-3. Controlling Connection Axial Force Demands (% Change).

Condition	Boundary Beam Connection	Girder Connection
Interior	-57%	-55%
Edge	-11%	-42%
Corner	+13%	+5%

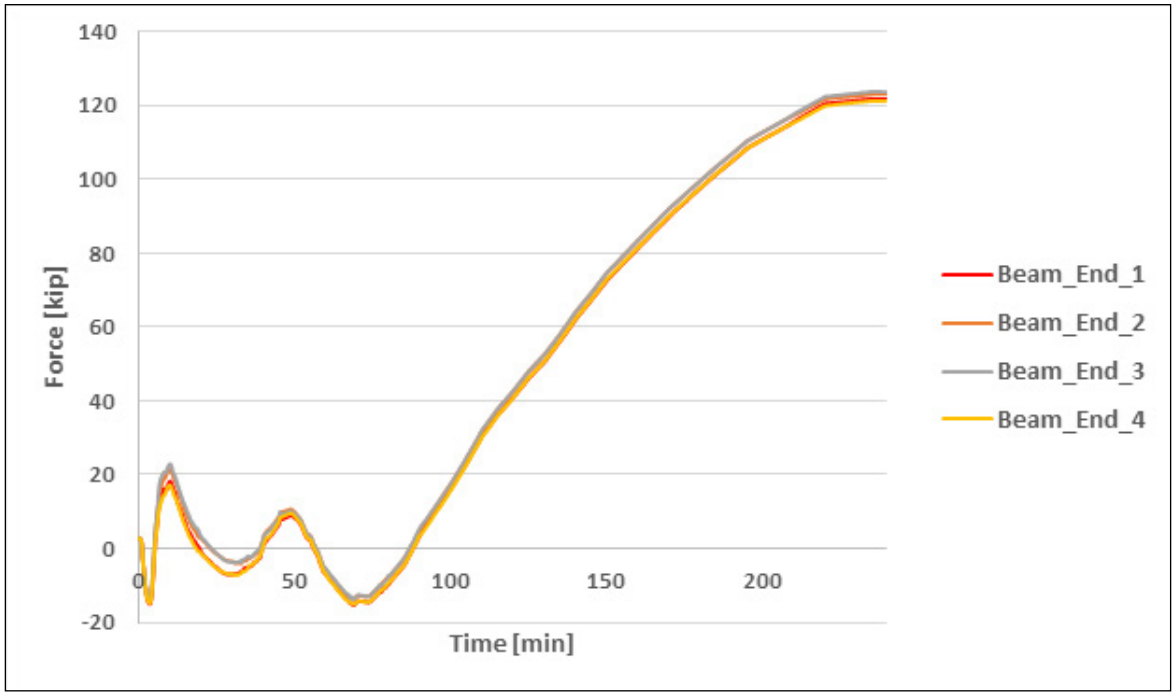

Figure 7-33. Boundary beam axial force histories (heating and cooling).
Source: Courtesy of Simpson Gumpertz & Heger (2019).

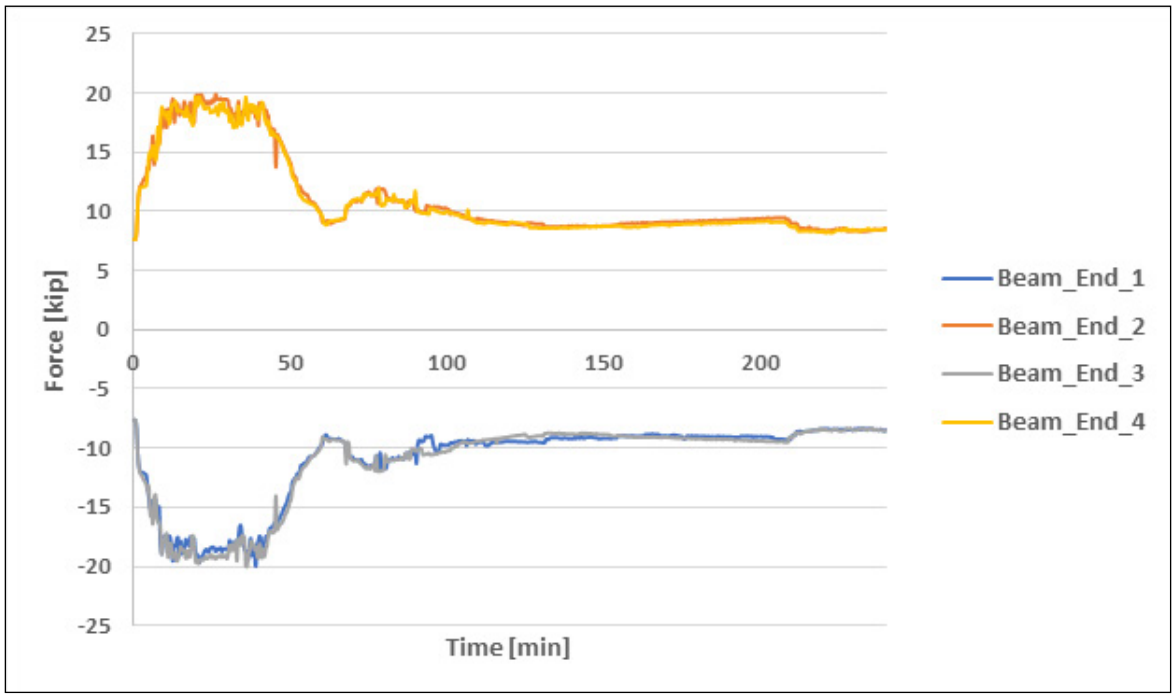

Figure 7-34. Boundary beam shear force histories (heating and cooling).
Source: Courtesy of Simpson Gumpertz & Heger (2019).

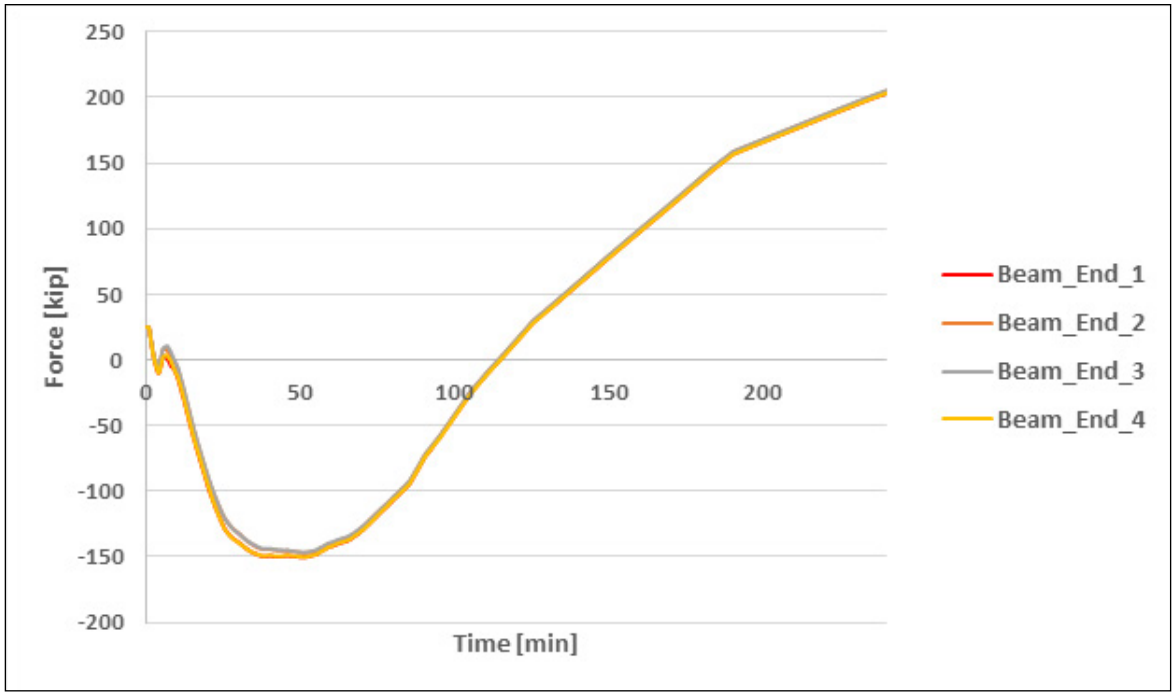

Figure 7-35. Girder axial force histories (heating and cooling).
Source: Courtesy of Simpson Gumpertz & Heger (2019).

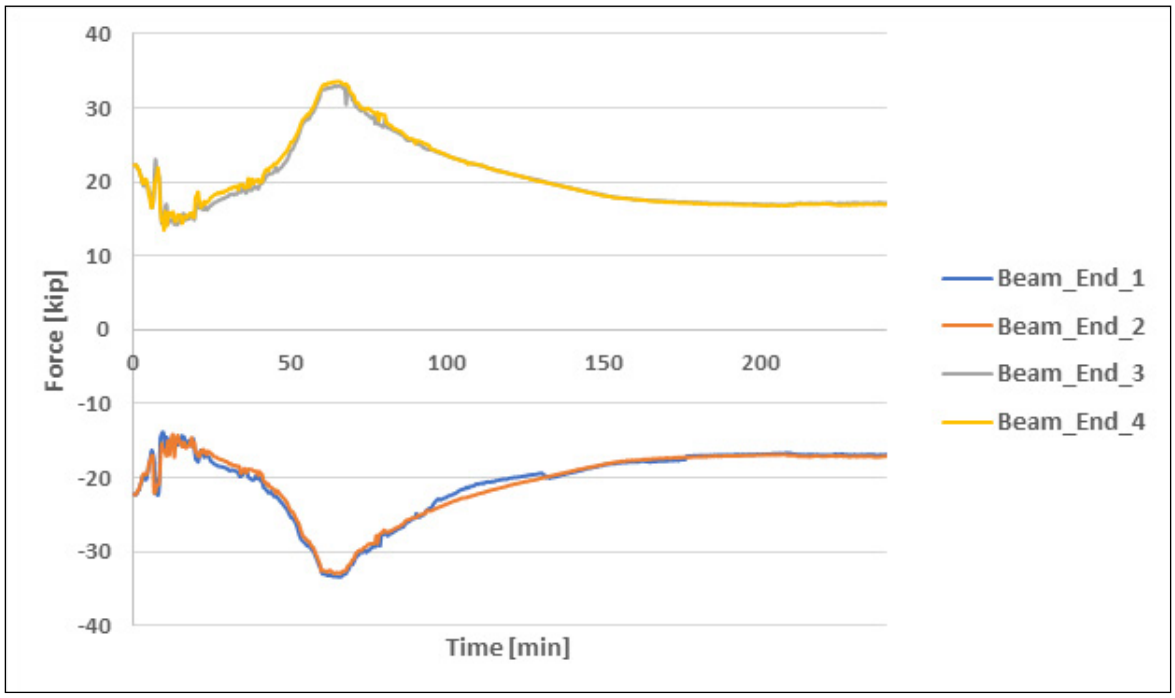

Figure 7-36. Girder shear force histories (heating and cooling).
Source: Courtesy of Simpson Gumpertz & Heger (2019).

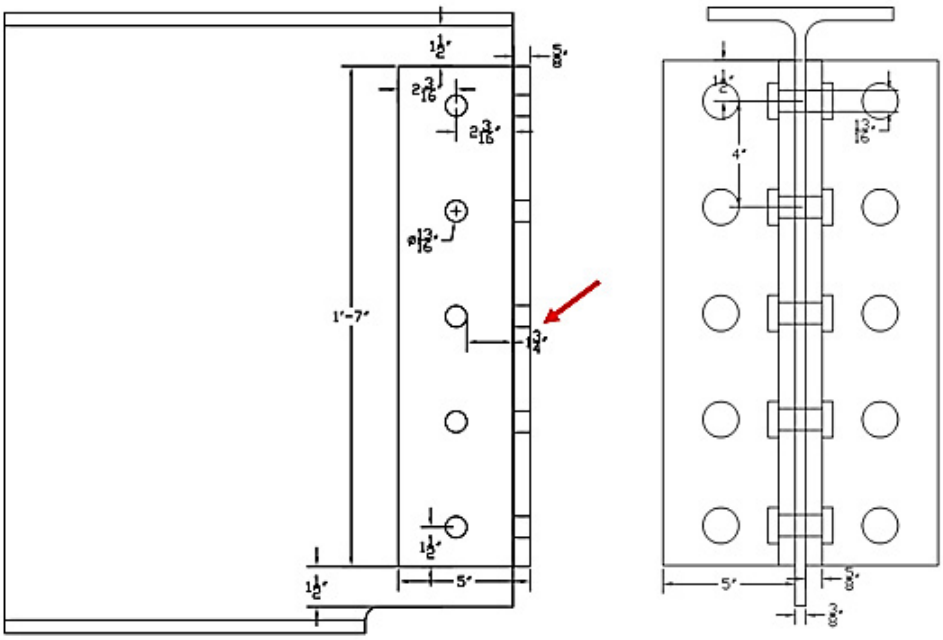

Figure 7-37. Girder–column connection.

Source: Courtesy of Simpson Gumpertz & Heger (2019).
Note: Enhancement is identified with arrow.

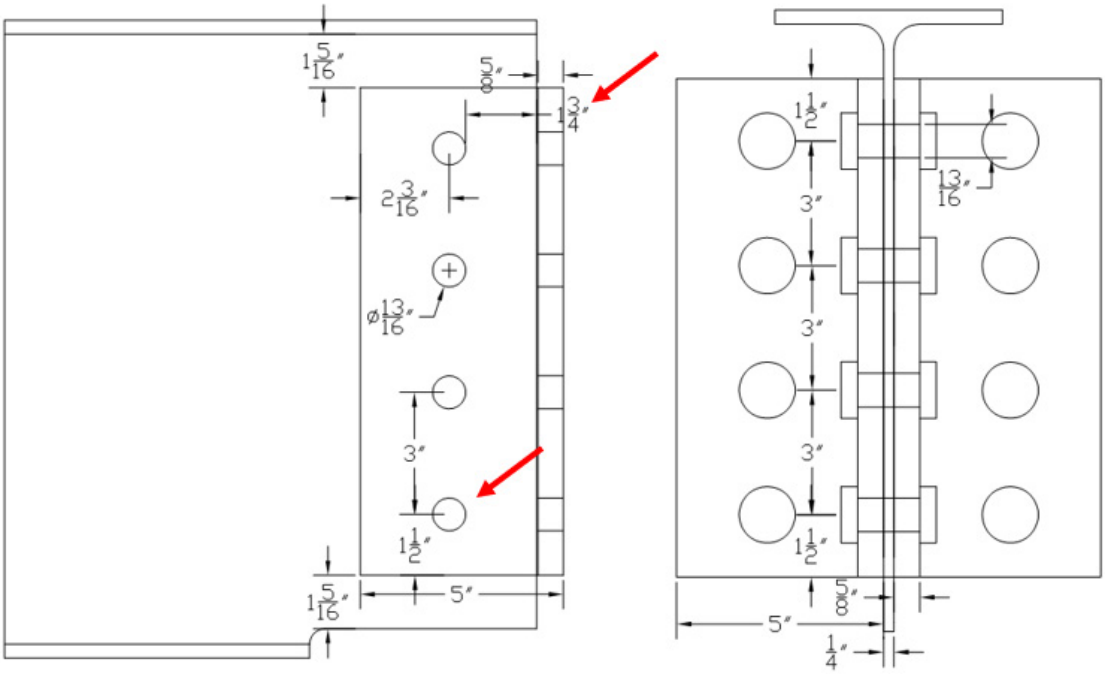

Figure 7-38. Boundary beam–column connection.

Source: Courtesy of Simpson Gumpertz & Heger (2019).
Note: Enhancement is identified with arrows.

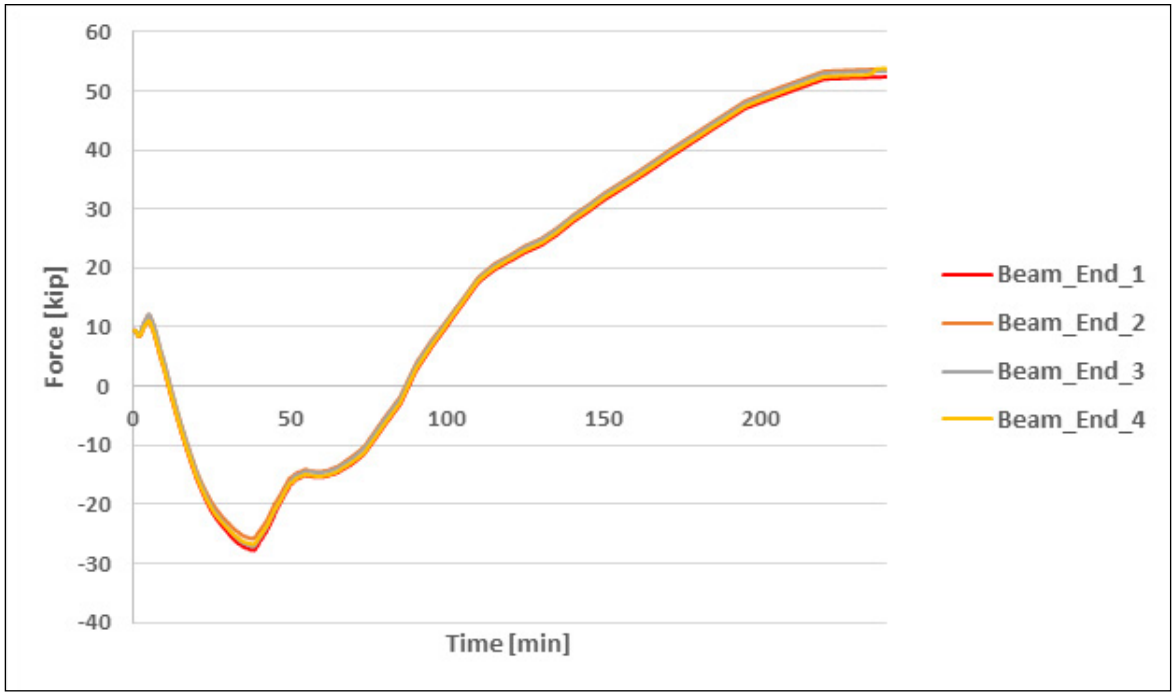

Figure 7-39. Boundary beam axial force histories (heating and cooling) (interior bay fire condition).

Source: Courtesy of Simpson Gumpertz & Heger (2019).

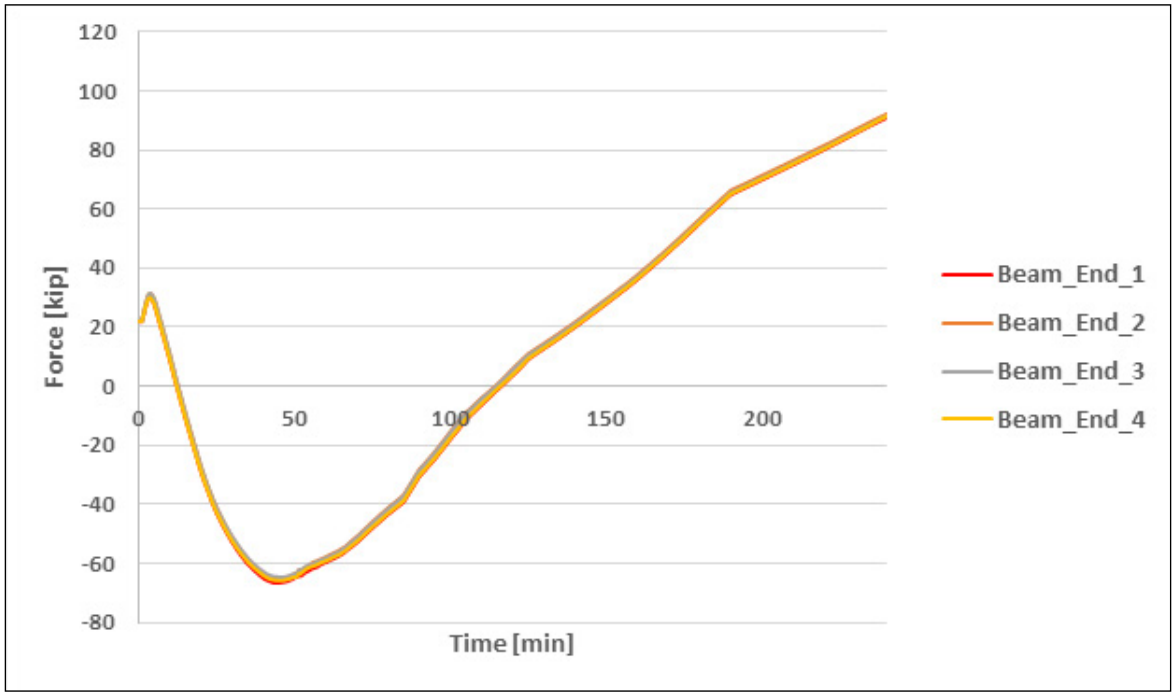

Figure 7-40. Girder axial force histories (heating and cooling) (interior bay fire condition).

Source: Courtesy of Simpson Gumpertz & Heger (2019).

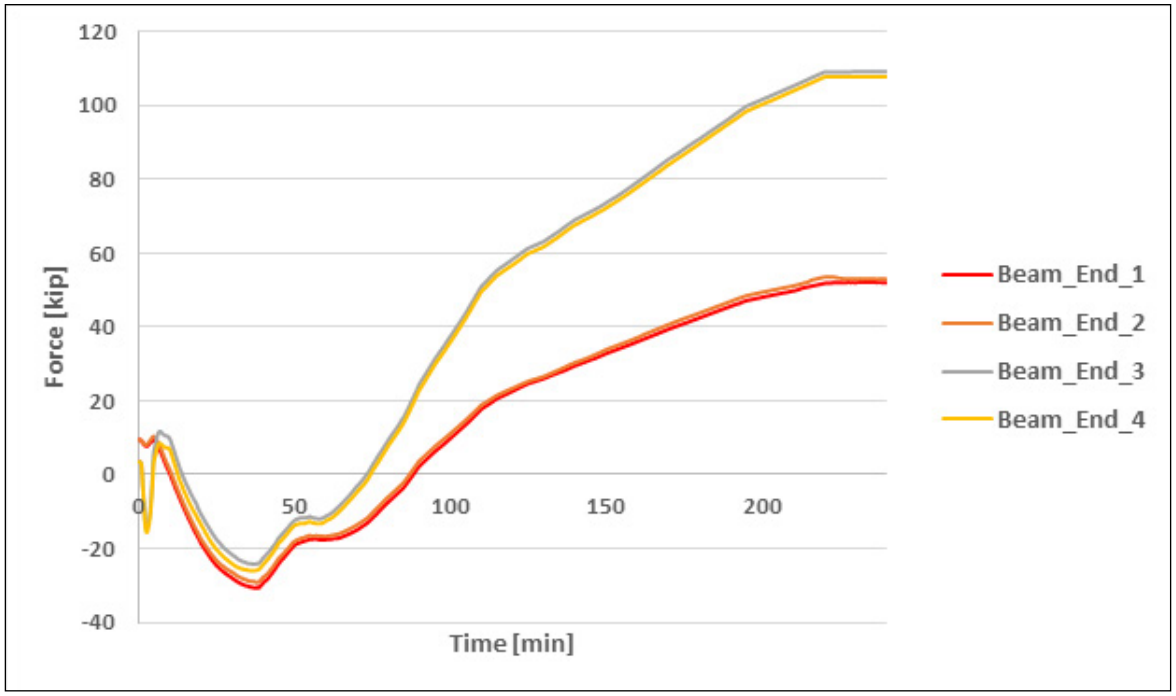

Figure 7-41. Boundary beam axial force histories (heating and cooling) (edge bay fire condition).

Source: Courtesy of Simpson Gumpertz & Heger (2019).

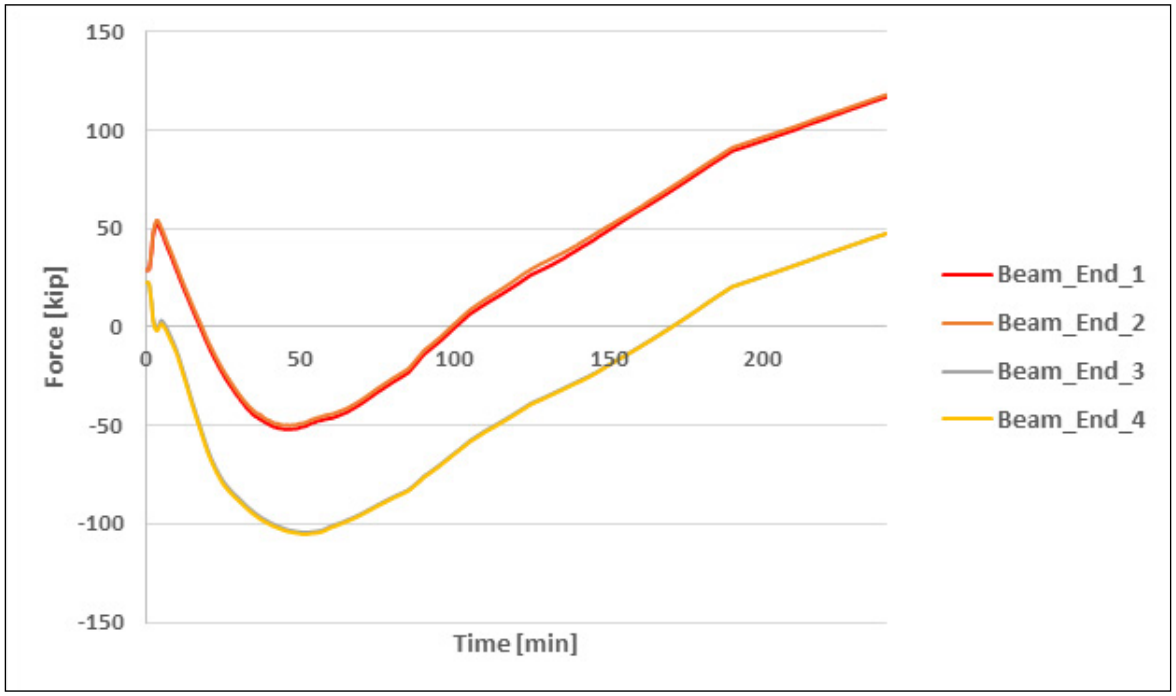

Figure 7-42. Girder axial force histories (heating and cooling) (edge bay fire condition).

Source: Courtesy of Simpson Gumpertz & Heger (2019).

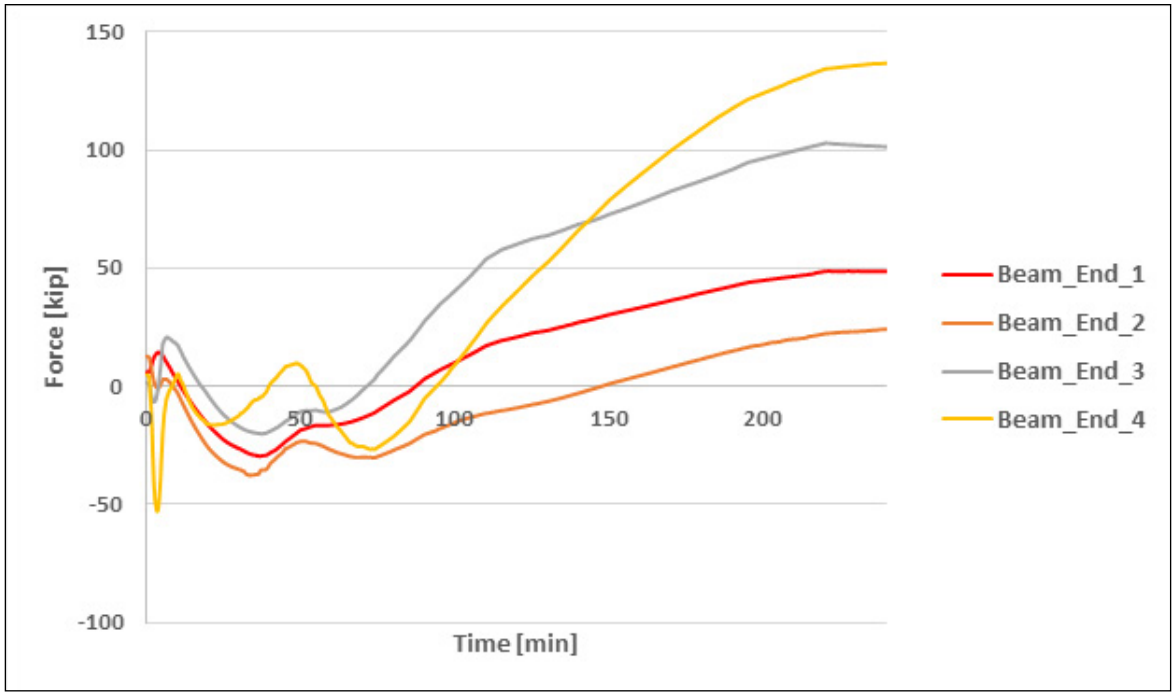

Figure 7-43. Boundary beam axial force histories (heating and cooling) (corner bay fire condition).

Source: Courtesy of Simpson Gumpertz & Heger (2019).

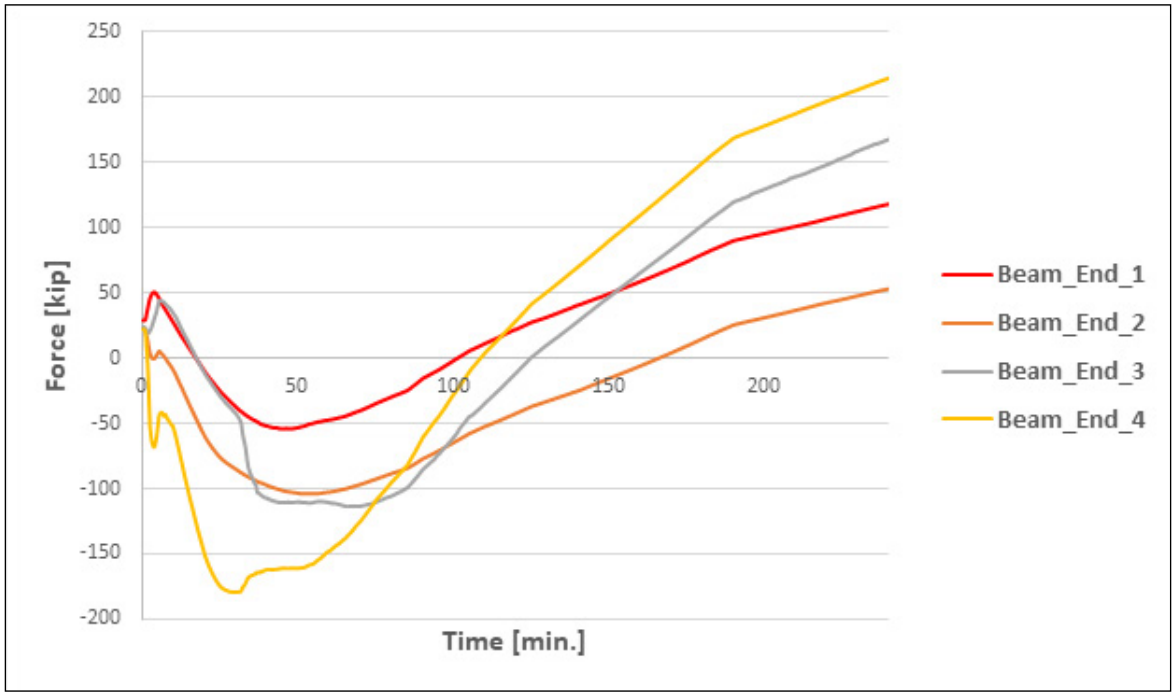

Figure 7-44. Girder axial force histories (heating and cooling) (corner bay fire condition).

Source: Courtesy of Simpson Gumpertz & Heger (2019).

7.6.6. Structural Columns

Hand calculations were conducted to check the strength of representative protected columns on various floor levels of the building. Comparing the calculated critical temperature for each representative column according to AISC 360, Appendix 4 to its maximum steel temperature (as discussed in Section 7.5) confirms that typical columns would survive full burnout. However, each perimeter column must be reoriented such that its strong axis is perpendicular to the building perimeter to adequately resist girder/boundary beam thermal expansion/contraction at the floor level above the fire exposure, as confirmed by hand calculations. There would be significantly less expansion/contraction at the floor level directly below the fire exposure owing to the insulating effect of the top slab and lack of buoyancy-driven hot gas exposure. Because the building utilizes braced frames at the core for its lateral-force-resisting system and the perimeter structure is not designed as a moment frame (i.e., moment connections are not present around the perimeter), reorienting the perimeter columns would not appreciably affect the lateral-force-resisting system of the building. At the corners of the building, hollow steel section (HSS) columns should be used instead of the nominally specified steel W-shape columns to adequately resist girder/boundary beam thermal expansion/contraction in two free-end directions simultaneously.

The perimeter and corner columns would not be heated uniformly as assumed for these calculations; however, such effects [i.e., increase in compression on the exterior (unheated) side owing to thermal bowing and increase in compression on the interior (heated) side owing to a shift in the neutral axis of the cross section toward the cooler side (Garlock and Quiel 2008)] can be reasonably neglected because these effects would control at the midheight of the fire floor, not at the ceiling level of the fire floor where floor expansion creates a controlling column bending condition, as considered previously. Also, the described effects resulting from nonuniform heating tend to cancel each other out to a certain extent (though not necessarily completely).

7.6.7 Roof Structures

As discussed in Section 7.4, the roof framing can be maintained at temperatures of 450 °C or lower with the inclusion of passive combination heat vents/skylights as permitted by Design 3. For this case, hand calculations per AISC 360, Appendix 4 were conducted to demonstrate that the majority of the roof framing members can be left unprotected. These calculations also demonstrate that roof member connections would experience very low rotations (1 degree or less with simplifying assumptions). Hence, these connections (if enhanced as described in Section 7.6.5) are judged as adequate under this condition when left unprotected and higher-order analyses are not necessary.

7.7 DESIGN SUMMARY

For Design 0, all structural steel members shall be protected with traditional spray-applied insulation as specified in Tables 4 to 6 of the Design Brief. For this case in isolation, structural performance would not be assessed.

As discussed in Section 7.1, Design 1 must satisfy the minimum performance expectations for safe occupant evacuation absent any structural modifications. However, because the ASET (approximately 12 min as discussed in Section 7.6.3) was determined to be less than the RSET (as discussed in Section 7.2) and increasing the level of insulation would not appreciably change these

results, Design 1 is not satisfied. Hence, Design 2 is not satisfied, which requires a higher level of performance as compared to Design 1. These designs are not viable (absent any structural upgrades) given the combination of the nominal structural design and the fire resistance rated floor assembly assigned. Notwithstanding, the results of Design 3 demonstrate that the beam/girder–column connections require modest enhancements to perform adequately, even though they are protected similarly. Also, the infill member-girder single shear tab connections may govern the capacity of the floor system (not specifically analyzed) because the nominal mesh is not adequate for stable slab two-way action as demonstrated by the results of Design 3. Overall, Design 1 and Design 2 share multiple structural fragilities at elevated temperatures, which make a reliable design infeasible to achieve when only the level of insulation can be adjusted.

Figures 7-44 through 7-50 summarize the distribution of structural insulation for Design 3. In this case, nearly all secondary floor beams may be left unprotected; the exception is those located within the core of the building in which the slab typically has large penetrations for utilities, elevators, stairs, and so on, which generally inhibit the ability of the slab to achieve reliable compressive-tensile membrane action in these areas. The protected floor members shall receive a 3/4 in thickness of traditional spray-applied insulation (*standard specification* option), or alternatively, these members may be protected with shop-applied thin-film (paint) intumescent that is certified by the manufacturer to limit the temperature of the girders and boundary beams to 500 °C and 600 °C (or lower), respectively, under a fire intensity that is deemed equivalent to, or greater than, the above-design fuel load with low ventilation fire case (*performance specification* option). Because of the relatively higher weight-to-heated-perimeter of the girders compared to the boundary beams, it is likely that a uniform mil thickness of intumescent paint would suffice for these performance requirements. Moreover, upsizing members typically allows for thinner coats of intumescent if deemed more economical. Bolts installed in the field shall be protected with commercially available premolded intumescent bolt caps, eliminating the need for field-spraying of connections. Otherwise, the bolts may be left unprotected if the intumescent coating on adjacent surfaces is deemed as capable of properly shielding the bolts on expansion of the coating according to the manufacturer. The faying surfaces of the beams and connection components must be appropriately masked off if intumescent spraying is conducted off-site to prevent difficulties during the steel erection process. As discussed in Section 4.2.1.1, the performance specification option is the far superior choice in many respects.

In addition to increasing the slab mesh reinforcement from 6x6-D2.9x2.9 to 4x4-D5.4x5.4, the mesh must be properly lapped and anchored to the composite girders/boundary beams at the outside edges of the building (spandrel beams), as discussed in Section 7.6.4. Columns shall receive an 11/16 in. thickness of traditional spray-applied insulation or, alternatively, an equivalent board-type encasement. The latter is strongly preferred as it would uphold the primary benefits of the performance specification option as discussed in Section 4.2.1.1. Also, each perimeter column must be reoriented such that its strong axis is perpendicular to the building perimeter, and HSS columns should be used instead of the nominally specified steel W-shape columns at the corners of the building. Lastly, modest girder/boundary beam–column connection enhancements are required as described in Section 7.6.5.

As illustrated in Figures 7-46 and 7-50, the majority of the roof structures may be left unprotected if standard 4 ft × 8 ft (165 °F) passive combination heat vents/skylights are installed (six vents evenly distributed within each 30 ft × 30 ft structural bay). The exception is the roof framing within the core of the building, in which the installation of heat vents would be difficult, given the many potential sources of interference, such as shaft enclosures.

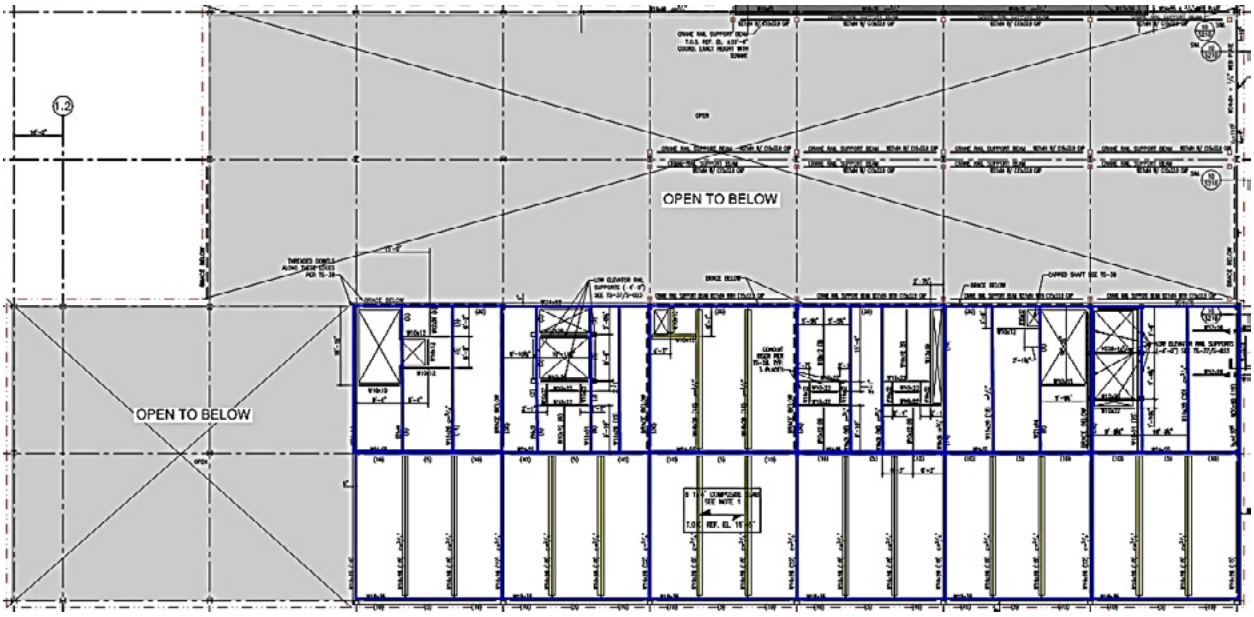

Figure 7-45. Design 3 Structural insulation distribution (Level 2 framing).

Source: Courtesy of Simpson Gumpertz & Heger (2019).

Note: Insulation is shown in blue; unprotected members are shown in yellow.

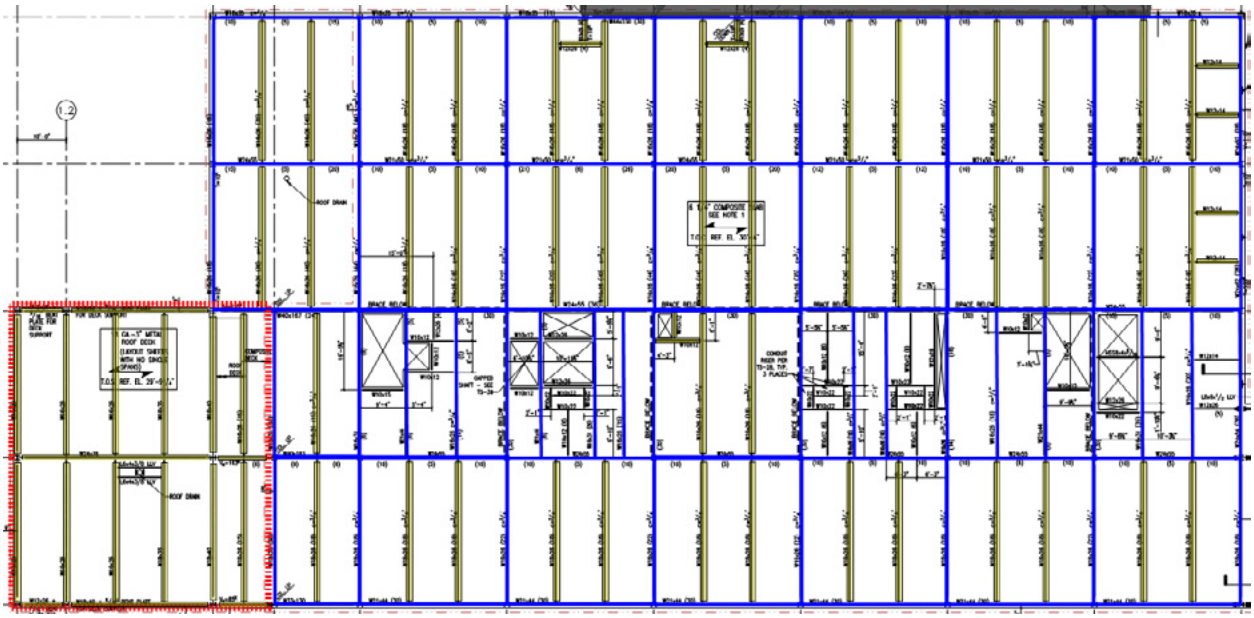

Figure 7-46. Design 3 Structural insulation distribution (Level 3 framing).

Source: Courtesy of Simpson Gumpertz & Heger (2019).

Note: Insulation is shown in blue; unprotected members are in yellow; roof area is designated in red.

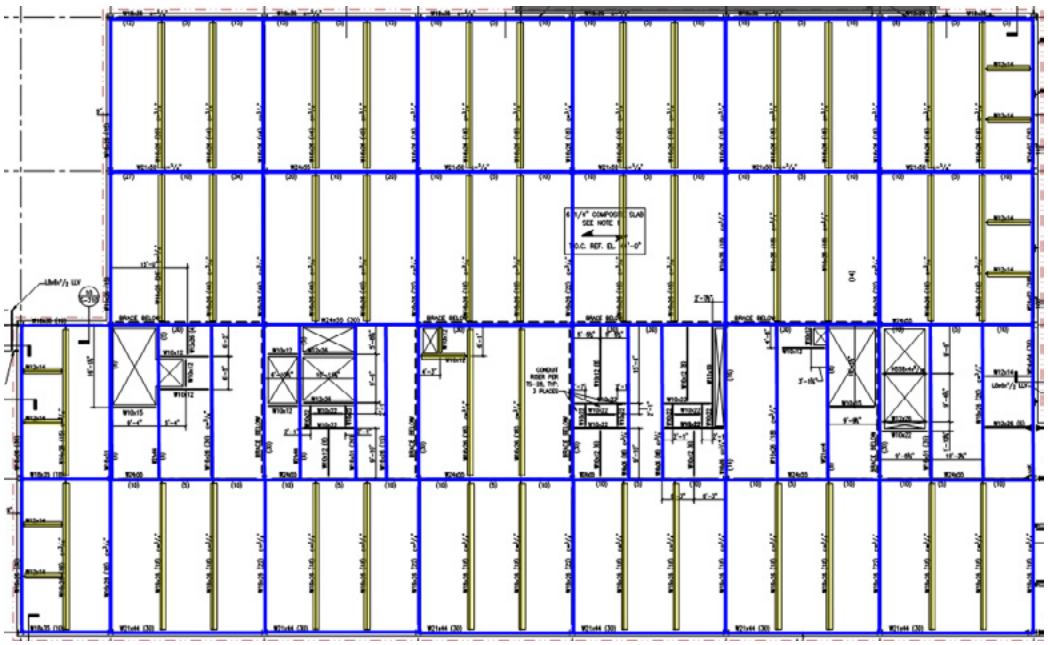

Figure 7-47. Design 3 Structural insulation distribution (Level 4 framing).

Source: Courtesy of Simpson Gumpertz & Heger (2019).

Note: Insulation is shown in blue; unprotected members are shown in yellow.

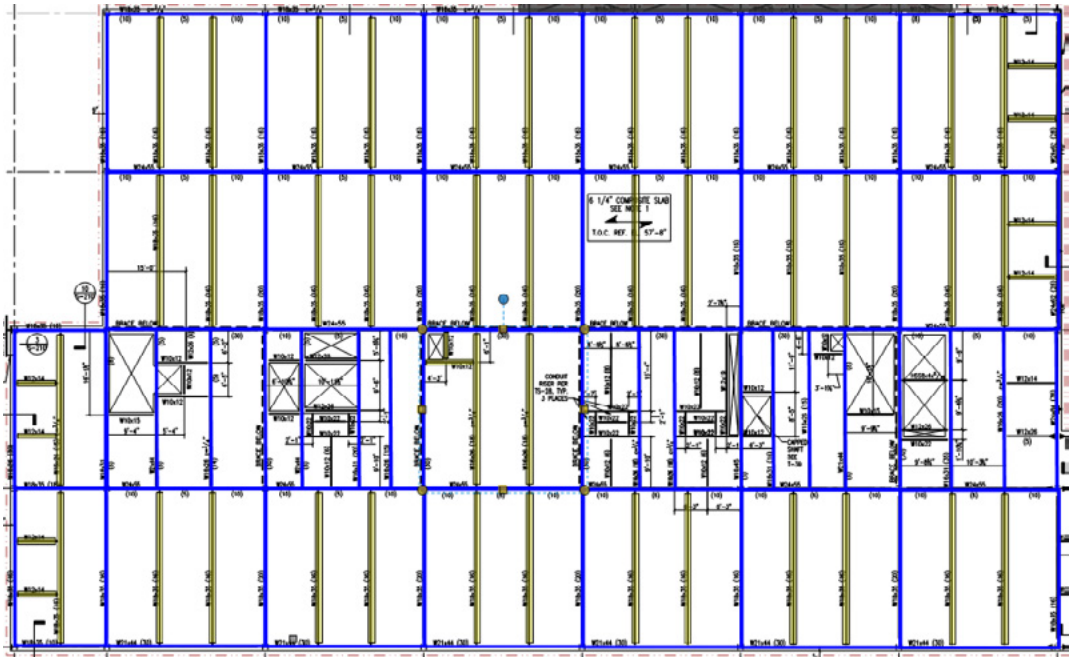

Figure 7-48. Design 3 Structural insulation distribution (Level 5 framing).

Source: Courtesy of Simpson Gumpertz & Heger (2019).

Note: Insulation is shown in blue; unprotected members are shown in yellow.

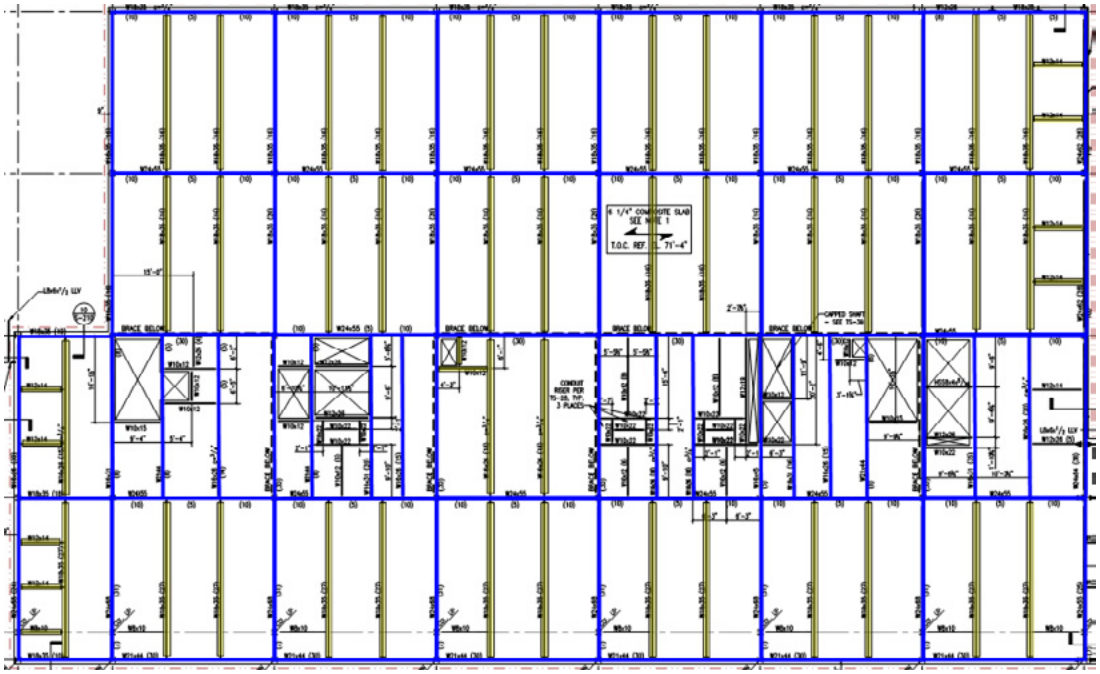

Figure 7-49. Design 3 Structural insulation distribution (Level 6 framing).

Source: Courtesy of Simpson Gumpertz & Heger (2019).

Note: Insulation is shown in blue; unprotected members are shown in yellow.

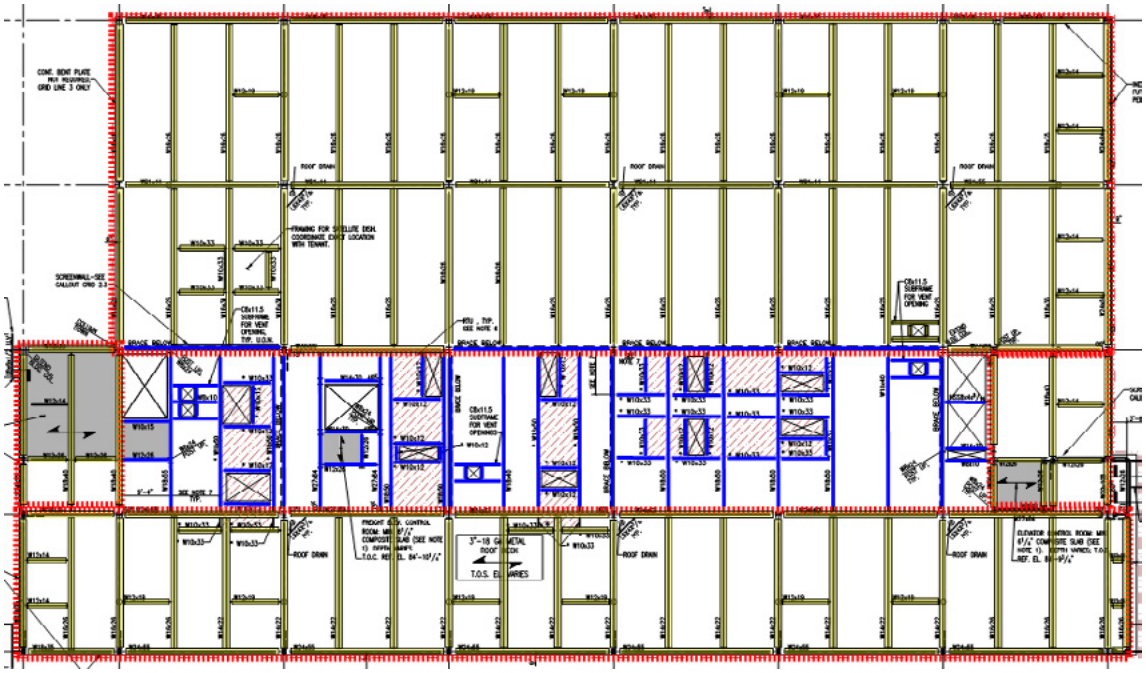

Figure 7-50. Design 3 structural insulation distribution (roof framing).

Source: Courtesy of Simpson Gumpertz & Heger (2019).

Note: Insulation is shown in blue; unprotected members are shown in yellow.

7.7.1 Potential Economic Impacts

Design 0 represents how steel structures are commonly protected from fire in the United States, in which spray-applied insulation (fireproofing) is applied to structural members on the site in a uniform fashion. PBSFD provides the potential to use alternative methods of fire protection which could provide beneficial economic impacts to a given project. For instance, by fine tuning the distribution and thicknesses of applied fire protection, some projects have the potential to benefit from improvements to construction schedule and/or material costs. As harnessed for Design 3, the shop-application of a thin-film intumescent coating (or any other protective material with similar attributes as described herein) has the potential to enhance construction efficiency; however, such coatings could be prohibitively expensive when required for all structural members, and prescriptive requirements may necessitate coating thicknesses that are not suitable for shop-application.

The SGH team used Design 3 to demonstrate how PBSFD allows for a targeted insulation strategy that shifts fire protection from reliance on insulative capacity to the intrinsic structural system strength. It is this shift that enables the use of a protective coating that is qualified for its ability to meet specific structural performance metrics (such as to uphold the slab yield line design assumption as described in Section 7.6.3). Also, the sizing of structural members can be modified to optimize protective coating thicknesses for a given structural system. For example, the cost of intumescent protection and the potential for damage during transport can both increase nearly exponentially as the coating thickness increases, so member size optimization in conjunction with a performance specification may prove critical (Newman et al. 2005).

The use of PBSFD with performance-specified off-site applied protection has the potential to improve the construction process related to schedule and material costs. Granted, such potential would vary from building to building depending upon the level of speculation (such as time to rent), construction complexity (such as tight access), and any other project-specific aspects. Hence, PBSFD in practice should include an exploratory phase that involves both the owner (to discuss the potential project impacts) and building authority (to discuss the acceptability of PBSFD), as the application of this approach does not necessarily guarantee cost savings, nor are building authorities obligated to accept this approach. Regardless, the application of PBSFD according to the requirements of ASCE 7-16, Appendix E does explicitly evaluate structural fire safety, which may justify its use, regardless of the economics or other potential project impacts.

7.7.2 Other Potential Impacts

Aside from the economic impact, Design 3 may provide other potential benefits described as follows.

Carbon Footprint

In recent years, the carbon footprint of building construction has gained increased attention from community stakeholders. PBSFD enables the design team to examine a variety of alternatives for fire protection that could contribute to achieving overall project goals.

Aesthetics

The potential to consider structural performance based on structural analysis could provide project owners and architects added design opportunity for a mix of exposed and coated structural elements with a reduced extent of concealment. Using PBSFD enables structural engineers to be strategic about fire protection methods for every area of the structure.

Quality Control and Site Safety

As demonstrated by Design 3, the use of PBSFD has the potential to improve fire protection quality control and site safety by facilitating the use of shop-applied methods, which are easier to control than field-applied methods.

7.8 CONCLUSIONS

Simpson Gumpertz & Heger analyzed a previously completed, 6-story, Risk Category II office building located on the East Coast to compare the safety and practical implications (including economics) of applying prescriptive (SFRD) and PBSFD approaches. The following conclusions were derived based on analysis of this specific building, and do not necessarily apply to all buildings or circumstances:

- PBSFD revealed key structural system vulnerabilities under fire exposure, which would not have been revealed if SFRD was employed.
- Thermal restraint dominates the behavior of the structural system (which cannot be addressed with insulation alone), with degradation of stiffness and strength a secondary factor (typically addressed with insulation) (LaMalva et al. 2020).
- Structural restraint of thermal expansion is predominately deleterious to structural system performance under fire exposure.
- Modest structural upgrades per PBSFD analysis dramatically increased the level of structural fire safety.
- Increasing the level of structural insulation (absent structural enhancements) does not appreciably improve the level of structural fire safety.
- PBSFD has the potential to significantly improve and enhance project economics, carbon footprint, aesthetics, quality control, and site safety conditions when harnessed with performance-specified off-site applied thin-film (paint) intumescent protection.
- Potential economic benefit of PBSFD increases as the level of project speculation and construction complexity increases.

- Potential cost savings provided by PBSFD may outweigh the cost of modest structural enhancements required and the increased material cost for intumescent may be offset and possibly advantaged as compared to traditional fireproofing.

- PBSFD burnout design may be justified, regardless of economic benefits to structural system, as it confirms adequate structural system performance under fire exposure, especially for buildings with a high consequence of failure.

- PBSFD requires structural engineering competency (SFPE 2018).

7.9 REPRESENTATIVE ENHANCED CONNECTION LIMIT STATE CHECK

As discussed in Section 7.6.5, Figures 7-51a through 7-51x provide a representative enhanced connection limit states check calculation.

Strength of Ductile All Bolted Double-Angle Shear Connections:
By: Adel Mashayekh
Checked By: Keith Palmer / Kevin LaMalva

Note: This is for beam to column connections in which only beam **bottom** flange is coped.

- Variables needed for strength calculations of double-angle bolted bolted connections:

Lm1xm2xtxL: Angle dimensions (m1, m2, t) and L is the length
eb: distance from bolt line on the beam web of the angle to the column flange
Fy, Fu: Yield and Ultimate strength of angles
g: gage length on angle to calculate prying action (see Fig. below)
Lev: distance from center of the top or bottom farthest bolt to edge of coped area on the beam web (see Fig. above)
Lright: distance from center of bolt on the beam web to the edge of angle (see Fig. below)
Lleft: distance from center of bolt on the beam web to the edge of beam web (see Fig. below) which needs to be 1.75 in however, to be general it is considered an input variable.

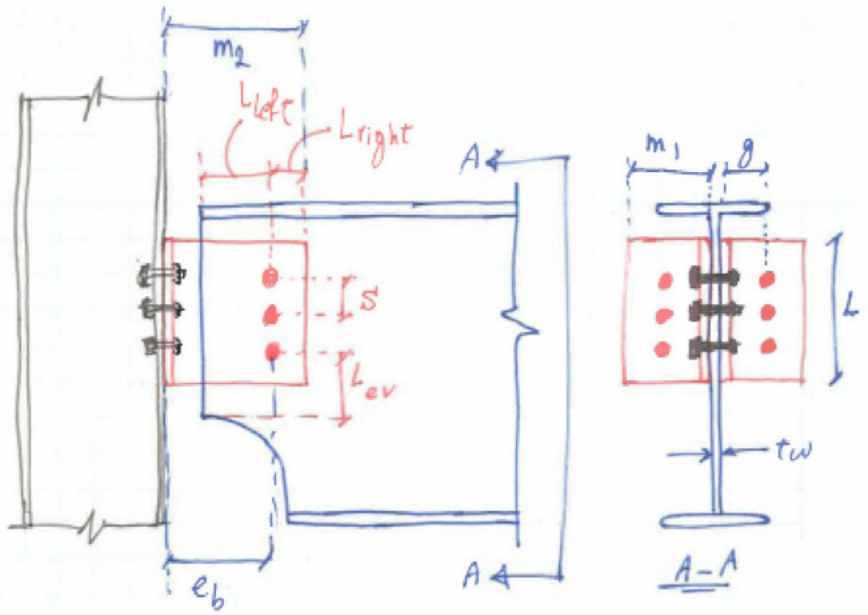

Created with PTC Mathcad Express. See www.mathcad.com for more information.

Figure 7-51a. Enhanced connection limit state check.
Source: Courtesy of Simpson Gumpertz & Heger (2019).

Ltoedge: distance from center of top/bottom hole to edge of angle

tw: beam web thcikness

Lcedge:clear distance from top/bottom hole to edge of angle
db: bolt diameter
Lcbolts: clear distance between holes
n: number of bolts along one line on one angle
ϕ_{75} and ϕ_{90} is an indication for type of failure (brittle = 0.75 and ductile = 0.9). They are set to 1.0 in this sheet as we only want the nominal strength.

Fub: bolt tensile strength
Ts: Temperature
S: Spacing between bolts
Fybw, Fubw: Yield and ultimate strength of beam web (50, and 65 ksi)
Typethread: Threads included (N) or Excluded (X)

The example below is for **W16x26 Boundary Beam** with **2L4X4X5/8x11.5** angles with **(4) 3/4 inch A325-N bolts.**
Vuv: Vertical Shear Force (kip)
Vuh: Horizontal Shear Force (kip)
NuC: Compressive Axial Force (kip)
NuT: Tensile Axial Force (kip)

Figure 7-51b. Enhanced connection limit state check.
Source: Courtesy of Simpson Gumpertz & Heger (2019).

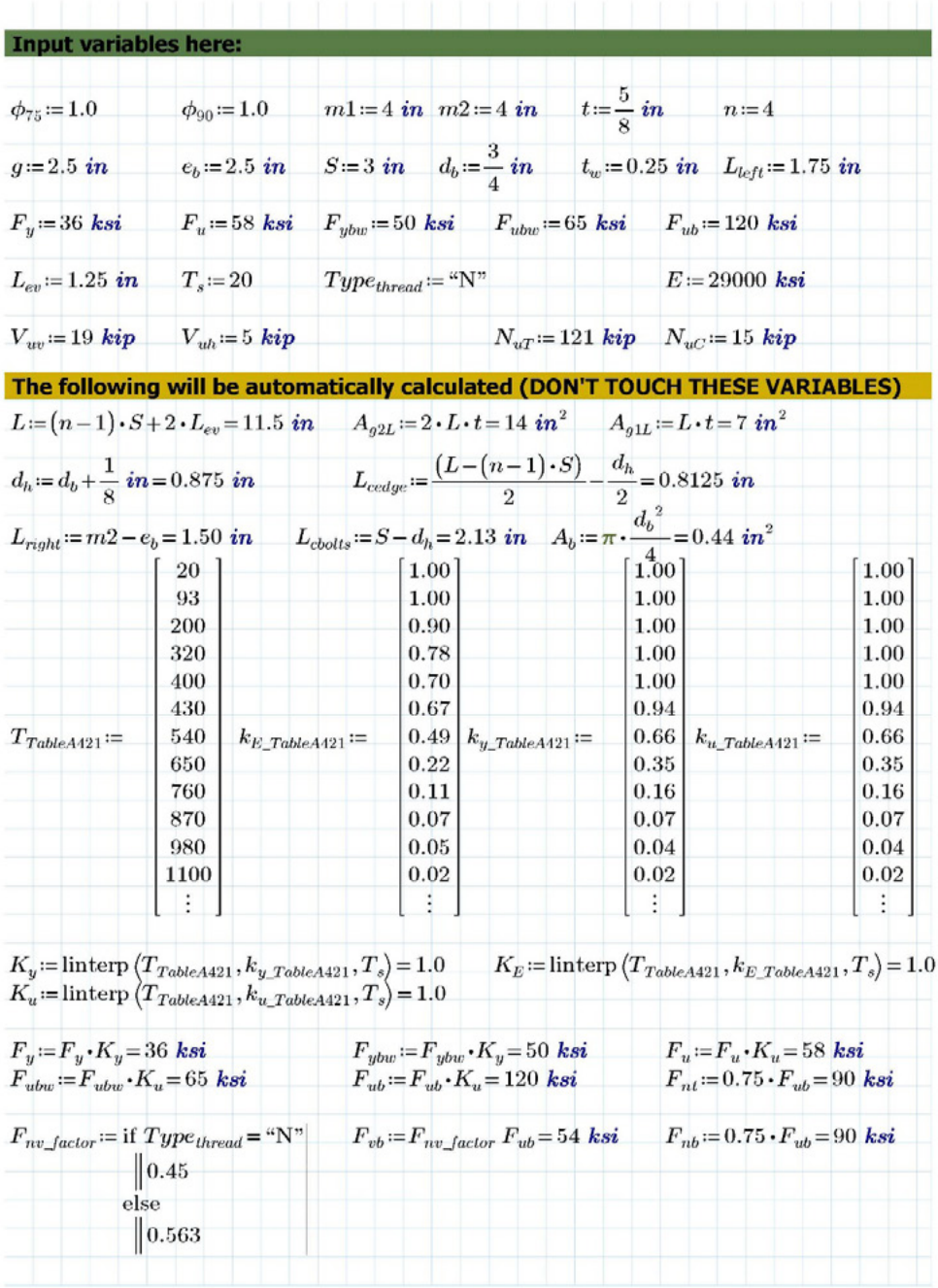

Figure 7-51c. Enhanced connection limit state check.

Source: Courtesy of Simpson Gumpertz & Heger (2019).

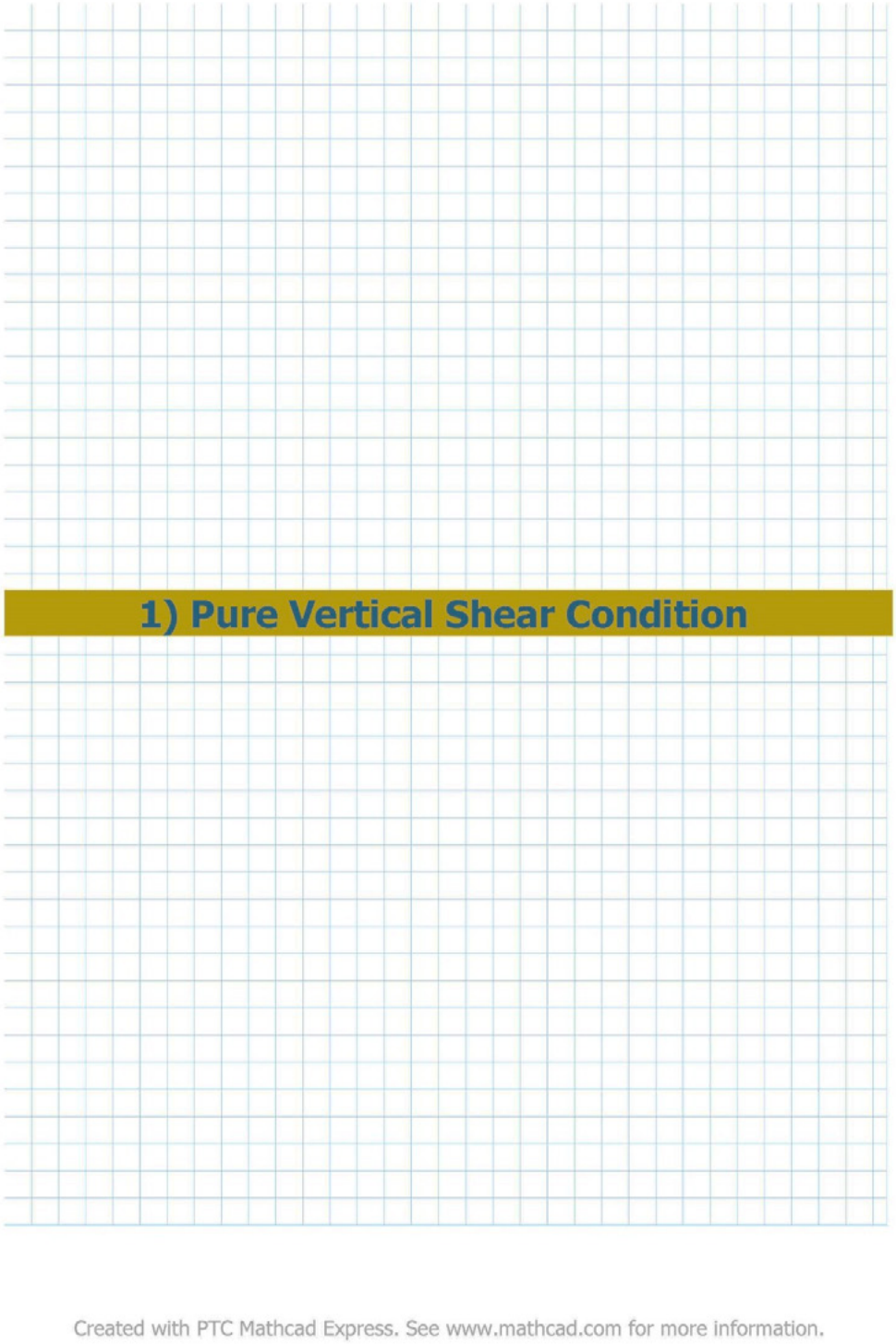

Figure 7-51d. Enhanced connection limit state check.
Source: Courtesy of Simpson Gumpertz & Heger (2019).

1) Yielding of Double Angles in Shear:

The first step in design is to select double angles and design them for shear yield failure mode by using the following equations in LRFD and ASD:

$V_u \le \phi_y V_y$ (LRFD) (2.3a)

$V \le V_y / \Omega_y$ (ASD) (2.3b)

In the above equations, $\phi_y V_y$ and V_y / Ω_y are design shear strength in LRFD and ASD respectively, and

V_u = applied factored shear to the connection in LRFD

V = applied shear to the connection in ASD

$V_y = 0.60 F_y A_g$

$\phi_y = 0.90$ (LRFD) and $\Omega_y = 1.50$ (ASD)

$A_g = 2Lt$

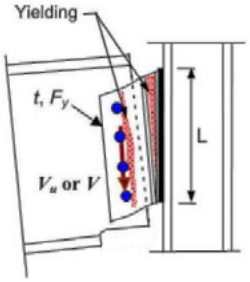

Figure 2.12. Yield Failure Mode

For definitions of the other terms in the above equations, please see the "Notations" section on page 4.

$$\phi_{90} V_{yLS1} := \phi_{90} \cdot 0.6 \cdot F_y \cdot \left(A_{g2L}\right) = 311 \ kip$$

$$DCR_1 := \frac{V_{uv}}{\phi_{90} V_{yLS1}} = 0.06$$

Figure 7-51e. Enhanced connection limit state check.

Source: Courtesy of Simpson Gumpertz & Heger (2019).

2) Bearing Failure of the Double Angle, Beam Web, or Supporting Member:

2.3.b. Bearing Failure of the Double Angle, Beam Web, or Supporting Member (Limit State 2)

For double angles, the limit state of the bearing failure should be checked against the shear yield capacity to ensure that the strength in the bearing is greater than the strength in the shear yielding:

$\phi_{br} V_{br} > \phi_y V_y$ (LRFD) (2.4a)
$V_{br}/\Omega_{br} > V_y / \Omega_y$ (ASD) (2.4b)

In the above equations, $\phi_{br} V_{br}$ and V_{br}/Ω_{br} are the design strength in LRFD and ASD, respectively, and

$V_{br}=\Sigma(1.2L_c t F_u \le 2.4\, d_b\, t F_u)$
$\phi_{br} = 0.75$ (LRFD) and $\Omega_{br} = 2.00$ (ASD)

The term $1.2L_c t F_u$ in the above equations is the bearing capacity of each bolt using its own L_c, where L_c is the greater of the distance from the edge of the bolt hole to the edge of the plate or to the edge of the adjacent bolt hole in the direction of the applied shear. For definitions of the other terms in the above equations, please see the "Notations" section on page 4.

Equation 2.4a or 2.4b should be applied not only to angles but also to the beam web and the flange of the supporting column, and the bearing capacity of all three elements needs to be greater than the shear yield capacity of the angles.

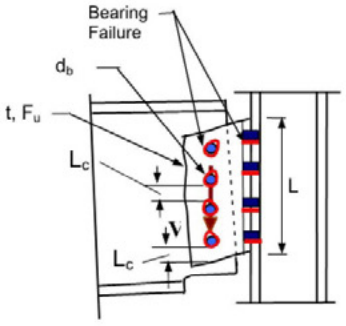

Figure 2.13. Bearing Failure Mode

on the angles

$$V_{br} := 2 \cdot \left(min\left(1.5 \cdot L_{cedge} \cdot t \cdot F_u, 3 \cdot d_b \cdot t \cdot F_u\right) + min\left(1.5 \cdot (n-1)\ \left(L_{cbolts} \cdot t \cdot F_u\right), 3 \cdot (n-1) \cdot d_b \cdot t \cdot F_u\right)\right) = 577.7\ \textit{k}$$

$$\phi_{75} V_{brLS2A} := \phi_{75} \cdot V_{br} = 577.7\ \textit{kip}$$

on the beam web

$$V_{br} := \left(3 \cdot d_b \cdot t_w \cdot F_{ubw} + min\left(1.5 \cdot (n-1)\ \left(L_{cbolts} \cdot t_w \cdot F_{ubw}\right), 3 \cdot (n-1) \cdot d_b \cdot t_w \cdot F_{ubw}\right)\right) = 146.3\ \textit{kip}$$

$$\phi_{75} V_{brLS2B} := \phi_{75} \cdot V_{br} = 146.3\ \textit{kip}$$

$$\phi_{75} V_{brLS2} := min\left(\phi_{75} V_{brLS2A}, \phi_{75} V_{brLS2B}\right) = 146.3\ \textit{kip}$$

$$DCR_2 := \frac{V_{uv}}{\phi_{75} V_{brLS2}} = 0.13$$

3) Edge Distance Failure in the Angles or in the Beam Web:

This failure is precluded by satisfying the AISC minimum edge distance requirement

Figure 7-51f. Enhanced connection limit state check.
Source: Courtesy of Simpson Gumpertz & Heger (2019).

4) Net-Area Fracture of the Double Angle:

2.3.d. Net-Area Fracture of the Double Angle (Limit State 4)

For the angles, the design shear strength for net area fracture in LRFD and the allowable shear force for net area fracture in ASD are $\phi_n V_n$ and V_n/Ω_n, respectively, where:

$$V_n = 0.60 F_u A_{nv}$$

$$\phi_n = 0.75 \text{ (LRFD) and } \Omega_n = 2.00 \text{ (ASD)}$$

The term A_{nv} in the above equations is the "net section for shear." Currently, the AISC specifications (AISC-ASD 1989 and AISC 1999) define the net area in shear to be the area along the centerline of the bolts. However, as discussed in Astaneh-Asl (2005), the actual net section fracture occurs not through the centerline of the bolts but through the line at the edge of the bolts, Figure 2.14.

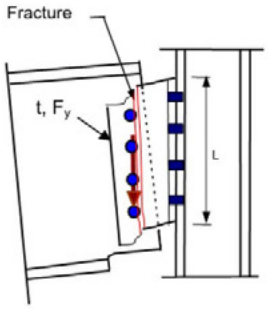

Figure 2.14. Net Section Fracture

$$A_{nv} := 2 \cdot \left(A_{g1L} - 0.5 \cdot n \cdot d_h \cdot t\right) = 12 \ in^2$$

$$\phi_{75} V_{nLS3} := \phi_{75} \cdot 0.6 \cdot F_u \cdot A_{nv} = 424 \ kip$$

$$DCR_4 := \frac{V_{uv}}{\phi_{75} V_{nLS3}} = 0.045$$

Figure 7-51g. Enhanced connection limit state check.
Source: Courtesy of Simpson Gumpertz & Heger (2019).

5) Fracture of Bolt Group:

a. Design of bolts on the beam web. The bolts connecting the beam web to the double angles are subjected to pure shear. The limit state of shear fracture of these bolts should be checked against the shear yield capacity of the double angles to ensure that bolt fracture, a brittle failure mode, does not occur prior to the shear yielding of the angles, which is the desirable ductile failure mode of this connection. This can be done by satisfying the following Equations 2.7a and 2.7b in LRFD and ASD formats, respectively:

$$\phi_b V_b > \phi_y V_y \quad \text{(LRFD)} \qquad (2.7a)$$

$$V_b/\Omega_b > V_y/\Omega_y \quad \text{(ASD)} \qquad (2.7b)$$

Where,

$V_b = 2nA_b F_b$

$\phi_b = 0.75$ and $\phi_y = 0.90$ (LRFD)

$\Omega_b = 2.0$ and $\Omega_y = 1.5$ (ASD)

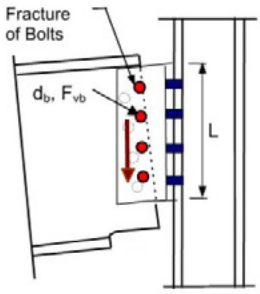

Figure 2.15. Fracture of Bolts

$$\phi_{75}V_{bLS5} := \phi_{75} \cdot 2 \cdot n \cdot A_b \cdot F_{vb} = 191 \ kip$$

$$DCR_5 := \frac{V_{uv}}{\phi_{75}V_{bLS5}} = 0.1$$

Figure 7-51h. Enhanced connection limit state check.

Source: Courtesy of Simpson Gumpertz & Heger (2019).

6) Design of bolts on the column flange:

To design the bolt groups for the combined effects of shear and bending moment, the circular interaction Equations 2.8a and 2.8b below are suggested. Selection of a circular interaction curve for shear and moment is based on RCSC (2000), which recommends a circular interaction curve for combined shear and tension. It should be mentioned that application of the RCSC recommendation, which is for combined shear and tension acting on a bolt group, to this case of combined shear and bending may be somewhat conservative. The reason is that, for the case of combined shear and tension studied by Chesson, Faustio, and Munse (1965), all the bolts are assumed to be subjected to the same combined shear and axial load, whereas in the case of combined bending and shear, a few bolts at the bottom part of the connection and in the compression zone are subjected to shear only. In the event, due to a lack of extensive test data on bolt groups subjected to combined shear and bending, the somewhat conservative circular interaction curve, recommended for V+N, was adapted for V+M as well.

$$\left(\frac{V_u}{\phi V_b}\right)^2+\left(\frac{M_u}{\phi M_b}\right)^2 \geq 1.0 \quad \text{(LRFD)} \quad (2.8a)$$

$$\left(\frac{V}{V_b/\Omega}\right)^2+\left(\frac{M}{M_b/\Omega}\right)^2 \geq 1.0 \quad \text{(ASD)} \quad (2.8b)$$

Where,

$V_u = V_y$ and $M_u = V_y e_b$ (LRFD)

$V = V_y/\Omega$ and $M = (V_y/\Omega)e_b$ (ASD)

$\Omega = 2.00$ (ASD)

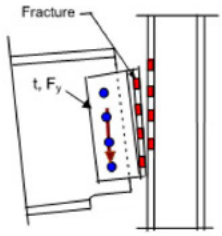

Figure 2.16. Fracture of Bolts

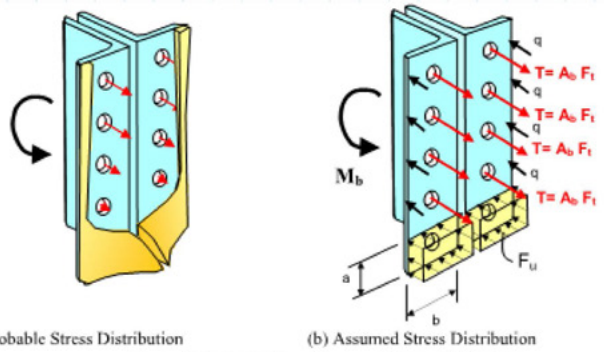

(a) Probable Stress Distribution (b) Assumed Stress Distribution

Figure 2.17. Probable and Assumed Stress Distribution

Note: We are solving for Vu in Equation 2.8a above (capacity result from interaction equation and not equal to Vy)

$V_b := 2 \cdot n \cdot A_b \cdot F_{vb} = 191\ kip$

to solve for Mb prying action formula is used:

Assuming that at the plastic level, demand/capacity in tension of each bolt is equal to 1:

Figure 7-51i. Enhanced connection limit state check.
Source: Courtesy of Simpson Gumpertz & Heger (2019).

$b := g - \frac{t}{2} = 2.2\ in$ $\quad b_{prime} := b - \frac{d_b}{2} = 1.8\ in$

$a := m1 - g = 1.5\ in$ $\quad a_{prime} := min\left(a + \frac{d_b}{2}, 1.25 \cdot b + \frac{d_b}{2}\right) = 1.9\ in$

$p := min(3.5 \cdot b, S) = 3\ in$

$d_{prime} := d_b + \frac{1}{16}\ in = 0.8\ in$ Per AISC Table J3.3

$\rho := \frac{b_{prime}}{a_{prime}} = 1$ $\quad BcTr := 1$ $\quad TrBc := 1$ Conservative assumption

$\beta := \frac{1}{\rho} \cdot (BcTr - 1) = 0$ $\quad \delta := 1 - \frac{d_{prime}}{p} = 0.7$ $\quad \alpha_{prime} := min\left(1, \frac{1}{\delta} \cdot \left(\frac{\beta}{1-\beta}\right)\right) = 0$

$B_c := A_b \cdot F_{nt} = 39.8\ kip$ Steel tips shows the bolts have reached to ultimate stress (T)

$t_c := \sqrt{\frac{(4 \cdot B_c \cdot b_{prime})}{p \cdot F_u}} = 1.3\ in$

$\alpha := \frac{1}{\delta} \cdot \left(TrBc \cdot \left(\frac{t_c}{t}\right)^2 - 1\right) = 4.4$

$\alpha := f(\alpha) = 1$

$q_r := B_c \cdot \left(\delta \cdot \alpha \cdot \rho \cdot \left(\frac{t}{t_c}\right)^2\right) = 6.6\ kip$

$f(\alpha) :=$ if $\alpha > 1$ then 1; else if $\alpha < 0$ then 0; else α

Solve for compression block "ablock" dimension via equilibrium at the interface:

$a_{block} := \frac{\langle 2 \cdot n \cdot A_b \cdot F_{nt} - 2 \cdot q_r \cdot n \rangle}{2 \cdot b \cdot F_u} = 1.045\ in$

$i := 1..n$

$L_{Mb_i} := L - L_{ev} - (i-1) \cdot S$ $\quad M_{bBOLTS} := 2 \cdot A_b \cdot F_{nt} \cdot L_{Mb}$ $\quad M_{bqrs} := 2 \cdot q_r \cdot L_{Mb}$

$ii := 1..n$

$ones_{ii} := 1$ $\quad M_{bBOLTStrans} := M_{bBOLTS}^{T}$ $\quad M_{bqrtrans} := M_{bqrs}^{T}$

$M_{bbolt} := M_{bBOLTStrans} \cdot ones = (1.83 \cdot 10^3)\ kip \cdot in$

$M_{bqr} := M_{bqrtrans} \cdot ones = 303.97\ kip \cdot in$

$M_{compblock} := 2 \cdot \frac{a_{block}^2}{2} \cdot b \cdot F_u = 138.61\ kip \cdot in$

Figure 7-51j. Enhanced connection limit state check.
Source: Courtesy of Simpson Gumpertz & Heger (2019).

$$M_b := M_{bbolt} - M_{bqr} - M_{compblock} = 1386.42 \ kip \cdot in$$

$$\phi_{75}V_b := \phi_{75} \cdot V_b = 190.9 \ kip$$

$$\phi_{75}M_b := \phi_{75} \cdot M_b = \left(1.4 \cdot 10^3\right) \ kip \cdot in$$

Solve for capacity:

$$\phi_{75}V_{pryingLS6} := \sqrt{\frac{1}{\left(\frac{1}{\phi_{75}V_b}\right)^2 + \left(\frac{e_b}{\phi_{75}M_b}\right)^2}} = 180.46 \ kip$$

$$DCR_6 := \frac{V_{uv}}{\phi_{75}V_{pryingLS6}} = 0.11$$

Figure 7-51k. Enhanced connection limit state check.
Source: Courtesy of Simpson Gumpertz & Heger (2019).

7) Block Shear Failure of the Double Angles or Beam:

2.3.g. Block Shear Failure of the Double Angles or Beam (Limit State 7)

This limit state can be a governing limit state in double-angle shear connections, especially when the beam web is coped. To check the block shear failure of the coped beam, the reader is referred to the procedures in the AISC-LRFD manual (2000).

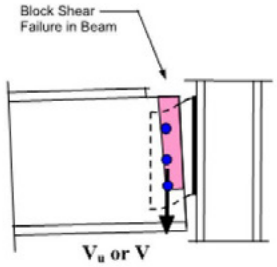

A) On Angles:

$A_{nvLS7L1} := 2 \cdot \left(L - L_{ev} - \left(n - 0.5\right) \cdot d_h\right) \cdot t = 8.98\ in^2$

$A_{gvLS7L1} := 2 \cdot \left(L - L_{ev}\right) \cdot t = 12.81\ in^2$

$A_{ntLS7L1} := 2 \cdot \left(L_{right} - 0.5 \cdot d_h\right) \cdot t = 1.33\ in^2$

$\phi_{75} V_{BSLS7L} := \phi_{75} \cdot min\left(\left(0.6 \cdot F_u \cdot A_{nvLS7L1} + F_u \cdot A_{ntLS7L1}\right), 0.6\ F_y \cdot A_{gvLS7L1} + F_u \cdot A_{ntLS7L1}\right) = 353.78\ kip$

$$DCR_7 := \frac{V_{uv}}{\phi_{75} V_{BSLS7L}} = 0.05$$

Figure 7-51l. Enhanced connection limit state check.
Source: Courtesy of Simpson Gumpertz & Heger (2019).

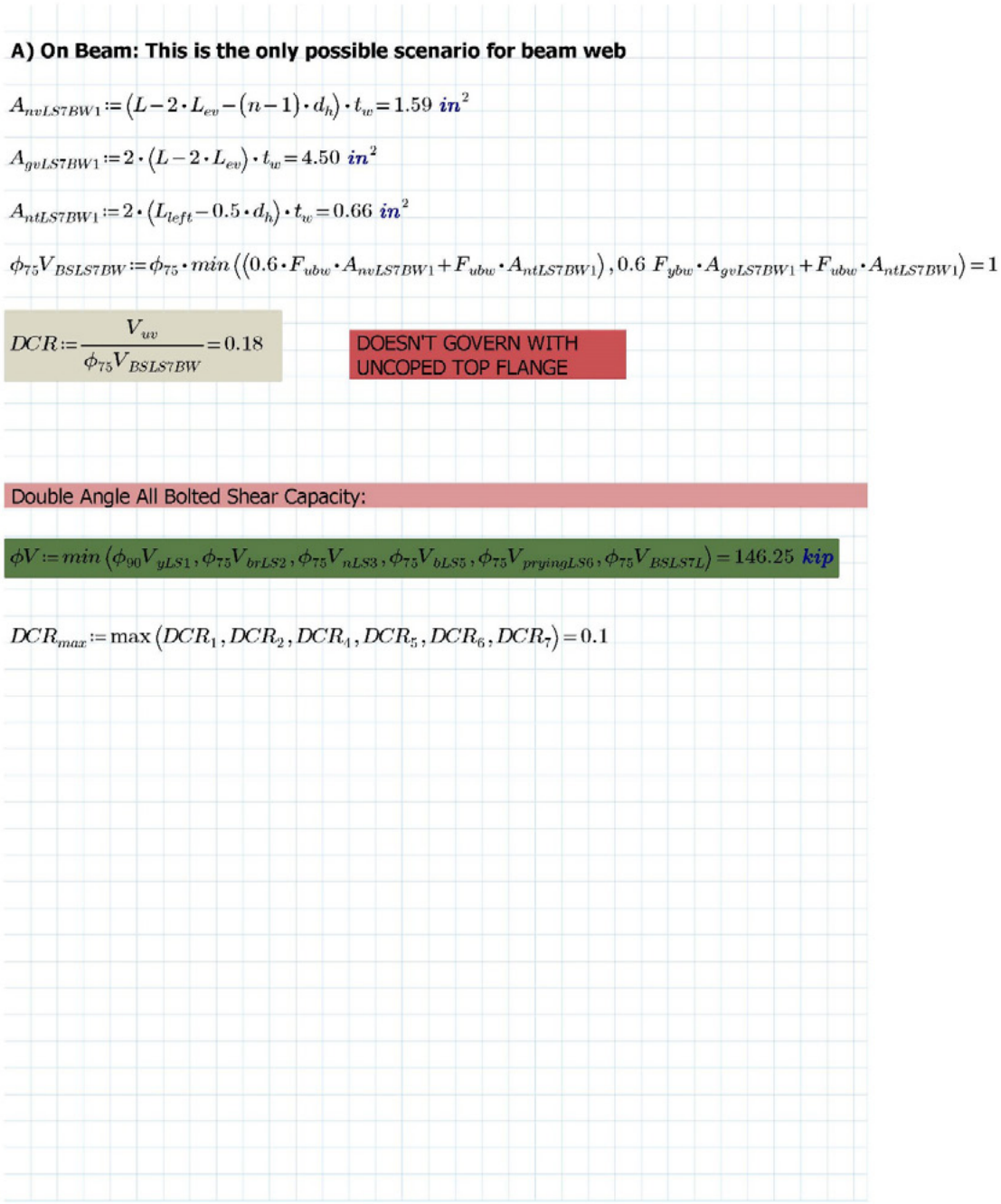

Figure 7-51m. Enhanced connection limit state check.

Source: Courtesy of Simpson Gumpertz & Heger (2019).

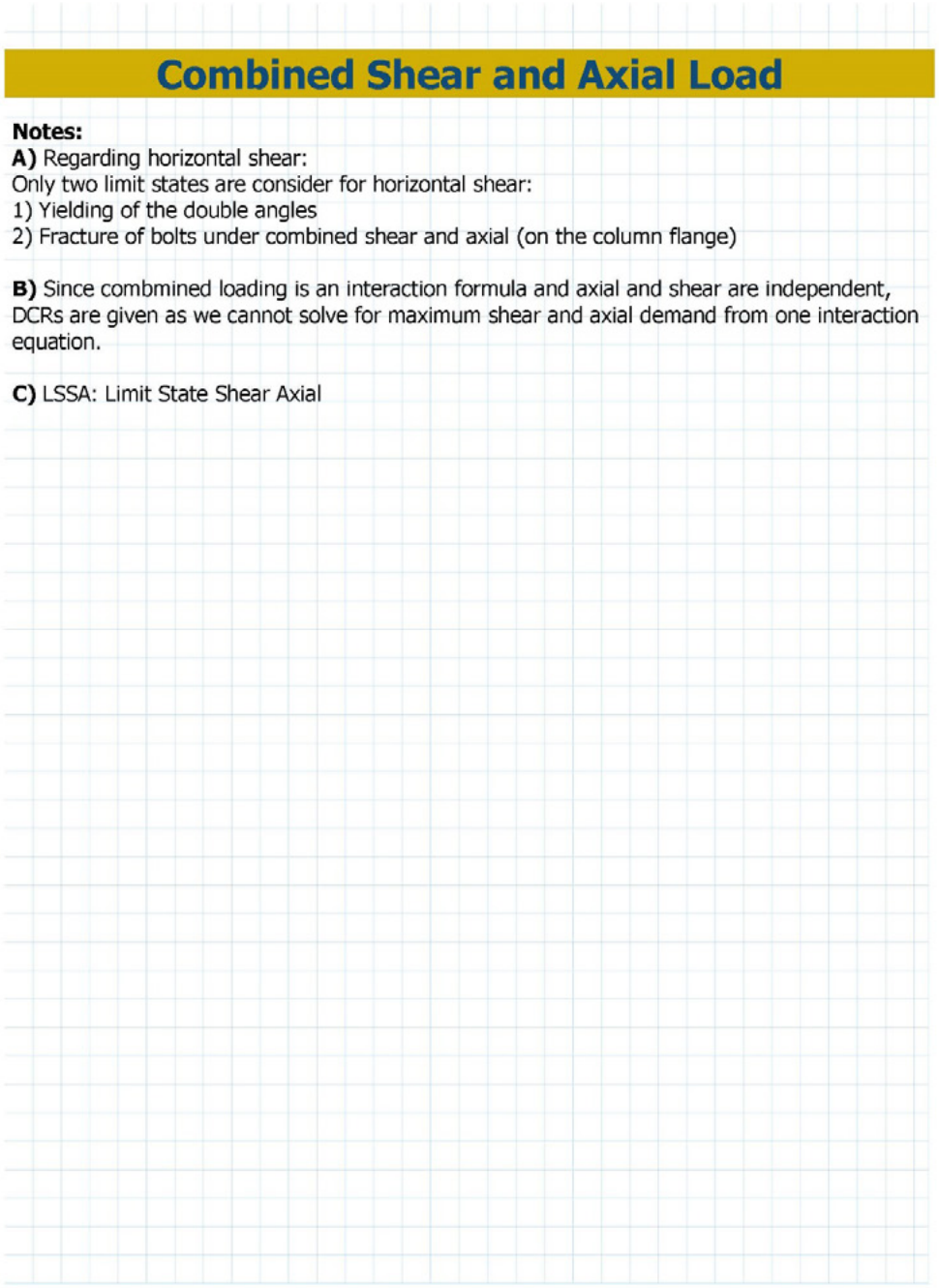

Figure 7-51n. Enhanced connection limit state check.
Source: Courtesy of Simpson Gumpertz & Heger (2019).

1) Yielding of the Double Ange under Combined Shear and Axial Load:

2.5.a. Yielding of the Double Angles under Combined Shear and Axial Load (Limit State 1)

For this failure mode, which involves yielding of the plate under combined shear and normal stresses, the Von Mises yield criterion and a circular interaction curve are used. The maximum factored axial force (in LRFD) and the maximum allowable axial force (in ASD) can be obtained from the following interaction equations:

$$\left(\frac{V_u}{\varphi_y V_n}\right)^2+\left(\frac{N_u}{\varphi_y N_n}\right)^2=1.0 \qquad \text{(LRFD)} \qquad (2.11a)$$

$$\left(\frac{V}{V_n/\Omega_y}\right)^2+\left(\frac{N}{N_n/\Omega_y}\right)^2=1.0 \qquad \text{(ASD)} \qquad (2.11b)$$

Where $\phi_y = 0.90$ (LRFD) and $\Omega_y = 1.50$ (ASD)

For definitions of the other terms in the above equations, see the "Notations" section on page 4.

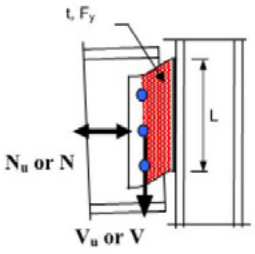

Figure 2.25

$\phi_{90}V_n := \phi_{90}\cdot 0.6\cdot A_{g2L}\cdot F_y = 310.5\ kip$

$\phi_{90}N_n := \phi_{90}\cdot A_{g2L}\cdot F_y = 517.5\ kip$

$\phi_{90}M_n := \phi_{90}\cdot 2\cdot L\cdot \frac{t^2}{4}\cdot F_y = 80.9\ kip\cdot in$ Capacity

$M_{vuh} := V_{uh}\cdot (e_b - t) = 9.4\ kip\cdot in$ Demand

Note: it is assumed that both angles are resisting bending moment from horizontal shear because the beam web will bear on the foreward angle and the bolts will engage the lee angle.

$$DCRLSSA1\phi_{90} := \left(\frac{M_{vuh}}{\phi_{90}M_n}\right)^2+\left(\frac{V_{uv}}{\phi_{90}V_n}\right)^2+\left(\frac{\max(N_{uT},N_{uC})}{\phi_{90}N_n}\right)^2 = 0.076$$

Figure 7-51o. Enhanced connection limit state check.
Source: Courtesy of Simpson Gumpertz & Heger (2019).

2) Bearing Failure of Double Angles under Combined Shear and Axial Load:

2.5.b. Bearing Failure of Double Angles under Combined Shear and Axial Load (Limit State 2)

Similar to the yielding of gross area, the Von Mises yield criterion is used for this failure mode as well. The maximum factored axial force in LRFD and the maximum allowable axial force in ASD can be obtained from the following interaction equations respectively:

$$\left(\frac{V_u}{\phi_{br} V_{br}}\right)^2 + \left(\frac{N_u}{\phi_{br} N_{br}}\right)^2 = 1.0 \quad \text{(LRFD)} \quad \text{(2.12a)}$$

$$\left(\frac{V}{V_{br}/\Omega_{br}}\right)^2 + \left(\frac{N}{N_{br}/\Omega_{br}}\right)^2 = 1.0 \quad \text{(ASD)} \quad \text{(2.12b)}$$

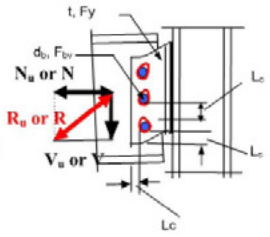

Figure 2.26

Where;
V_{br} = bearing capacity of the bolt group in the direction of shear (vertical direction)
N_{br} = bearing capacity of the bolt group in the direction of axial force (horizontal direction)
ϕ_{br} = 0.75 (LRFD) and Ω_{br} = 2.00 (ASD)

For definitions of the terms in the above equations, please see the "Notations" section on page 4.

CASE A: Angles:

$$\phi_{75}V_{brL} := \phi_{75}\cdot 2\cdot\left(min\left(1.5\cdot L_{cedge}\cdot t\cdot F_u, 3\cdot d_b\cdot t\cdot F_u\right) + min\left(1.5\cdot(n-1)\left(L_{cbolts}\cdot t\cdot F_u\right), 3\cdot(n-1)\cdot d_b\cdot t\cdot F_u\right)\right) =$$

$$\phi_{75}N_{brTL} := \phi_{75}\cdot 2\cdot n\cdot min\left(1.5\cdot\left(L_{right}-\frac{d_h}{2}\right)t\cdot F_u, 3\cdot d_b\cdot t\cdot F_u\right) = 462.2\ \textit{kip}$$

$$\phi_{75}N_{brCL} := \phi_{75}\cdot 2\cdot n\cdot 3\cdot d_b\cdot t\cdot F_u = 652.5\ \textit{kip}$$

$$DCRLSSA2TL := \left(\frac{V_{uv}}{\phi_{75}V_{brL}}\right)^2 + \left(\frac{N_{uT}}{\phi_{75}N_{brTL}}\right)^2 = 0.074$$

$$DCRLSSA2CL := \left(\frac{V_{uv}}{\phi_{75}V_{brL}}\right)^2 + \left(\frac{N_{uC}}{\phi_{75}N_{brCL}}\right)^2 = 0.002$$

CASE B: Beam web:

$$\phi_{75}V_{brBW} := \phi_{75}\cdot\left(3\cdot d_b\cdot t_w\cdot F_{ubw} + min\left(1.5\cdot(n-1)\left(L_{cbolts}\cdot t_w\cdot F_{ubw}\right), 3\cdot(n-1)\cdot d_b\cdot t_w\cdot F_{ubw}\right)\right) = 146.3\ \textit{kip}$$

$$\phi_{75}N_{brTBW} := \phi_{75}\cdot n\cdot min\left(1.5\cdot\left(L_{left}-\frac{d_h}{2}\right)t_w\cdot F_{ubw}, 3\cdot d_b\cdot t_w\cdot F_{ubw}\right) = 128\ \textit{kip}$$

$$\phi_{75}N_{brCBW} := \phi_{75}\cdot n\cdot 3\cdot d_b\cdot t_w\cdot F_{ubw} = 146.3\ \textit{kip}$$

$$DCRLSSA2TBW := \left(\frac{V_{uv}}{\phi_{75}V_{brBW}}\right)^2 + \left(\frac{N_{uT}}{\phi_{75}N_{brTBW}}\right)^2 = 0.971$$

$$DCRLSSA2CBW := \left(\frac{V_{uv}}{\phi_{75}V_{brBW}}\right)^2 + \left(\frac{N_{uC}}{\phi_{75}N_{brCBW}}\right)^2 = 0.027$$

$$\left(\frac{V_{uv}}{\phi_{75}V_{brBW}}\right) = 0.1$$

$$\left(\frac{N_{uT}}{\phi_{75}N_{brTBW}}\right) = 1$$

Figure 7-51p. Enhanced connection limit state check.
Source: Courtesy of Simpson Gumpertz & Heger (2019).

3) Edge Distance Failure in the Angles or in the Connected Members:

2.5.c. Edge Distance Failure in the Angles or in the Connected Members (Limit State 3)

This failure mode is the same as the edge distance failure under pure shear discussed in Section 2.4 earlier. The required minimum edge distances for the beam web are equal to those given in the AISC-LRFD (2000) specifications or two times the bolt diameter, whichever is greater.

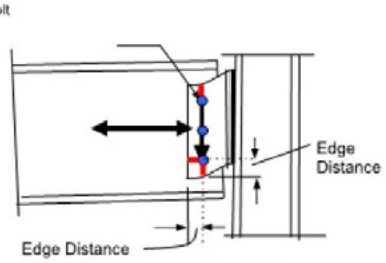

Figure 2.27

This failure is precluded by satisfying the AISC minimum edge distance requirement

Figure 7-51q. Enhanced connection limit state check.
Source: Courtesy of Simpson Gumpertz & Heger (2019).

4) Net-Area Fracture of the Plate under Combined Shear and Axial Force:

2.5.d. Net-Area Fracture of the Plate under Combined Shear and Axial Force (Limit State 4)

Similar to the yielding of gross area, the Von Mises yield criterion is used for this failure mode as well. The maximum factored axial force in LRFD and the maximum allowable axial force in ASD can be obtained from the following interaction equations, respectively:

$$\left(\frac{V_u}{\varphi_n V_n}\right)^2+\left(\frac{N_u}{\varphi_n N_n}\right)^2=1.0 \quad \text{(LRFD)} \qquad (2.13a)$$

$$\left(\frac{V}{V_n/\Omega_n}\right)^2+\left(\frac{N}{N_n/\Omega_n}\right)^2=1.0 \quad \text{(ASD)} \qquad (2.13b)$$

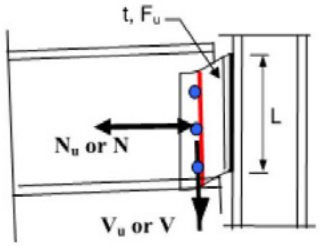

Figure 2.28

Where:
$V_n = 0.60F_u A_{nv}$
$N_n = F_u A_n$
$A_{nv} = 2[A_g - 0.5n(d_h + 1/8 \text{ inch})]$
$A_n = 2[A_g - n(d_h + 1/8 \text{ inch})]$

For definitions of the terms in the above equations, please see the "Notations" section on page 4.

$$\phi_{75}V_n := \phi_{75}\cdot 0.6\cdot F_u\cdot 2\cdot\left(A_{g1L}-0.5\cdot n\cdot d_h\cdot t\right)=424.1\ \textit{kip}$$

$$\phi_{75}N_n := \phi_{75}\cdot F_u\cdot 2\cdot\left(A_{g1L}-n\cdot d_h\cdot t\right)=580\ \textit{kip}$$

$$DCRLSSA4TC := \left(\frac{V_{uv}}{\phi_{75}V_n}\right)^2+\left(\frac{\max\left(N_{uT},N_{uC}\right)}{\phi_{75}N_n}\right)^2=0.048$$

Figure 7-51r. Enhanced connection limit state check.
Source: Courtesy of Simpson Gumpertz & Heger (2019).

5) Fracture of Bolts under Combined Shear and Axial Force (Case a on Beam Web):

2.5.e. Fracture of Bolts under Combined Shear and Axial Force (Limit State 5)

a. Design of bolts on the beam web. The shear and axial force applied to the connection created only shear in the bolts connecting the beam to the double angles. Therefore, the strength of the bolt group in shear, $\phi_b V_b$ in LRFD and V_b/Ω in ASD, should satisfy the following equations:

$$\left(\varphi_y V_y\right)^2 + \left(\varphi_y N_y\right)^2 \le \left(\varphi_b V_b\right)^2 \quad \text{(LRFD)} \quad (2.14a)$$

$$\left(V_y/\Omega_y\right)^2 + \left(N_y/\Omega_y\right)^2 \le \left(V_b/\Omega_b\right)^2 \quad \text{(ASD)} \quad (2.14b)$$

Where,

$V_b = 2nA_b F_b$

$\phi_b = 0.75$ and $\phi_y = 0.90$ (LRFD)

$\Omega_b = 2.0$ and $\Omega_y = 1.5$ (ASD)

For definitions of the terms in the above equation, see the "Notations" section on page 4.

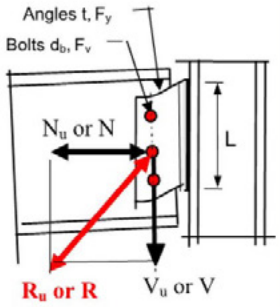

Figure 2.29

$$DCRLSSA5TCa := \left(\frac{V_{uv}}{\phi_{75} V_b}\right)^2 + \left(\frac{\max\left(N_{uT}, N_{uC}\right)}{\phi_{75} V_b}\right)^2 = 0.439$$

Figure 7-51s. Enhanced connection limit state check.
Source: Courtesy of Simpson Gumpertz & Heger (2019).

5) Fracture of Bolts under Combined Shear and Axial Force (Case b on Column Flange):

b. Design of bolts on the column flange. The bolts on the column flange, Figure 2.30, should be designed for the combined effects of direct shear, axial force, and bending moment. To design the bolt groups for the combined effects of shear, axial load and bending moment, the circular interaction Equations 2.15a and 2.15b below are suggested:

$$\left(\frac{V_u}{\varphi_b V_b}\right)^2+\left(\frac{N_u}{\varphi_b N_b}\right)^2+\left(\frac{M_u}{\varphi_b M_b}\right)^2=1.0 \qquad \text{(LRFD)} \qquad (2.15a)$$

Where,

V_u = factored applied shear

N_u = factored applied axial force

M_u = factored applied bending moment

V = unfactored applied shear

N = unfactored applied axial force

M = unfactored applied bending moment

V_b = shear strength of the bolt group under pure shear

N_b = tensile strength of the bolt group under pure tension

M_b = plastic moment capacity of the bolt group in bending given in Section 2.3.e above.

$\phi_b = 2.00$ (LRFD) and $\Omega_b = 2.0$ (ASD)

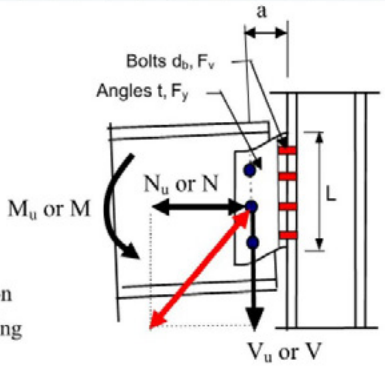

Figure 2.30

$\phi_{75}N_b := \phi_{75} \cdot 2 \cdot n \cdot A_b \cdot F_{nb} = 318.1$ *kip*

$N_{Mvuh} := V_{uh} \cdot \frac{e_b}{2 \cdot g} = 2.5$ *kip*

$\phi_{75}V_b$ and $\phi_{75}M_b$ can be found under limit state 6 of pure shear, page 11

$$DCRLSSA5TCb := \left(\sqrt{\left(\left(\frac{V_{uh}}{\phi_{75}V_b}\right)^2+\left(\frac{V_{uv}}{\phi_{75}V_b}\right)^2\right)}\right)^2+\left(\frac{N_{uT}+N_{Mvuh}}{\phi_{75}N_b}\right)^2+\left(\frac{V_{uv} \cdot e_b}{\phi_{75}M_b}\right)^2 = 0.172$$

Figure 7-51t. Enhanced connection limit state check.
Source: Courtesy of Simpson Gumpertz & Heger (2019).

6) Block Shear Failure of Double Angles or Beam Web under Combined Shear and Axial Force (Case A Double Angles):

This limit state can be a governing limit state in double-angle shear connections, especially when the beam web is coped.

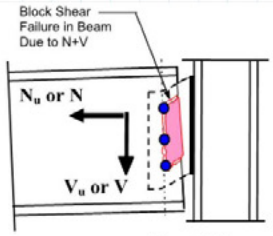

Figure 2.32

A) On Angles Case 1: Case **A1**

Under Shear

$\phi_{75}V_{LSSA6A1V} := \phi_{75}V_{BSLS7L} = 353.78\ kip$

Under Tension

$A_{ntLSSA6} := 2 \cdot \left(L - L_{ev} - \left(n - 0.5\right) \cdot d_h\right) \cdot t = 8.98\ in^2$

$A_{nvLSSA6} := 2 \cdot \left(L_{right} - 0.5 \cdot d_h\right) \cdot t = 1.33\ in^2$

$A_{gvLSSA6} := 2 \cdot \left(L_{right}\right) \cdot t = 1.88\ in^2$

$\phi_{75}V_{LSSA6A1T} := \phi_{75} \cdot min\left(\left(0.6 \cdot F_u \cdot A_{nvLSSA6} + F_u \cdot A_{ntLSSA6}\right), 0.6\ F_y \cdot A_{gvLSSA6} + F_u \cdot A_{ntLSSA6}\right) = 561.59\ kip$

$$DCRLSSA6A1 := \left(\frac{V_{uv}}{\phi_{75}V_{LSSA6A1V}}\right)^2 + \left(\frac{N_{uT}}{\phi_{75}V_{LSSA6A1T}}\right)^2 = 0.052$$

A) On Angles Case 2: Case **A2**

Under Shear

$A_{nvLS7L2} := 2 \cdot \left(L - 2 \cdot L_{ev} - \left(n - 1\right) \cdot d_h\right) \cdot t = 7.97\ in^2$

$A_{gvLS7L2} := 2 \cdot \left(L - 2 \cdot L_{ev}\right) \cdot t = 11.25\ in^2$

$A_{ntLS7L2} := 2 \cdot 2 \cdot \left(L_{right} - 0.5 \cdot d_h\right) \cdot t = 2.66\ in^2$

$\phi_{75}V_{BSLS7L2} := \phi_{75} \cdot min\left(\left(0.6 \cdot F_u \cdot A_{nvLS7L2} + F_u \cdot A_{ntLS7L2}\right), 0.6\ F_y \cdot A_{gvLS7L2} + F_u \cdot A_{ntLS7L2}\right) = 397.06\ kip$

$\phi_{75}V_{LSSA6A2V} := \phi_{75}V_{BSLS7L2} = 397.06\ kip$

Figure 7-51u. Enhanced connection limit state check.

Source: Courtesy of Simpson Gumpertz & Heger (2019).

Under Tension

$A_{ntLSSA6A2} := 2 \cdot \left(L - 2 \cdot L_{ev} - (n-1) \cdot d_h\right) \cdot t = 7.97\ in^2$

$A_{nvLSSA6A2} := 2 \cdot 2 \cdot \left(L_{right} - 0.5 \cdot d_h\right) \cdot t = 2.66\ in^2$

$A_{gvLSSA6A2} := 2 \cdot 2 \cdot \left(L_{right}\right) \cdot t = 3.75\ in^2$

$\phi_{75} V_{LSSA6A2T} := \phi_{75} \cdot min\left(\left(0.6 \cdot F_u \cdot A_{nvLSSA6A2} + F_u \cdot A_{ntLSSA6A2}\right), 0.6\ F_y \cdot A_{gvLSSA6A2} + F_u \cdot A_{ntLSSA6A2}\right) = 543.19$

$$DCRLSSA6A2 := \left(\frac{V_{uv}}{\phi_{75} V_{LSSA6A2V}}\right)^2 + \left(\frac{N_{uT}}{\phi_{75} V_{LSSA6A2T}}\right)^2 = 0.055$$

6) Block Shear Failure of Double Angles or Beam Web under Combined Shear and Axial Force (Case B Beam Web):

B) On Beam Web Case 1: (This is the only possible case for beam web to be combined shear and axial) Case **B1**

Under Tension

$A_{ntLSSA6B1T} := \left(L - 2 \cdot L_{ev} - (n-1) \cdot d_h\right) \cdot t_w = 1.59\ in^2$

$A_{nvLSSA6B1T} := 2 \cdot \left(L_{left} - 0.5 \cdot d_h\right) \cdot t_w = 0.66\ in^2$

$A_{gvLSSA6B1T} := 2 \cdot \left(L_{left}\right) \cdot t_w = 0.88\ in^2$

$\phi_{75} V_{LSSA6B1T} := \phi_{75} \cdot min\left(\left(0.6 \cdot F_{ubw} \cdot A_{nvLSSA6B1T} + F_{ubw} \cdot A_{ntLSSA6B1T}\right), 0.6\ F_{ybw} \cdot A_{gvLSSA6B1T} + F_{ubw} \cdot A_{ntLSSA6B}$

$V_{resultant} := \sqrt{N_{uT}^{\ 2} + V_{uv}^{\ 2}} = 126.4\ kip$

$$DCRLSSA6B1 := \left(\frac{V_{resultant}}{\phi_{75} V_{LSSA6B1T}}\right)^2 = 0.958$$

$DCR_{max} := \max\left(DCRLSSA1\phi_{90}, DCRLSSA2TL, DCRLSSA2CL, DCRLSSA2TBW, DCRLSSA2CBW, DC\right.$

Figure 7-51v. Enhanced connection limit state check.
Source: Courtesy of Simpson Gumpertz & Heger (2019).

Summary of DCRs and Limit States (under tension and shear)

Ductile limit states:

1) Yielding of double angles:

$$DCR_{Yieldingofdoubleangles} := DCRLSSA1\phi_{90} = 0.08$$

2) Beaing failure:

$$DCR_{Bearingfailures} := \text{if } 1.5 \cdot \left(L_{left} - \frac{d_h}{2}\right) t_w \cdot F_{ubw} < 3 \cdot d_b \cdot t_w \cdot F_{ubw} \text{ "BRITTLE" else } DCRLSSA2TBW$$

$$DCR_{Bearingfailures} = \text{"BRITTLE"}$$

Brittle Limit States:

2) Bearing failure:

$$DCR_{Bearingfailrues} := \text{if } 1.5 \cdot \left(L_{left} - \frac{d_h}{2}\right) t_w \cdot F_{ubw} < 3 \cdot d_b \cdot t_w \cdot F_{ubw} \; DCRLSSA2TBW \text{ else "DUCTILE"}$$

$$DCR_{Bearingfailrues} = 0.97$$

3) Edge distance failure: Not a concern

4) Net area fracture:

$$DCR_{Netareafracture} := DCRLSSA4TC = 0.05$$

5) Fracture of bolts:

$$DCR_{Fractureofbolts} := \max\left(DCRLSSA5TCa, DCRLSSA5TCb\right) = 0.44$$

6) Block shear failure:

$$DCR_{Blockshearfailure} := \max\left(DCRLSSA6A1, DCRLSSA6A2, DCRLSSA6B1\right) = 0.96$$

Figure 7-51w. Enhanced connection limit state check.
Source: Courtesy of Simpson Gumpertz & Heger (2019).

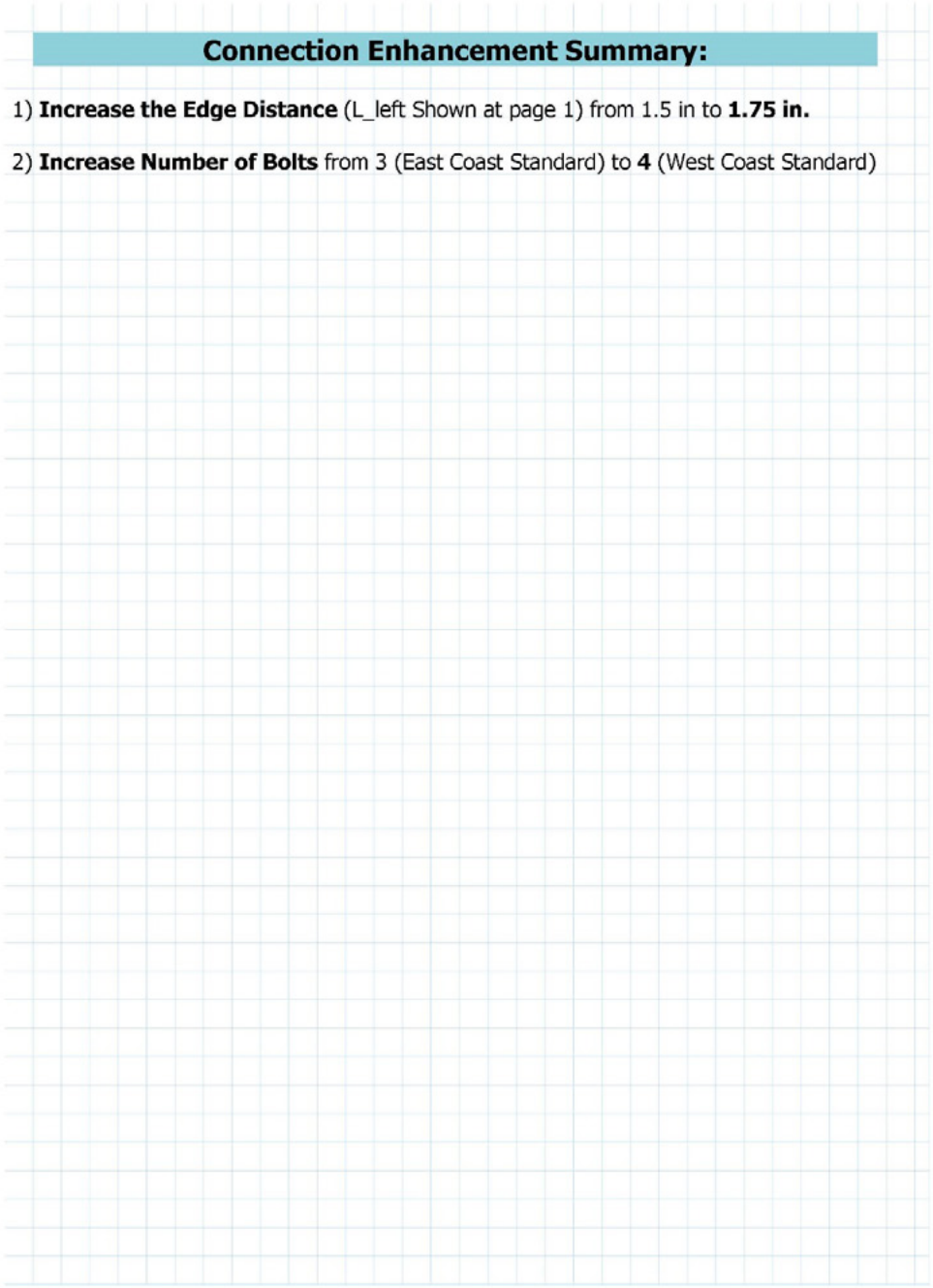

Figure 7-51x. Enhanced connection limit state check.
Source: Courtesy of Simpson Gumpertz & Heger (2019).

Chapter 8. Building 2: Magnusson Klemencic Associates (MKA)

Participants

The Structural Engineering Institute of ASCE acknowledges the work of the participants in this project.

Industry Champions

The Magnusson Klemencic Associates (MKA) design team comprised the following contributors:

Ron Klemencic, P.E., S.E., Hon. AIA, *Industry Champion*

Robert Baxter, S.E.

Amy Garras, P.E.

Chris Lubke, S.E.

Mike Valley, S.E.

BUILDING 2

Building 2 is a 12-story, 63,000 m^2, acute care facility with surgery, diagnostic, radiology, cardiology, and emergency departments, as well as 368 general patient and intensive care beds. The exterior cladding system is composed of glass and metal panels.

Each patient floor has a total area of 4,800 m^2 arranged in two wings of patient rooms joined by a central connector with offices and family lounges as shown in Figure 8-1. The story height of the patient floors is 4.3 m.

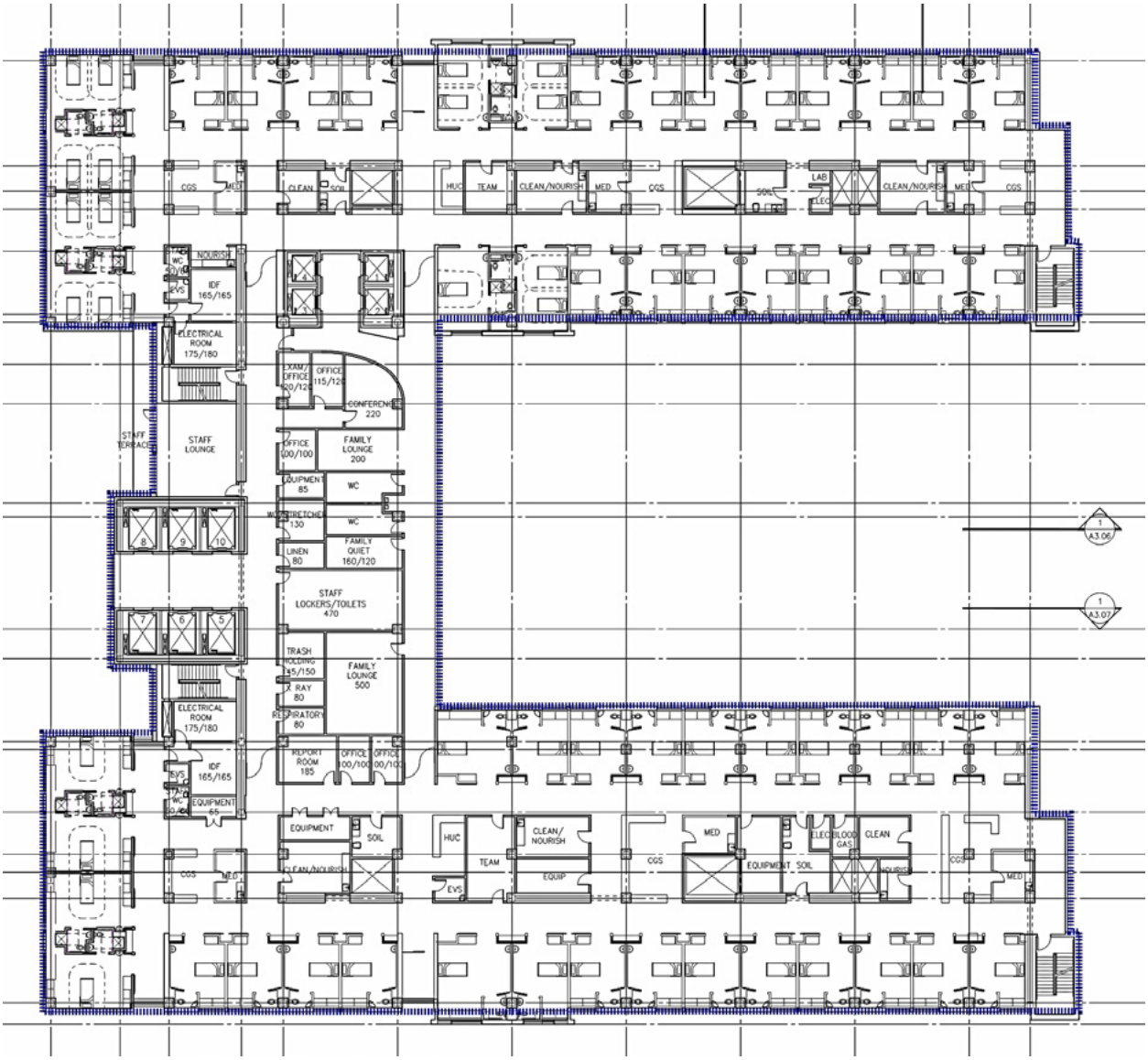

Figure 8-1: Building 2 patient floor plan.

Source: Courtesy of Magnusson Klemencic Associates (2019).

The Building 2 structure is steel, framed with composite slabs and a buckling-restrained brace lateral system. The composite slab consists of 64-mm-thick, normal-weight concrete topping over a 76-mm-deep, 20-gauge steel deck. The slab is reinforced with #3 bars at 450 mm on center, each way, at middepth of the topping. The composite slab profile section is shown in Figure 8-2.

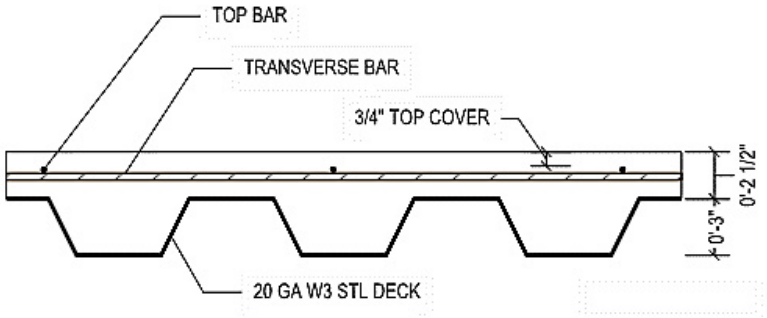

Figure 8-2. Composite slab profile.

Source: Courtesy of Magnusson Klemencic Associates (2019).

The slab spans a maximum of 3.4 m between W16 beams that are oriented parallel to the long direction of each patient wing. The W16 beams are supported by W21 girders and W14 columns on the grid lines, which are spaced at 9.1 m. The floor framing of a typical bay in a patient wing is shown in Figure 8-3.

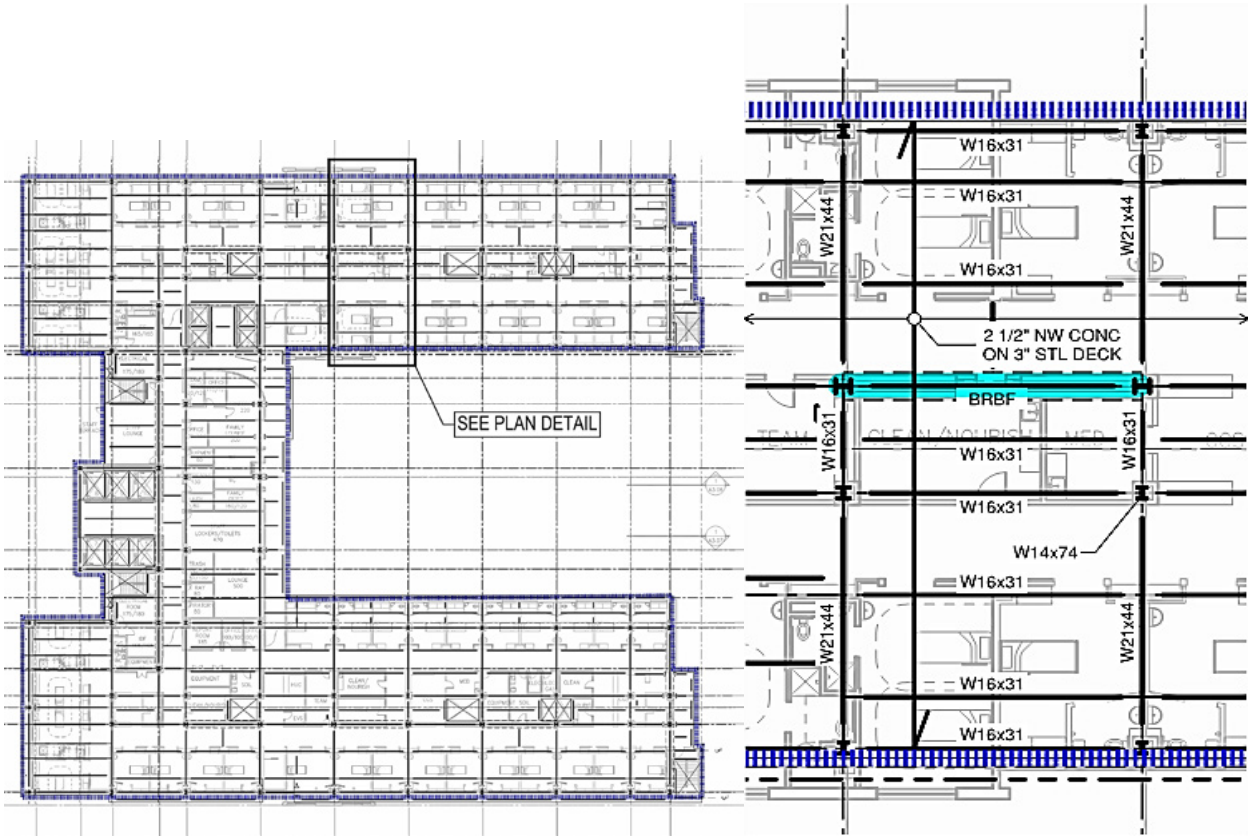

Figure 8-3. Building 2 structural framing plan.

Source: Courtesy of Magnusson Klemencic Associates (2019).

The building's structural design was optimized for the effects of gravity, wind, and seismic loads. The vertical deflection of the floor beams is limited to the requirements of IBC, Chapter 16 (ICC 2018) and the acceleration associated with footfall-induced vibrations is limited to 0.5% g according to the provisions of AISC *Design Guide 11*. The gravity design loads are summarized in Table 8-1. The self-weight of the structure is considered in addition to the loads indicated in Table 8-1.

Table 8-1. Uniform Gravity Loads.

Distributed Live Load: Hospital Corridor	3.8 kN/m^2
Distributed Dead Load: Partitions + Suspended Ceiling / MEP	1.4 kN/m^2
Exterior Cladding: Glass / Metal Panel Curtain Wall	1.0 kN/m^2

The building is classified as Construction Type IB according to IBC, Chapter 5 (ICC 2018). This classification was relaxed from Type IA because of supervised sprinkler control valves and waterflow devices on every floor.

The fire protection for Building 2 is applied based on prescriptive requirements of the IBC. The required ratings of the structural elements and the associated thickness of spray-applied fire resisting material (SFRM) are noted in Table 8-2.

Table 8-2. Fire Protection of Structural Elements.

Element	Rating	UL Design No	SFRM Thickness
Columns at Floors	3 h	X701	43 mm
Floor Beams	2 h	D925	27 mm
64 mm Conc on 76 mm Stl Deck	2 h	D739	M

8.1 DESIGN STRATEGY

For the purpose of this study, one representative bay of Level 8 extending the width of the floor was modeled and analyzed. To fully evaluate the structural performance, an extended model or additional models would be required to evaluate all the varying conditions of support, restraint, and loading.

The representative bay was evaluated for Design 0 using prescriptive fireproofing thicknesses.

Removal of the slab fireproofing was the primary target for Design 2, because this had the greatest potential economic value without otherwise altering the structural system. In addition, SFRM thicknesses were adjusted iteratively to achieve the performance objectives of Design 2, full burnout without collapse of the structure. Because the structure is a hospital, complete and safe evacuation was not feasible, and the Design 1 fire scenario was not considered.

For Design 3, the secondary beams were targeted for SFRM removal in addition to removing the SFRM from the slab. The temperature of unprotected steel members closely follows the compartment temperature and quickly loses load-carrying capacity. Therefore, slab membrane action was considered as an alternative load path. The slab reinforcement was enhanced to allow the gravity load of a framing bay to be supported by membrane action. The slab panel method, as presented by Clifton (2006), was used to estimate the gravity load-carrying capacity enhancement associated with reinforced slab membrane action. A three-dimensional model was run to validate the design.

8.2 DESIGN FUEL LOAD

For the purposes of this study, only post-flashover compartment fires were considered.

The design fuel loads are determined in accordance with Eurocode 1 (CEN 2001). The occupancy of the Building 2 area under review is primarily hospital patient rooms. The characteristic fire load density used for all fire scenarios is 280 MJ/m^2, corresponding to the 80% fractile value for fuel load densities of hospital rooms according to Table E.4 of Eurocode 1.

The fires within the hospital are assumed to consume mostly cellulosic materials; therefore, a combustion factor, m, of 0.8 has been considered for all fire scenarios.

The fire scenarios include two different compartment sizes, 1,000 m^2 and 30 m^2. The size and location of the compartments on one of the typical patient room floors are shown in Figure 8-4. Eurocode 1, Annex A-1 limits the size of valid fire compartments to 500 m^2 of floor area. One of the fire compartments under consideration exceeds this limit, but it is common practice to use the parametric temperature curves for compartments larger than 500 m^2, because alternative models for larger compartment sizes are unavailable. The compartment size risk factor associated with the respective compartment floor areas, d_{q1}, is accordingly interpolated from Table E.1 of Eurocode 1.

The fire activation risk factor associated with occupancy, d_{q2}, as defined in Eurocode 1, Table E.1, is assumed to be 1.0 for all fire scenarios. The patient room occupancy is not specifically listed in Table E.1, so the values for a residence or hotel room were used.

For the purposes of this evaluation, complete compartment fuel burnout is assumed and no manual or automatic fire suppression or fire detection methods are utilized. Therefore, all factors, d_n, from Table E.2 of Eurocode 1 are taken as 1.0 for the fire scenarios considered.

A medium fire growth rate has been considered for the hospital occupancy based on Table E.5 of Eurocode 1. This growth rate is associated with a 20 min duration until peak compartment temperature is reached for a fuel-controlled fire.

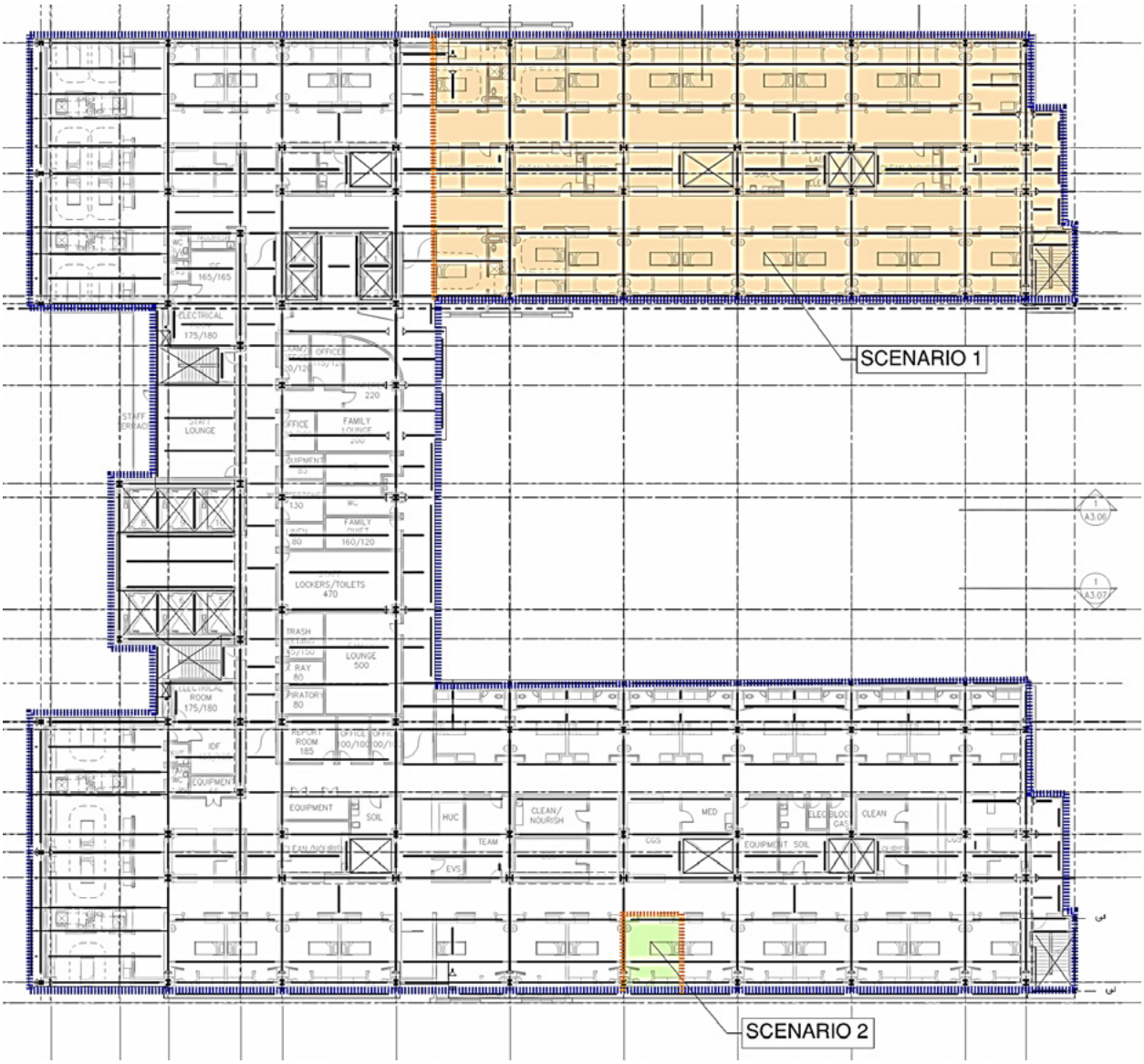

Figure 8-4. Design fire compartments.

Source: Courtesy of Magnusson Klemencic Associates (2019).

8.3 STRUCTURAL DESIGN FIRES

Design fires are dependent on fuel load, compartment geometry, compartment wall opening configuration, and compartment thermal properties. Eurocode 1 has been used to consider these parameters in development of the design fires for this structure. Table 8-3 summarizes the basic parameters for each design fire, and Figure 8-5 plots the time–temperature curve for each scenario.

Table 8-3. Design Fire Parameters.

Design Fire	S1A	S1B	S1C	S1D	S2A	S2B
Compartment Floor Area, m^2	1,000	1,000	1,000	1,000	30	30
Compartment Wall Opening Area, m	240	110	50	50	10	5
Average Opening Height, m	3.8	3.7	3.6	3.6	3.2	1.8
Opening Factor, $m^{1/2}$	0.18	0.08	0.04	0.04	0.14	0.05
Boundary Thermal Factor, $J/m^2s^{1/2}K$	1,000	950	950	1600	750	750
Design Fire Load, MJ/m^2	389	389	389	389	254	254

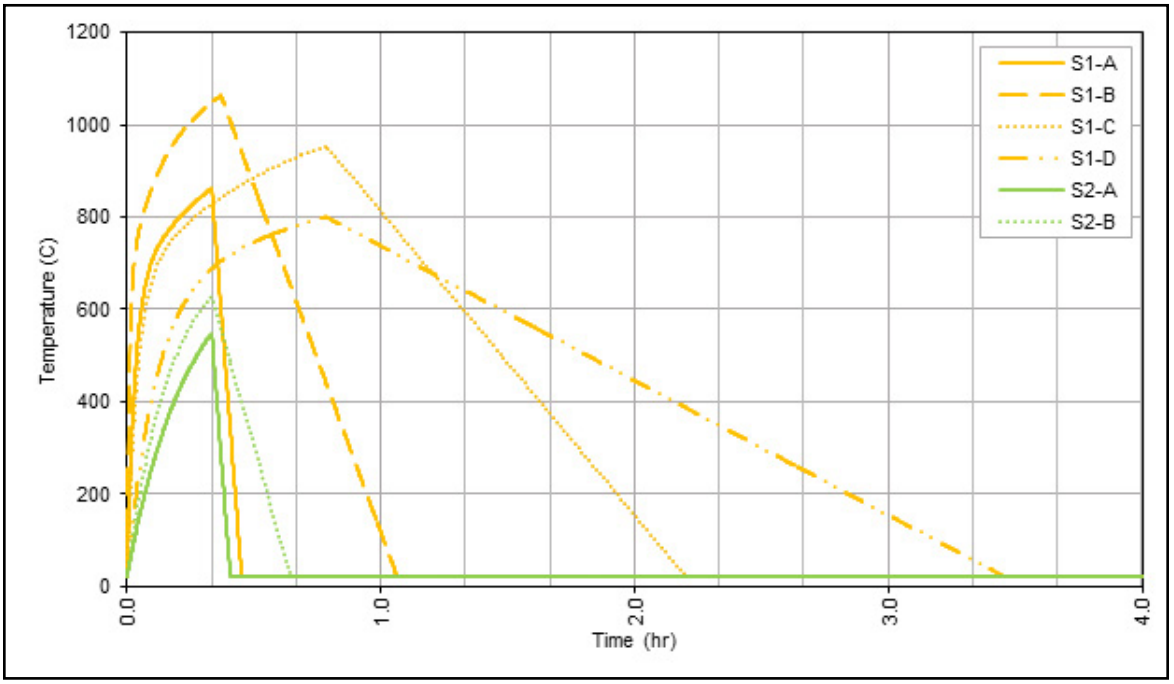

Figure 8-5. Design fire time–temperature curves.

Source: Courtesy of Magnusson Klemencic Associates (2019).

Eurocode 1 limits the applicability of the parametric curves to the set of opening factors, O, bounded between 0.02 and 0.20 $m^{0.5}$. Given the large number of full-height interior walls on the patient floors, the floor plan becomes highly compartmentalized, and a wide range of opening factors need to be considered. Design fires S1A, S1B, and S1C each have the same compartment size and thermal properties but consider different ventilation conditions. Scenario S1A has the largest wall opening area and the highest opening factor, O = 0.18 $m^{0.5}$, which is near the upper limit of the parametric curve applicability. The opening conditions for Scenario S1A, shown in Figure 8-6, consider all the exterior windows breaking and interior openings occurring at each of the corridors. This leads to a fuel-controlled design fire in which the entire fuel mass is depleted rapidly, the hot gasses are evacuated quickly, and the structure is exposed to elevated temperatures for a very short duration.

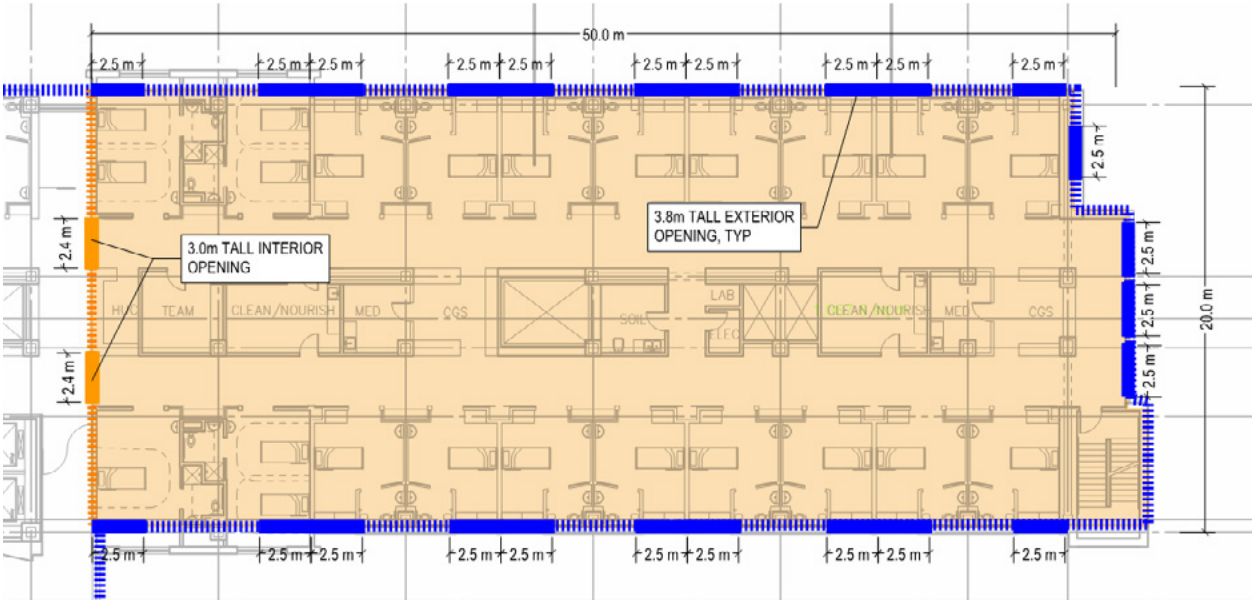

Figure 8-6. Wall openings of fire scenario S1A.

Source: Courtesy of Magnusson Klemencic Associates (2019).

Scenario S1B, shown in Figure 8-7, has a lower opening factor than Scenario S1A, leading to a ventilation-controlled fire. This design fire has the highest compartment temperature.

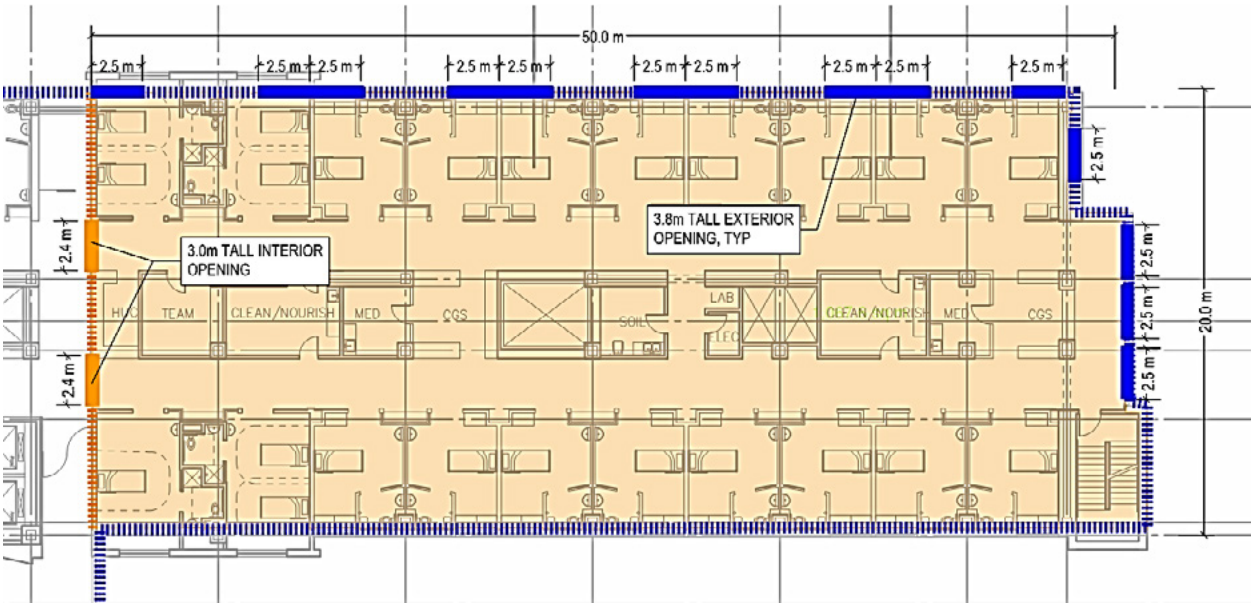

Figure 8-7. Wall openings of fire scenario S1B.

Source: Courtesy of Magnusson Klemencic Associates (2019).

Scenarios S1C and S1D have the smallest wall opening area and, therefore, the lowest opening factor, O = 0.04 $m^{0.5}$, near the lower bound of the parametric curve limits. The opening conditions

for Scenarios S1C and S1D, shown in Figure 8-8, correspond to the end-wall exterior windows breaking while the rest stay intact, and interior openings occurring at each of the corridors. Scenarios S1C and S1D yield lower peak compartment temperatures because the ventilation is more restricted than in Scenario S1B, the other ventilation-controlled fire scenario, but Scenarios S1C and S1D have significantly longer durations.

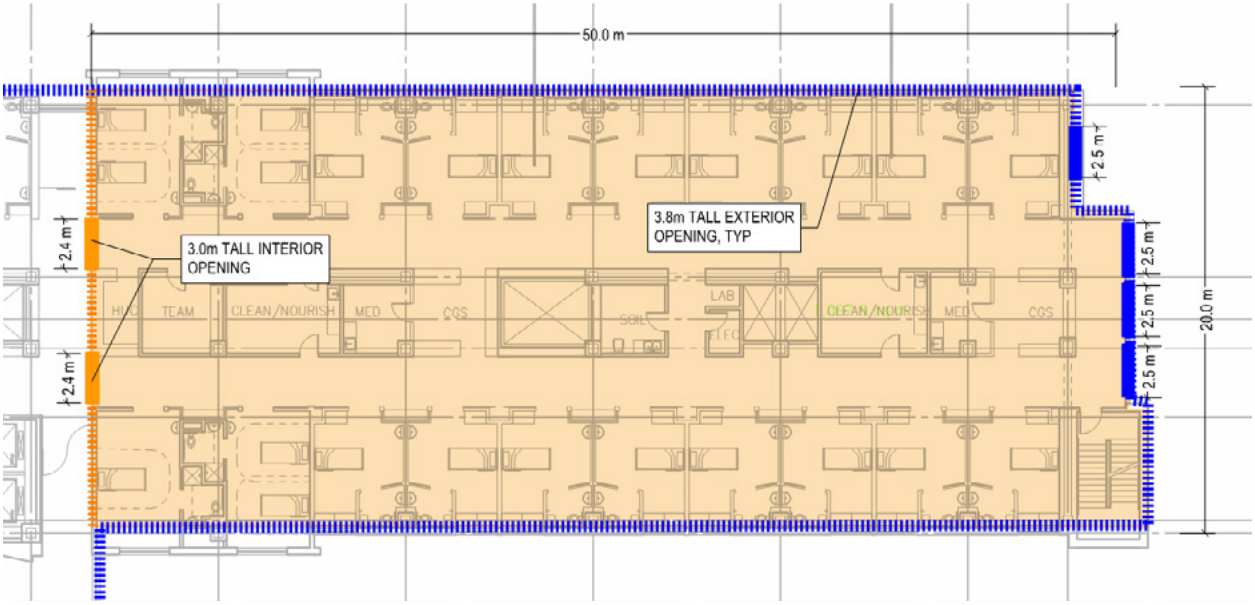

Figure 8-8. Wall openings of fire scenario S1C and S1D.

Source: Courtesy of Magnusson Klemencic Associates (2019).

The only difference between Scenarios S1C and S1D is the compartment thermal properties. Because the composite structural slab is relatively thin, SFRM is applied to the underside of the deck to achieve the 2 h prescriptive level of fire protection. All scenarios other than S1D consider the SFRM thermal properties for the compartment ceiling. S1D uses the thermal properties for normal-weight concrete instead of SFRM, leading to a significant change in compartment thermal factor. The result is that peak compartment temperatures of S1D are lower than those of S1B and S1C, but the total duration is much longer. Scenario S1D is considered for Design 2 and Design 3, in which the SFRM is removed from the deck.

This study has assumed that the fire does not breach the indicated compartments. The detailing of the interior and exterior walls needs to be reviewed to confirm whether it is sufficient to accommodate the estimated structural deflections and temperatures that are associated with the fire scenarios.

8.4 STRUCTURAL MEMBER TEMPERATURE HISTORIES

Thermal analysis in Abaqus was used to determine structural element temperatures because of the imposed time–temperature curves for Scenarios S1A through S1D. For each condition, a two-dimensional cross-section model was assembled, including the steel beam, concrete slab, beam SFRM (when occurring), and concrete SFRM (when occurring). Slab extent was modeled

for one full flute on each side of the beam, beyond which through-thickness effects dominate. Figure 8-9 shows the temperature contours across a beam and slab profile at one time step of the member temperature history.

Temperature-dependent thermal material properties according to the Design Brief were assigned to each element. The design fire temperatures were applied to all exposed surfaces below the slab, and the gas temperature at the top of the slab was held at 20 °C.

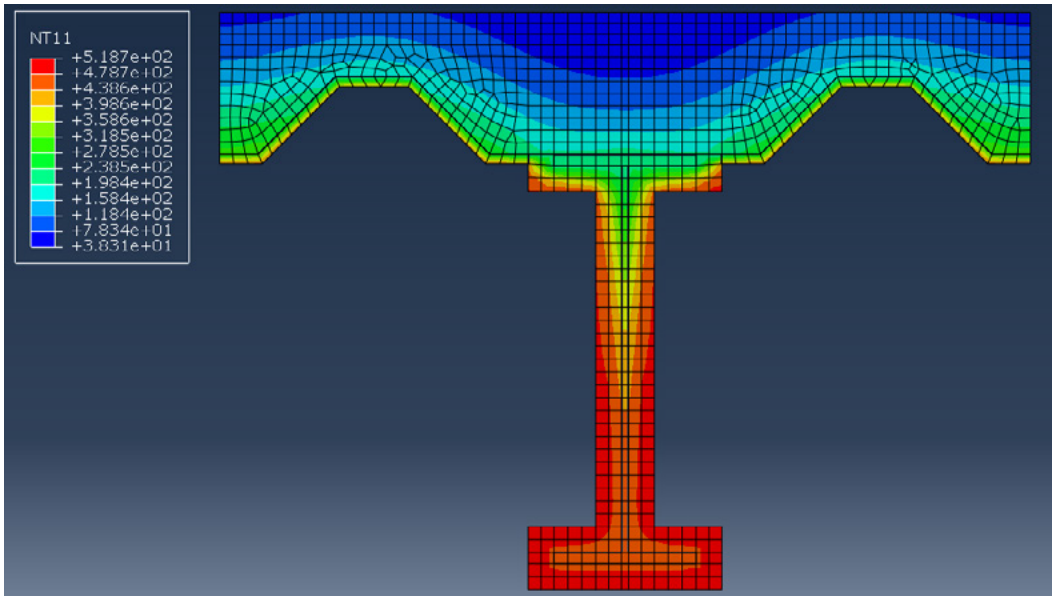

Figure 8-9. Temperature plot of an W16x31 insulated beam and slab.

Source: Courtesy of Magnusson Klemencic Associates (2019), and software © Abaqus.
Note: Scenario S1C, Beam SFRM = 26 cm; Slab SFRM = 10 mm, Time = 1.5 h.

Owing to the large number of cases to be run, the model building process was automated using the Abaqus scripting interface. This allowed many iterations of beam size, slab thickness, SFRM thickness, and time–temperature curve to be rapidly evaluated. An example suite of temperature histories for a W16x31 beam at varying levels of fireproofing is shown in Figure 8-10.

Analysis results were postprocessed to determine controlling bottom flange, web, top flange, and through thickness slab temperatures at each time step. These controlling temperatures were used for temperature load input to the structural analysis model.

8.5 STRUCTURAL ANALYSES

Three-dimensional, quasi-static structural analyses with geometric and material nonlinearity were performed in Abaqus to assess the structural response associated with elevated member temperatures. The extent of the model and the elements represented is shown in Figure 8-11.

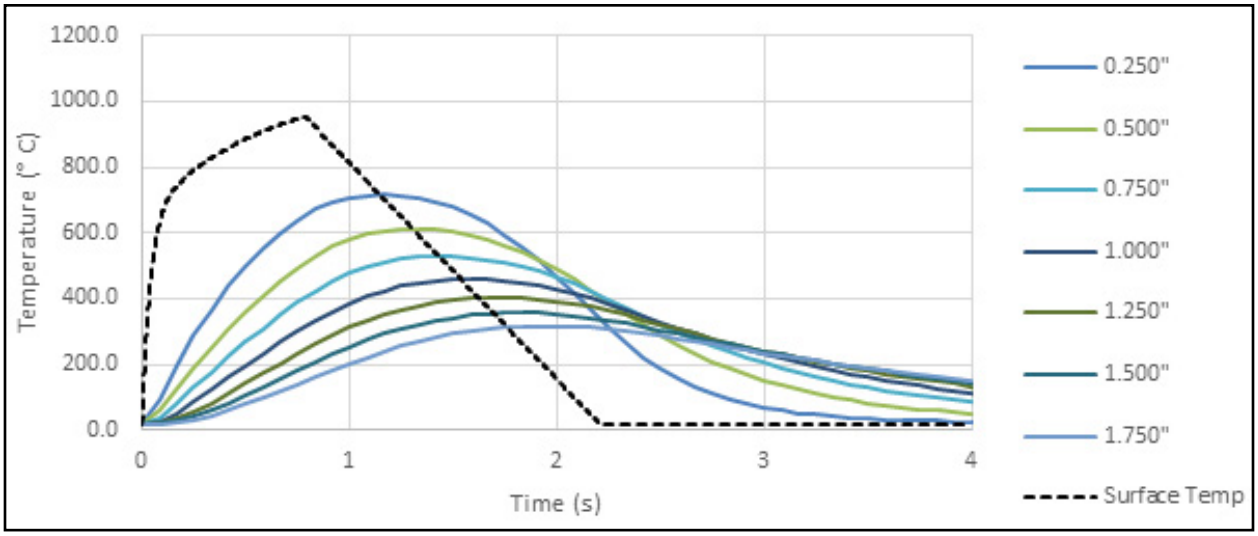

Figure 8-10: Bottom flange temperature.
W16x31 Beam, S1C, equal beam and slab SFRM thickness.

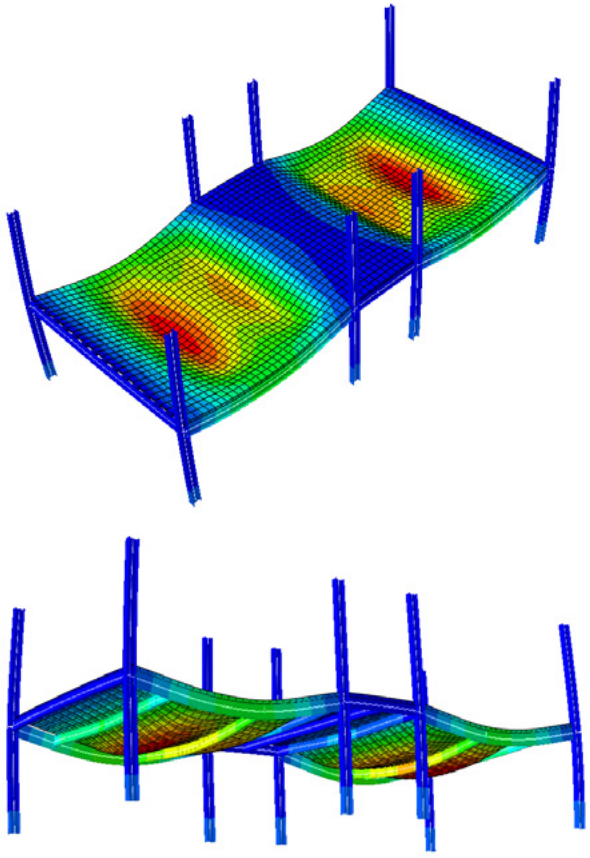

Figure 8-11. 3D structural model.
Source: Courtesy of Magnusson Klemencic Associates (2019), and software © Abaqus.

8.5.1 Nonlinear Model

The model is composed of two-node beam elements and four-node shell elements, coupled with rigid nodal constraints. The columns above and below the analyzed floor plate were modeled to simulate the restraint condition at the slab. Columns are pinned at the base and restrained horizontally at the top. They are restrained from twist at the top, at the bottom, and at the floor level. The model is also restrained horizontally at the floor level to account for stability provided by the lateral system.

At the edges of the model along the girder lines, rotational restraints are applied to simulate continuity outside the bounds of the model. Rotational restraints are not applied to the edges along the spandrel beams where the slab does not continue. The analysis does not consider a condition with a spandrel girder with unrestrained slab rotations, because the end bay of the building is much shorter than the typical condition and would not be a controlling design case.

Sensitivity to rotational fixity of beam-to-column and beam-to-beam connections was studied by comparing models with fully fixed connections to fully pinned connections. The pinned connection models showed more realistic behavior because the observed end-moment demands in the fixed-connection case exceeded the capacity of the connections, which are not specifically modeled. Slab shell element nodes are rigidly linked to beams, but are not linked to columns at the slab–column interface. This is done to eliminate slab–beam coupling at the columns, which could induce artificial bending moments.

Temperature-dependent nonlinear material models are used for both concrete and steel. The concrete is defined using the Concrete Damaged Plasticity model in Abaqus with the temperature-dependent compressive model taken from Eurocode 2 (CEN 2004). The tensile behavior of the concrete is defined using CEB-FIP Model Code 90 using the power law for brittle shear and unidirectional failure for brittle normal failure.

The model for the A992 Gr. 50 steel is based on Eurocode 3 (CEN 2005a). This model captures degradation of elastic and plastic response with elevated temperature, and ductile damage evolution of a set displacement (20 mm) following an ultimate strain of 0.1 mm/mm. The steel reinforcement model is similar, with temperature-dependent parameters taken from Eurocode 2.

The concrete shell elements utilize a layered element model in which the reinforcement is idealized as a continuous layer at the average depth of reinforcement, in the middle of the topping slab. The reinforcement for Designs 0 and 2 matches the original design. Reinforcement density is altered to meet performance objectives in Design 3. Shell element thicknesses were modeled in alternating 1 ft strips in the longitudinal direction to account for the stiffness of the profiled deck, as shown in Figure 8-12. The steel deck is included as a reinforcement layer in the slab to more accurately capture the condition at the end of the gravity case. The metal deck property stiffness is reduced to a negligible level once the temperature is elevated to simulate delamination from the slab. Shell element temperatures are assigned through the thickness of the material as shown in Figure 8-13.

Wide flange beam sections are defined using the built-in I-section definition in Abaqus. This section definition allows for temperature variation through the width and depth of the section using the predefined points in Figure 8-13. In this analysis, a uniform temperature is applied at each of the flanges and to the web, so the temperature varies in one axis only.

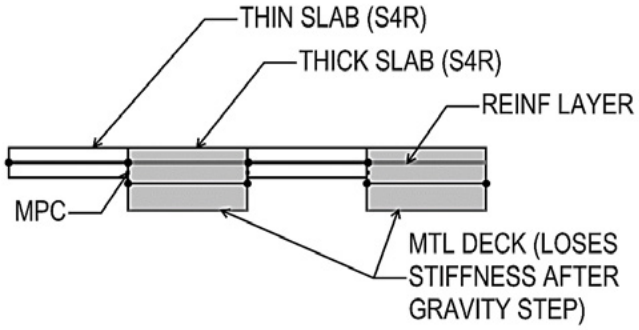

Figure 8-12. Slab element definition.

Source: Courtesy of Magnusson Klemencic Associates (2019).

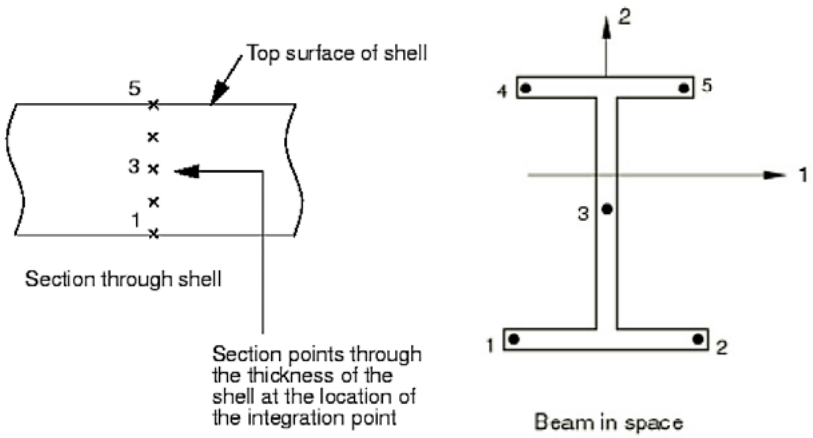

Figure 8-13. Temperature definition at beam and shell elements.

Source: Courtesy of Magnusson Klemencic Associates (2019).

A multistep analysis was performed to capture the effects of temperature over the duration of the fire event. An initial temperature of 20 °C was applied, and then factored gravity loads using the structural load combination for extraordinary events of ASCE 7-16 (2017), Section 2.5.2.2. Gravity loading includes factored self-weight, a uniform load applied to the slab, and line loads to account for cladding and to simulate adjacent bays where the slab continues outside of the model bounds. Point loads are applied at tops of columns to account for loads above the modeled floor. The applied gravity loads are shown in Figure 8-14.

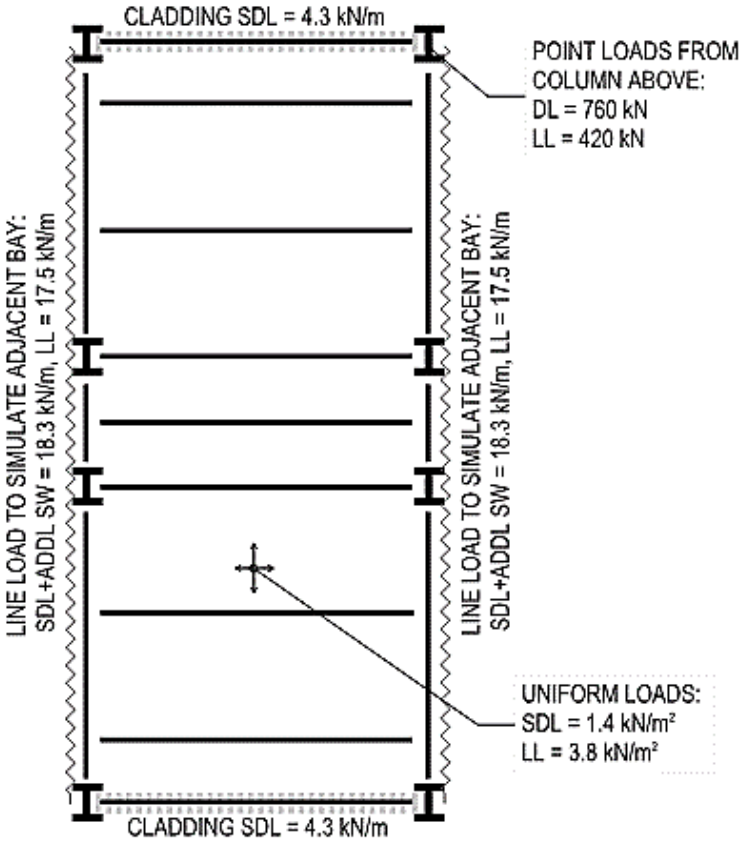

Figure 8-14. Applied gravity loads.

Source: Courtesy of Magnusson Klemencic Associates (2019).

After the gravity loading step, temperature loads are applied to beam and shell elements at time steps representing five minute increments. The temperatures vary through the element thickness based on the member temperature histories developed with the thermal analysis. The analysis duration of six hours was set to capture the member temperature histories and to allow the members to return to near 20 °C.

8.5.2 Member Design

The strength of the structural steel members is determined using the provisions of AISC 360 (AISC 2016b), Appendix 4. The ultimate member demands are based on the structural load combination for extraordinary events of ASCE 7-16, Section 2.5.2.2.c.

$$(0.9 \text{ or } 1.2)D + A + 0.5L + 0.2S \quad (8\text{-}1)$$

where

D = Dead load,
A = Load effect resulting from extraordinary event,
L = Live load, and
S = Snow load.

Member strengths, connection strengths, and floor deflections were evaluated at the locations shown in Figure 8-15.

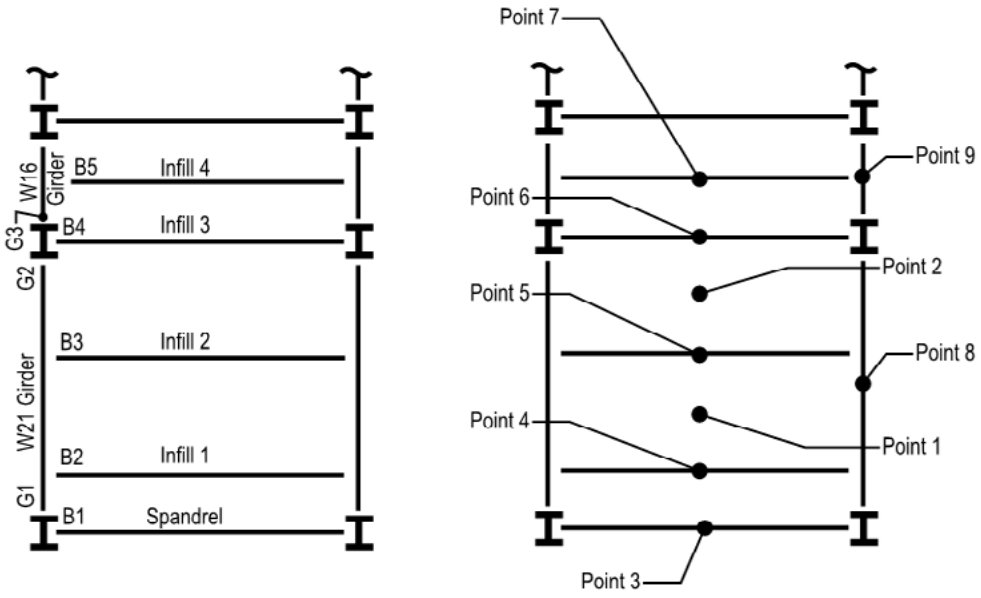

Figure 8-15: Key plan for strength and deflection results.

The strength and stiffness of structural steel, concrete, and concrete reinforcement varies with temperature. The temperature-dependent properties of structural steel have been determined from Eurocode 3. The temperature-dependent properties of concrete and concrete reinforcement are determined from Eurocode 2. The steel reinforcement is assumed to be hot rolled and therefore has the same temperature-dependent capacity reductions as structural steel.

The strength of the composite floor beams and girders is calculated in accordance with AISC 360, Appendix 4.2.4d. With the restraint provided by the slab, the beams and girders experience net compression and tension loads; therefore, interaction of flexure with axial loads is considered. The composite slab is assumed to provide lateral-torsional bracing of the top flange of both beams and girders. Given the lateral-torsional restraint, the positive flexural strength of the beams and girders is determined from AISC 360, Chapter F rather than using the AISC 360, Equations A-4-3 through A4-3-10. In some instances, the bottom flange of the beam is in compression. In these cases, the full length of the beam was considered unbraced for moment capacity calculations of the bare steel section.

When accounting for compressive loads, the slab was assumed to restrain beams and girders against weak-axis buckling, but constrained-axis torsional buckling is considered as a limit state. The composite slab provides torsional bracing of beams based on slab bending stiffness and sufficient beam web stiffness to brace the beam bottom flange. The girders are braced against torsion only at incoming beam connections. The limiting compression capacity of the beams and columns for the limit state of torsion is determined from Helwig and Yura (1999).

Beam demand/capacity ratios were assessed in two ways. First, the steel member forces in the analysis model were compared to the bare steel section capacity, accounting for bracing assumptions. In addition, element nodal forces in the slab and beam were combined into a resultant composite section demand and compared to the strength of the composite section calculated using the plastic stress distribution and temperature-dependent material properties. Example beam demand-to-capacity results for beams designed as composite sections and as bare steel can be seen in Figures 8-16 and 8-17, respectively, for the Design 0 case.

The strength of the columns is determined in accordance with AISC 360, Appendix 4.2.4b, using the temperature-dependent material properties and assuming uniform heat, which is consistent with the thermal analysis. Thermal gradients across the column sections were not considered, given the discussion in the commentary to AISC 360, Appendix 4.4d.

Because column continuity past the floor is included in the model, significant column moments develop at the floor level. The buckling behavior of the column was captured directly with the nonlinear analysis, so buckling is not considered in the capacity calculation. Lateral-torsional buckling of the column owing to the moment is considered but does not control beyond the plastic moment capacity. Figure 8-18 shows the column demand-to-capacity ratios in the Design 0 case. The results demonstrate plastic hinge formation when section capacity is reached just before the 1 h mark.

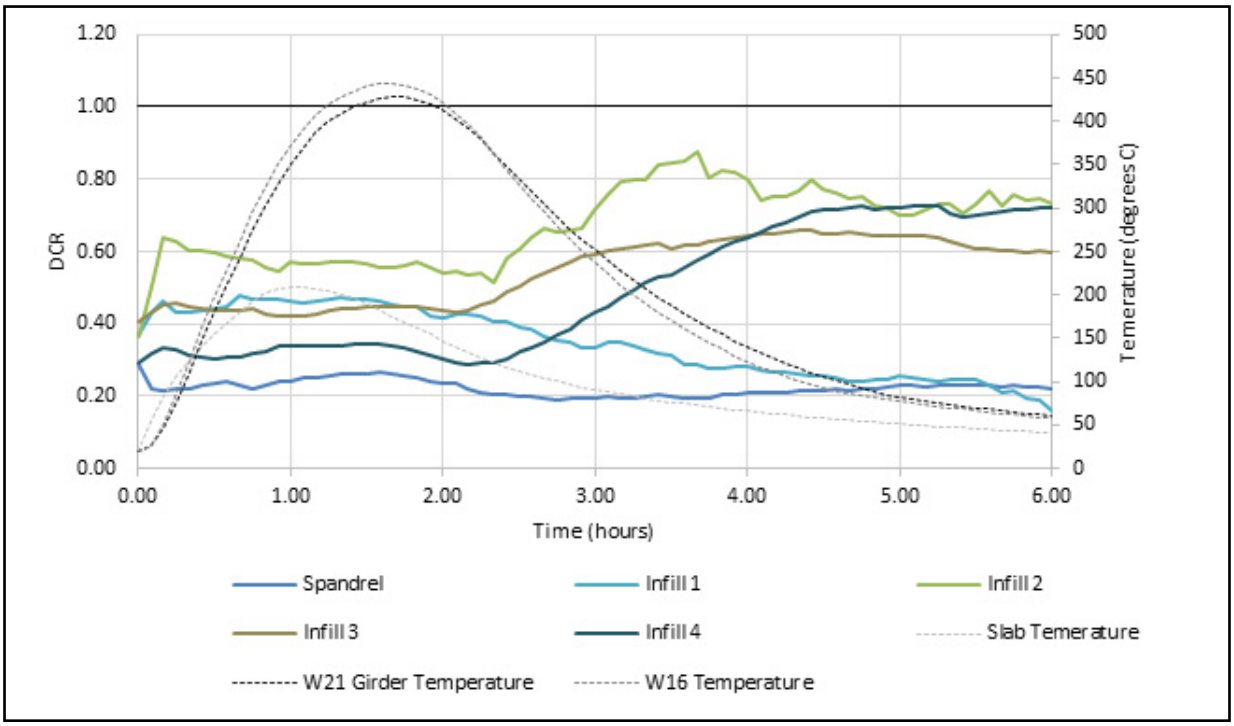

Figure 8-16: Design 0 demand/capacity ratios at beam midspans, composite sections.

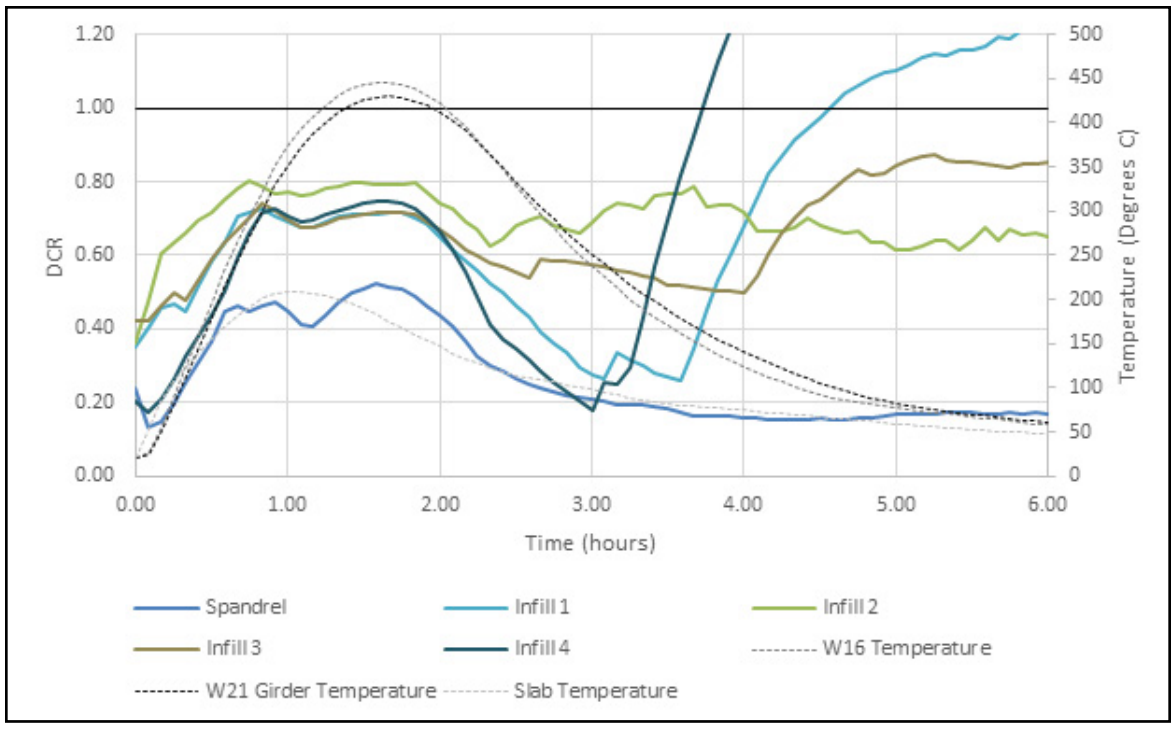

Figure 8-17: Design 0 demand/capacity ratios at beam midspans, steel only.

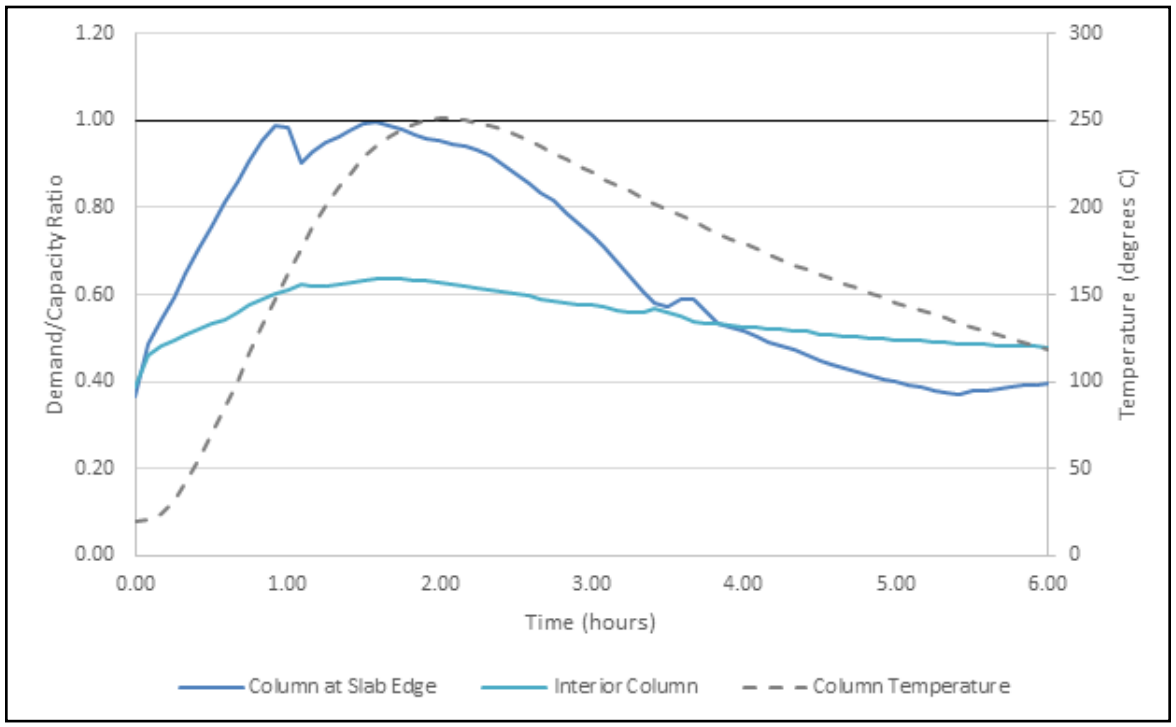

Figure 8-18: Design 0 demand/capacity ratios at columns.

8.5.3 Connections

Beam-to-column and beam-to-girder connections are represented as pins in the analytical model. Nodal forces developed in the model at these points of connection are checked against the strength and rotational capabilities of the connections. The beam connections for Building 2 are simple shear tabs with 22 mm diameter Group A bolts. Connection strength checks account for reduced strength of the bolts, welds, and steel connection material, using the beam bottom flange temperature, reduced in accordance with Annex D.3 of Eurocode 3, for temperature-dependent properties. The connections are checked for limit states of AISC 360, Chapter J with consideration of combined axial, bending, and shear stresses. Limiting stresses are based on plastic stress distributions.

In addition to the strength limit states, connections rotations more than 0.08 radians are considered to indicate failure. Shear tabs have been shown, (Astaneh-Asl 2005, Davison et al. 2010), to have rotational ductility more than this magnitude.

Figures 8-19 and 8-20 show the girder end rotations and connection strength for the Design 0 case at representative girder connections.

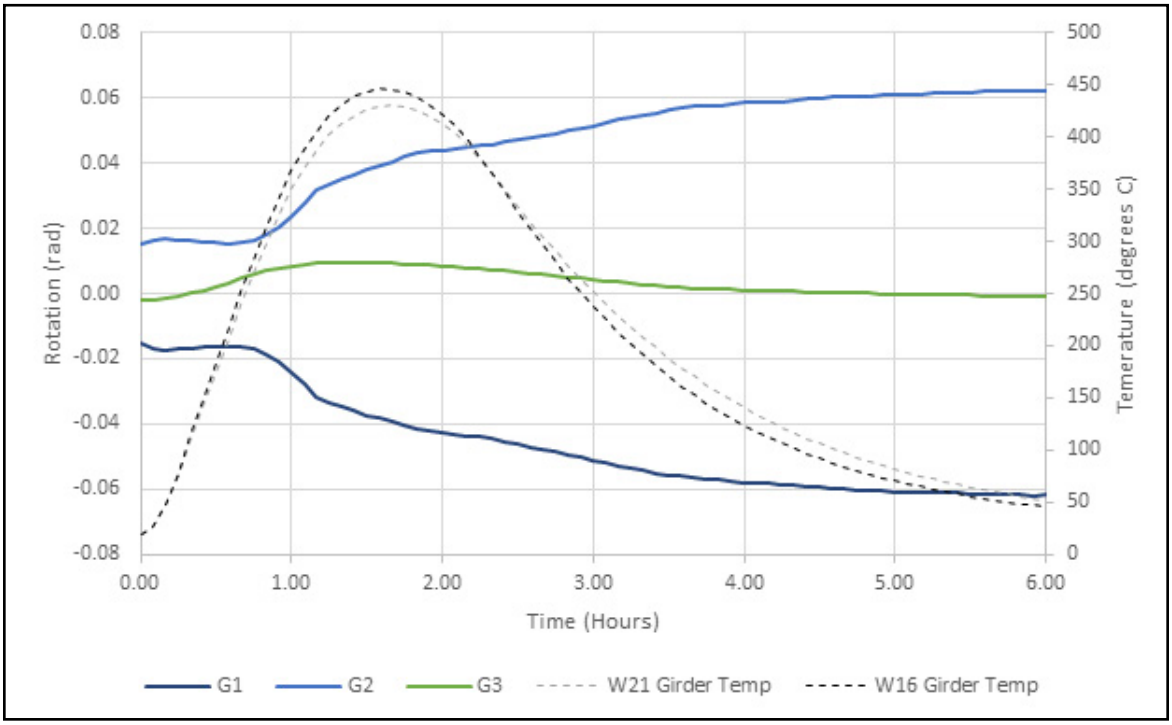

Figure 8-19: Design 0 girder end rotations

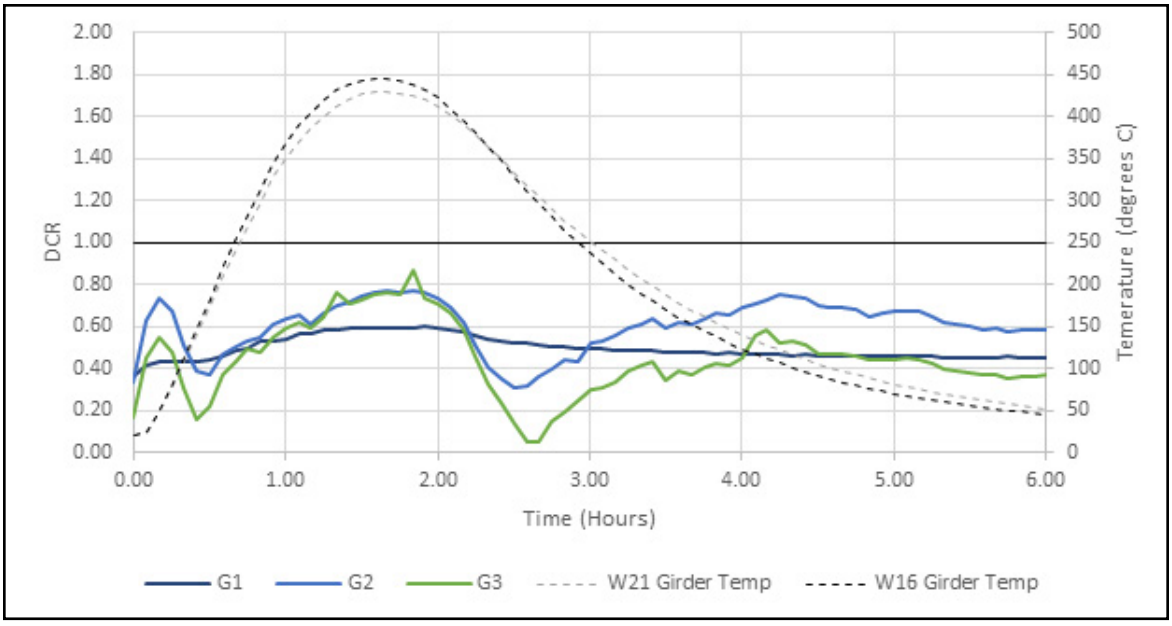

Figure 8-20: Design 0 girder end connection strength DCR.

8.6 DESIGN SUMMARY

8.6.1 Design 0

The structure, as considered, was able to maintain integrity for a duration of approximately 3.5 h when exposed to fire Scenario S1C. Beyond this duration, the demand/capacity ratio of one of the infill beams evaluated using the bare steel section properties exceeds 1.0. The relative deflection of the slab spanning between infill beams begins to exceed the L/20 limit (170 mm) at approximately 3.5 h.

8.6.2 Design 1

The structure was not evaluated for Design 1 because the building occupancy is an in-patient hospital, and safe egress of the occupants is not possible.

8.6.3 Design 2

For Design 2 — where only changes to the level of applied insulation is permitted — the SFRM is removed from the underside of the slab, and S1D is the controlling fire scenario.

In addition to increasing temperatures in the slab, removing slab SFRM changes the parameters for the fire time–temperature curve, resulting in a lower peak gas temperature and a longer duration. In contrast to Design 0, slab temperatures increased much more rapidly in the heating phase than did the beam and girder temperatures. Large tensile forces which exceeded connection capacity developed in the girder-to-interior-column connections as a result of girder-line axial

continuity. This tensile force is developed through differential self-strain of the beam and slab, which is resolved as a force couple in the rigidly linked slab and beam elements. It is reasonable to assume that this force has been amplified because stud slip is not accounted for in the model, but more sophisticated modeling is needed for confirmation.

To mitigate the effect of differential slab and beam strain in this simplified modeling approach, the thickness of SFRM applied to the girders was reduced to decrease the temperature differential. Connection axial load decreased but was still more than the available capacity. Connection rotations more than 0.08 radians were observed before the connection axial load could be reduced below its capacity. Further refinement of stud-slip and connection modeling would be needed to confirm the viability of the connections for Design 2. The columns, beams and slab were sufficient to resist the fire effects for Design 2.

Given the low demand/capacity ratios of the infill beams with full SFRM, the thickness of SFRM was reduced to 20 mm. Considering the slabs, beams, girders, and columns, the amount of SFRM provided in Design 2 was reduced by 40% from Design 0. A summary of the SFRM thickness is provided in Section 8.6.3.

8.6.4 Design 3

The objective of Design 3 is to remove fireproofing from infill elements by making structural enhancements to slab reinforcement and to provide additional capacity for the slab to support the gravity load with membrane action of the slab. The slab panel method (Clifton 2006) shows that the reinforcement in the slab needs to be upgraded to allow for the SFRM to be removed from the infill beams. Two levels of enhanced reinforcement were evaluated, as summarized in Table 8-4. The Design 0 slab reinforcement is shown for reference. Both reinforcement schemes 3A and 3B are structurally viable, depending on the acceptable level of midbay deflection. The reinforcement weight information in Table 8-4 does not include additional quantity for lap splices.

Table 8-4. Design 3 Slab Reinforcement Enhancement.

Design Scheme	0	3A	3B
Top Reinforcement	#3 @ 450 mm	W2.9 @ 150 mm	#3 @ 450 mm
Transverse Reinforcement	#3 @ 450 mm	W2.9 @ 150 mm	#3 @ 450 mm
Bottom Reinforcement	-	#3 @ 300 mm	#3 @ 300 mm
Total Reinforcement Area	320 mm^2/m^2	490 mm^2/m^2	550 mm^2/m^2
Total Reinforcement Weight	24 N/m^2	37 N/m^2	42 N/m^2
Midbay Deflection	–	440 mm	350 mm

Without changing the modeling assumptions, the W21 girder to column connections needed to be enhanced from a 6-bolt shear tab connection to an 8-bolt shear tab connection in a 2 × 4 pattern to accommodate the axial loads induced in the girder connections. Similarly, the W16 girder to column connections needed to be enhanced from a 6-bolt shear tab connection (2 × 3) to an 8-bolt (2 × 4) shear tab connection. Alternatively, the connections could be changed to 3-bolt and 4-bolt double angle connections at the W16 and W21 girders, respectively. More refined modeling of the nonlinear properties of the connections may show better performance of the girder connections

by relieving some of the axial forces to be transferred through the end connections and eliminate the need to enhance the connections beyond the requirements of the gravity design.

Although the infill beam end connections become overstressed when exposed to the elevated temperatures of the beam, the weak axis shear capacity of the slab can support the full vertical reaction of the slab panel along each girder line.

Consideration was given to reduction in thickness of SFRM along the girders to minimize the axial forces to be transmitted through the connection. A nominal reduction in the axial force is realized, but not enough to significantly change the connection requirements.

Considering the slabs, beams, girders, and columns, the amount of SFRM provided in Design 3 was reduced by 60% from Design 0. A summary of SFRM thicknesses for the three design scenarios can be found in Table 8-5. The beam and girder groupings for SFRM thickness iterations are defined in Figure 8-21.

Table 8-5. SFRM Thickness Summary.

Design Case	Design 0	Design 2	Design 3
Slab (mm)	10	0	0
W21 Girder (mm)	27	27	27
W16 Girder (mm)	27	12	27
Perimeter Beam (mm)	27	20	27
Infill Beam (mm)	27	20	0
Column (mm)	43	43	43

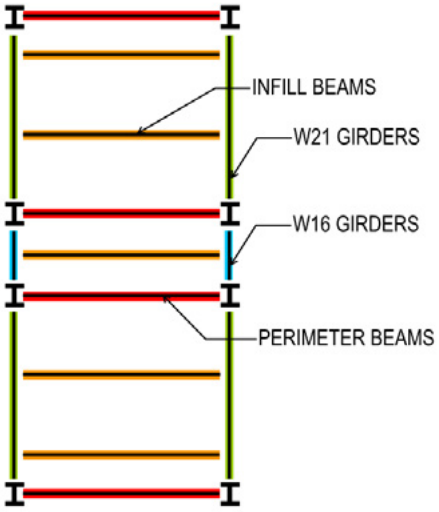

Figure 8-21. Beam categories for SFRM thickness.
Source: Courtesy of Magnusson Klemencic Associates (2019).

To illustrate the relative quantity of SFRM applied to each element, the total SFRM applied to the bay is calculated and divided by the total bay area. As shown in Figure 8-22, Design 0, the largest volumes of SFRM are associated with the slab and the beams.

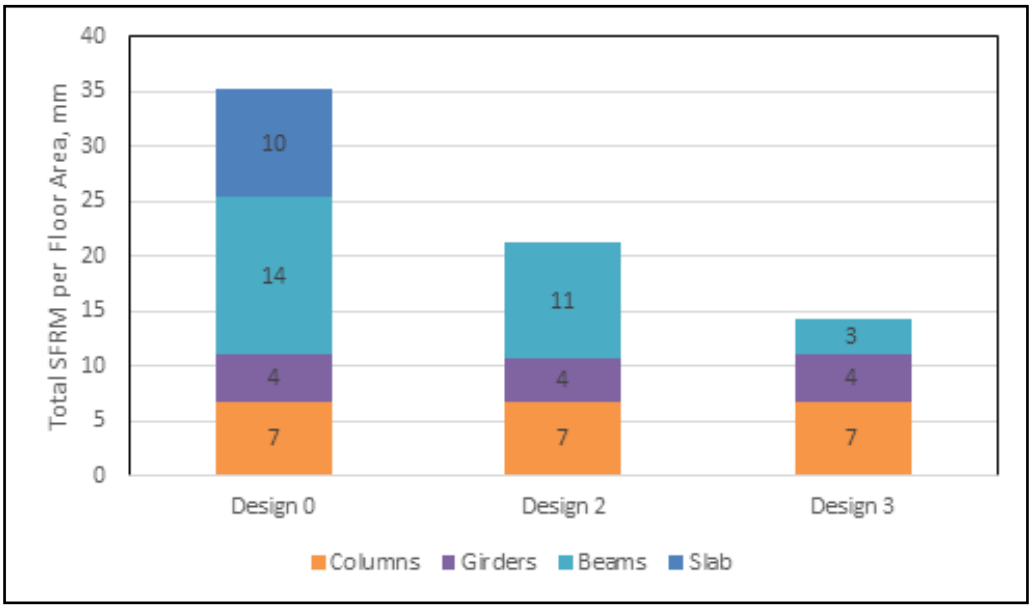

Figure 8-22. Beam categories for SFRM thickness iteration.
Source: Courtesy of Magnusson Klemencic Associates (2019).

8.7 DISCUSSION

8.7.1 Thermal Analysis Comparison

Lumped mass calculations were performed in accordance with Eurocode 4 (CEN 2005b), Part 1.2, Section 4.3.4.2.2 for composite beam temperatures, and were compared to the temperature histories using finite-element heat transfer. AISC does not provide guidance for lumped-mass modeling of composite members in its fire provisions. In the scenarios considered, the lumped mass model predicted a peak temperature 5% to 20% higher than the finite-element analysis (FEA) model. Based on these results, the lumped mass model as proposed by Eurocode provides a reasonable and conservative approximation of expected temperatures. A comparison of top flange, web, and bottom flange temperatures for a W21x44 beam subjected to the gas temperatures in Scenario 1-D is shown in Figure 8-23.

Column temperatures determined through finite element methods (FEM) were compared to the lumped mass calculation guidelines in the AISC 360, Appendix 4.2.2 commentary. As with the composite beam lumped mass calculation, the peak temperature prediction was conservative when compared with FEM, but within 20%. Lumped mass calculations are a useful alternative when FEM are unavailable. Scenario S1-D, W14x74 column temperature values using FEA and AISC 360, Appendix 4.2.2 commentary (LM) is shown in Figure 8-24.

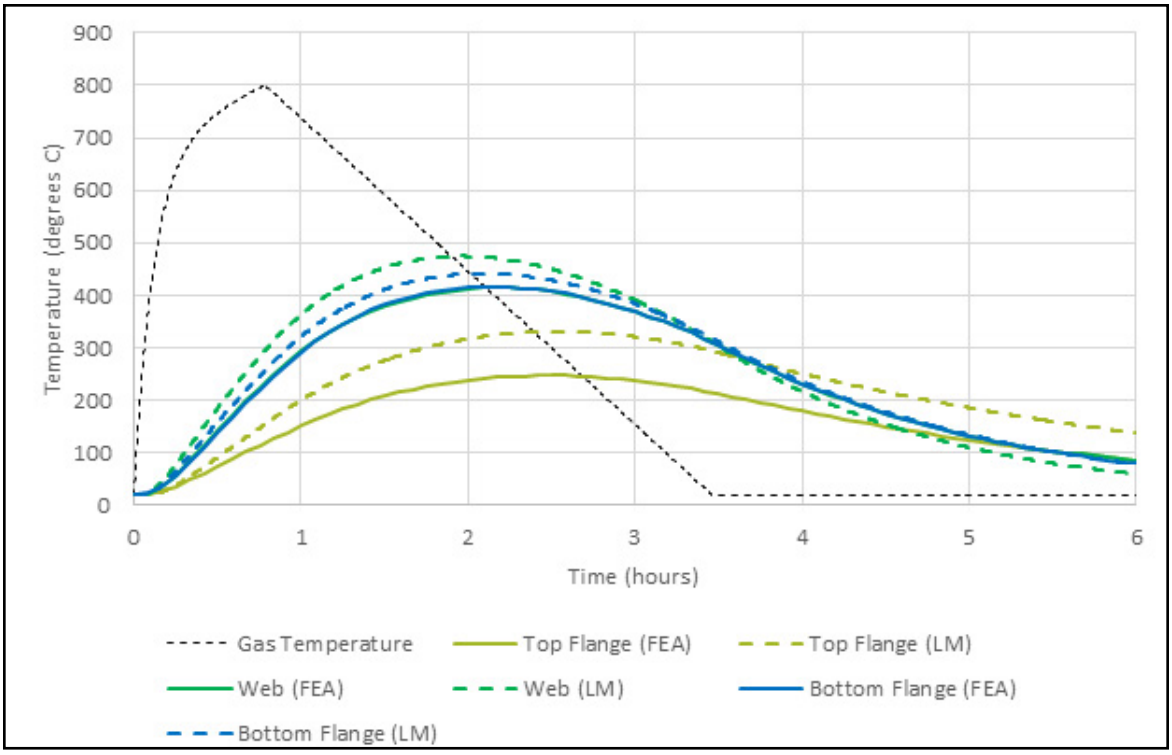

Figure 8-23. Scenario S1-D, W21x44 composite beam temperature values using FEA and Eurocode 4, Part 1.2, Section 4.3.4.2.2 (LM).

Source: Courtesy of Magnusson Klemencic Associates (2019).

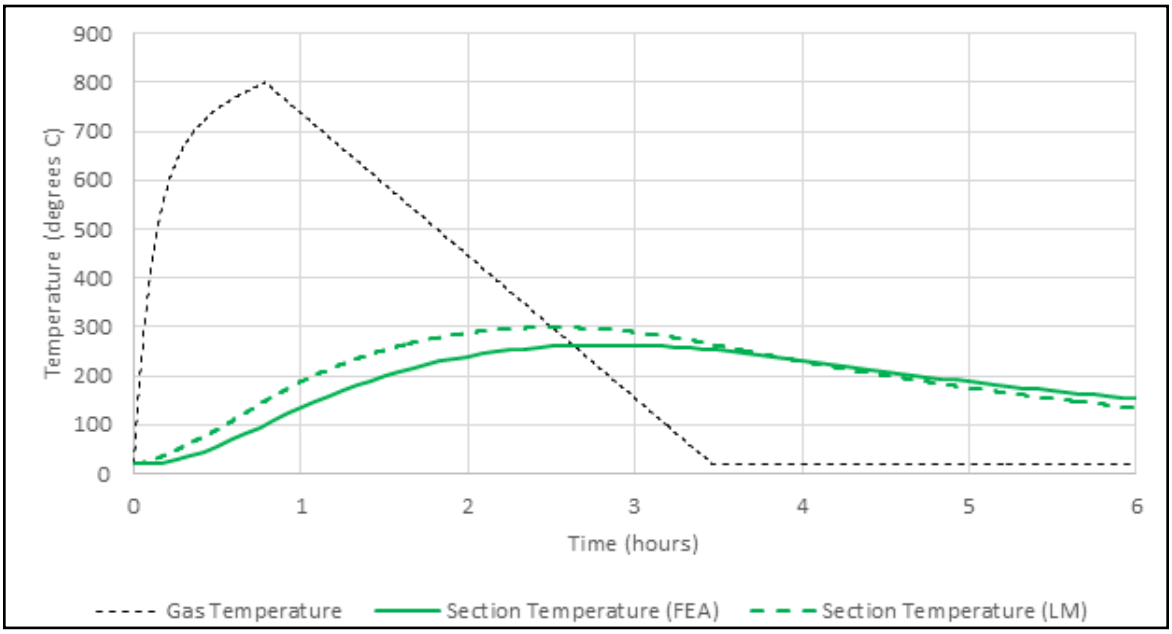

Figure 8-24. Scenario S1-D, W14x74 column temperature values using FEA and AISC 360, Appendix 4.2.2 commentary (LM).

Source: Courtesy of Magnusson Klemencic Associates (2019).

8.7.2 Beam and Girder End Constraints

The three-dimensional model considered beam end conditions with and without strong axis flexural continuity. With consideration of flexural continuity, very large moments are developed at connections to columns. The magnitudes of the moments are not compatible with the simple shear connections that are provided at the beam-to-column connections. Therefore, as a lower-bound solution for the load-carrying capacity of the floor system, the member end connections were idealized without flexural continuity. The member end rotations were then compared to the connection rotations that have been validated through testing (Choe et al. 2019) to confirm that they have sufficient deformation compatibility to accommodate the expected rotations of the beam ends. This is a similar approach to the justification of connections of members that are not part of the seismic force-resisting system as discussed in the commentary of AISC 341, Section D3. For shear tab connections, the maximum rotation of a shear tab connection can be determined based on the available end offset distance, g, as shown in Figure 8-25 (Astaneh-Asl 2005).

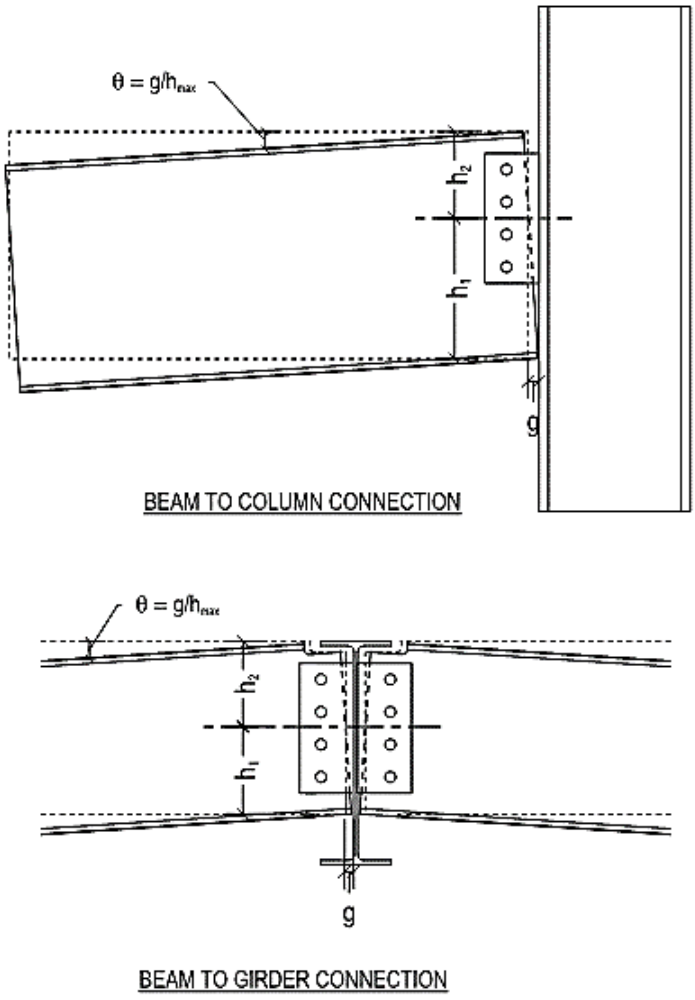

Figure 8-25. Rotation of shear tab connection.

Source: Courtesy of Magnusson Klemencic Associates (2019).

8.7.3 Slab Modeling

It has been observed in fire events that at elevated temperatures the steel deck debonds from the underside of composite slabs (Lim 2003, Li et al. 2017) and is no longer capable of acting as positive flexural reinforcement for the slab. As a result of early deck debonding, it is common practice to model only the concrete topping slab (Gernay et al. 2020) and ignore the participation of the metal deck and concrete in the flutes. When only the concrete topping slab is considered in the analysis of Building 2, gravity deflections are vastly overpredicted before temperature loads are applied. If a slab profile is modeled that represents both the thin and thick portions of the composite slab and includes metal deck stiffness in the gravity loading step, the slab can span to the secondary beams without relying on membrane action for gravity loads, and the associated large displacements are mitigated. There is significantly more negative bending capacity at the beam lines because the effective depth of the section extends down from the topping reinforcement to the bottom of the deck flutes.

Because the slab reinforcement from original design, which includes reinforcement placed low in the deck flutes, is more robust than traditional slab-on-deck welded-wire-fabric reinforcement placed above the deck flutes, the design team did additional analyses to appropriately examine and account for the capacity of the original slab especially the deck rib reinforcement. Modeling of the thin and thick portions of the slab also allows for reinforcement to be analytically placed low in the deck flutes to be appropriately leveraged for maximizing the load carrying capacity of a slab panel.

Figure 8-26 shows the geometric options considered for the slab profile. The alternating strips of thick and thin elements in Option (d) were found to produce the best longitudinal behavior while limiting error in in the weak axis. This option was favored over Option (c), where similar deflection results were seen, because the smaller quantity of shell elements reduces runtime and composite section cut results are easier to post-process. Option (b), where a truss element is added below the slab with area equal to the flute area, was rejected because there was not an easy way to include the contribution of the metal deck without adding another element, which was found to be important in predicting initial deflection. Gravity-step deflections for a one-bay test model of the floor system using each slab geometry option can be seen in Figure 8-27.

8.7.4 Slab Panel Methodology

The slab panel method (SPM) as described in the literature (Clifton 2006) was used to develop preliminary designs to be verified with the three-dimensional model. Additional limitations were imposed on the panel deflections to target the maximum allowable rotations of the beam and girder connections. The SPM was a reasonable prediction of the system behavior when compared to three-dimensional analysis. Given that only two secondary beams occur within the slab panel under consideration, and SPM relies on a reasonably distributed reinforcement assumption, the beams were not assumed to contribute to the strength of the slab panel.

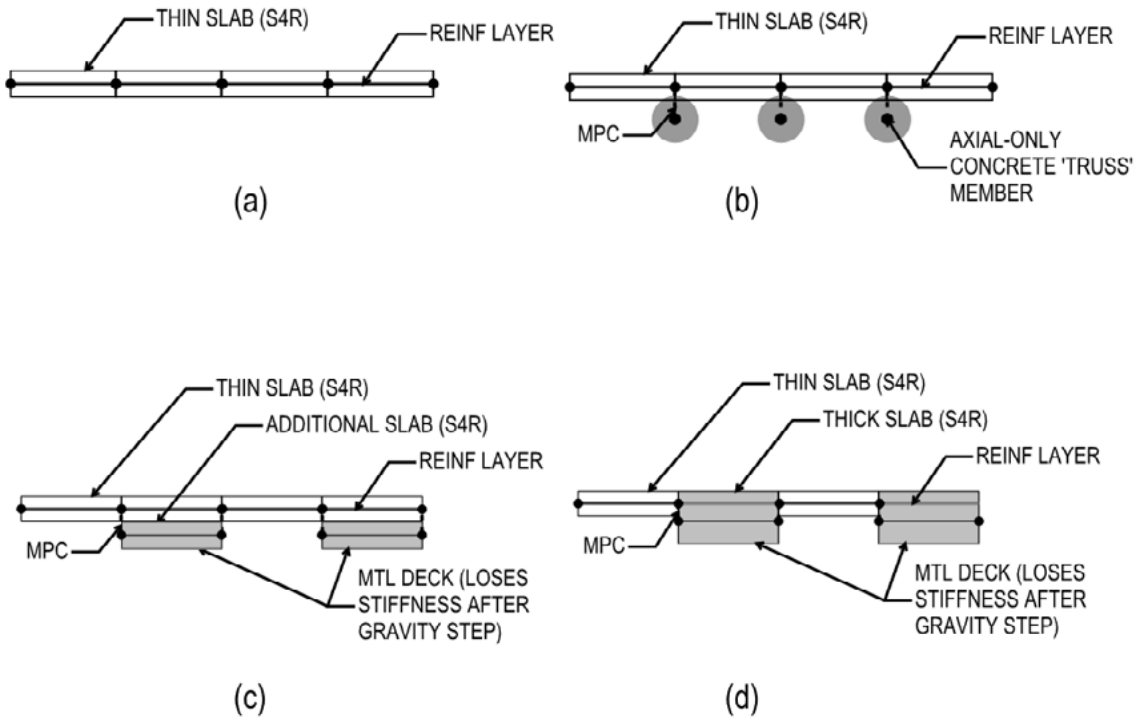

Figure 8-26: Slab Geometry Options: (a) Topping-only, (b) Topping with truss elements rigidly connected, (c) Topping with additional flute elements rigidly connected, and (d) Alternating thick-thin elements with rigid connection.

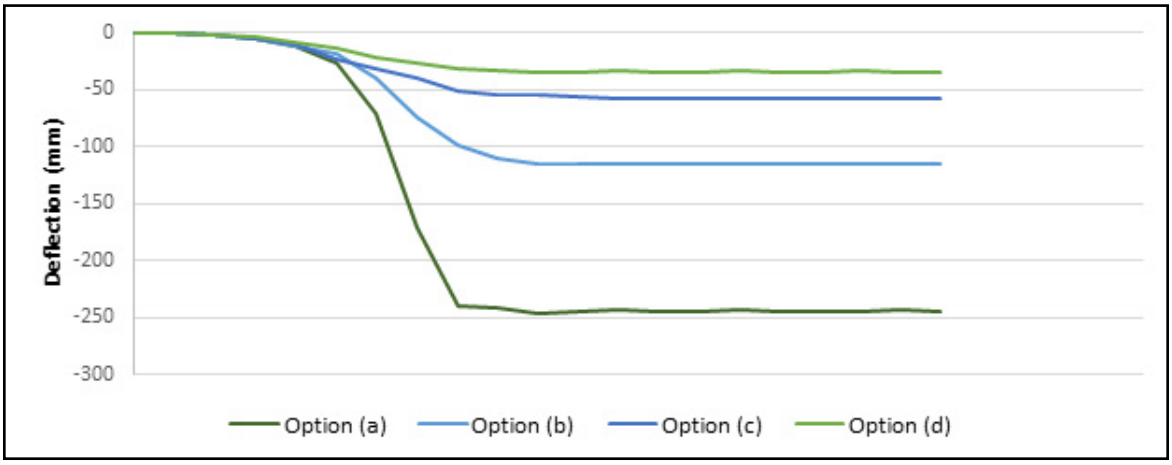

Figure 8-27: Comparison of deflections over the gravity step for slab geometry options: (a) Topping-only, (b) Topping with truss elements rigidly connected, (c) Topping with additional flute elements rigidly connected, and (d) Alternating thick-thin elements with rigid connection.

8.7.5 Column Design

The exterior columns experience significant shear and bending moments associated with the growth of the floor subjected to a fire event as shown in Figure 8-28. To maintain the global stability, the columns need to be able to accommodate the thermal expansion of the building.

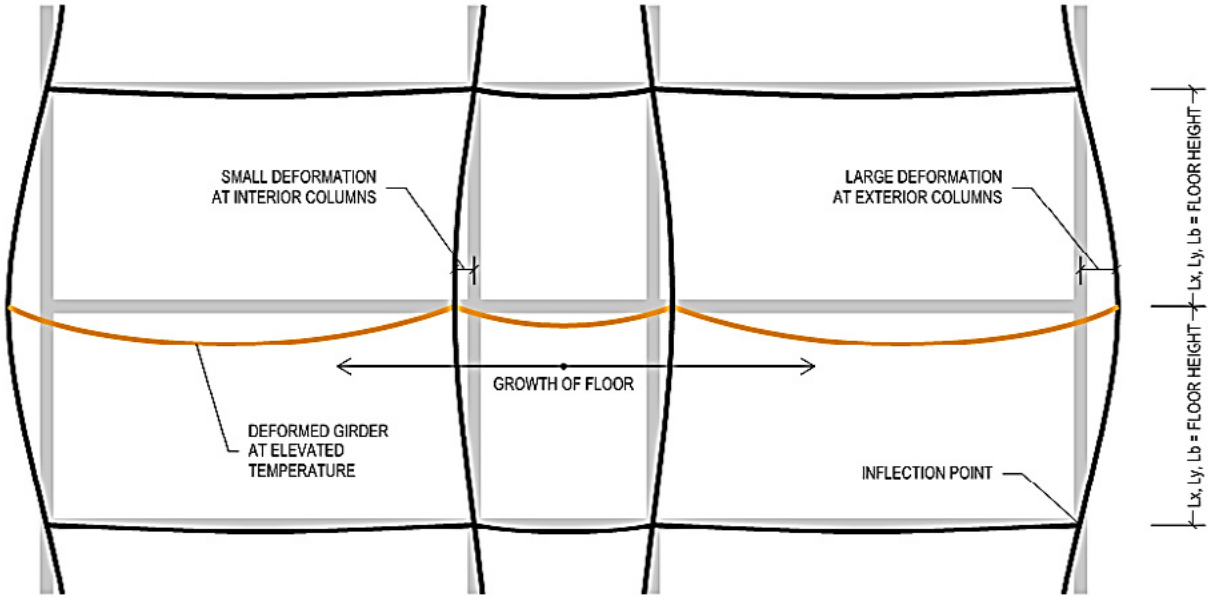

Figure 8-28. Exterior column bending.

Source: Courtesy of Magnusson Klemencic Associates (2019).

Given that Building 2 has been designed to the provisions of Seismic Design Category D, the column splices have the shear capacity to develop the plastic moment capacity of the columns in accordance with AISC 341 for columns that are not part of the seismic force-resisting system. This precludes a shear failure at columns under a fire event.

The columns were designed to support gravity loads assuming the unbraced length between floors. Therefore, gravity load-carrying capacity is maintained as long as flexural hinges can develop at the top and bottom of the columns. Because there is a load path to support the resulting lateral loads and the columns do not buckle laterally or in torsion prior to the development of the plastic moment, axial capacity is maintained.

Flexural members that are unbraced along their length in single curvature can assume a Cb = 1.67. For rolled shapes, when the slenderness ratio of the column, L/r, is less than 130, the lateral-torsional buckling capacity would exceed the plastic moment capacity. Higher values of Cb and the resulting L/r can be justified for columns in double curvature, provided that there is enough stiffness to restrain the column rotation at the floors above and below. Because the location of the inflection point is dependent on the stiffness of the beams and connections at adjacent floors and the floor-to-floor heights, it is simple and conservative to assume Cb = 1.67 for the column design.

8.7.6 Composite Beam Section Capacity

AISC 360, Appendix 4.2.4d (d) addresses composite beam design for flexure in a fire event. Using the AISC method, capacities are either determined using AISC 360, Chapter I with reduced yield stresses consistent with temperature variation or using the nominal flexural capacity at ambient temperature multiplied by a retention factor, *r(T)*, to account for losses resulting from reduced strength and stiffness.

The results presented for Building 2 use reduced material properties. A comparison of the approaches for the Design 0 case are presented in Figure 8-29, with thick lines indicating the use of retention factors and thin lines representing reductions to material properties.

The retention factor approach consistently under-predicts capacity compared with the material property modification approach. This is intuitive because it is a simplification of several variables and was developed to be a lower bound on observed behavior.

The retention factor approach implies a baseline moment capacity calculation that can be used at each step in the temperature history. This is only valid if significant net tensile and compressive forces in the composite section are not observed. Per AISC 360, Appendix 4.2.4d(f), combined flexure and axial force must be considered where it occurs. Tensile and compressive forces vary throughout the temperature history because of changes in the steel and concrete temperature differential, so the moment capacity is also variable based on the axial-flexural interaction. Because the capacity for combined forces must be calculated at each time step, it is straightforward to also include the variation in material properties directly. The retention factor approach predicts a lower capacity and does not provide a significant benefit in reducing computation complexity.

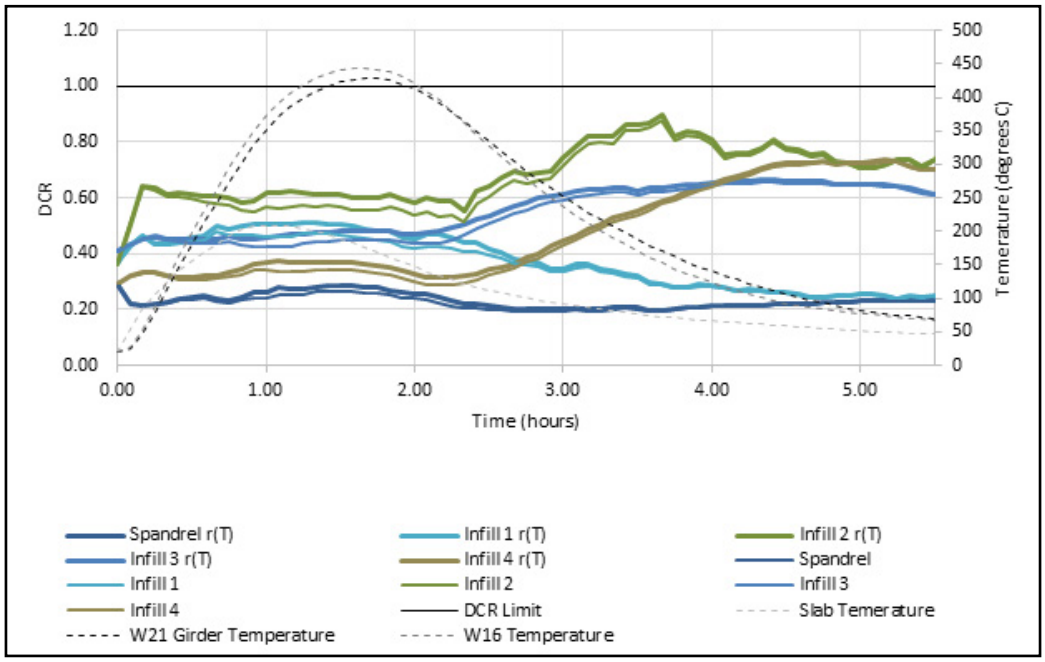

Figure 8-29. Design 0 demand/capacity ratios at beam midspans, composite sections. Comparison of retention factor, *r*(*T*), to reduction in material properties.

Source: Courtesy of Magnusson Klemencic Associates (2019).

8.8 CONCLUSIONS

Magnusson Klemencic Associates analyzed the structural integrity of the Risk Category IV Building 2, which was originally designed for West Coast loads. The structural behavior was evaluated using PBSFD and derived the following conclusions:

- Prescriptive fireproofing in Design 0 showed good performance when subjected to a fire exposure considering full burnout.

- Structural response to fire exposure is highly dependent on the restraint imposed on the structural system. The strength and stiffness reductions to concrete and steel mechanical properties are not a significant contributor to the structural response. Removing prescriptive-based SFRM from the underside of composite slabs is achievable with minimal changes to the structural design if the thermal strains can be balanced with the beam thermal strains. This may require modifications to the SRFM thicknesses on beams and girders.

- Design process for improving performance by balancing fireproofing thicknesses is iterative because of the many nonlinear and interdependent parameters defining the thermal and structural behavior of the system.

- Slab panel method accurately represented membrane action from added slab reinforcement in Design 3.

- Relying on slab reinforcement for membrane action is an effective method to improve the structural response to fire exposure because it is insulated by concrete and is typically already included in the floor assembly.

- For each of the design options presented, the girder to column connections are the limiting factor. More refined connection modeling may show better performance by reducing stiffness and allowing slip at bolts, but greatly increases the model complexity.

- Minor upgrades to the slab reinforcement and girder to column connections can result in significant reductions to the volume of SFRM required in a conventionally framed steel building and allow the owner and engineer to establish performance objectives that are absent from traditional prescriptive methods.

REFERENCES

AISC (American Institute of Steel Construction). 2016a. *Seismic provisions for structural steel buildings,* AISC 341. Chicago: American Institute of Steel Construction.

AISC. 2016b. *Specification for structural steel buildings*, AISC 360. Chicago: American Institute of Steel Construction.

ASCE. 2017. *Minimum design loads and associated criteria for buildings and other structures*, ASCE 7-16. Reston, VA: ASCE.

Astaneh-Asl, A. 2005. “Design of shear tab connections for gravity and seismic loads.” *Steel Tips.* Lafayette, CA: Structural Steel Educational Council, June.

CEN (European Committee for Standardization). 2001. EN 1991-1-2. *Eurocode 1 – Actions on structures – Part 1-2: General actions – Actions on structures exposed to fire*. Brussels: CEN.

CEN. 2004. EN 1992-1-2. *Eurocode 2 – Design of concrete structures – Part 1-2: General rules – Structural fire design*. Brussels: CEN.

CEN. 2005a. EN 1993-1-2. *Eurocode 3 – Design of steel structures – Part 1-2: General rules – Structural fire design*. Brussels: CEN.

Choe, L. Y., S. Ramesh, M. S. Hoehler, M. S. Seif, M. F. Bundy, J. Reilly, et al. (2019). “Compartment fire experiments on long-span composite beams with simple shear connections Part 2: Test Results.” *Tech Note, TN 2055*. Gaithersburg, MD: NIST.

CEN. 2005b. EN 1994-1-2 *Eurocode 4 – Design of steel structures. Part 1-2: General rules. Structural fire design*. Brussels: CEN.

Clifton, G. C. 2006. “Design of composite steel floor systems for severe fires.” *HERA Report R4-131*. Manukau City, Auckland, NZ: New Zealand Heavy Engineering Reach Association.

Davison, J. B., I. W. Burgess, R. J. Plank, H. Yu, and Y. Hu. 2010. “Ductility of simple steel connections in fire.” In *Proc., SDSS’ Rio 2010: International Colloquium*, Rio de Janeiro: Federal University of Rio de Janeiro, 441−448.

Helwig, T. A., and J. A. Yura. 1999. “Torsional bracing of columns.” *J. Struct. Eng.* 125 (5): 547−555.

ICC (International Code Council). 2018. *International building code*. Washington, DC: International Code Council.

Wang, Y. C., X. H. Dai, and C. G. Bailey. 2011. “An experimental study of relative structural fire behaviour and robustness of different types of steel joints in restrained steel frames.” *J. Construct. Steel Res.* 67(7): 1149–1163.

Chapter 9. Building 3: Thornton Tomasetti (TT)

Participants

The Structural Engineering Institute of ASCE acknowledge the work of the participants in this project.

Industry Champions

The TT (Thornton Tomasetti) design team comprised the following contributors:

Najib Abboud, Ph.D., P.E., *Industry Champion*

Zeynab Abbasi, Ph.D.

Ali Ashrafi, Ph.D., P.E., LEED AP

Pierre Ghisbain, Ph.D., P.E.

Jaimin Korat

Mostafa Mobasher, Ph.D.

Jenny Sideri, Ph.D., P.E.

Zhi Zhang, Ph.D.

BUILDING 3

Building 3 is a Type I-A mixed-use, 50-story-tall building (Figure 9-1). The building design is generic and representative of a common type of modern high-rise building design in the United States. The building is comprised of two distinct structural systems; the 20 upper floors are residential floors with concrete columns and two separate concrete cores to resist lateral loads. The 30 lower floors are office floors with steel perimeter columns, steel beams, and a single larger concrete core to resist lateral loads (Figure 9-2). The transition between the upper and lower structural systems is achieved by several interconnected steel transfer trusses located at the 30th floor. The trusses transfer loads from a denser column spacing in the upper residential floors to a wider column spacing in the lower office floors. Two features of the building are considered for performance-based fire design: a typical bay of the steel frame of the 30 lower floors, and the transfer trusses as a unique structural feature of the building (Figure 9-1).

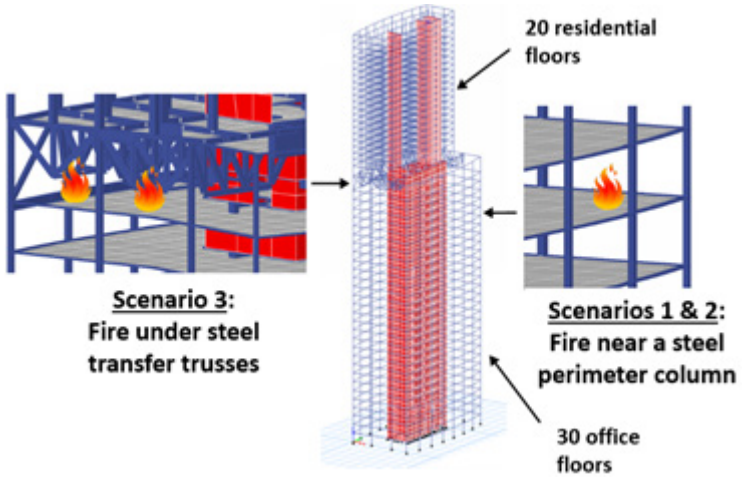

Figure 9-1. Building geometry and locations considered for performance-based fire engineering.

Source: Courtesy of Thornton Tomasetti (2019).

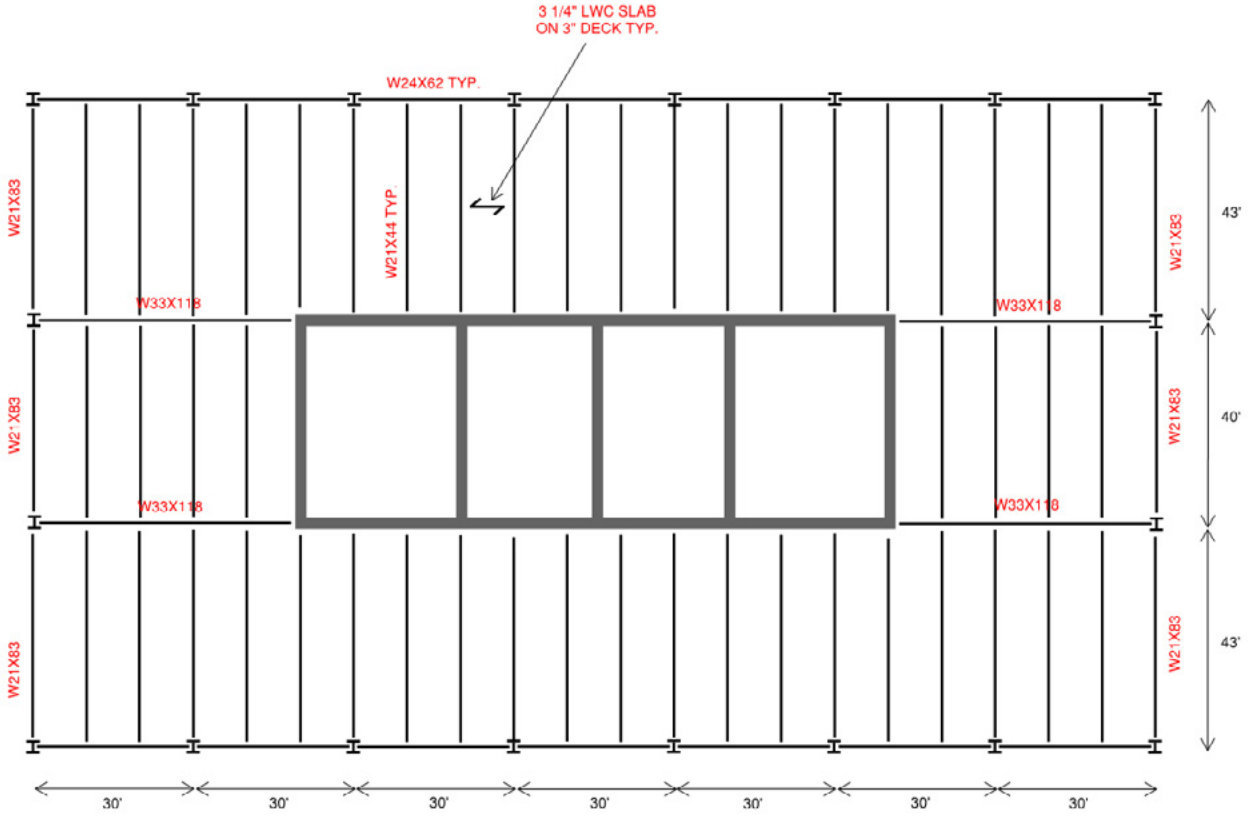

Figure 9-2. Typical office floor framing plan.

Source: Courtesy of Thornton Tomasetti (2019).

9.1 DESIGN STRATEGY

For Design 1, the performance objective regarding occupant egress requires providing enough time for the occupants to travel safely to refuge areas within the building or exit the building to a public area. Full evacuation for this high-rise building may require hours, practically making this requirement into designing for full burnout. Depending on the specifics of a design, a similar project that relies on refuge in place strategies could provide for a shorter survival duration for the typical floor framing. Such an approach would not be acceptable for the transfer trusses in any situation because their failure would affect the refuge floors as well. For this project, it has been determined that Design 1 is not applicable to either design location. Design 2 consists of providing full burnout capacity by only adjusting the fireproofing of the building, and Design 3 consists of providing full burnout capacity by adjusting both the structure and the fireproofing. Designs 2 was not possible for typical bay because the connection demands could not be accommodated by only adjusting fireproofing without modifying the connections. Design 3 was developed for the typical bay and Designs 2 and 3 are similar for the transfer trusses.

9.1.1 Typical Bay

For the typical floor framing, Design 2 was considered including the maximum fireproofing thickness for beams according to UL N743, regardless of how a beam is classified (2 15/16 in.). Nonetheless, connection demands were large enough to require that connections be changed to provide more strength or deformation capacity. Hence, Design 2 is not achievable. For Design 3, connections have been changed by providing slots that can accommodate the movements resulting from the structural response to fire. The bolts and slots are covered with premade laths that are under the fireproofing such that any movement does not affect the fireproofing next to the bolts. If a small unprotected area of the connection is exposed when a beam pulls away from the connection, the connection capacity is evaluated, considering the temperature effects. Connections for primary members are designed as slip-critical at ambient temperatures and provide adequate bracing forces for the columns. In a fire, the bolts can slide to relieve large thermal forces, but the connection has adequate capacity in other limit states to be able to sustain column bracing loads. The columns are checked for their ability to carry their loads when deformed as a result of the thermal expansion. The option of providing increased connection capacity was not selected as it required substantial strengthening of the connections and sometimes the columns. For secondary interior beams framing into spandrels, the connections are designed with slots and finger-tight bolts to accommodate the movement due to structural response to fire and prevent imposition of large weak axis bending and torsional loads on spandrels. For all connections, additional fireproofing has been provided locally to limit the reduction of their capacities during fire. Overall, the fireproofing in beams including primary and secondary interior beams and the spandrels changed by +7% in the most severe fire scenario and by -41% in the more moderate fire scenario. The wire mesh in the floor system is also adjusted to increase the confidence that it can span between the supporting beams for the required duration.

For typical columns, high enough reserve capacity has been found to be able to reduce the fireproofing by 38%. There is no need for adjustment to the structural design.

9.1.2 Transfer Trusses

For the transfer trusses, Design 2 involves changes to the fireproofing to achieve burnout capacity. Because the response of the transfer trusses to fire can impact all the upper supported floors, several Design 2 options have been provided, all of which satisfy the performance criteria, but with different potential impacts on the structure. The project team would select one of these designs on the basis of the project owner preferences. For Design 3, the project team has the option of modifying the structure to achieve the same performance. The failure mode in the trusses is buckling of structural members, and the solution could be a combination of providing additional strength or additional fireproofing. Providing additional fireproofing locally has limited additional cost and is the most straightforward solution. Unlike typical areas in a structure, the alternative solution of creating alternative load paths is not reasonable for the transfer trusses that are main structural features of the building. Hence, Design 3 is the same as Design 2.

9.2 DESIGN FUEL LOAD

The choice of fuel load has a significant impact on the response. The designer should consider several factors such as specific requirements by the AHJ, different factors affecting likelihood and intensity of a severe fire, and whether there is a long-term tenant who has a more defined layout and office use that can be incorporated in the design. For this study, both characteristic fuel loads of $q_{f,k}$ = 511 MJ/m^2 and 656 MJ/m^2, corresponding to 80% and 95% fractile for office occupancy as given in Eurocode 1, Annex E (EC-1), are considered. The 95% fractile value is calculated based on the Gumbel distribution parameters provided in Eurocode 1. The design fuel load $q_{f,d}$ is adjusted in each fire scenario by several parameters. This project considers danger of activation factor δ_{q1} based on compartment area, danger of activation factor δ_{q2} =1 for office occupancy, and combustion factor m = 0.8 for mainly cellulosic materials. No reduction is considered for any of the fire detection or suppression methods, except that the sprinkler reduction factor is considered for the 80% fractile scenario. The area under transfer trusses is a mechanical space, with a tightly defined description of its content. For this study, a conservative fuel load similar to the office load is considered.

9.3 STRUCTURAL DESIGN FIRES

The fire load on the structure can be defined in the context of time histories of effective temperatures (typically adiabatic surface temperature) acting on the structure. Beyond the design fuel, other factors such as the opening factor and the material of the boundaries of the compartment have a significant impact on these histories, including the duration, shape, and peak of temperature.

The opening factor affects the fire regime and represents the amount of ventilation available to the fire, as described by the size of openings in relation to the size of compartments. The size of compartments in a typical office building and the openings on the interior side (doors) could vary significantly, depending on the tenants. However, if long-term tenants are present with relatively defined spaces, such information could be available for design. On the other hand, openings on the exterior (through windows and louvers) are design parameters set early in the design process and can be easily considered for determination of fire scenarios. If incorporated early in the design process, the fire impact could be another input into the design process for the building exterior

system. For this design, variations on the size of openings on the exterior have been considered, as well as a range for openings on the interior to explore critical fire scenarios.

Compartment fires are modeled using the parametric temperature–time curve methodology of Annex A in Eurocode 1. Depending on the amount of ventilation available, highest compartment temperatures typically happen in a ventilation-controlled, as opposed to fuel-controlled, regime. Furthermore, between two fires with the same maximum compartment temperature, the ventilation-controlled fire would have the longer duration (Thomas and Heselden 1972, Drysdale 2011). A range of factors affecting the design fire are being investigated to show how the parameters of design or preferences of regulatory bodies can affect the final fire loads. The temperature time histories of the fire scenarios considered in this study are shown in Figure 9-8.

9.3.1 Typical Bay

Fire Scenario 1: Localized Fire

One of the fire scenarios considered for the typical bay is a localized but intense fire originating from a workstation near a perimeter column and three framing beams. The Heat Release Rate (HRR) is selected from experimental tests of ignited workstations performed by the National Institute of Standards and Technology (NIST) (Ohlemiller 2005) as one of the longest and most intense scenarios (Figure 9-3). The peak HRR is much higher than the HRR produced by a distributed compartment fire over the same area. This fire scenario also allows for consideration of structural response to asymmetric thermal loading on beams and columns.

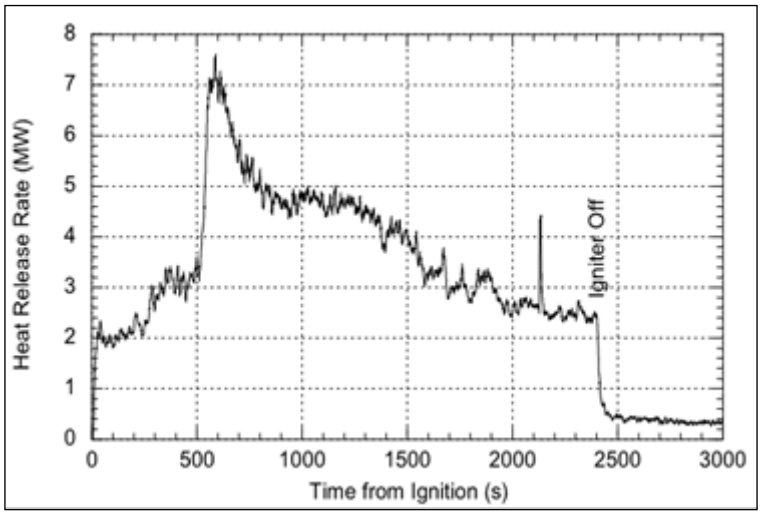

Figure 9-3. Heat release rate of ignited workstation, based on experimental tests by NIST
Source: Courtesy of Thornton Tomasetti (2019).

The localized fire is simulated in the Fire Dynamics Simulator (FDS) (McGrattan 2017), a Computational Fluid Dynamics (CFD) program developed and extensively validated with experimental tests at NIST. A CFD approach to modeling fire effects is warranted when localized effects are to be considered, either because it is a good representation of the fire, or because the spatial

distribution of fire effects is important to the structural response. The FDS model entails a 27 m^2 computational space with an open or broken glass of 4 m^2 behind the column that provides ventilation. The geometry of the room, as well as the size and location of the opening, are specifically selected so that sufficient ventilation is provided to approximate the expected HRR and that the flames engulf the structural members (Figure 9-4). A larger compartment with more openings could result in a fire that is more remote from the column. The fire is located over a 2.5 m × 2.5 m area, consistent with the NIST experimental set up. The wide-flange sections of the members are geometrically approximated by rectangular cross sections for the sake of simplicity; an approximation that does not significantly affect the global fluid flow inside the room (Figure 9-4). Thermocouples are placed at each side of the members every 0.5 m to obtain adiabatic surface temperatures (AST) (Wickström 2007). Time histories of AST (Figure 9-5) are then transferred as input information in the form of radiative and convective surface interactions for the subsequent finite-element thermal analysis. Figure 9-5 illustrates the AST time histories for this scenario.

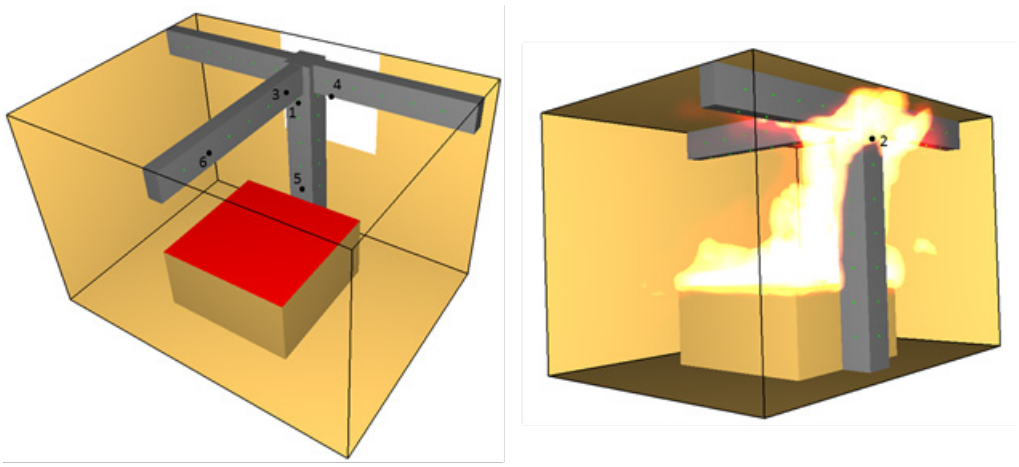

Figure 9-4. FDS model of Fire Scenario 1 with reference points 1–6.

Source: Courtesy of Thornton Tomasetti (2019).

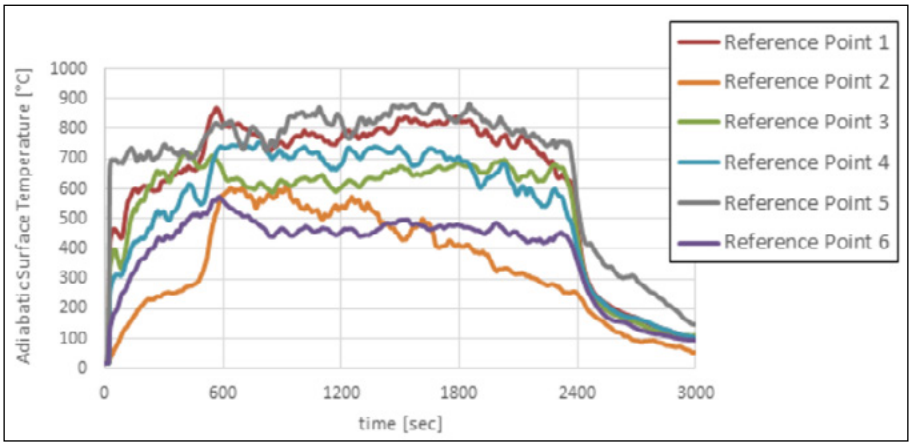

Figure 9-5. Adiabatic surface temperature time histories from FDS model of Fire Scenario 1 at reference points 1–6.

Source: Courtesy of Thornton Tomasetti (2019).

Fire Scenarios 2A and 2B: Compartment Fires for Typical Bay

A large compartment size of 13 m × 37 m is considered in this study, with an area of 480 m^2, close to the maximum applicable range of the Eurocode equation, resulting in larger assumed fuel load density. The lowest realistic opening factor for this space is 0.042, based on 30% opening in the exterior and no opening on the interior (assuming no open floor design and all doors closed). The boundary properties are selected based on a weighted average of lightweight concrete at floors and ceilings and gypsum at the walls. Additional opening in the façade or on the interior results in larger opening factors, with slightly higher temperatures, but at significantly shorter durations. Thermal analysis showed that the smallest opening factor in this case produced the maximum thermal impact on the structure. Therefore, the 95% fractile fuel without reduction due to sprinklers are considered in this scenario to create the most severe impact fire scenario for the building. This case represents a more conservative regulatory environment and a building with minimal openings representing older construction. This is Fire Scenario 2A (Figure 9-6). If a long-term anchor tenant with good information on the layout is available, such information might be incorporated to inform the calculation of the opening factor, including additional interior openings for the compartment. To the extent that such information is subject to uncertainty, the designer has to be conservative but realistic in selection of parameters.

For Fire Scenario 2B (Figure 9-6), an 80% opening in the exterior with no interior opening is considered, resulting in an opening factor of 0.103. This scenario also includes 80% fractile fuel density and reduction of fuel density by a factor of 0.610, based on the presence of sprinklers. This design reflects a regulatory environment, compatible with Eurocode fuel recommendations and an opening factor more in line with that of modern buildings. This fire is fuel-controlled, with any additional openings reducing both the duration and the temperature and resulting in less impact on the structure.

Separate designs of the typical bay are developed to consider Fire Scenario 1 and either Scenario 2A or Scenario 2B. In all cases, the local fire scenario did not govern.

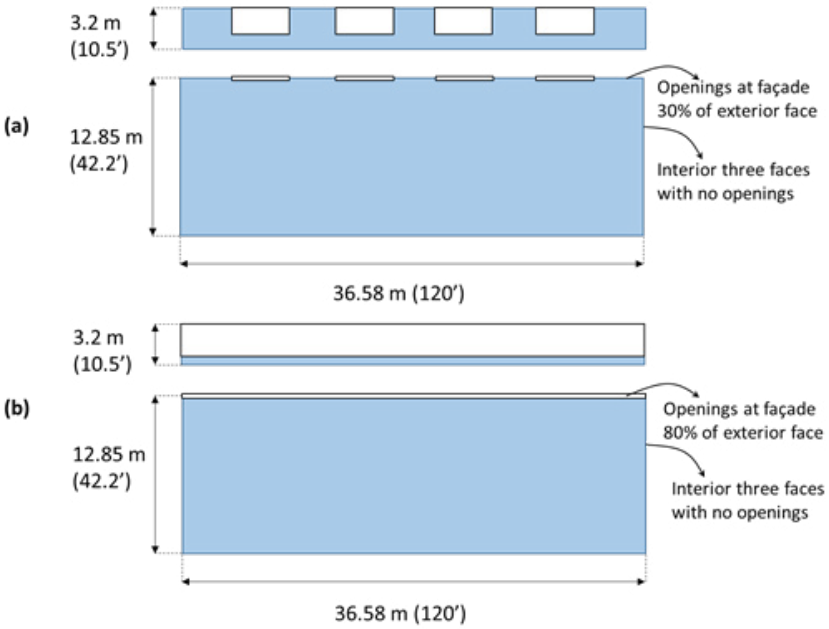

Figure 9-6. Layout and openings of typical bay for Fire Scenarios 2A and 2B

Source: Courtesy of Thornton Tomasetti (2019).

9.3.2 Transfer Trusses

Fire Scenarios 3A and 3B: Compartment Fires for Transfer Trusses

Compartment fire scenarios are developed using the parametric temperature–time curve methodology in Eurocode 1. Based on the large area encompassed by the trusses, it was decided that a compartment fire is more critical than a local fire. The transfer trusses are 4 m deep and occupy an L-shaped compartment area of 340 m^2 with a ceiling height of 7 m. The boundary properties are selected based on a weighted average of lightweight concrete at floors and ceilings and gypsum at the walls.

As for the typical bay, two variants of the fire scenario are considered based on different fire parameters. Fire Scenario 3A (Figure 9-7) has 30% opening on one exterior face and no other external or internal openings, resulting in an opening factor of 0.062. This design includes 95% fractile fuel and no fuel reduction for sprinklers. Additional opening in the façade or on the interior result in larger opening factors, with slightly higher temperatures, but at significantly shorter durations. Thermal analysis showed that the smallest opening factor in this case produced the maximum thermal impact on the structure.

Fire Scenario 3B (Figure 9-7) also has 30% opening, but on both exterior faces for this room, with no interior openings, resulting in opening factor of 0.124. This design includes 80% fractile fuel and fuel reduction owing to sprinklers (a factor of 0.61). This fire is fuel-controlled, with any additional openings reducing both the duration and the temperature and resulting in less impact on the structure. Given the short duration of fire in this scenario, additional scenarios with more opening are not considered in this design.

The two fires represent significantly different impacts on the structure within the reasonable range of design parameters. The application of Eurocode 1 parametric fire method for a compartment height exceeding the 4 m limit of Eurocode 1 is a conservative assumption, because taller compartments do not accumulate heat as intensely as described in Eurocode 1. Because of this feature, a designer could choose to use CFD to have a better representation of the fire effects.

9.4 ANALYSIS

Two different analytical tools are used in this study. One is Abaqus (Dassault Systèmes Simulia Corp. 2011), a general 3D finite-element program with capabilities to model many phenomena, including thermal and structural responses of building systems. The general 3D feature of this program makes it most useful when spatial variations in structural behavior or thermal input are important or features such as connections need to be modeled in detail. The other tool is SAFIR (Franssen and Gernay 2017), also a finite-element program. This program is geared toward analysis of structures in fires and can perform thermal analysis of 2D sections, as well as structural analysis of frame and shell fiber elements. This program has the advantage of ease of use for applications where performance of 3D features such as connections or complex 3D thermal gradients are not important to the response. For the beam–slab–column assembly, in which the impact of connections on the complex structural behavior is considered and one of the fire scenarios is localized, Abaqus is used. For the transfer truss, in which a uniform temperature is being studied

and the substantial gusset plates of the connections are not expected to have a prominent impact on the response, SAFIR is used.

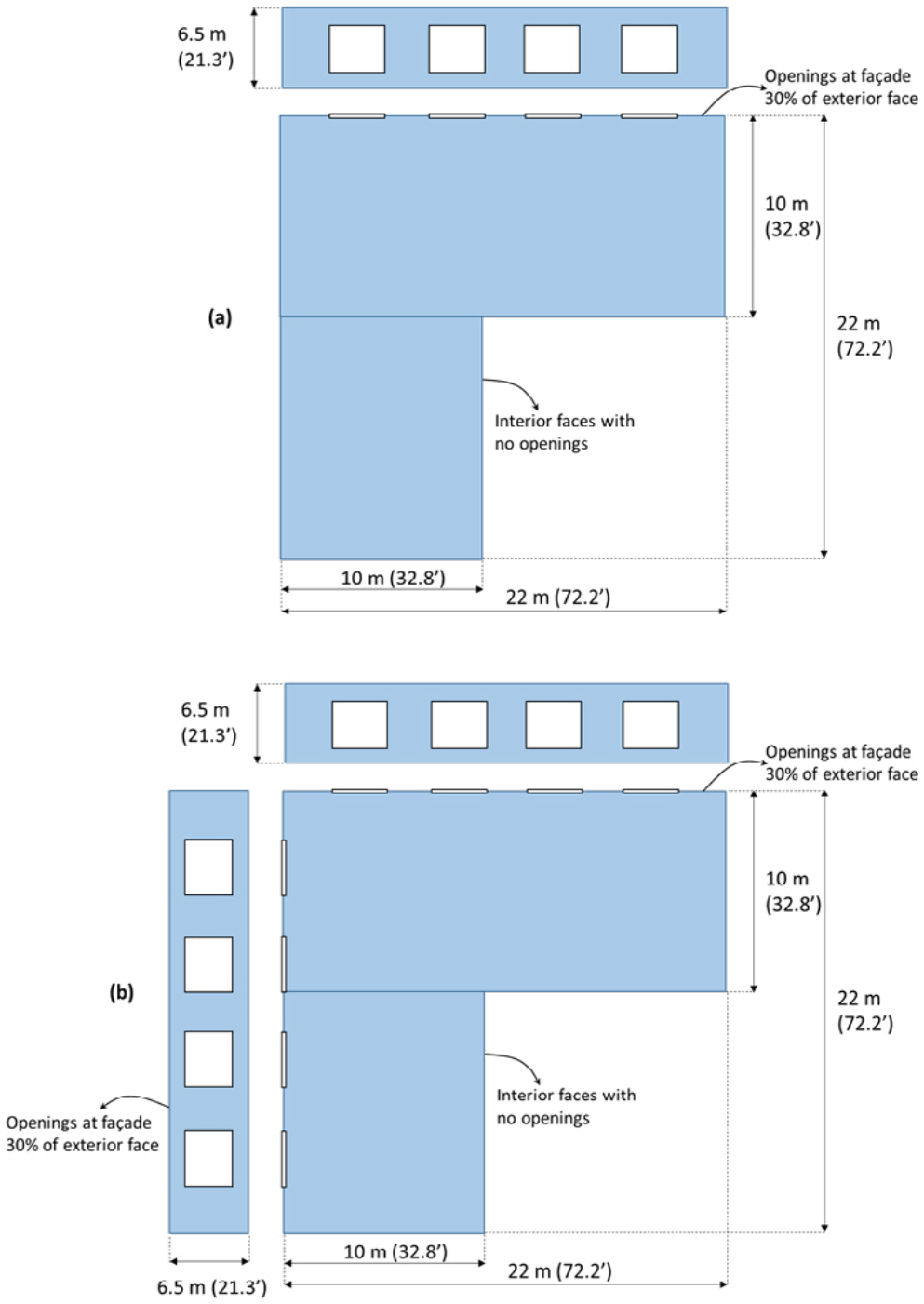

Figure 9-7. Layout and openings of transfer trusses for Fire Scenarios 3A and 3B

Source: Courtesy of Thornton Tomasetti (2019).

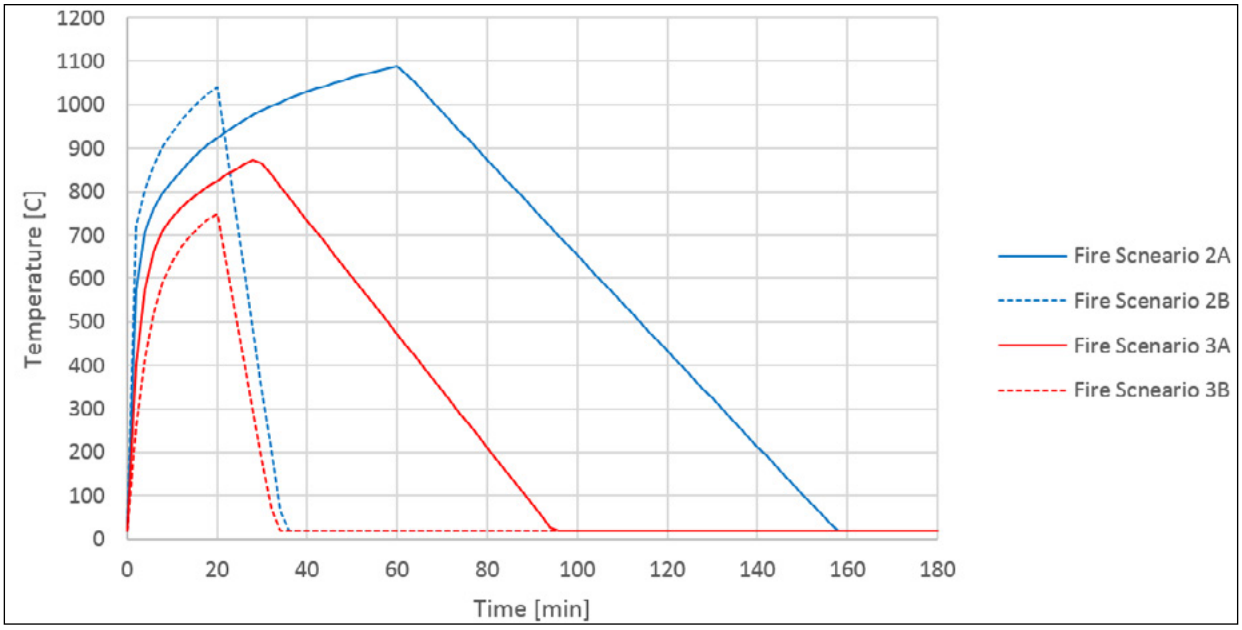

Figure 9-8. Temperature–time histories per Eurocode for compartment fire scenarios 2A, 2B, 3A and 3B.

Source: Courtesy of Thornton Tomasetti (2019).

9.4.1 Typical Bay

Model

The floor system at this typical office location is comprised of 3.25 in. lightweight concrete with 4 ksi strength on 20-gauge, 3-in.-deep metal deck with 6x6 W2.9/W2.9 welded wire mesh. The steel column sizes vary from W14x99 to built-up columns heavier than W14x730. The finite- element model uses a W14x500 column section which represents a very stiff boundary resisting thermal effects of fire (Figure 9-9). The column is modeled one floor above and one floor below the affected floor, with moment fixities at the neighboring floors. The floor heights are 4.27 m (14 ft). The perimeter beams are W24x62 sections of 9.14 m (30 ft) length. The interior beams are W21x44 sections of 12.85 m (42 ft, 2 in.) length and in principle, there is no difference between those framing into the columns versus those framing into the spandrels, except that those framing into columns are considered primary members by code. The steel beams that support the floor system are designed as fully composite members using welded steel studs on top of the flange. A framing plan for the typical floor is shown in Figure 9-2. The finite-element model of the beam–slab–column subassembly includes equivalent slab strips to account for the composite action of the steel beams. The slab strip width is determined based on AISC provisions on composite members. The ribbed portion of the slab, as well as the metal deck, are not included in the finite-element model. The top concrete considered in the model is considered with the 3 in. offset for structural analysis. The primary and secondary interior beams have the same design for gravity loads and are subjected to the same fire loads, except that secondary beams are restrained less by the columns and hence, should have lower connection demands. As such, a design similar to primary members is satisfactory for them. Considering this fact and the limited capacity of

the slab above the deck to redistribute loads at higher temperatures, it was decided that a model representing one-way composite action of the primary interior beams and the spandrels, including their connections, would provide adequate information for design.

The wide-flange sections of the steel members, as well as the concrete slab, are modelled with 4-node composite layered shell elements that can model local failure modes (e.g., web or flange local buckling) and can be easily modified to change their fireproofing. The concrete slab shell elements are offset relative to the beam top flange shell elements to simulate the actual geometry. Tie constraints are applied at contact between the bottom slab surfaces and the beam top flange surfaces to transfer forces and heat between the two materials. The material for the steel members is A992 with yield stress of 345 MPa and ultimate stress of 450 MPa at ambient temperature conditions. Temperature-dependent thermal and mechanical properties including stress–strain are defined according to Eurocode 3. Concrete slab material properties are derived from Eurocode 2, including thermal properties and changes of concrete modulus of elasticity with temperature. The strength of concrete is not explicitly modeled. Rather, the total slab force from analysis is checked and it is verified that either concrete remains in compression in the majority of cases, or when temporarily in tension, its tensile stresses remain below the tensile capacity of concrete. With steel plasticity and buckling explicitly modeled and concrete forces checked against capacity, the failure of the beam through buckling, loss of capacity resulting from reduced steel strength or overstressing concrete is detectable using this model. None of the analyses showed beam member failure under loads. Connections are discussed separately.

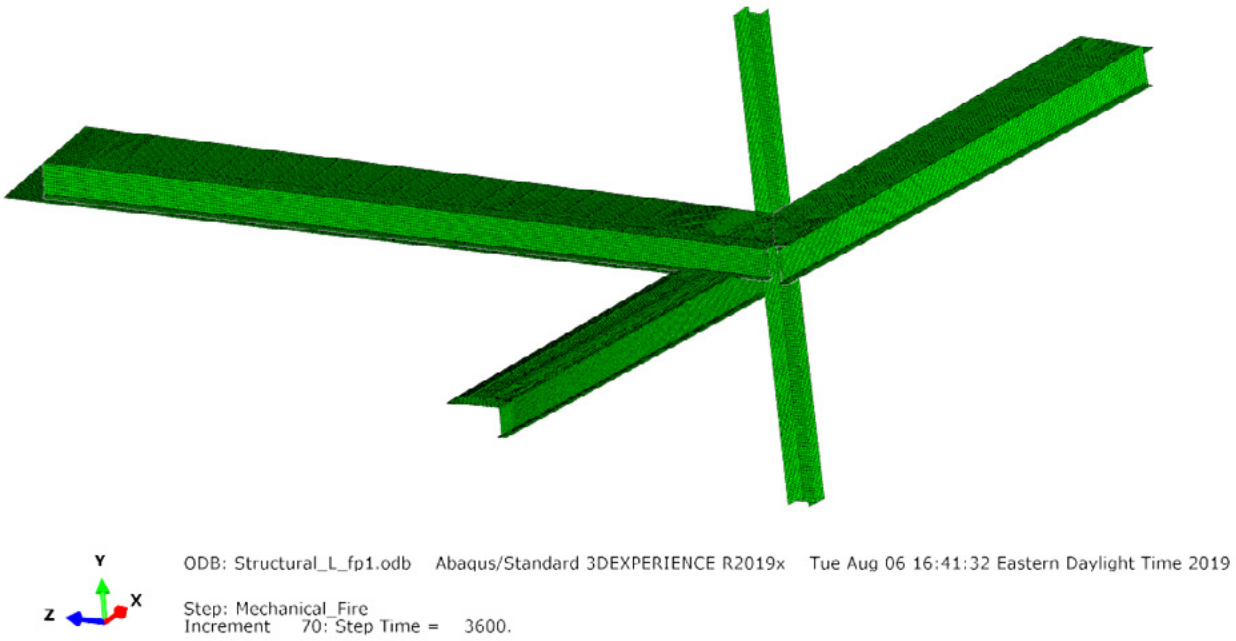

Figure 9-9. Abaqus model of typical bay

Source: Courtesy of Thornton Tomasetti (2019).

Design Iterations

Heat transfer and structural analysis are performed in Abaqus to capture the response of the structural system under Fire Scenarios 1, 2A, and 2B.

The heat transfer analysis is performed by applying the temperature time histories derived from the FDS model for Fire Scenario 1, and from Eurocode 1 parametric fire curves for Fire Scenarios 2A and 2B, as convection and radiation interactions to the exterior surfaces of the model. For the localized Fire Scenario 1, only the part of the structure located inside the small enclosure is heated, and the spatial variability of heating in the 3D space is considered (Figure 9-10). For the compartment Fire Scenarios 2A and 2B, all members are considered to be heated uniformly along their entire lengths, assuming uniform compartment temperature conditions consistent with the Eurocode 1 methodology. Fire Scenarios 2A and 2B produced more significant thermal impact and structural response compared to Fire Scenario 1.

The model is initially subjected to gravity loads according to the extreme event load combination of ASCE7 (1.2 DL + 0.5 LL + 0.2 S + Fire) and subsequently subjected to the temperature time-histories mapped from the previous heat transfer analysis.

Figures 9-11 to 9-14 illustrate a set of results for a representative case; Fire Scenario 2B and 1 h rated members. Results are presented in terms of

- Section cut forces of slabs at beam midspan plotted against concrete capacity (reduced per elevated temperatures) for interior beam,
- Beam sag (vertical displacement) for interior beam, and
- Steel temperature at web of interior beam and flange of column.

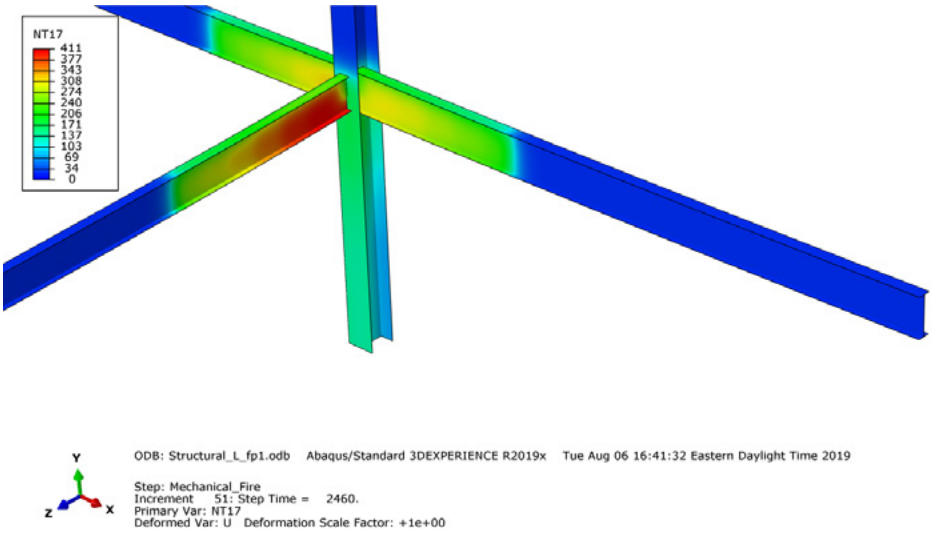

Figure 9-10. Steel temperatures for localized Fire Scenario 1 at t = 2460 sec (maximum temperatures observed).

Source: Courtesy of Thornton Tomasetti (2019).

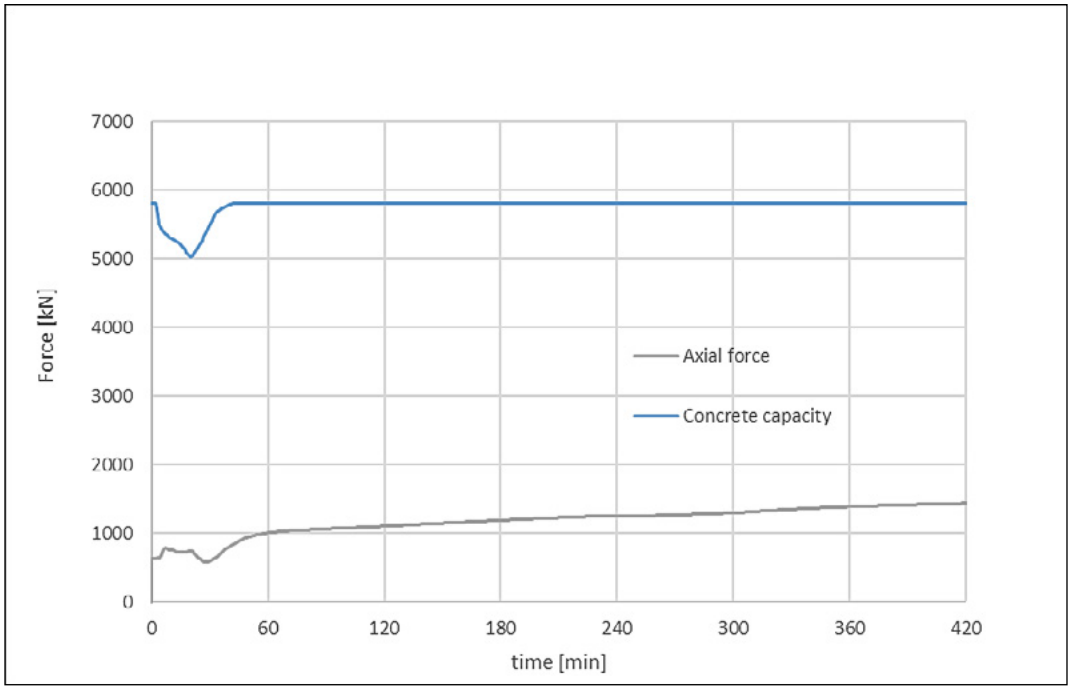

Figure 9-11. Section cut at slab above interior beam at midspan: Fire Scenario 2B and 1 h rating.

Source: Courtesy of Thornton Tomasetti (2019).

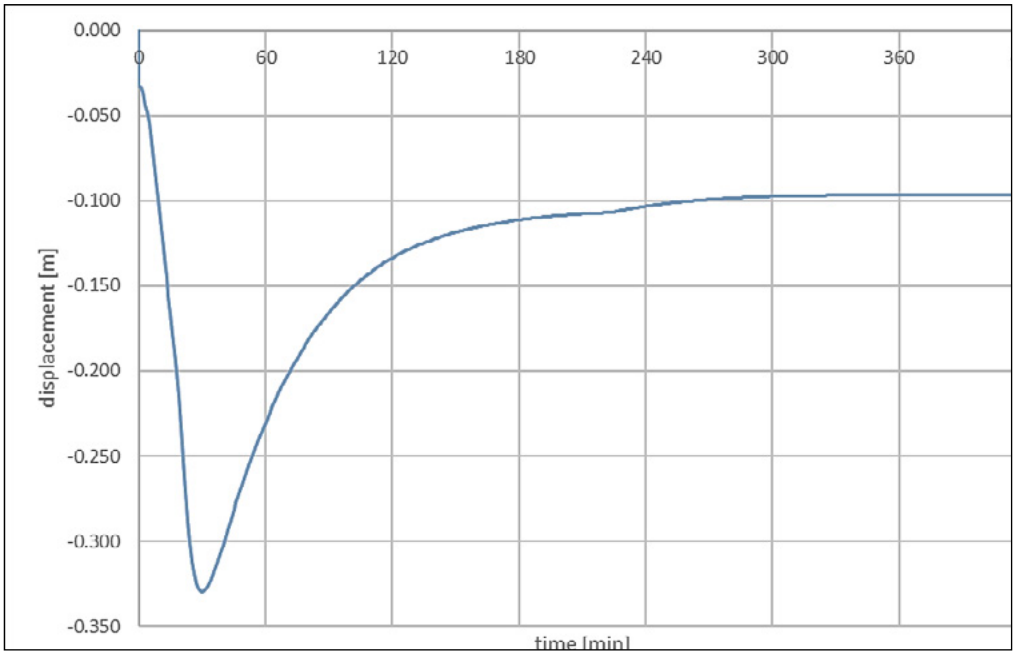

Figure 9-12. Slab sag at midspan above interior beam: Fire Scenario 2B and 1 h rating.

Source: Courtesy of Thornton Tomasetti (2019).

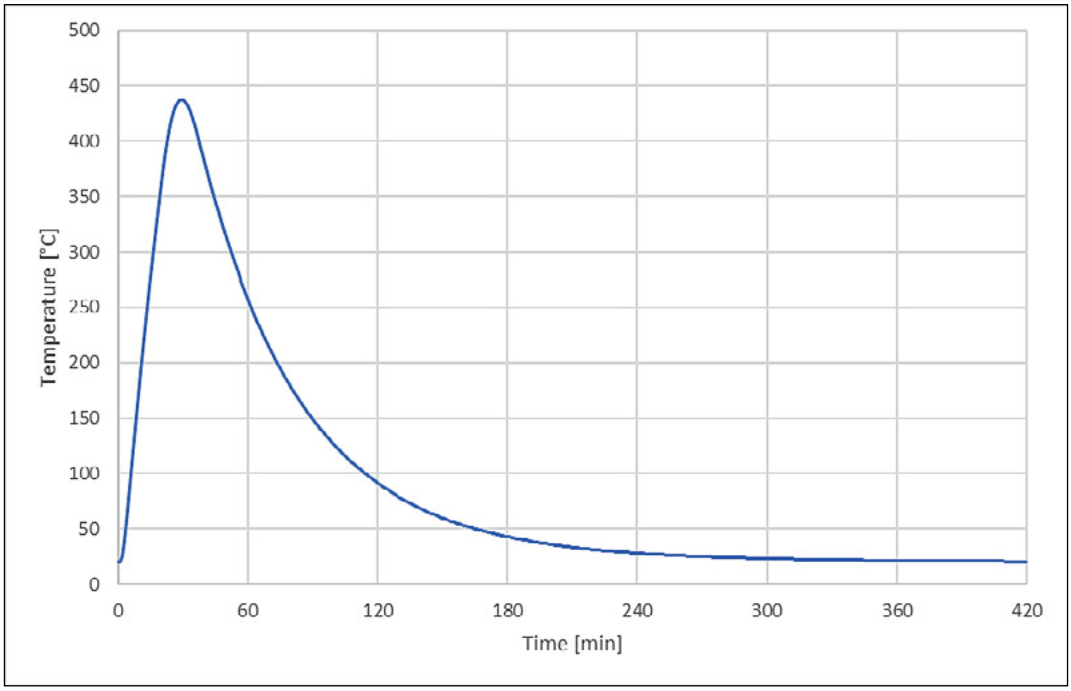

Figure 9-13. Steel temperature at Interior beam web: Fire Scenario 2B and 1 h rating

Source: Courtesy of Thornton Tomasetti (2019).

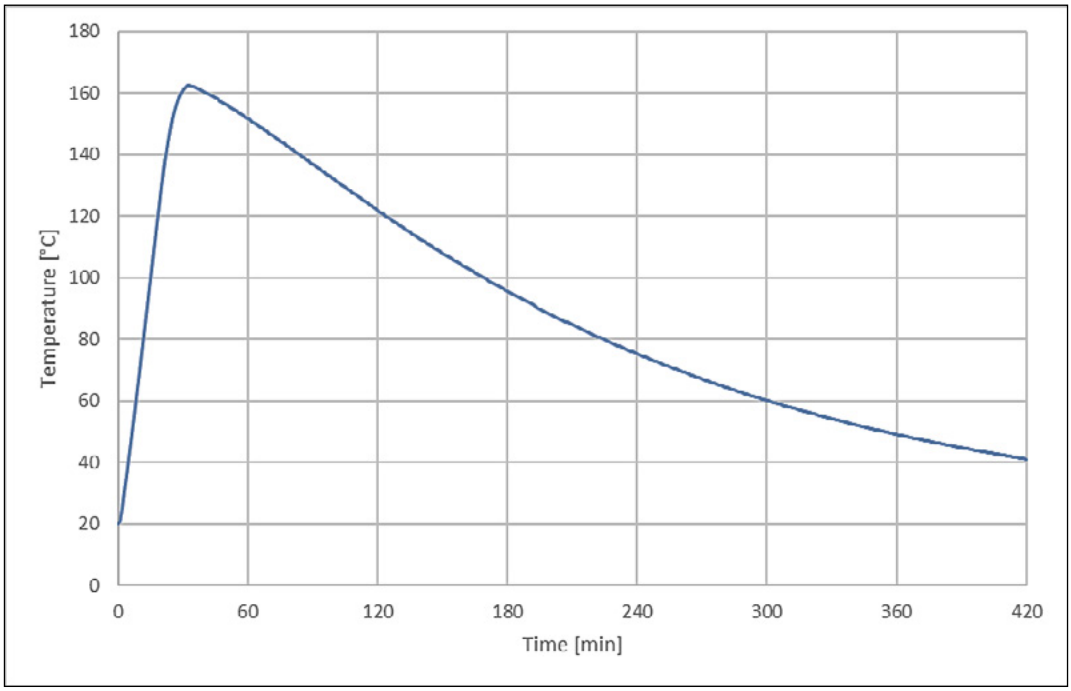

Figure 9-14. Steel temperature at column flange: Fire Scenario 2B and 1 h rating.

Source: Courtesy of Thornton Tomasetti (2019).

Analysis results showed the significant difference in fireproofing requirements and structural behavior, depending on the fire scenarios. In all scenarios, the connections had to be modified for adequate performance of the structure. However, the fireproofing could be lowered for all the beams to what would be equivalent to a prescriptive 2 h rating for Fire Scenario 2A, and 1 h rating for Fire Scenario 2B. Additional fireproofing at connections offset some of these reductions, resulting in a total fireproofing change in the beams of +7% in Fire Scenario 2A and -41% in Fire Scenario 2B.

Connections

In theory, any offset between the centroid of the connection and the centroid of the composite member can cause axial forces in the connections owing to gravity loads. However, such forces are not considered in standard connection design practice and are not known in the technical literature to be an important factor for several reasons, including that the concrete weight is initially imposed when it is wet, and also that a small sliding at the bolts can relieve the forces. Therefore, the boundary conditions at the ends of the interior and perimeter beams in the finite-element model are initially set as rollers during the gravity load and then changed to pins to capture the response to fire. These pins are applied at the centroid of the actual connections. The shear tab connection is modeled using elastic shell elements. This model is provided to approximately capture the initial stiffness of a shear tab and its impact on the structural behavior, without going to the level of detail of modeling bolts, holes, slip behavior, and local plasticity.

In addition, to capture the potential boundary forces acting on the slab owing to the response to fire, compression only springs are modeled between the beams and column. Similarly, to capture the potential contact forces between the bottom flange of the beams and the adjacent structure owing to thermal expansion of the beams, contact is explicitly modeled between the bottom portion of the beams and the interface with the column. An example contact scenario is depicted in Figure 9-15 from two different angles, which occurs at t = 6,900 s for Fire Scenario 2A and 2 h rated members, along with Von Mises stress contours on the steel. In this figure, the bottom flange and the lower web of both beams are in full contact with the adjacent column, whereas local buckling is observed at the beams' ends.

Figure 9-16 illustrates results regarding the following connection forces for the same representative case; Fire Scenario 2B and 1 h rated members; section cut forces at the shear tab location, concrete contact forces from the compression only springs between slab and column, and steel contact forces between beam bottom flange/lower web and column for the interior beam.

As discussed, Design 2 was not viable based on analysis results because fireproofing alone could not reduce the connection forces to within capacity. Design 3 for connections changes both fireproofing and connection geometry. For fireproofing, the connection, along with an additional 3 ft for Fire Scenario 2A and 1 ft for Fire Scenario 2B, are protected with additional fireproofing to limit the reduction in connection strength during fire. In addition, deformation demands in the connections are calculated and then accommodated using horizontal slots. Based on past experiments, a deformation of 1/2 in. or more is expected in a single plate connection before the connection fails (Guanyu 2011). However, this value is not explicitly considered and serves as an additional margin for the design.

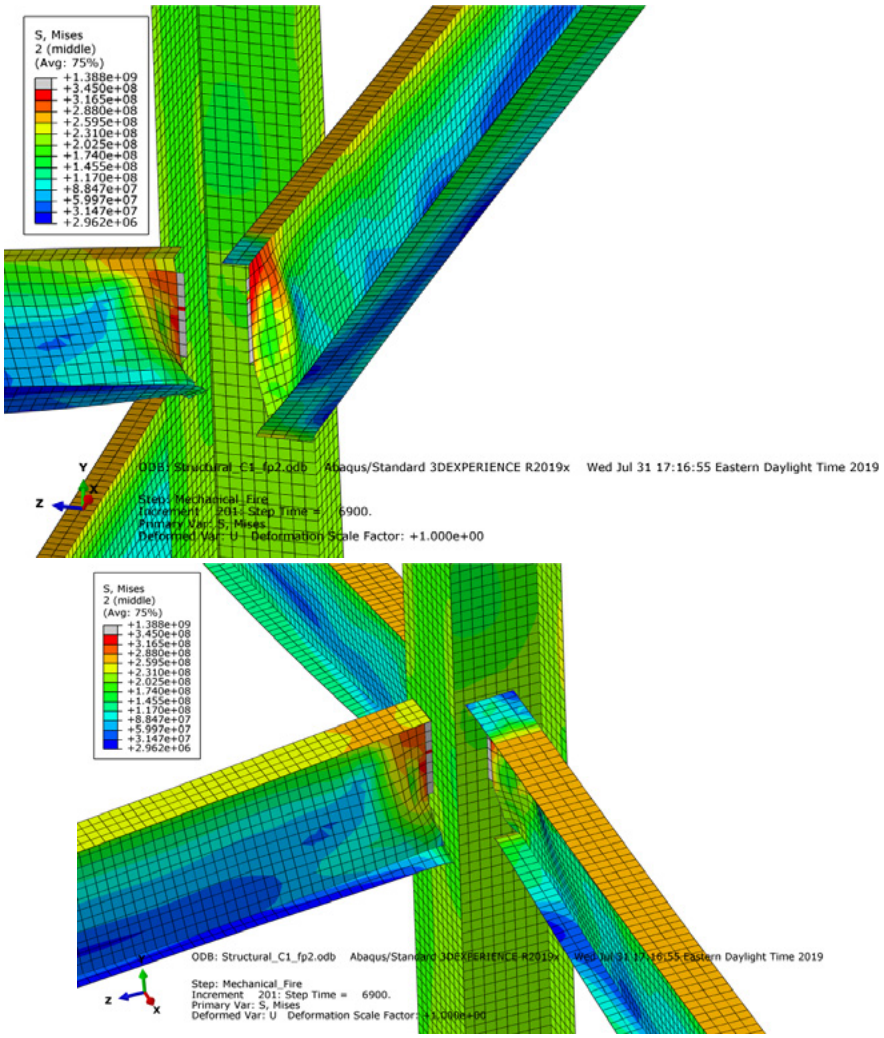

Figure 9-15. Contact between beam bottom flange and lower web with column flange, for Fire Scenario 2A and 2 h fire rated members at t = 6,900 s, along with Von Mises stress contours.

Source: Courtesy of Thornton Tomasetti (2019).

During the beam expansion during heating, the bottom flange comes in contact with the support and continues to push as the beam expands, resulting in local deformations and buckling and contact between part of the web and the support. However, concrete contact with the support at the top prevents closing of the gap at the top of the beam. The deformation demand in the bolts can be estimated using the contact point at the bottom of the bottom flange or web and the initial beam edge gap of 1 in. maintained at the top because of concrete contact. However, the estimate would be somewhat unconservative, given the elasticity of the connection. In this study, the initial beam edge distance of 1 in. has been set as the upper bound for the bolt deformation demand toward support.

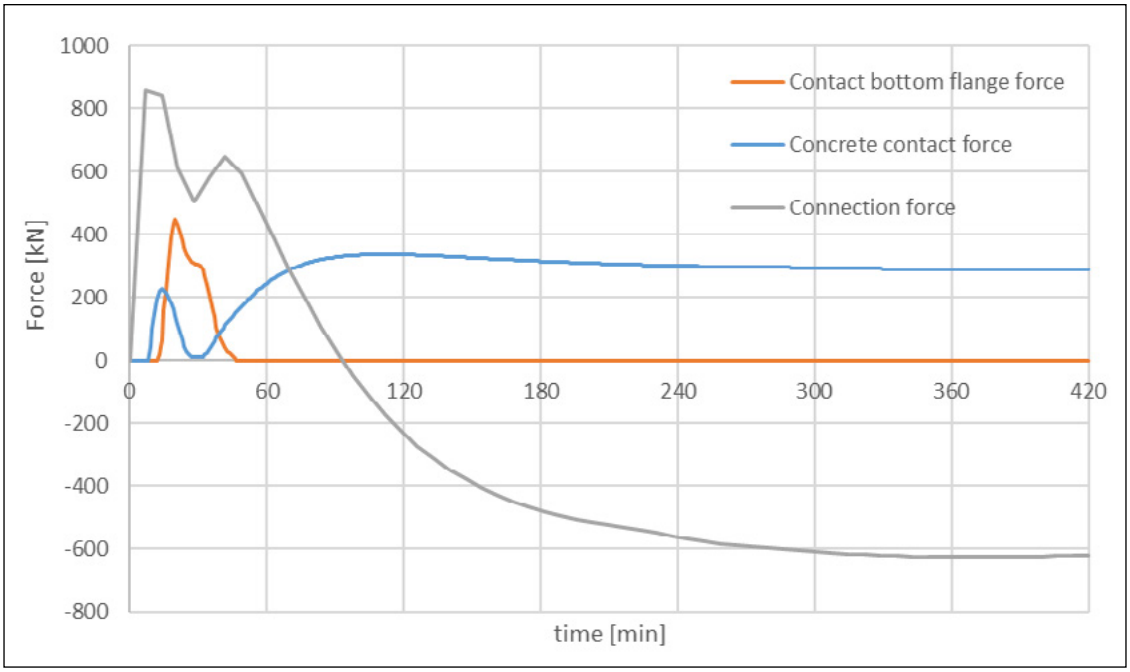

Figure 9-16. Comparison of forces around connection of interior beam to column: Fire Scenario 2B and 1 h rating.

Source: Courtesy of Thornton Tomasetti (2019).

Additional heating softens the beam and increases sagging, resulting in both large end rotations and shortening of the beam owing to large deformations in addition to the thermal expansion resulting from heating. During cooling, the beam recovers from some of the sagging hence has smaller end rotation and large-deformation shortening, but is also under less thermal expansion. The interaction between the end rotation resulting from sagging, beam shortening because of sagging, and thermal expansion can cause the connection or parts of it to pull away during the heating or cooling phase of the fire. The end rotation and large-deformation shortening at maximum sag are used to provide a reasonable conservative estimate of required bolt stroke in tension. The total length of slot is determined based on the bolt diameter plus the required strokes in tension and compression. The connections are designed such that limit states other than sliding do not govern the design, and weld capacity is more than plate capacity. It should also be noted that for this design, the position of the bolts within the slots should be specified and explicitly inspected during construction. Figure 9-17 demonstrates the results summary for slot length calculations.

Although slotted connection is very common in construction and the effects of potential movement of bolts on fireproofing are not considered, it was decided for this study that the bolts and slots should be covered with premade laths that would be under the fireproofing such that any movement does not affect the fireproofing next to the bolts. Whenever a small unprotected area of the connection is exposed when a beam is pulling away from the connection, the connection capacity is evaluated, considering the actual temperatures to ensure the adequacy of the connection to carry the gravity loads.

Fire scenario		2A	2A	2B	2B	2B
Fireproofing (in)		1.375" (3-hr rating)	0.875" (2-hr rating)	1.375" (3-hr rating)	0.875" (2-hr rating)	0.5" (1-hr rating)
Beam	Max connection force in compression (Kips)	246	194	204	203	193
	Max connection force in tension (Kips)	106	82	48	117	140
	Maximum tensile stroke (in)	1.91	3.08	0.34	0.6	1.45
	Required plate width (in)	6.03	7.2	4.46	4.72	5.57
	Required length of slot (in)	3.66	4.83	2.09	2.35	3.2
Spandrel	Max connection force in compression (Kips)	273	265	274	258	267
	Max connection force in tension (Kips)	391	393	155	268	421
	Maximum tensile stroke (in)	0.65	1.23	0.34	0.48	0.58
	Required plate width (in)	4.77	5.35	4.46	4.6	4.7
	Required length of slot (in)	2.4	2.98	2.09	2.23	2.33

Figure 9-17. Slot length calculations results summary.

Source: Courtesy of Thornton Tomasetti (2019).

Connections for spandrels and primary interior beams could alternatively be designed using much heavier double angle connections to resist the forces from the analysis. However, this would also require locally strengthening the columns in many locations and hence, was not considered. Strengthening for secondary interior beams framing into the spandrels was not considered because it is desirable to limit exertion of weak axis bending and torsion forces on spandrels.

Columns

Columns are gravity only. They were thermally analyzed in SAFIR and their capacities were determined at elevated temperatures using standard equations with temperature-dependent properties. Columns showed adequate reserve capacity to survive with lower fireproofing (Figure 9-18). Additional bending demand on the columns owing to thermal push is acceptable, as a plastic hinge does not compromise the load carrying capacity. The adequacy of the column to carry the loads at the offset due to thermal expansion was verified.

Slab Catenary Action

The typical slab is 3-1/4 in. thick lightweight concrete, on top of a 20-gauge, 3-in. metal deck, with 6x6-W2.9xW2.9 wire mesh reinforcement placed 3/4 in. below the slab surface and lapped 6 in.,

such that 50% of its tensile capacity can be mobilized. The metal deck is unprotected in Design 0 and is intended to be unprotected in Design 3. The wire mesh is relied on to develop catenary action in the direction of the metal deck during fire, as the exposed metal deck would rapidly lose capacity during a fire. It was determined that in the more severe fire scenario 3A, whose heat lowers the wire mesh strength by 10%, equilibrium is reached with a slab deflection of 11.1 in. This deflection is acceptable, considering the other large deflections experienced by the floor steel framing during a fire. The deflection is 9.2 in. in Fire Scenario 3B, for which the wire mesh strength is not affected.

Catenary action can only develop if the wire mesh can be held in tension at the ends of the slab span. This is achieved through continuity and/or lapping of the mesh over interior beams. At the perimeter, the concrete in the 2 ft long cantilever could balance the wire mesh tensile forces. However, lowering the mesh by 1.25 in. over the perimeter beams is recommended to engage the shear studs.

The strength of the wire mesh is limited by the partial lap typically used, which can only transfer 50% of the tensile capacity of the mesh. The deflections resulting from catenary action can therefore be lowered by doubling the wire mesh laps and mobilizing 100% of the mesh in tension. If this is done, the deflections decrease to 5.2 in. and 4.7 in. for Fire Scenarios 3A and 3B, respectively.

9.4.2 Transfer Trusses

Model

The gravity system of the 20 upper residential floors is comprised of concrete columns and slabs, all supported by steel transfer trusses. This upper portion of the building is modeled in the finite-element analysis program SAFIR, in which the two-way flat slab system is approximated by equivalent slab strips defined according to the ACI 318 provisions (Figure 9-19). At the transfer level, in which the top chords of the trusses are encased in the slab, the slab system is approximated by T-beams defined according to the ACI 318 provisions. The steel members and the slab strips are modeled as beam elements.

Design Iterations

For the transfer trusses, only Design 2 is considered, when fireproofing can be adjusted, as long as the structural frame does not collapse after burnout. Design 3 is considered similar to Design 2 because structural modifications do not provide a more efficient way of achieving the performance goals. Design 2 was implemented separately for Fire Scenarios 3A and 3B, which represent more severe and moderate fires, respectively. For each fire scenario, several heat transfer and structural analyses were performed with different fireproofing thicknesses applied to the transfer truss members. Because of the large number of steel sizes for trusses, hourly ratings according to UL Y725 were used as a unified benchmark to vary fireproofing thicknesses across all members during analysis iterations. After each analysis, any member or system failure and the D/C ratios of the still-intact steel and concrete members were reviewed to analyze the impact of the selected fireproofing.

W14X99	Fire Rating [hours]	SFRM thickness per UL Y725 [in]	max. T [°C]	$k_{y,\theta}=f_{y,\theta}/f_y$	$k_{E,\theta}=E_{a,\theta}/E_a$	Capacity [kips]	Demand @ 1.2DL + 0.5 LL [kips]	D/C
Scenario 2A	1	0.477	688	0.258	0.151	302.9	776.6	> 1 (rejected)
	2	0.954	492	0.798	0.608	962.0	776.6	0.807
	3	1.431	375	1	0.725	1200.0	776.6	0.647
Scenario 2B	1	0.477	350	1	0.750	1203.4	776.6	0.645
	2	0.954	198	1	0.902	1220.7	776.6	0.636
	3	1.431	125	1	0.975	1227.1	776.6	0.633

W14X193	Fire Rating [hours]	SFRM thickness per UL Y725 [in]	max. T [°C]	$k_{y,\theta}=f_{y,\theta}/f_y$	$k_{E,\theta}=E_{a,\theta}/E_a$	Capacity [kips]	Demand @ 1.2DL + 0.5 LL [kips]	D/C
Scenario 2A	1	0.329	630	0.397	0.255	934.8	1775.6	> 1 (rejected)
	2	0.658	446	0.898	0.654	2133.9	1775.6	0.832
	3	0.987	344	1	0.756	2382.5	1775.6	0.745
Scenario 2B	1	0.329	303	1	0.797	2391.1	1775.6	0.743
	2	0.658	179	1	0.921	2412.6	1775.6	0.736
	3	0.987	126	1	0.974	2420.3	1775.6	0.734

W14X370	Fire Rating [hours]	SFRM thickness per UL Y725 [in]	max. T [°C]	$k_{y,\theta}=f_{y,\theta}/f_y$	$k_{E,\theta}=E_{a,\theta}/E_a$	Capacity [kips]	Demand @ 1.2DL + 0.5 LL [kips]	D/C
Scenario 2A	1	0.250	539	0.659	0.487	3030.2	3023.4	0.998 (rejected)
	2	0.426	409	0.980	0.691	4490.5	3023.4	0.673
	3	0.638	318	1	0.782	4614.1	3023.4	0.655
Scenario 2B	1	0.250	235	1	0.865	4641.2	3023.4	0.651
	2	0.426	160	1	0.940	4661.7	3023.4	0.649
	3	0.638	117	1	0.983	4672.1	3023.4	0.647

Figure 9-18. Column reserve capacity.

Source: Courtesy of Thornton Tomasetti (2019).

W14X500	Fire Rating [hours]	SFRM thickness per UL Y725 [in]	max. T [°C]	$k_{y,\theta}=f_{y,\theta}/f_y$	$k_{E,\theta}=E_{a,\theta}/E_a$	Capacity [kips]	Demand @ 1.2DL + 0.5 LL [kips]	D/C
Scenario 2A	1	0.250	470	0.846	0.630	5273.0	4488.4	0.851
	2	0.345	395	1.000	0.705	6211.2	4488.4	0.723
	3	0.517	309	1	0.791	6253.9	4488.4	0.718
Scenario 2B	1	0.250	192	1	0.908	6299.3	4488.4	0.713
	2	0.345	152	1	0.948	6312.1	4488.4	0.711
	3	0.517	113	1	0.987	6323.9	4488.4	0.710

W14X730	Fire Rating	SFRM thickness per UL Y725 [in]	max. T [°C]	$k_{y,\theta}=f_{y,\theta}/f_y$	$k_{E,\theta}=E_{a,\theta}/E_a$	Capacity [kips]	Demand @ 1.2DL + 0.5 LL [kips]	D/C
Scenario 2A	1	0.250	391	1.000	0.709	9149.3	6922.2	0.757
	2	0.265	312	1.000	0.788	9200.2	6922.2	0.752
	3	0.397	240	1	0.860	9239.4	6922.2	0.749
Scenario 2B	1	0.250	148	1	0.952	9280.3	6922.2	0.746
	2	0.265	113	1	0.987	9294.1	6922.2	0.745
	3	0.397	84	1	1.000	9299.0	6922.2	0.744

*Notes

1. For column sections heavier than the ones shown in each table, the same SFRM thickness applies as the lightest section.
2. The given SFRM thickness is benchmarked against the fire rating (in hours) for restrained beam per UL N.743 design.
3. For all column section: L=14ft, k=0.65 and ϕ=0.9

Figure 9-18. Column reserve capacity (con't).

Source: Courtesy of Thornton Tomasetti (2019).

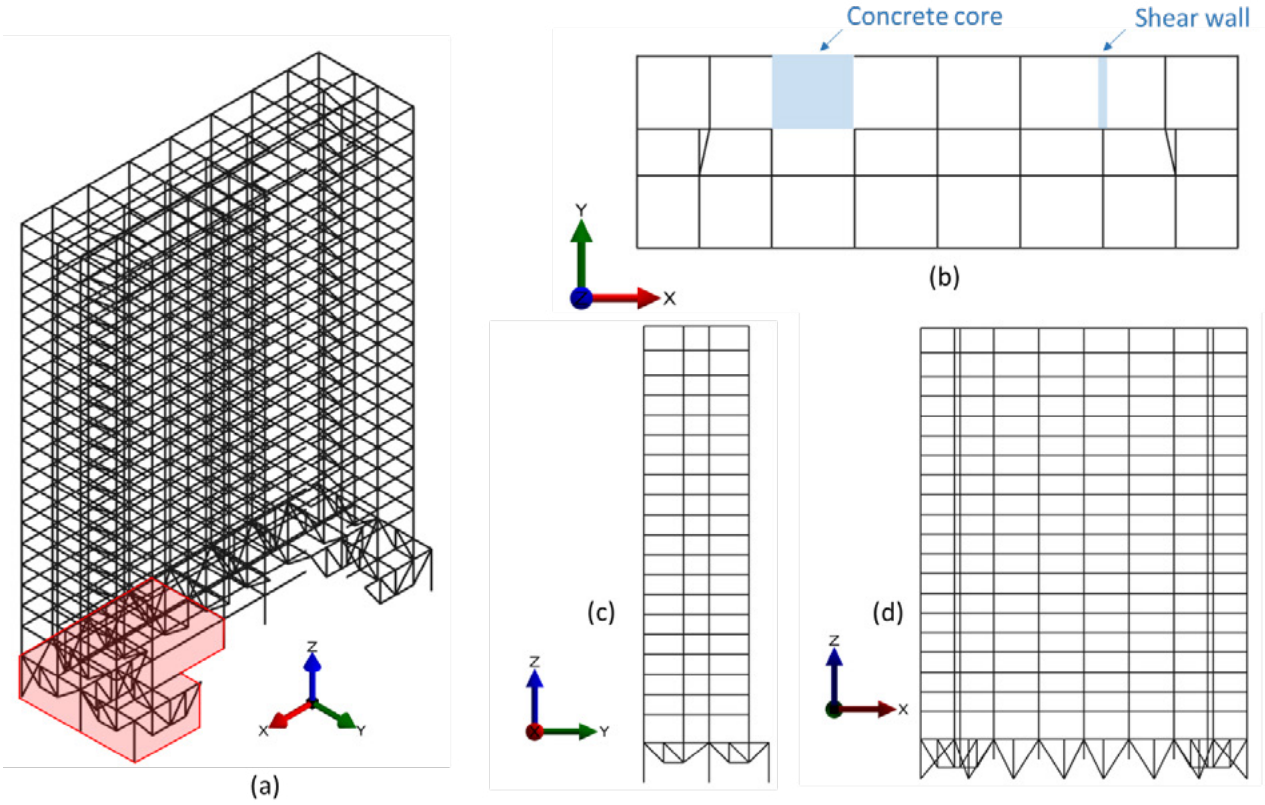

Figure 9-19. Building geometry in SAFIR: (a) isoparametric view, (b) plan XY view of the 20 residential floors with concrete core and shear wall locations, (c) side YZ view, and (d) side XZ view.

Source: Courtesy of Thornton Tomasetti (2019).

Figure 9-20 illustrates the temperatures along the cross section of a typical W14x145 section of the transfer trusses protected with a 1 h fire rating during Fire Scenario 3A, at time t = 7,200 s. The time histories of the temperatures at fireproofing surface and the steel web during Fire Scenario 3A with 1 h, 2 h and 3 h fire rating are also shown. Figure 9-21 illustrates temperature contours at t = 7,200 s for an example thermal 2D analysis of the two types of T-beams located at the transfer level, for fire exposure only at the bottom.

The more severe Fire Scenario 3A was first applied to the transfer structure protected with a 3 h fire rating (Design 0). The analysis shows that a diagonal member of the perimeter truss initiates buckling after 40 min, but load redistribution through the rest of the structure prevents collapse, and no other member fails. The prescriptive design therefore satisfies the performance objective of Design Scenario 2. Fire Scenario 3A was then applied to the structure with fireproofing corresponding to 1 h and 2 h ratings. With the 2 h rating, two members of the perimeter truss initiate buckling within the first 45 min of the fire, and the concrete structure experiences larger deflections and D/C ratios. Yet, load redistribution prevents collapse of the transfer system, and the 2 h rating satisfies the performance objective of Design Scenario 2. With the 1 h rating, three members of the perimeter truss buckle within the first 30 min of the fire and the transfer structure cannot continue to carry the loads.

In all the aforementioned analyses, buckling always occurred in the perimeter truss. Therefore, two more optimized designs were tested, in which the perimeter truss receives a 3 h fire rating, while the interior trusses are protected with only 1 h or 2 h ratings. The results showed that the interior trusses can survive Fire Scenario 3A with only a 1 h fire rating, whereas the perimeter truss experiences the same single member buckling as before with its 3 h rating. This design therefore satisfies the performance objectives of Design 2.

Similar analyses are performed with the more moderate Fire Scenario 3B. In this case, the 2 h rating is sufficient to prevent any steel member failure. With the 1 h rating, one member of the perimeter truss initiates buckling, but load redistribution prevents collapse of the transfer structure and no other member subsequently fails. Therefore, when considering Fire Scenario 3B, the 1 h rating satisfies the performance objectives of Design Scenario 2. However, the project owner or the AHJ may consider the buckling of a primary gravity member as near-collapse and not an acceptable level of performance. In that case, the 2 h rating would be selected as Design 2 for that member.

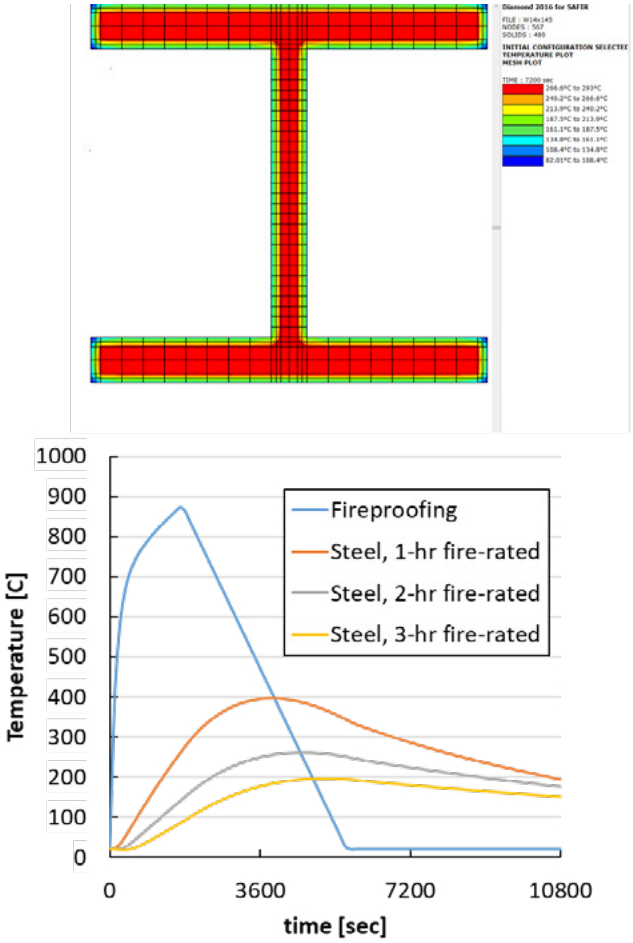

Figure 9-20. Temperature contours of the SAFIR 2D model of a transfer truss W14x145 member at t = 7,200 s, protected with a 1 h fire rating, along with time history of steel temperatures at the section web for different fire ratings.

Source: Courtesy of Thornton Tomasetti (2019).

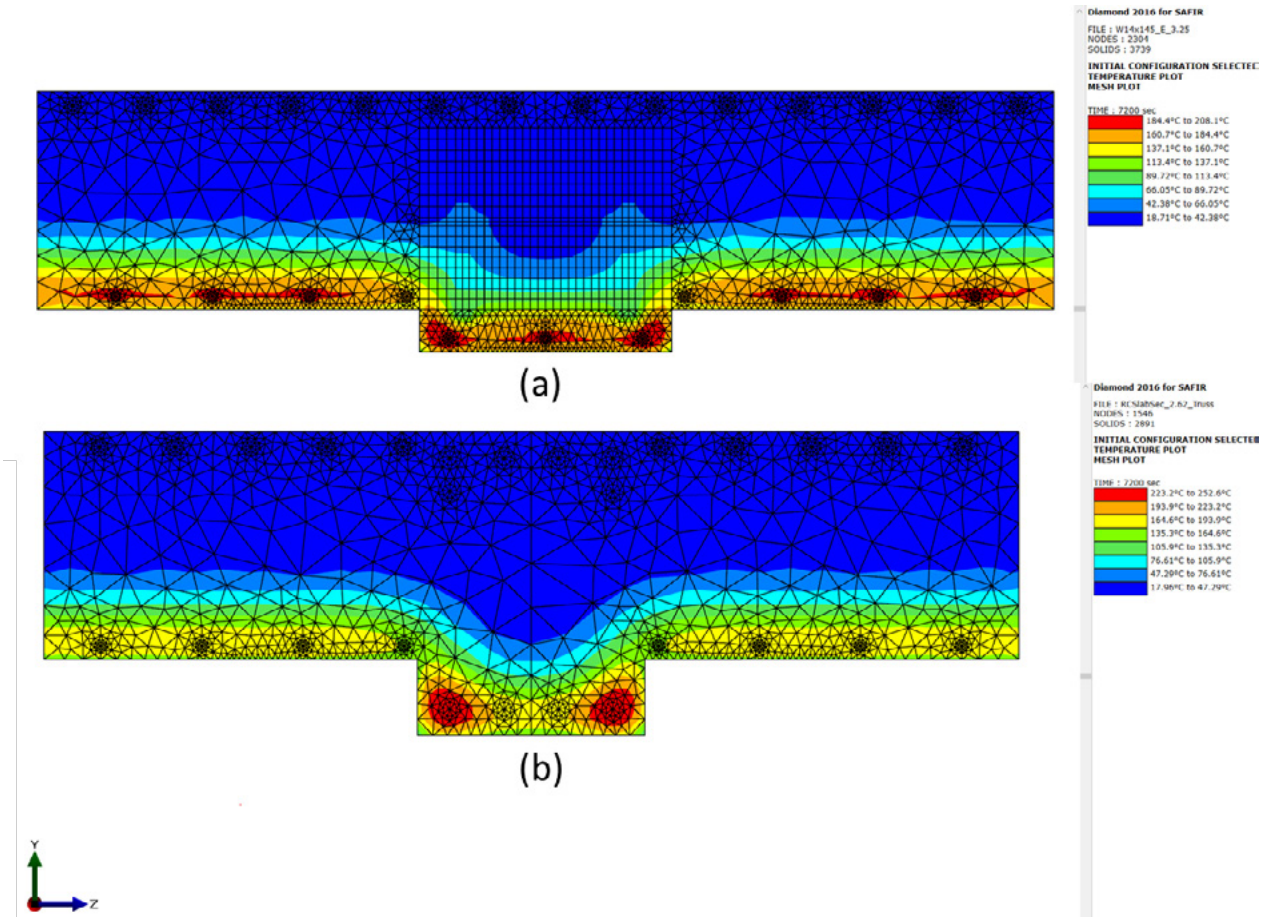

Figure 9-21. Temperature contours of the SAFIR 2D model of (a) concrete-encased top chords of transfer trusses and (b) concrete T-beams, at t = 7,200 s, both exposed to fire at the bottom.

Source: Courtesy of Thornton Tomasetti (2019).

Truss Connections

The members of the transfer trusses are W14 sections oriented such that the flanges are vertical and bolted together with gusset plates at the connections. Common practice for fireproofing gusset plates is to match the maximum fireproofing thickness of the connected members, and the additional steel thickness would result in lower temperatures in the connection than in the connected members. In this study, it was decided that the actual connection capacities remain adequate and no additional fireproofing was required, based on: the reduction in bolt capacity by 37% at maximum truss temperature of 464 °C; the reduced gravity load demand in truss axial forces of at least 15% for fire load combination; the fact that bolt design has a strength reduction factor of 0.75; and the fact that the actual temperature at the connection is lower than the value stated because of additional thermal mass. However, additional local fireproofing at critical connections may be added at minimal cost.

Table 9-1. Summary of Transfer Truss Analysis Results.

Fire scenario	Interior truss fire-proofing	Perimeter truss fire-proofing	Perimeter truss member buck-ling time(s)	Maximum truss deflection owing to fire	Maximum DCR of slabs above	Design
3A	1 h	1 h	16, 28, and 30 min	Collapse	Collapse	Unacceptable
		3 h	37 min	L/250	95%	Minimum Design 2
	2 h	2 h	28 and 53 min	L/397	90%	Acceptable Design 2
		3 h	41 min	L/441	90%	Acceptable Design 2
	3 h	3 h	40 min	L/548	83%	Design 0
3B	1 h	1 h	18 min	L/500	85%	Minimum Design 2
	2 h	2 h	None	L/885	79%	Acceptable Design 2
	3 h	3 h	None	L/1280	74%	Design 0

9.5 DESIGN SUMMARY

9.5.1 Typical Bay

For the typical floor framing, beam behavior was checked through capturing steel plasticity and buckling explicitly in the model and checking concrete forces against capacity, accounting for thermal changes in properties of steel and concrete. The beams remained capable of carrying the loads with fireproofing reduced to 2 h rating for Fire Scenario 2A, and 1 h rating for Fire Scenario 2B. However, connection demands were large enough that connections would have to be changed, even when beam fireproofing was increased to the maximum fireproofing thickness for beams with any classification per UL N743 (2-15/16 in.). Therefore, Design 2 is not achievable.

For Design 3, connections have been changed by providing slots that can accommodate the movements resulting from the structural response to fire. The bolts and slots are covered with premade laths that will be under the fireproofing such that any movement does not affect the fireproofing next to the bolts. If a small unprotected area of the connection is exposed when a beam is pulling away from the connection, the connection capacity is evaluated considering the temperature effects. Connections for primary members are designed as slip critical at ambient temperatures and provide adequate bracing forces for the columns. In a fire, the bolts can slide to relieve large thermal forces, but the connection has adequate capacity in other limit states, so they do not govern. The columns are checked to be able to carry their loads when deformed as a result of the thermal expansion. The option of providing increased connection capacity was not selected, as it required substantial strengthening of the connections and sometimes the columns. For secondary interior beams framing into spandrels, the connections are designed with slots and finger-tight bolts to accommodate the movement because of structural response to fire and

to prevent imposition of large weak axis bending and torsional loads on spandrels. Given that the connections are essential to the structural integrity in fire, additional fireproofing has been provided locally to beam connections to limit the reduction of their capacities, particularly of the bolts, during fire. The additional fireproofing covers the connection plus an additional 3 ft for Fire Scenario 2A and 1 ft for Fire Scenario 2B.

Overall, the fireproofing for all the beams was lowered to what would be equivalent to a prescriptive 2 h rating for Fire Scenario 2A, and 1 h rating for Fire Scenario 2B. Additional fireproofing at connections offset some of these reductions, resulting in a total fireproofing change in the beams of +7% in Fire Scenario 2A and -41% in Fire Scenario 2B.

The floor system at this typical office location is comprised of 3.25 in. light-weight concrete with 4 ksi strength on 20-gauge 3-in.-deep metal deck, with 6x6-W2.9/W2.9 welded wire mesh reinforcement placed 3/4 in. below the slab surface and lapped 6 in. The metal deck is unprotected in Design 0 and it will be kept as such in Design 2 and Design 3. The wire mesh was relied on to develop catenary action in the direction of the metal deck during fire, as the exposed metal deck would rapidly lose capacity during a fire. In the more severe fire scenario 3A, equilibrium was reached with a slab deflection of 11.1 in. This deflection is acceptable, considering the other large deflections experienced by the floor steel framing during a fire. The deflection was 9.2 in. in Fire Scenario 3B. For Design 2, the floor system works with catenary action. At the building perimeter, the behavior relies on catenary reaction being developed within the approximately 2 ft cantilever slab past the spandrel. Design 3 improves the certainty of the outcome of this behavior by specifying that the wire mesh be lowered by 1.25 in. at the slab edges to engage the studs. Increasing the wire mesh lap splice to 12 in. can further increase the floor capacity and lower its deflection during fire by half.

The steel column sizes vary from W14x99 to built-up columns heavier than W14x730. High enough reserve capacity was found to be able to reduce the fireproofing by 38%. There is no need for adjustment to the structural design (Table 9-2).

9.5.2 Transfer Trusses

For the transfer trusses, Design 2 involves changes to the fireproofing to achieve burnout capacity. Because the response of the transfer trusses to fire can affect all the upper supported floors, Design 2 was provided with several options, all of which satisfy the performance criteria, but with different extent of impacts on the upper floors. The design team would select one of these designs based on the building owner's preferences. For Design 3, the design team has the option of modifying the structure to achieve the same performance. The failure mode in the trusses is buckling of structural members, and the solution could be a combination of providing additional strength, or additional fireproofing. Providing additional fireproofing locally has limited additional cost and is the most straightforward solution. Unlike typical areas in a structure, the alternative solution of creating alternative load paths is not reasonable for the transfer trusses, which are main structural features of the building. Hence, Design 3 is the same as Design 2.

Table 9-2. Summary of Typical Bay Framing for Design Scenarios.

Design scenario	Fire scenarios considered	Beam fireproofing thickness	Column fireproofing thickness	Shear tab connection
0	n/a	Primary: 1-3/8 in. (3 h) Secondary: 7/8 in. (2 h)	Varies (3 h)	t=1/4 in., (4) 3/4 in. A-325 bolts
1	n/a	n/a	n/a	n/a
2	1 + 2A	n/a	n/a	n/a (no acceptable design without modifying connections)
	1 + 2B	n/a	n/a	n/a (no acceptable design without modifying connections)
3	1 + 2A	7/8 in. (2 h)	Varies (1 and 2 h)	Primary interior beams and spandrel beams: t=3/8 in., (6) 1 in. A-490 slip critical bolts with slotted holes, more fireproofing Secondary interior beams: t=3/8 in., (4) 7/8 in. A-490 finger-tight bolts with slotted holes, more fireproofing
	1 + 2B	½ in. (1 h)	Varies (1 h)	Primary interior beams and spandrel beams: t=3/8 in., (6) 1 in. A-490 slip critical bolts with slotted holes, more fireproofing Secondary interior beams: t=3/8 in., (4) 7/8 in. A-490 finger-tight bolts with slotted holes, more fireproofing

Truss connections are proportioned to carry the design forces. Based on the reduction in bolt capacity by 37% at maximum truss temperature of 464 °C, the reduced gravity load demand in truss axial forces of at least 15% for fire load combination, and the fact that bolts are designed with a resistance factor of 0.75, the actual connection capacities will remain adequate, and no additional fireproofing was required. However, additional local fireproofing at critical connections may be added at minimal cost (Table 9-3).

Table 9-3. Summary of Transfer Trusses for Design Scenarios.

Design Scenario	Fire Scenarios considered	Allowable damage	Inner trusses fireproofing	Perimeter truss fireproofing
0	n/a	n/a	3 h	3 h
1	Performance objectives not applicable to high-rise			
2	3A	Cosmetic damages above, initiation of limited buckling in some truss members	1 h	3 h
2	3A	Minimal	Increase fireproofing compared to Design 0 as needed	
2	3B	Minimal damages above, initiation of limited buckling in some truss members	1 h	1 h
2	3B	Minimal	2 h	2 h
3	Similar to Design 2; structural upgrade not cost-effective versus fireproofing for transfer trusses			

9.6 DISCUSSION

This study on a high-rise building highlighted the significant impact of the design choices on the fire performance of the building and the role of PBSFD in ensuring that the performance goals presumed in a prescriptive design are actually achieved. This analysis showed that at least in some cases, there might not be a realistic acceptable design without changes to the design of the structure. However, with structural fire engineering incorporated into the design from early stages, it is possible to both increase the integrity of a building during fire and reduce the fireproofing.

As shown in Section 9.2 starting with fuels loads, it is shown how different regulatory environments can have a meaningful impact on the fire load considered for design of a building. It was also shown in Section 9.3 how information regarding openings in the façade, as well as from the interior layout of the building, can have a profound impact on the fire loads. Increasingly, the different features of a façade including its window sizes are part of a parametric study at the beginning, considering the holistic impact on the building performance including lighting, energy usage, and aesthetics. If quantified, the impact on fire performance can also be added to the mix of factors being considered. Similarly, many new high-rise designs start with anchor tenants with long term leases and a clear general understanding of the type of interior layout. While the designer must be conservative within the range of uncertainty of design parameters, such layout information can be incorporated into the design when appropriate.

One of the most important findings of this study was that the prescriptive design was incapable of providing the presumed life safety goals and that this deficiency could not be fully remedied by just adjusting fireproofing; see discussion of Design 2 in Section 9.1. This finding highlights the importance of performance-based fire engineering. Although this is currently not a code requirement,

being able to quantify this effect can allow owners and developers to make decisions when they want to increase the reliability of their buildings, especially for sensitive buildings.

It is also noteworthy that PBSFD does not necessarily mean more expensive design. Indeed, if both modifications to the structure and fireproofing are permitted, a building might benefit both from better safety and reduced material costs. In addition, the better fire performance of a building may be leveraged to reduce the insurance premiums on the building, providing additional benefit.

Finally, this design showed a reduction of up to 42% in the quantity of fireproofing in the moderate fire scenario and a slight increase of 4% in the severe fire scenario. In addition to the reduced material cost, the reduced fireproofing can result in lowering the labor cost and the installation time, compression of the construction schedule, and even a reduction in the carbon footprint of the building.

9.7 CONCLUSIONS

The large range of building performances obtained when considering the full design space for the same building highlights the limitations of a prescriptive approach in providing a solution that is specific to a project and meets the appropriate performance goals. The presented design example has identified deficiencies of the prescriptive code when a code compliant design might not perform adequately for structural safety or adequately limit the extent of damage. Many circumstances in which PBSFD can reduce the fireproofing needs of a structure while achieving the required safety goals have also been identified. Being a rational design approach that explicitly studies the parameters of the design space and adjusts them based on their impact, PBSFD allows for achieving better safety and performance for the same cost, or better economy for the same performance and safety. In addition, PBSFD helps quantify the expected behavior of buildings during fire, allowing for informed decisions and reliable performance.

Within the context of PBSFD, this analysis also showed that just being able to adjust the fireproofing has its limitations and cannot always result in a satisfactory outcome, even when it can improve performance in comparison with the prescriptive design. Only the incorporation of modifications to structural design in addition to fireproofing provides the designer with all the tools required to achieve performance goals for the buildings considering their specific features. Fortunately, this approach can frequently improve both safety and economy of a design.

REFERENCES

Dassault Systèmes Simulia Corp. 2011. Abaqus software. Johnston, RI: Dessault Systèmes Simulia Corp.

Drysdale, D. 2011. *An introduction to fire dynamics*, 3rd ed. Hoboken, NJ: Wiley.

Franssen, J.-M., and T. Gernay. 2017. “Modeling structures in fire with SAFIR®: Theoretical background and capabilities.” *J. Struct. Fire Eng.* 8 (3), 300−323.

Guanyu, H. 2011. “Behavior of beam shear connections in steel buildings subject to fire.” Ph.D. diss., Univ. of Texas, Austin, TX.

McGrattan K., Hostikka, S., McDermott, R., Floyd, J., Weinschenk, C. and Overholt, K. 2013. “Fire dynamics simulator user’s guide.” *NIST special publication, 1019(6).*

Ohlemiller, T. J., G. W. Mulholland, A. Maranghides, and J. J. Filliben. 2005. *Fire tests of single office workstations*. Gaithersburg, MD: NIST, National Institute of Standards and Technology Federal Building and Fire Safety Investigation of the World Trade Center Disaster.

Thomas, P. H., and A. J. M. Heselden. 1972. “Fully developed fires in single compartments. Fire Research Station. A cooperative research programme of the Conseil Internationale du Bâtiment.” *Conseil Internationale du Bâtiment Report No. 20, Fire Research Note No. 923*. Borehamwood, UK: Fire Research Station.

Wickström U., D. Dat Duthinh, and K. McGrattan. 2007. “Adiabatic surface temperature for calculating heat transfer to fire exposed structures.” In *Proc., 11th International Interflam Conference.* London: Interscience Communications, 943−954.

Chapter 10. Building 4: Walter P Moore (WPM)

Participants

The Structural Engineering Institute of ASCE acknowledges the work of the participants in this project.

Industry Champions

The WPM (Walter P Moore) design team comprised the following contributors:

Lawrence G. Griffis, P.E., *Industry Champion*

Ozgur Atlayan, Ph.D., P.E.

Samuel J. Baer

Sridhar Baldava, P.E.

Addison L. Bliss

Viral B. Patel, P.E., S.E.

BUILDING 4

Walter P Moore studied a 6-story steel braced framed building in Florida, which was constructed in 2014 according to the *International Building Code* 2009. The risk category of this office building is II and occupancy classification is B (business). The construction type is IB (fully sprinklered), which requires a 2 h fire-resistance rating. IBC allows for Type IIA construction (1 h fire rating) in 6-story buildings up to 85 ft when equipped with an automated sprinkler system. However, because of large floor-to-floor heights, this building is 87 ft tall, and thus, Type IB construction was required. Gross floor area per floor is about 30,000 sf and composite-floor systems with 3.5 in. thick lightweight concrete on 3-in.-deep metal deck are used at all floor levels. Typical bay size is 30 ft 0 in. × 41 ft 6 in. (Figure 10-1).

10.1 DESIGN STRATEGY

The main design strategy for Design 3 of the Design Brief, in which structural modifications are permitted to achieve optimum performance through full fire, is to leave the central beams of the floors unprotected, in other words, remove the spray-applied fire resisting material (SFRM) from the central beams, and, if possible, reduce the SFRM thickness of the perimeter beams (boundary beams and girders at column gridlines) of the floors. This is achieved through the utilization of tensile membrane action (TMA) in the composite slab. The perimeter beam connections are improved as necessary to accommodate additional forces generated by these modifications. Column demands are also compared to reduced capacities at elevated temperatures, and if possible, column SFRM thicknesses are reduced.

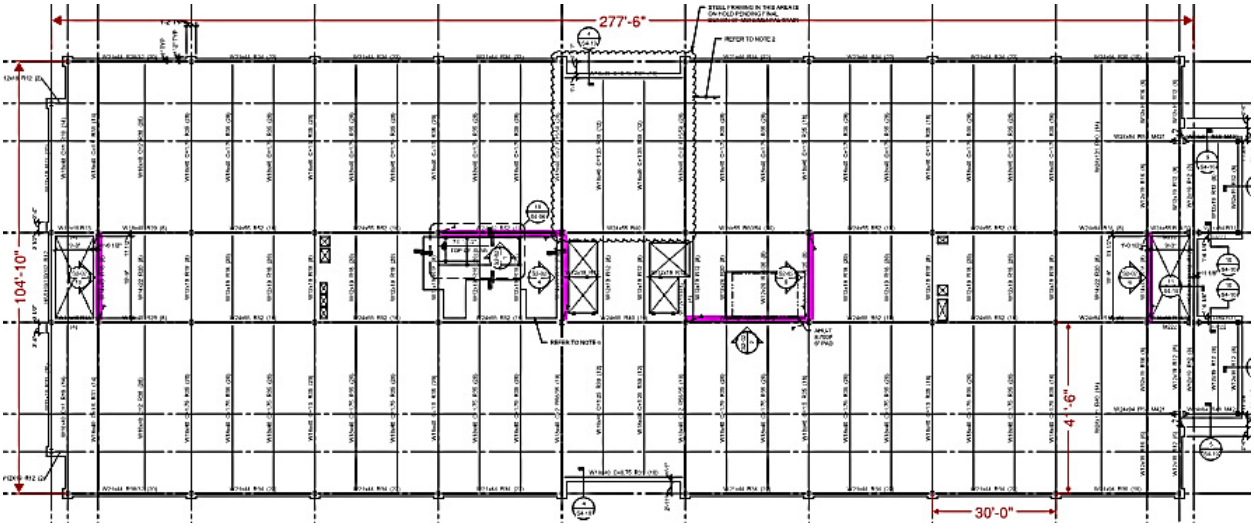

Figure 10-1. Typical floor plan with braced frame lines highlighted.

Source: Courtesy of Walter P Moore (2019).

When central beams are left unprotected (i.e., bare steel), they lose their load-carrying capacity during a fire event and slab forces are transferred through a redundant load path via TMA, where the slab reinforcement starts carrying the vertical load by acting like a tensile net. The slab supports the load by TMA at the central region of the slab and compressive membrane action forming a supporting compression ring around the perimeter of the slab. For this load path to work, the boundary beams need to remain close to their original location vertically, that is, they need to be stiff enough to have minimal deflections, and the vertical supports (columns) need to be minimally affected by fire to maintain continuity in the overall load path and general stability of the structure. To utilize TMA in the slab, the position of the reinforcement is changed within practical limits and the amount of reinforcement within the slab is increased. Perimeter beams may also need to be revised if they deflect too much during fire, owing to change in the load distribution. Figure 10-2 shows formation of membrane action when the central beams are left unprotected.

In Design 1 and Design 2, as defined in the Design Brief document, the structural engineer gets involved at a late stage of the design, and thus structural modifications are not permissible. The insulation (SFRM) thickness of the floor beams is optimized for Design 1 and Design 2. Whereas Design 1 goals are to achieve minimum code-mandated performance (stability up to required safety egress time (RSET), Design 2 requires full fire burnout optimum performance. RSET was calculated as 11.9 min. using the occupancy and exit capacity information obtained from the life safety drawings of the building. The procedure outlined in Proulx (2002) was followed for the RSET calculation.

10.2 DESIGN FUEL LOAD

Design fuel load was calculated according to Eurocode 1, Annex E (CEN 2001). Danger of fire activation factors, d_{q1} and d_{q2}, are 1.56 and 1.00 for compartment floor area of 600 m^2 and office occupancy. A combustion factor, m, of 0.8 was used. For the baseline fire, as defined in design brief, an 80% fractile fire load density, q_{fk}, of 511 MJ/m^2 was used. The only active fire-fighting

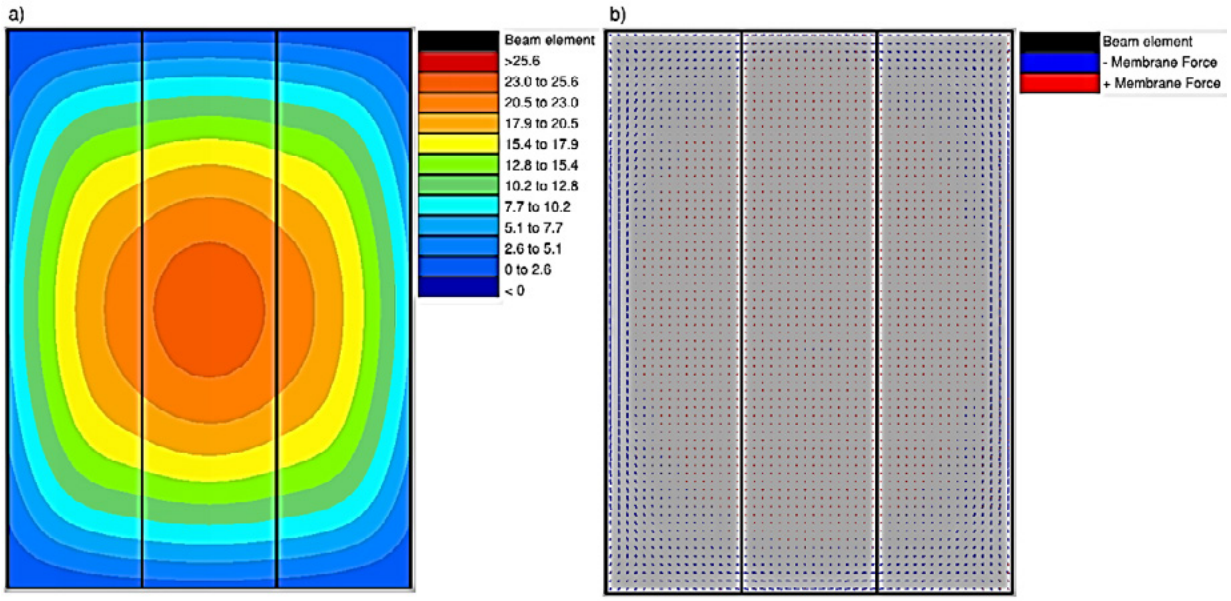

Figure 10-2. SAFIR snapshots for: (a) vertical displacement contours (legend values in inches), and (b) membrane forces when slab center displacement is maximum.

Source: Courtesy of Walter P Moore (2019).

measure considered was the sprinkler reduction factor, d_{n1}, of 0.61. The design fire load, q_{fd}, is 389 MJ/m^2 for the baseline fire.

Two alternative design fuel loads were also calculated for robustness and sensitivity. As a first alternative, fire load density is increased from 80% fractile to 95% fractile to increase the level of conservatism. 655 MJ/m^2 is used as 95% fractile fire load density, , which is calculated using a coefficient of variation of 0.3 and based on a Gumbel Type I distribution (Vassart et al. 2014). The design fire load, q_{fd}, for the first alternative is 499 MJ/m^2. As a second alternative, the fire load density was maintained at the 80% fractile but no active firefighting reductions (including sprinklers) were considered. The design fire load, q_{fd}, for the second alternative is 638 MJ/m^2.

10.3 STRUCTURAL DESIGN FIRES

The building occupancy is open office with workstations on the north and south sides of each typical floor and a core consisting of mechanical equipment, restrooms, conference rooms, elevators and stairs in the central portion of each floor. Because the connection between the north and south sides is limited, it is highly unlikely that there would be fire at both sides at the same time. The highlighted area in Figure 10-3, which is the largest possible continuous area on plan, is the selected compartment for this study. The two connection hallways between the north and south sides are treated as openings in Eurocode 1, Annex A ventilation calculations.

Although Annex A equations are for compartments up to 500 m^2 of floor area and 4 m maximum heights, they were nevertheless used conservatively for this building with a compartment area of about 600 m^2 and a 4.2 m story height.

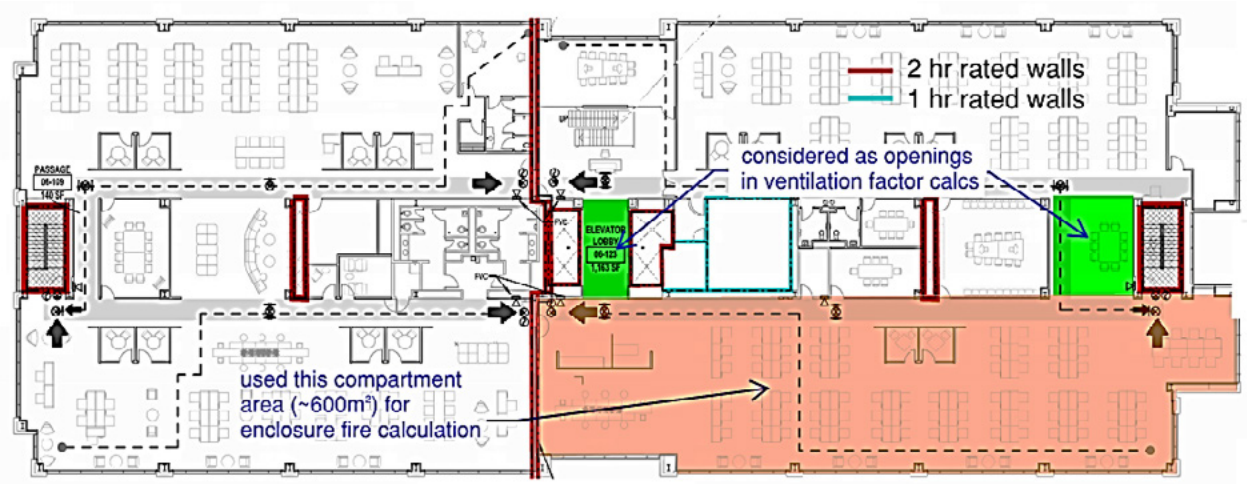

Figure 10-3. Fire compartment for enclosure fire calculations of Eurocode 1, Annex A.

Source: Courtesy of Walter P Moore (2019).

Because the window breakage during the fire is difficult to estimate, three different ventilation assumptions were made, with the percentage of broken windows varying as 25%, 50%, and 100% of the total. Combining the three different fire loads, as explained previously, with three different ventilation assumptions, nine different fire scenario cases were developed. Four out of the nine fire cases are ventilation-controlled and are longer and more severe because in fuel-controlled fires the excess air entering the compartment would likely have a cooling effect on room temperature. Table 10-1 and Figure 10-4 display the details and time–temperature curves of all fire scenarios studied for this building.

10.4 STRUCTURAL TEMPERATURE HISTORIES

Thermal analyses of the slabs, beams, and columns were conducted with SAFIR (Franssen and Gernay 2017).

A unidirectional thermal analysis was conducted on the slabs (see Figure 10-5). An effective thickness of 5 in. was used for thermal analyses to model the composite slabs with 3.5 in. thick concrete on 3 in. deep metal deck. Only the height above the deck, 3.5 in., is used for structural analyses; that is, 1.5 in. thick concrete at the bottom of the section is considered as thermal equivalent concrete to model the thermal effects of the ribs. The slab is heated from the base with the gas temperature and an ambient temperature of 20 °C is applied at top of the slab section.

Figure 10-6 shows the structural temperature histories under Cases 1 and 9 (envelope cases) for slab top and bottom, wire mesh, and beam bottom flange, compared with the gas temperatures. Slab bottom and unprotected beam bottom flange temperature histories generally follow the gas temperatures. The time of maximum temperature response varies for every scenario. Figure 10-7 displays the effect of insulation on the thermal response of beam bottom flanges for the same envelope fire scenarios. As the thickness of SFRM increases, the maximum temperature decreases and occurs later.

Table 10-1. Time–Temperature Curves and Details for All Fire Scenarios for Building 4.

Case	Fire Load Density Fractile	Ventilation	Active Fire Fighting Reductions according to EC-1	Controlled by	Design Value of Fire Load Density, qf,d [MJ/m²]	Opening Factor
1	80%	high	sprinklers only	fuel	389	0.19
2	80%	moderate	sprinklers only	fuel	389	0.10
3	80%	low	sprinklers only	ventilation	389	0.06
4	95%	high	sprinklers only	fuel	499	0.19
5	95%	moderate	sprinklers only	fuel	499	0.10
6	95%	low	sprinklers only	ventilation	499	0.06
7	80%	high	no reduction	fuel	638	0.19
8	80%	moderate	no reduction	ventilation	638	0.10
9	80%	low	no reduction	ventilation	638	0.06

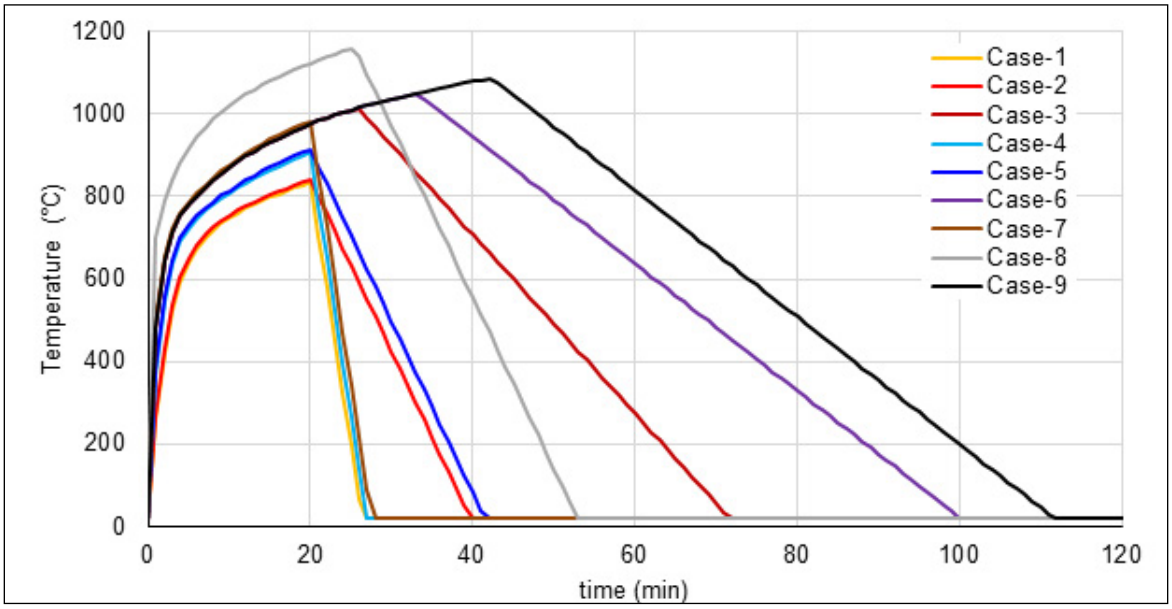

Figure 10-4. Time–temperature curves according to Eurocode 1 (EC-1) Annex A.

Source: Courtesy of Walter P Moore (2019).

Figures 10-8 and 10-9 show thermal contour snapshots from SAFIR at the time of maximum temperatures. While the maximum temperature of 784 °C occurs at the 20th minute for unprotected beams under Case 1, the maximum temperature of 151 °C occurs at the 38th minute with the insulation required by prescriptive design. Similarly, the maximum temperature of 1081 °C occurs at the 42nd minute for unprotected beams under Case 9 and the maximum temperature of 466 °C occurs at the 90th minute with prescriptive insulation. The variation in the thermal response is a product of robust fire scenarios generated with varying ventilation and design fuel load assumptions. Similar thermal analyses were performed on the slabs and columns.

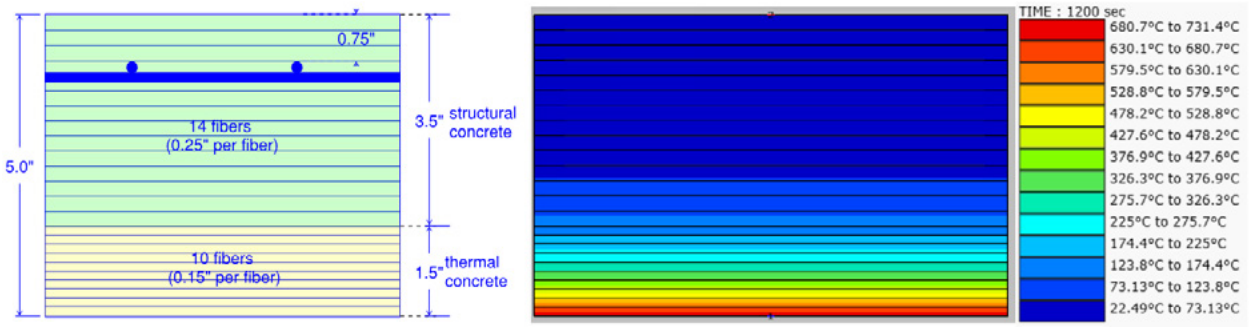

Figure 10-5. Slab modeling for thermal analyses and a sample response (Fire Case 1).

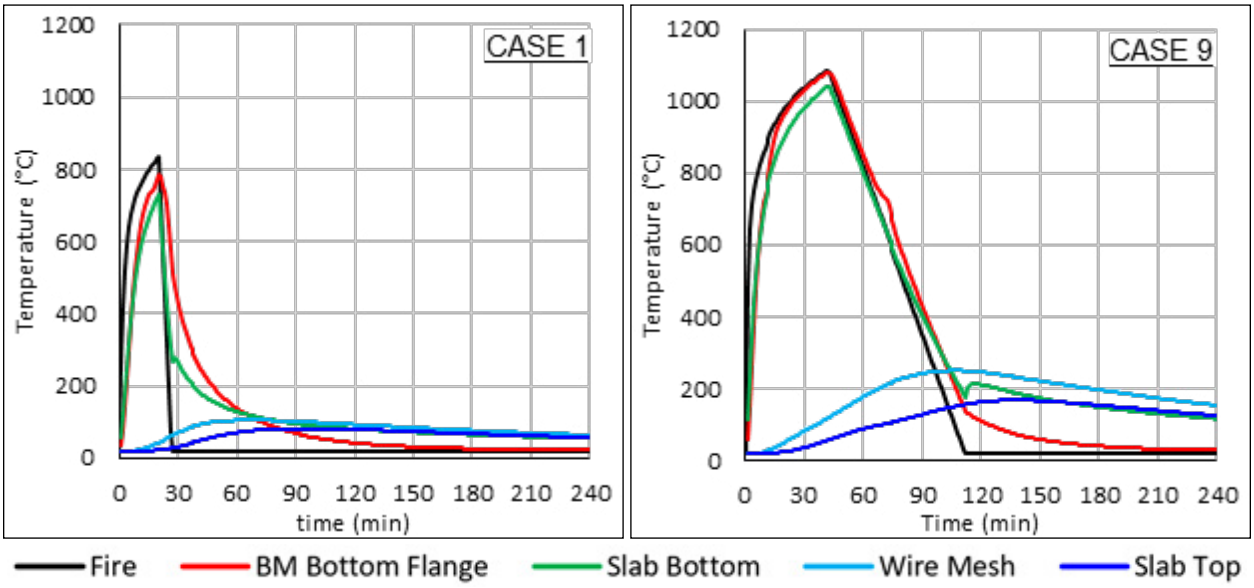

Figure 10-6. Temperature histories of slab, wire mesh (at 1.75 in. from surface), and unprotected beam bottom flange under Fire Scenarios Case 1 and Case 9.

Source: Courtesy of Walter P Moore (2019).

10.5 STRUCTURAL ANALYSES

10.5.1 Floor System

This study focuses on the effect of fire on a typical gravity floor bay, which has higher utilization ratios compared to lateral frames. All floors (including roof level) are composite-floor systems with 3.5-in.-thick lightweight concrete on 3-in.-deep metal deck with 6x6-W2.9xW2.9 welded wire-mesh reinforcement (0.058 in^2/ft steel area in each direction) placed 3/4 in. away from the surface. The slab includes only one layer of reinforcement, which is close to the surface, and there is no reinforcement in the flutes. Owing to the high temperatures observed at the bottom of the slabs, the effect of the metal deck was neglected in structural analyses. A single-bay model (41ft 6 in. × 30 ft. 0 in.) was used for parametric studies conducted with SAFIR. The effect of the restraints owing to surrounding bays was studied utilizing a multibay model.

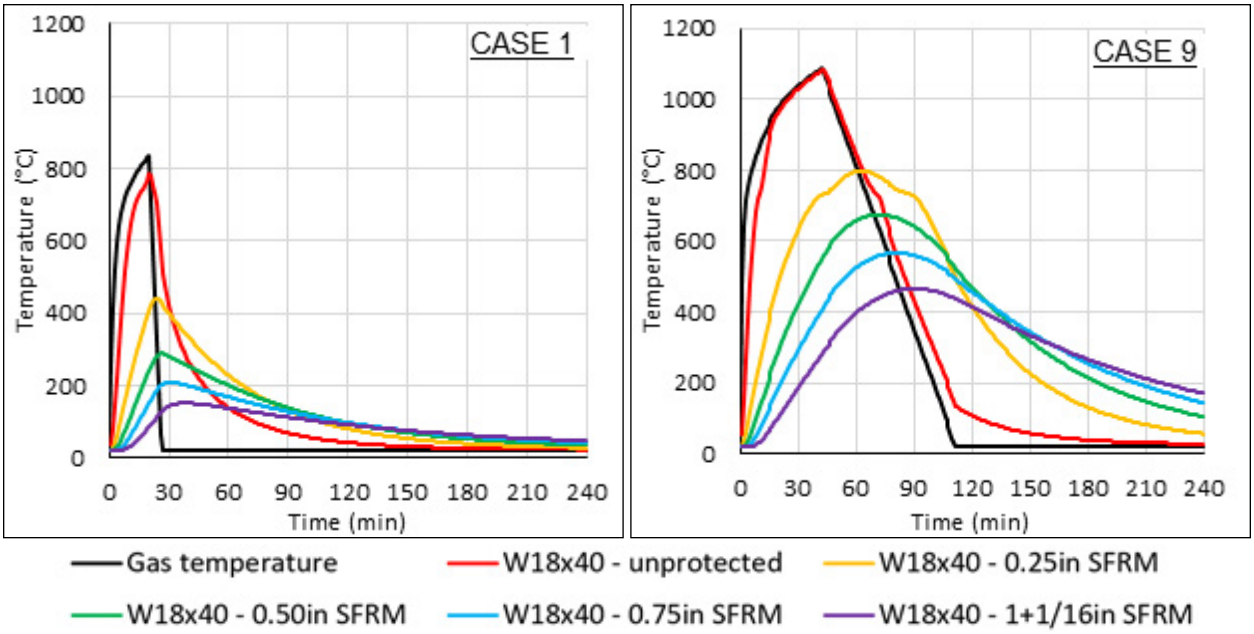

Figure 10-7. Beam bottom flange temperature histories for various insulation under Fire Scenarios Case 1 and Case 9.

Source: Courtesy of Walter P Moore (2019).

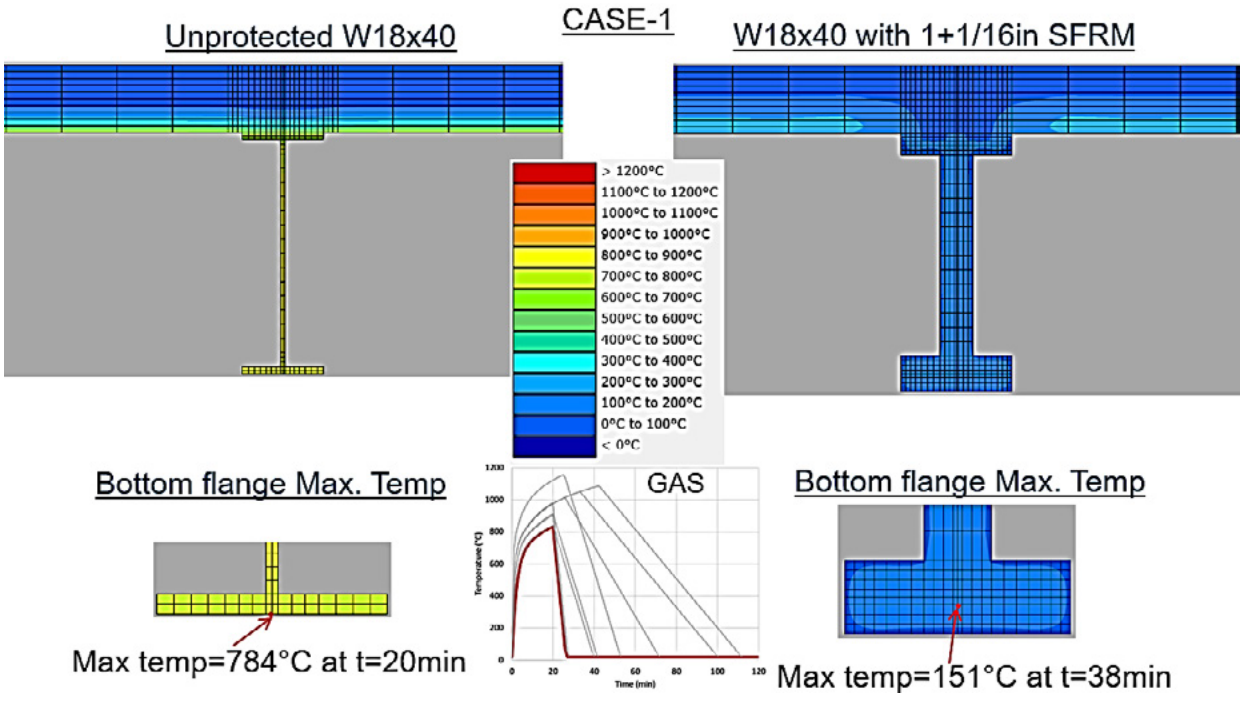

Figure 10-8. Thermal model responses at the time of maximum bottom flange temperatures for unprotected and protected beams under Fire Scenario Case 1.

Source: Courtesy of Walter P Moore (2019).

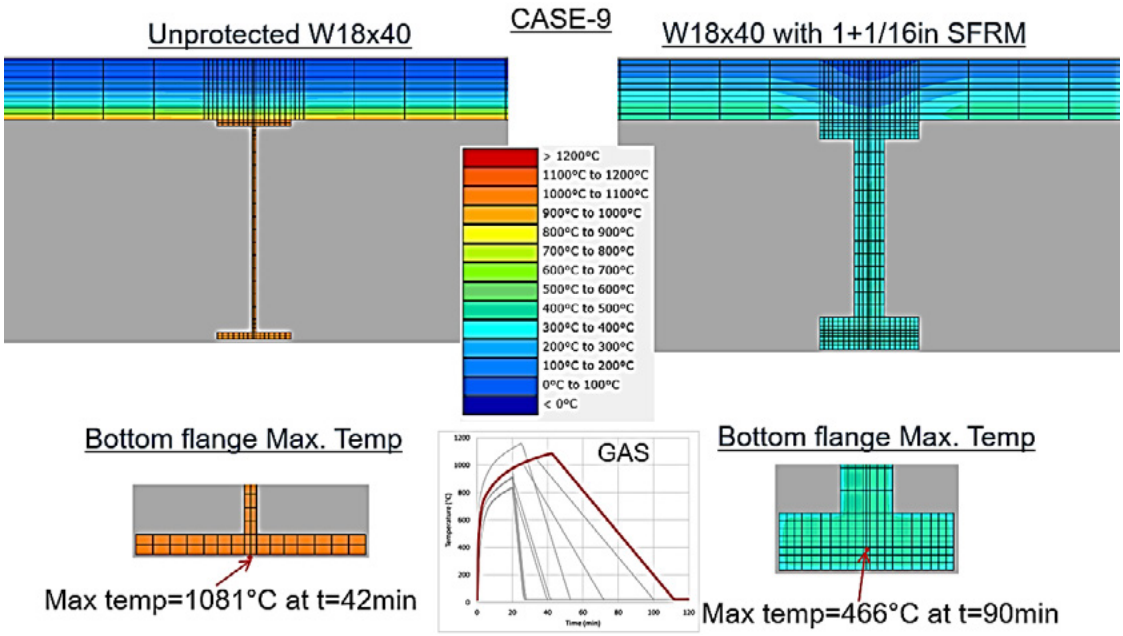

Figure 10-9. Thermal model responses at the time of maximum bottom flange temperatures for unprotected and protected beams under Fire Scenario Case 9.

Source: Courtesy of Walter P Moore (2019).

A comparison was made between a single-bay model, which is an exterior bay, and a six-bay model in which all the surrounding bays were also modeled. East and west sides of the central bay of the six-bay model are also under fire according to the compartment definition; however, the north bays stay cold. Figures 10.10 and 10.11 show response comparisons between the two models under Fire Case 1. Design-3 with unprotected central beams and 0.120 in^2/ft wire mesh reinforcement is used for both models. The displacement contour plot shows the comparison at the time of the peak gas temperature of 20 min. As may be seen in the response history comparison, a very good match could be obtained from the two models after applying minor modeling adjustments on the single-bay model to reduce the conservatism of the single-bay model used for parametric studies.

Figures 10-12 and 10-13 show sample displacement response histories of bay center nodes under Fire Cases 1 and 9, respectively. The responses of all design types (0 to 3) are shown in the figures. Figure 10-12 shows that stability for full fire burnout can be achieved under Case 1 with unprotected central beams when slab reinforcement is increased from 0.058 in^2/ft to 0.120 in^2/ft and by also repositioning the level of the bars from 0.75 in. to 1.75 in. away from the surface (see Design 3).

Note that ACI-318 provides a relationship for the spacing and yield strength of the reinforcement and the clear cover to control cracking. With 4 in. to 6 in. spacing of the wire mesh reinforcement, clear cover could be ~ 3.5 in. per ACI-318 equation, but for practical purposes it was decided to use 1.75 in. clear cover.

The reinforcement had to be increased to 0.360 in^2/ft to achieve stability through the fire burnout time under Fire Case 9 for Design 3, Option 1 (see Figure 10-13). The reason for this substantial

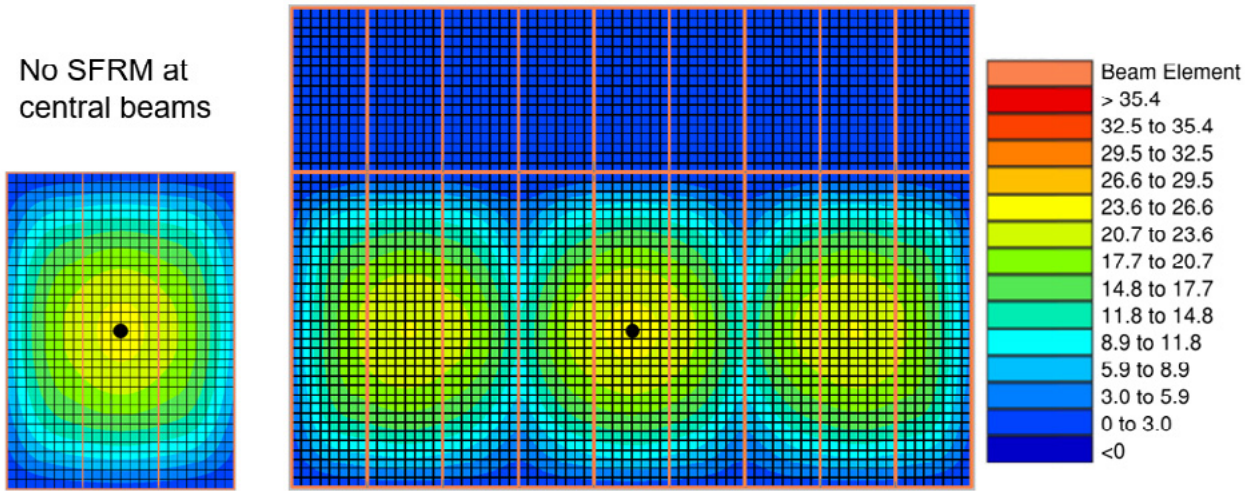

Figure 10-10. SAFIR single- and multibay model displacement contour at 20th min for Fire Case 1.

Source: Courtesy of Walter P Moore (2019).
Note: Legend is in inches.

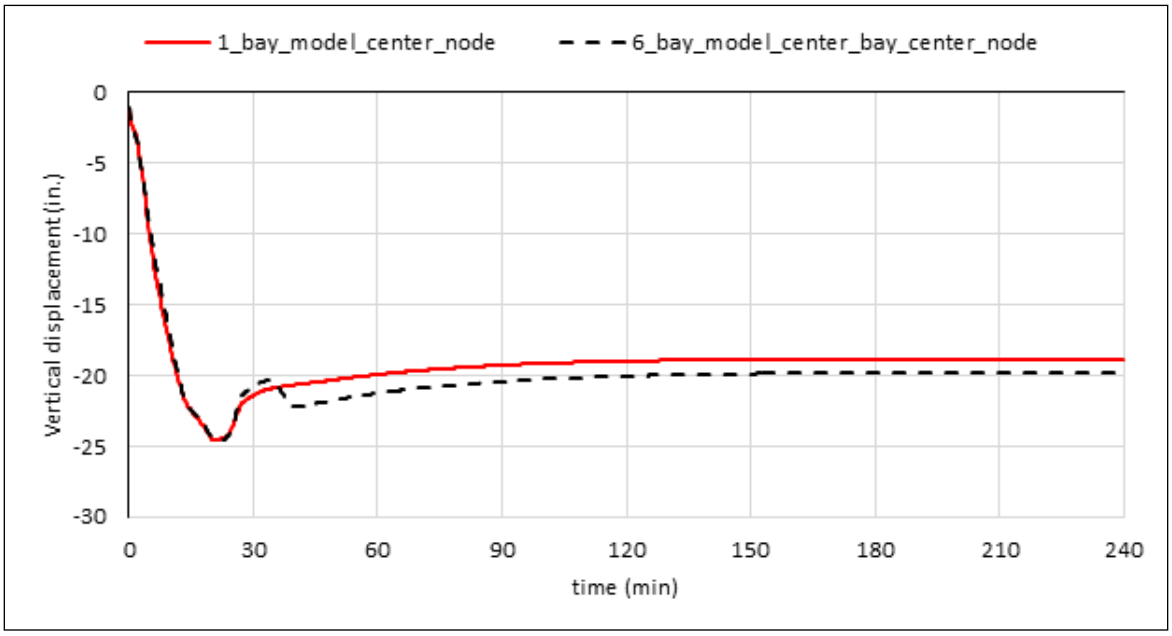

Figure 10-11. Vertical displacement response comparison between single- and multibay models' center nodes (black highlighted dots in Figure 10-10).

Source: Courtesy of Walter P Moore (2019).

increase is the yielding of the perimeter beams. The failure mechanism of this case is discussed subsequently in this section. When perimeter beam size is increased from W18x40 to W21x44, 0.240 in^2/ft reinforcement was adequate (see Design 3, Option 2 in Figure 10-10). A partially protected central beam option is also provided for Case 9 (see Design 3-3 in Figure 10-13). The required slab reinforcement dropped to 0.120 in^2/ft with 1/2 in. thick central beam insulation.

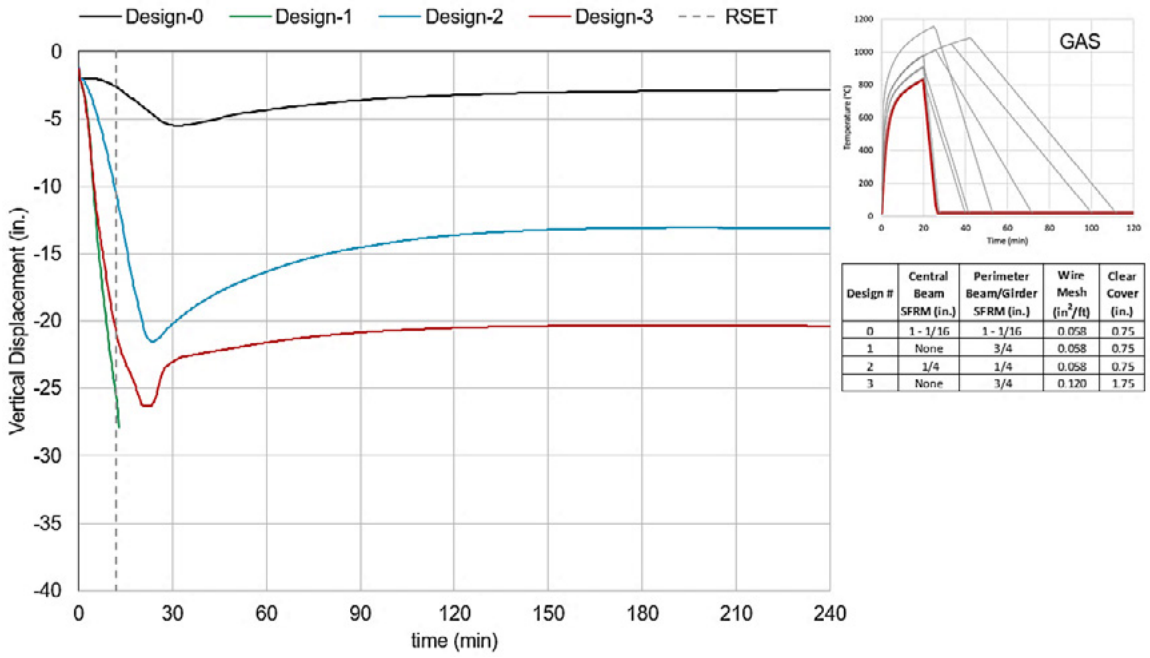

Design #	Central Beam SFRM (in.)	Perimeter Beam/Girder SFRM (in.)	Wire Mesh (in^2/ft)	Clear Cover (in.)
0	1 - 1/16	1 - 1/16	0.058	0.75
1	None	3/4	0.058	0.75
2	1/4	1/4	0.058	0.75
3	None	3/4	0.120	1.75

Figure 10-12. Vertical displacement response histories under Fire Case 1.

Source: Courtesy of Walter P Moore (2019).

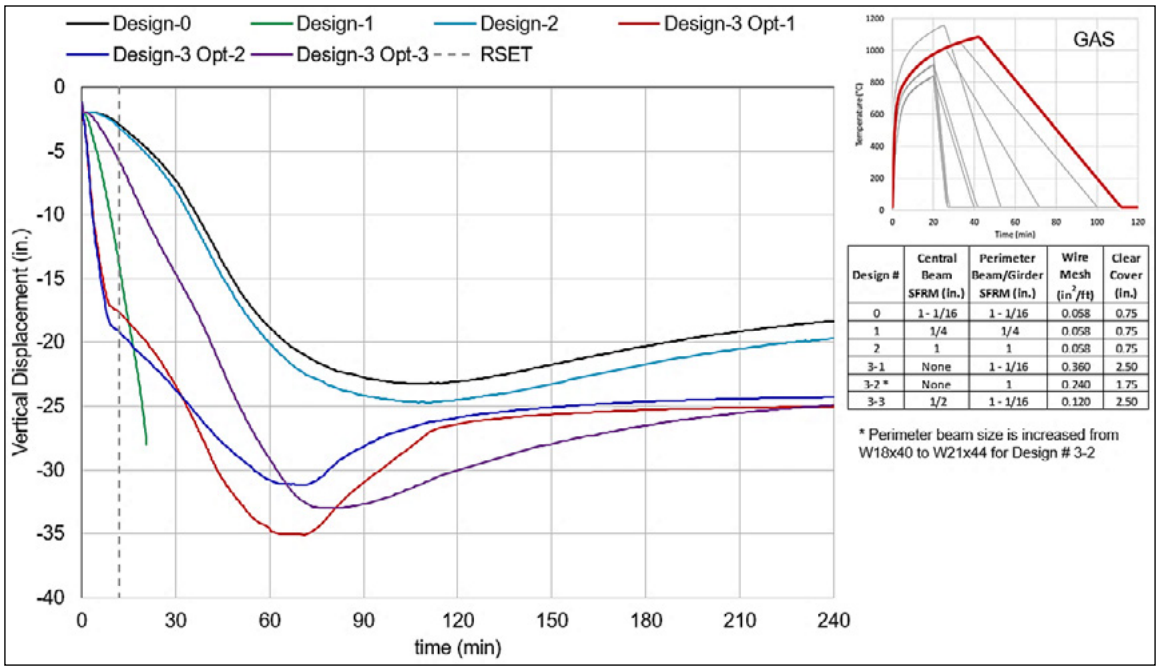

Design #	Central Beam SFRM (in.)	Perimeter Beam/Girder SFRM (in.)	Wire Mesh (in^2/ft)	Clear Cover (in.)
0	1 - 1/16	1 - 1/16	0.058	0.75
1	1/4	1/4	0.058	0.75
2	1	1	0.058	0.75
3-1	None	1 - 1/16	0.360	2.50
3-2 *	None	1	0.240	1.75
3-3	1/2	1 - 1/16	0.120	2.50

* Perimeter beam size is increased from W18x40 to W21x44 for Design # 3-2

Figure 10-13. Vertical displacement response histories under Fire Case 9.

Source: Courtesy of Walter P Moore (2019).

The position of the reinforcement within the slab is a critical parameter in TMA. When the slab reinforcement is located away from the slab surface (close to the deck), the flexural resistance of the slab increases due to increase in the lever arm. However, at the same time the lower the

position of the reinforcement, the higher temperature it will face. Thus, the position of the reinforcement within the slab should be decided carefully.

Figures 10-14 shows a comparison of the slab reinforcement temperature and bay center vertical displacement history under fire Case 9. The comparison was made on a Design-3-2 model in which the mesh reinforcement was increased from 0.058 in^2/ft to 0.240 in^2/ft and perimeter beams were changed from W18x40 to W21x44 as structural modifications. Slab reinforcement reaches higher temperatures with increased clear cover. The change of clear cover from 0.75 in. to 1.75 in. did not increase the temperatures significantly for this 5-in.-deep effective slab section; however, the mesh reinforcement reaches almost 500 °C with 3.50 in. clear cover. The small increase in clear cover from 0.75 in. to 1.75 in. helped to reduce the displacements with more bending resistance. However, lowering the reinforcement further at 3.50 in. clear cover has a detrimental effect with high reinforcement temperatures and the stability could not be achieved due to the yielding of slab reinforcement and perimeter beams.

After finalizing the slab reinforcement and position for Design 3, the perimeter beam SFRM thicknesses were gradually reduced in the SAFIR model until instability occurred. A similar approach was followed for Design 1 and Design 2 in which SFRM thicknesses were reduced without making any structural modifications.

An independent verification of the structural model was made using MACS+ software (Vassart and Zhao 2012) which uses a simplified design method of concrete slab plastic yield line theory combined with tensile membrane action.

Vertical displacement contour plots are provided in Figures 10-15 to 10-17 from Fire Cases 1, 3, and 9 for Design 3. Displacement contours are plotted at 15th and 30th min and after 1, 2, 3, and 4 h of response.

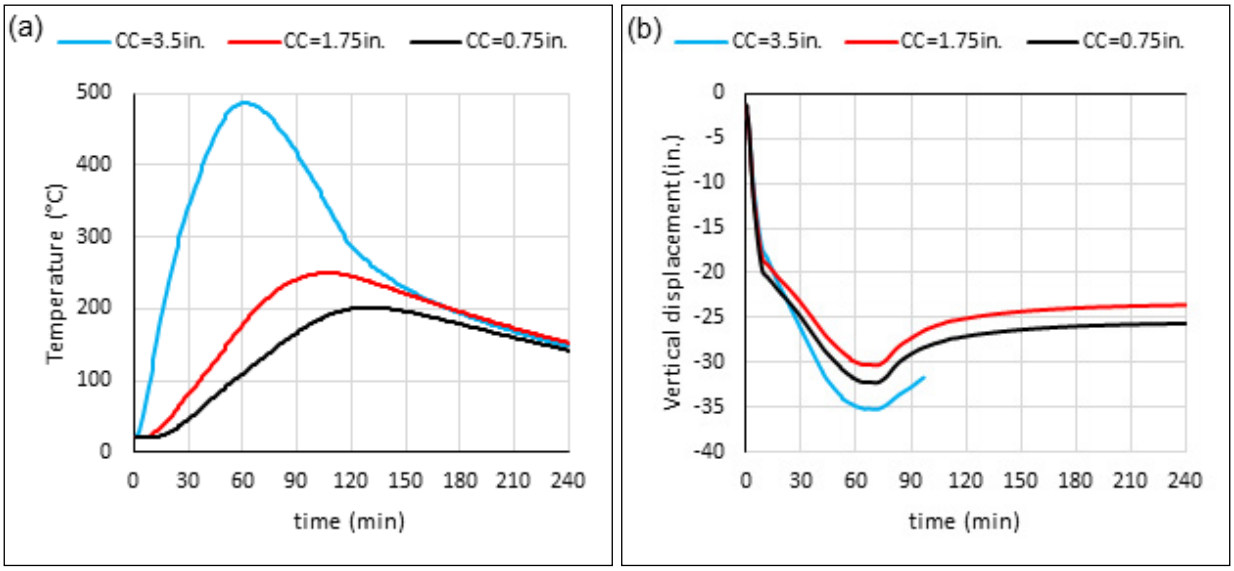

Figure 10-14, Effect of clear cover on: (a) reinforcement temperature, and (b) center bay vertical displacement response for Fire Case 9.

Source: Courtesy of Walter P Moore (2019).

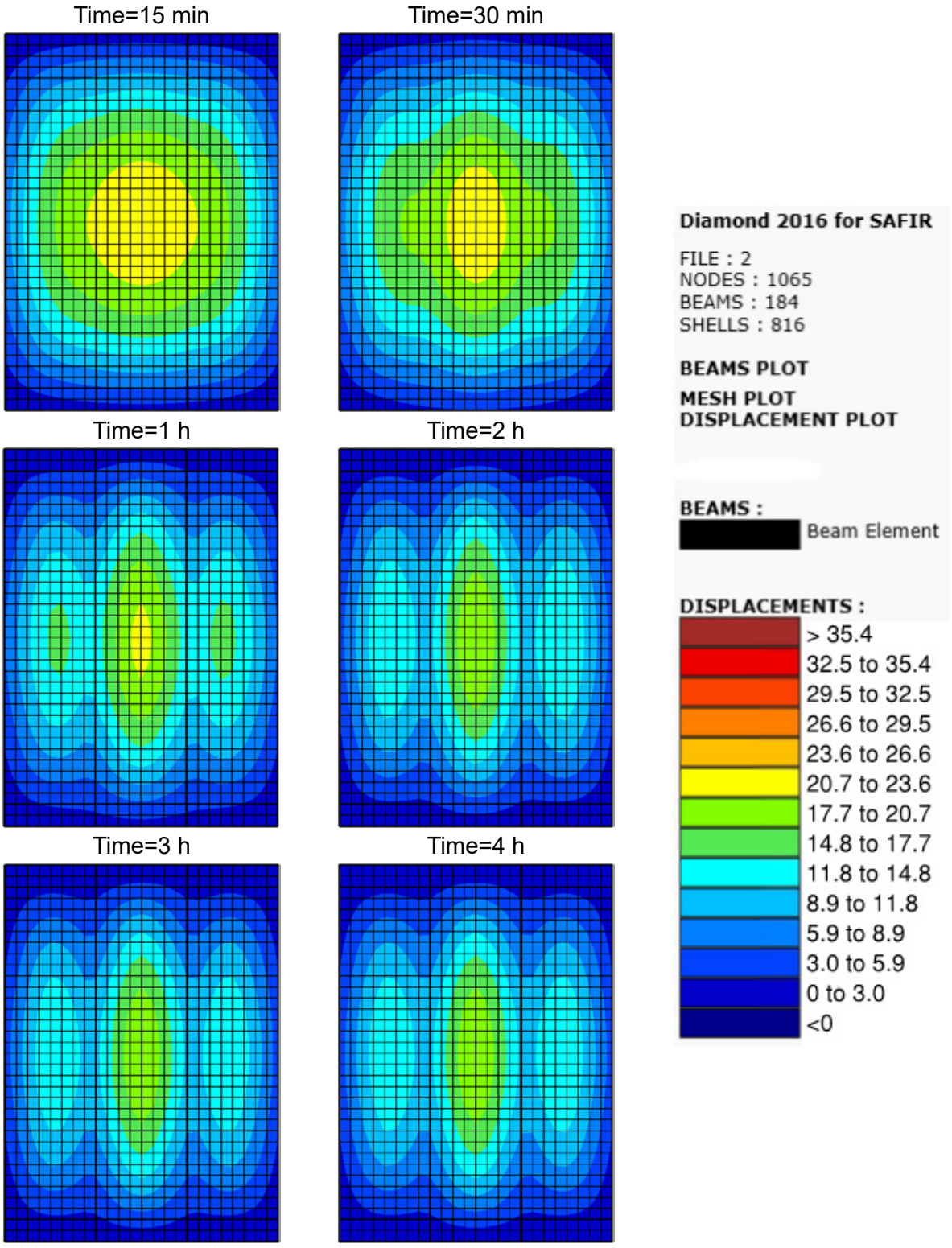

Figure 10-15. Vertical displacement contours of Design 3 with Fire Case 1.

Source: Courtesy of Walter P Moore (2019).
Note: Legend is in inches.

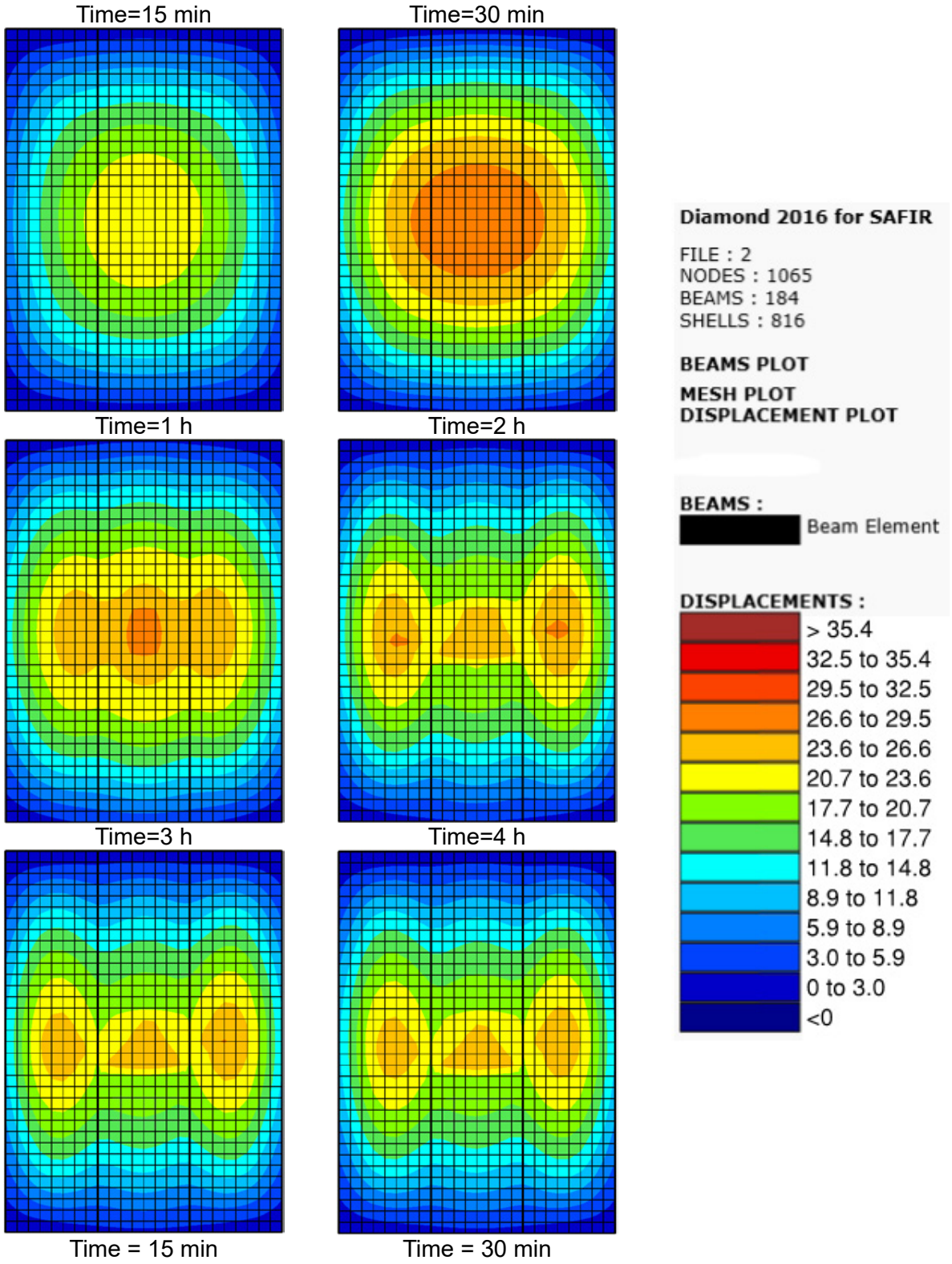

Figure 10-16. Vertical displacement contours of Design 3 with Fire Case 3.

Source: Courtesy of Walter P Moore (2019).
Note: Legend is in inches.

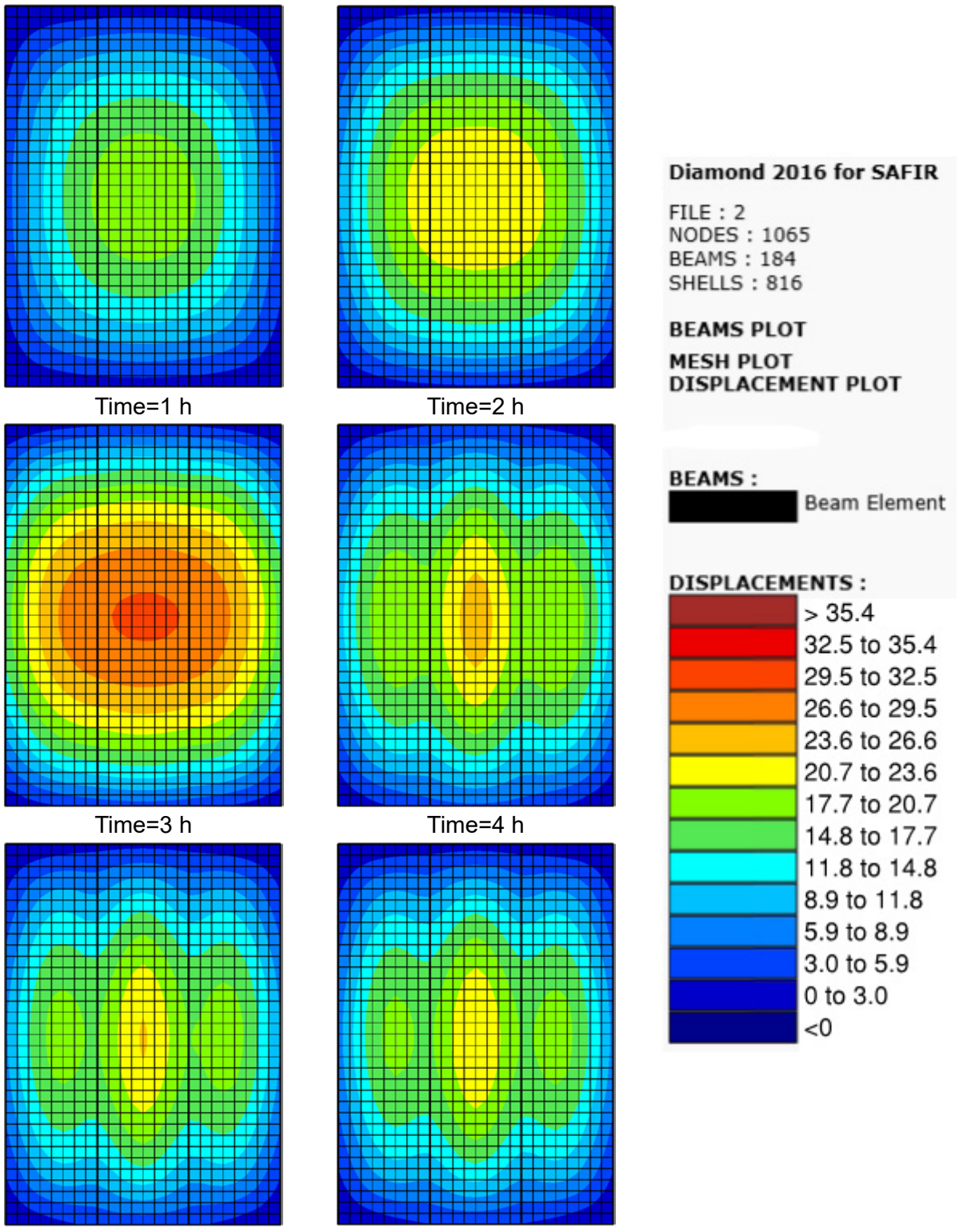

Figure 10-17. Vertical displacement contours of Design-3, Option 2 with Fire Case 9.

Source: Courtesy of Walter P Moore (2019).
Note: Legend is in inches.

Figure 10-18 (a) shows a sample response at the time of instability in which a failure mechanism with excessive deflections was observed under Fire Case 9 due to yielding of the boundary beams. Central beams are unprotected for this case and slab reinforcement is increased to 0.240 in^2/ft with clear cover of 1.75 in. As may be seen in Figure 10-18 (b), when the boundary beam sizes were increased from W18x40 to W21x44, full fire burnout stability was achieved with maximum displacement of about 30in. at the center of the slab. Note that boundary beams carry more load during fire after the central beams become ineffective because the load distribution changes from one-way to two-way action (Elhami Khorasani et al. 2017).

Other failure mechanisms result from yielding of the steel reinforcement when central beams are unprotected and when there is not enough reinforcement in the slab to develop tensile membrane action. For this rectangular bay, the failure mode is due to a concrete fracture across the shorter span, that is, the reinforcement in longer span yields because it cannot support the tensile forces.

10.5.2 Connections

The component method was used for connection checks. An assembly of nonlinear springs representing plate- and web-bearing, bolt shear, and friction of the plate surfaces were created for all different connection types and combined in Strand7 (Strand7 2010) to get the connection capacity curves, which were compared with the resultant shear and axial force demands calculated by

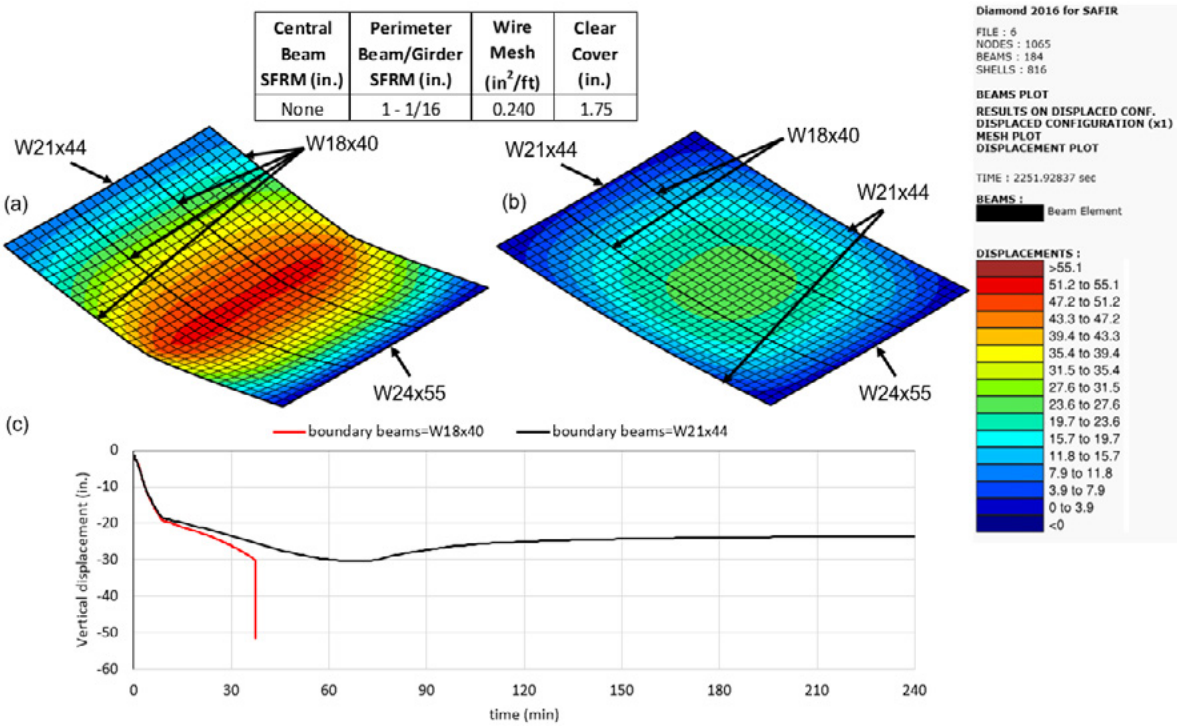

Figure 10-18. Displaced shapes at ~ 40th minute under Fire Case 9: (a) boundary beams with W18x40, and (b) boundary beams with W21x44 (c) bay center node displacement history comparison.

Source: Courtesy of Walter P Moore (2019).
Note: Displacement legend is in inches.

SAFIR. The nonlinear springs of the component method were created as outlined in Sarraj (2007). While all connections were checked for Design 1 and Design 2, only perimeter beam and girder connections to columns were checked for Design 3, because there was no need to rely on central beam to girder connection for Design 3 in which the central beams are left unprotected. The average temperature of the two connecting elements was used as the connection temperature. Note that connection temperature is usually lower than the average temperature of the two connecting elements. Thus, a conservative approach was followed for this study. Double angle connections were converted to shear tabs to be able to use with the component method. Shear tab connections with equivalent double angle capacities have five to seven 3/4 in. diameter ASTM F3125 Grade A325-Type N bolts, depending on the connection demand. Because of the low utilization ratios of the existing building connections, there was no need to make structural adjustments for any designs under any fire cases. The highest forces occurred at the cooling phase. When the connection is at peak temperature, the force demand is notably less than the peak. As the temperature asymptotically drops, so does the force asymptotically increase. Therefore, as the demand on the connection increases, the connection capacity similarly increases. Figure 10-19 shows a sample plot for the resultant force (axial and shear) and temperature response history.

10.5.3 Columns

The effect of elevated temperatures on the columns is assessed using the equations and elevated temperature mechanical property tables of AISC 360-16, Appendix 4. The rotational restraints of the cooler columns at the stories above or below are considered in column slenderness formulas (Agarwal and Varma 2011). For baseline fire (Cases 1, 2, and 3), insulation thickness could be reduced from 1-1/8 in. to 11/16 in. (the equivalent of 1 h fire resistance rating). For more severe fires (Cases 6, 8, and 9), 7/8 in. thick SFRM was adequate, except for the W14x53 column under Fire Case 9, in which 1-1/8 in. insulation was required because of its high slenderness ratio. Table 10-2 tabulates the limit temperatures at the design load levels from AISC Appendix 4 method and the maximum temperatures of the column steel sections with various SFRM.

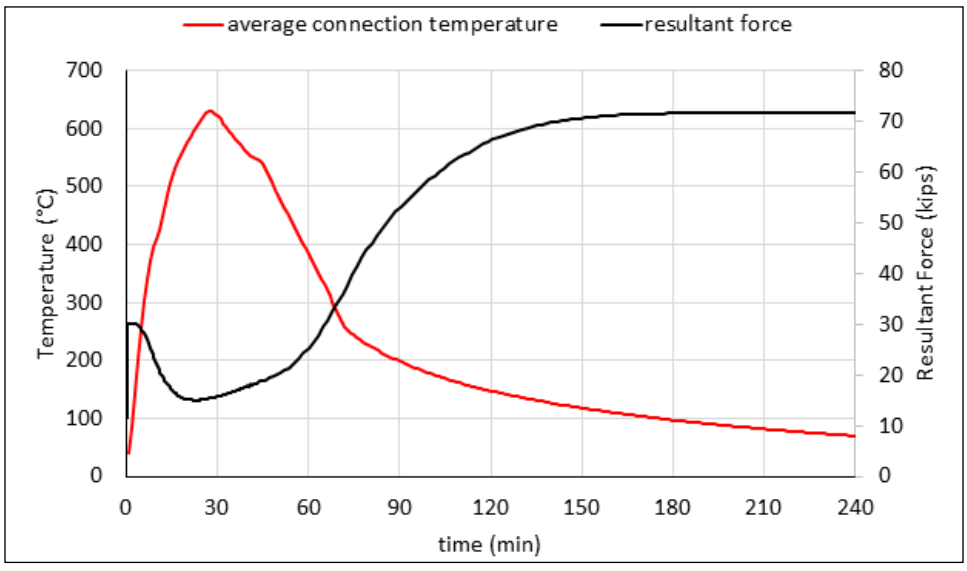

Figure 10-19. Sample resultant force versus temperature response history.
Source: Courtesy of Walter P Moore (2019).

Table 10-2. Limit temperatures at the design load levels from AISC, Appendix 4 method.

Fire Case	Column Location	Column Size	Limit Temp (°C) from AISC App.4	Max Steel temperature (°C) with different SFRM			
				SFRM= 1 1/8in.	SFRM = 7/8 in.	SFRM = 11/16 in.	SFRM = 1/2 in.
1	INT (top)	W14x74	461	122	158	198	258
	INT (bottom)	W14x145	537	95	120	150	195
	EXT (top)	W14x53	451	138	177	225	292
	EXT (bottom)	W14x90	515	124	160	201	262
2	INT (top)	W14x74	461	151	190	232	295
	INT (bottom)	W14x145	537	117	145	178	228
	EXT (top)	W14x53	451	170	210	262	331
	EXT (bottom)	W14x90	515	153	193	236	300
3	INT (top)	W14x74	461	258	315	374	457
	INT (bottom)	W14x145	537	200	245	294	365
	EXT (top)	W14x53	451	290	343	416	504
	EXT (bottom)	W14x90	515	262	320	380	464
4	INT (top)	W14x74	461	136	176	219	285
	INT (bottom)	W14x145	537	105	133	165	216
	EXT (top)	W14x53	451	154	197	249	322
	EXT (bottom)	W14x90	515	138	179	222	289
5	INT (top)	W14x74	461	169	212	258	327
	INT (bottom)	W14x145	537	130	162	198	253
	EXT (top)	W14x53	451	191	235	292	367
	EXT (bottom)	W14x90	515	171	215	262	333
6	INT (top)	W14x74	461	326	391	455	543
	INT (bottom)	W14x145	537	257	310	366	446
	EXT (top)	W14x53	451	365	421	502	592
	EXT (bottom)	W14x90	515	332	397	462	551
7	INT (top)	W14x74	461	150	195	241	312
	INT (bottom)	W14x145	537	115	146	181	237
	EXT (top)	W14x53	451	170	217	239	353
	EXT (bottom)	W14x90	515	152	197	244	317
8	INT (top)	W14x74	461	258	321	385	480
	INT (bottom)	W14x145	537	197	245	297	376
	EXT (top)	W14x53	451	292	353	433	533
	EXT (bottom)	W14x90	515	262	326	392	487
9	INT (top)	W14x74	461	372	443	512	605
	INT (bottom)	W14x145	537	294	353	415	501
	EXT (top)	W14x53	451	414	475	562	655
	EXT (bottom)	W14x90	515	378	450	519	612

10.6 DESIGN SUMMARY

Design 1 requires 1/4-in.-thick SFRM on all central and peripheral beams/girders, and Design 2 requires 1/2-in.- and 3/4-in.- thick SFRM on central and peripheral beams, respectively, under baseline fires (Cases 1, 2, and 3). For Design 3, about 40% of the beams can be left unprotected (see Figure 10-20). Slab wire-mesh reinforcement is increased from 0.058 in^2/ft to 0.162 in^2/ft and repositioned at 1.75 in. from the surface. The SFRM of the peripheral beams can be reduced to 1 in. Column SFRM thicknesses can be reduced from 1-1/8 in. to 7/8 in. for each of the Designs 1, 2, and 3. There is no need to make changes in the connections in any of the designs under the baseline fire cases.

Table 10-3 summarizes the slab wire mesh reinforcement and position, central beam, boundary beam/girder, and column SFRM thicknesses used for all designs under all fire cases.

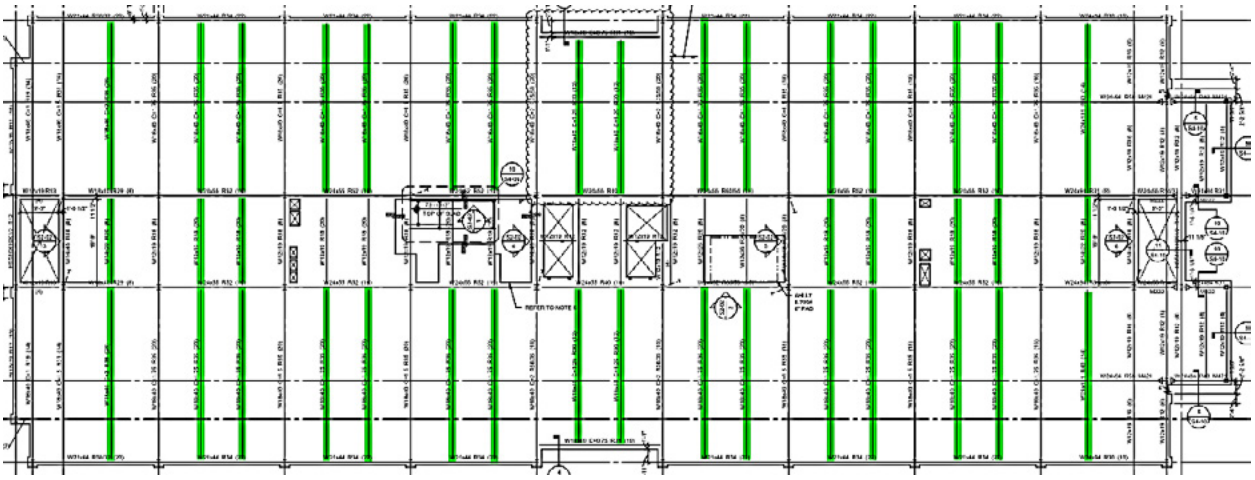

Figure 10-20. Typical floor with unprotected beams highlighted.

Source: Courtesy of Walter P Moore (2019).

Table 10-3. Summaries for Slab Wire Mesh Reinforcement and Position, Central Beam, Boundary Beam/Girder, and Column SFRM Thicknesses for All Designs.

Fire Case	Parameter	Design 0b	Design 1	Design 2	Design 3
1	Central Beam SFRM (in.)	1-1/16	None; 1/4	1/4	None
	Wire Mesh (in^2/ft)	0.058	0.058	0.058	0.120
	Mesh clear cover (in.)	0.75	0.75	0.75	1.75
	Boundary Beam / Girder SFRM (in.)	1-1/16	3/4, 1/4	1/4	3/4
	Column SFRM (in.)	1-1/8	11/16	11/16	11/16
2	Central Beam SFRM (in.)	1-1/16	1/4	1/4	None
	Wire Mesh (in^2/ft)	0.058	0.058	0.058	0.120
	Mesh clear cover (in.)	0.75	0.75	0.75	1.75
	Boundary Beam / Girder SFRM (in.)	1-1/16	1/4	1/4	3/4
	Column SFRM (in.)	1-1/8	11/16	11/16	11/16

Table 10-3. Summaries for Slab Wire Mesh Reinforcement and Position, Central Beam, Boundary Beam/Girder, and Column SFRM Thicknesses for All Designs (con't).

Fire Case	Parameter	Design 0b	Design 1	Design 2	Design 3
3	Central Beam SFRM (in.)	1-1/16	1/4	1/2	None
	Wire Mesh (in^2/ft)	0.058	0.058	0.058	0.162
	Mesh clear cover (in.)	0.75	0.75	0.75	1.75
	Boundary Beam / Girder SFRM (in.)	1-1/16	1/4	3/4	1
	Column SFRM (in.)	1-1/8	7/8	7/8	7/8
4	Central Beam SFRM (in.)	1-1/16	1/4	1/4	None
	Wire Mesh (in^2/ft)	0.058	0.058	0.058	0.120
	Mesh clear cover (in.)	0.75	0.75	0.75	1.75
	Boundary Beam / Girder SFRM (in.)	1-1/16	1/4	1/4	3/4
	Column SFRM (in.)	1-1/8	11/16	11/16	11/16
5	Central Beam SFRM (in.)	1-1/16	1/4	1/4	None
	Wire Mesh (in^2/ft)	0.058	0.058	0.058	0.162
	Mesh clear cover (in.)	0.75	0.75	0.75	1.75
	Boundary Beam / Girder SFRM (in.)	1-1/16	1/4	1/2	3/4
	Column SFRM (in.)	1-1/8	11/16	11/16	11/16
6	Central Beam SFRM (in.)	1-1/16	1/4	3/4	None
	Wire Mesh (in^2/ft)	0.058	0.058	0.058	0.240
	Mesh clear cover (in.)	0.75	0.75	0.75	1.75
	Boundary Beam / Girder SFRM (in.)	1-1/16	1/4	1	1-1/16
	Column SFRM (in.)	1-1/8	7/8	7/8	7/8
7	Central Beam SFRM (in.)	1-1/16	1/4	1/4	None
	Wire Mesh (in^2/ft)	0.058	0.058	0.058	0.162
	Mesh clear cover (in.)	0.75	0.75	0.75	1.75
	Boundary Beam / Girder SFRM (in.)	1-1/16	1/4	1/2	3/4
	Column SFRM (in.)	1-1/8	11/16	11/16	11/16
8	Central Beam SFRM (in.)	1-1/16	1/4	1/2	None
	Wire Mesh (in^2/ft)	0.058	0.058	0.058	0.200
	Mesh clear cover (in.)	0.75	0.75	0.75	1.75
	Boundary Beam / Girder SFRM (in.)	1-1/16	1/4	3/4	1-1/16
	Column SFRM (in.)	1-1/8	7/8	7/8	7/8
9	Central Beam SFRM (in.)	1-1/16	1/4	1	None; None[a]; 1/2
	Wire Mesh (in^2/ft)	0.058	0.058	0.058	0.360; 0.240[a]; 0.120
	Mesh clear cover (in.)	0.75	0.75	0.75	2.50; 1.75[a]; 2.50
	Boundary Beam / Girder SFRM (in.)	1-1/16	1/4	1	1-1/16; 1[a]; 1-1/16
	Column SFRM (in.)	1-1/8	1-1/8 (ext) 7/8 (int)	1-1/8 (ext) 7/8 (int)	1-1/8 (ext) 7/8 (int)

[a] Boundary beam sizes are increased to W21x44 from W18x40 for this design.

[b] Design 0 is the nonengineered prescriptive design for insulation.

10.7 DISCUSSION AND SUMMARY OF RESULTS

10.7.1 Building 4 (WPM)

Performance-based structural fire engineering was implemented on a 6-story braced frame building in Florida. Under prescriptive code requirements, this building required a 2 h fire rating for the primary structural frame, owing to slightly exceeding the IBC height limits of Type IIA construction that allows for a 1 h fire rating. The occupancy of the building is open office, with typical floor plans. One fire compartment with the biggest possible area on the plan was selected and nine fire scenario cases were generated using different fire load densities, ventilation assumptions, and active fire-fighting measure assumptions to achieve a robust design.

The main design strategy for Design 3 was to take advantage of the enhanced load-carrying capacity of the reinforced concrete composite slab through TMA by removing the fire protection from the central beams and adjusting the amount and the position of the slab reinforcement and, if necessary, increasing the boundary beam sizes. The performance goal was to allow localized damage as long as the overall stability of the building is maintained, and this is achievable by utilizing tensile membrane action in the slab.

The position of the reinforcement within the slab is important in TMA. Typical designs only use slab reinforcement close to the surface for cracking control. For Design 3, slab reinforcement position was lowered from 0.75 in. to 1.75 in. from the surface, and then the reinforcement amount was increased until the stability was achieved, following the design strategy explained in the previous sections. Although lowering the reinforcement within the slab increases the lever arm for bending resistance, depending on the fire case, lowered reinforcement also faces higher temperatures that can affect the response and the stability of the slab. Placing the reinforcement at about half the depth of the slab above the flutes worked well for this study in terms of not reaching high temperatures and increasing the bending resistance.

For baseline fire (Cases 1 to 3), the design was governed by the ventilation-controlled Fire Case 3. Full fire burnout stability was achieved when the wire mesh reinforcement was increased from 0.058 in^2/ft to 0.162 in^2/ft, leaving the central beams unprotected. When all nine fire cases are considered, the slab reinforcement needs to be increased to 0.360 in^2/ft, owing to governing long duration ventilation-controlled Fire Case 9. The maximum required slab reinforcement of all other eight cases is 0.24in^2/ft. The failure mechanism of Case 9 was the yielding of the boundary beams, which led to excessive deflections and prevented the utilization of tensile membrane action. When the boundary beam sizes are increased from W18x40 to W21x44, the slab reinforcement could be reduced to 0.24 in^2/ft for Case 9 as well. Note that the other failure mechanism for the rectangular bay of this study was the yielding of the slab reinforcement in the longer span, which occurs because of concrete fracture across the shorter span.

For baseline fire Cases 1 to 3, peripheral beam and all column SFRM thicknesses could be reduced to 1 in. and 7/8 in., respectively. The small reduction of the peripheral beams resulted from the high utilization ratios of the boundary beams of the studied bay. Thinner insulation on the boundary beams could be achieved if the boundary beams had been stiffened up by changing their sizes. This was not done, except for Fire Case 9. The utilization ratios of the columns were relatively lower than the beams for the existing design, and thus, more reduction could be made on the column insulation for most of the fire cases. When all nine fire cases are considered, the

governing Fire Case 9 resulted in 1-in.-thick SFRM on the peripheral beams, 1-1/8 in. SFRM on exterior columns, and 7/8 in. SFRM on interior columns.

Most of the beam-to-girder or beam-to-column connections of this existing building are double angle connections. These connections were converted to shear tab connections to use them with the component method and evaluate them at high temperatures. Connection shear and axial force time histories obtained from SAFIR were compared against the capacity curves created with component method using Strand7. There was no need to make any changes on the existing connections.

Table 10-4 shows the reduction in SFRM thicknesses (in percent) of Designs 1, 2, and 3 compared to the prescriptive Design 0. Fire scenarios are grouped as *baseline fire* (80% fractile fire load density with EC reduction for sprinklers only), Alternative 1: *high density* (95% fractile fire load density with sprinkler reductions), and Alternative 2: *no EC reduction* (80% fractile fire load density with no reductions according to EC). There is reduction in SFRM for all engineered designs. Note that there are 40 central beams that are left unprotected for Design 3. This represents about 40% of the total lengths of the beams of the floor. Peripheral beam SFRM thicknesses could not be reduced significantly for long duration fires of Design 2 and Design 3 because of high utilization (low stiffness) of the boundary beams.

Table 10-4. Reduction in SFRM Thicknesses.

	Reduction of SFRM for Design 1			**Reduction of SFRM for Design 2**			**Reduction of SFRM for Design 3**		
Fire scenario	**Central beams**	**Periph-eral beams**	**Col-umns**	**Central beams**	**Periph-eral beams**	**Col-umns**	**Central beams**	**Periph-eral beams**	**Col-umns**
Baseline fire (Cases 1 to 3)	76%	76%	22%	53%	29%	22%	100%	6%	22%
Alternative - 1 High density (Cases 4 to 6)	76%	76%	22%	29%	6%	22%	100%	0%	22%
Alternative - 2 No EC reduction (Cases 7 to 9)	76%	76%	9%	6%	6%	9%	100%	6%	9%

Table 10-5 includes a volumetric SFRM comparison of the nonengineered prescriptive Design 0 and engineered Designs 1, 2, and 3. Tabulated SFRM volumes are per story. When the total SFRM volumes are compared, there is about 64% reduction (71.7 cu yd to 26.0 cu yd) in Design 1, which only satisfies the minimum performance objective of RSET stability. Design 2 results in about 35% reduction (71.7 cu yd to 46.4 cu yd) under baseline fire, 17% reduction (71.7 cu yd to 59.2 cu yd) under Alternative 1(high-density) fire scenarios, and only 7% reduction (71.7 cu yd to 66.6 cu yd) for the last Alternative 2 (no EC reduction fire scenarios). The reason for the low reduction with Design 2 for the alternative severe scenarios is the low amount of slab reinforcement and its high position within the slab. Note that Design 0 prescriptive design center-bay node displacements already reach 19 in. (~ 48 cm) and 23 in. (~ 60 cm) under fire scenario Cases 6

and 9, respectively. Because structural modifications are not permissible for Design 2, it was not possible to reduce the SFRM volume further with the existing slab condition. Design 3, which requires full fire burnout optimum performance like Design 2, allowed more reduction (~ 35% under all fire scenarios), compared to Design 2, because insulation optimization is much easier with the ability to modify the structural system. Thus, it is important for the structural engineer to become involved early in the design stage for better optimization.

Table 10-5. Volumetric SFRM Comparison of the Nonengineered Prescriptive Design 0 and Engineered Designs 1, 2, and 3.

	Total beam SFRM (cu yd) for all Designs				Total column SFRM (cu yd) for all Designs				Total SFRM (cu yd) for all Designs			
Fire scenario	**0**	**1**	**2**	**3**	**0**	**1**	**2**	**3**	**0**	**1**	**2**	**3**
Baseline fire (Cases 1 to 3)	53.5	12.2	32.6	31.5	18.3	13.8	13.8	13.8	71.7	26.0	46.4	45.4
Alternative 1 igh density Cases 4 to 6)	53.5	12.2	45.4	33.6	18.3	13.8	13.8	13.8	71.7	26.0	59.2	47.4
Alternative 2 No EC reduction (Cases 7 to 9)	53.5	12.2	50.2	31.5	18.3	13.8	16.4	16.4	71.7	26.0	66.6	47.9

Table 10-6 summarizes the changes in structural quantities for Design 3 for all fire scenario groups. Quantities are provided in terms of the total weight per floor area and per unit area.

Table 10-6. Summary of Changes in Structural Quantities for Design 3.

	Increase in quantity for Design 3		
Fire scenario	**Slab reinforcement**	**Beam sizes**	**Connections**
Baseline fire (Cases 1 to 3)	+ 10.9 tons (0.75psf)	None	None
Alternative 1 High density (Cases 4 to 6)	+19.2 tons (1.32psf)	None	None
Alternative 2 No EC reduction (Cases 7 to 9)	+19.2 tons (1.32psf)	+ 1.95 tons (0.13 psf)	None

10.8 CONCLUSIONS

Current prescriptive practice in the United States only considers component level safety and does not provide insight on structural system behavior. Structural integrity is maintained in engineered approaches by understanding system behavior and failure mechanisms through structural analyses. It is ideal to set the performance criteria on the basis of stakeholder and design objectives at an early stage of the design process to give the structural design engineer more flexibility on possible economical and efficient solutions.

WPM studied a 6-story, 87-ft-tall building which has a 2 h fire-resistance rating owing to barely exceeding the IBC height limit (85 ft). The sensitivity of the structure was studied in the context of various uncontrolled fire scenarios to achieve a robust design.

Significant reduction (~ 64%) in the fire insulation of the beams and columns could be achieved under Design 1, where only a minimum code-mandated performance objective of structural stability up to RSET time was considered. The savings for Design 2, which requires full fire burnout optimum performance without structural modifications, depends on the fire hazard scenario considered. The reduction of SFRM changes from 35% to 17% to 7% from the baseline fire to more conservative Alternative 1 and Alternative 2 fire scenarios.

It was revealed that about 40% of the beams in the composite floor system can be left unprotected with the development of membrane action in the slab and that the total SFRM volume used on beams and columns could be reduced by about 35% under all fire scenario groups for Design 3. This can lead to substantial material and labor savings. The consequences of leaving the central beams unprotected include the additional slab reinforcement and other potential peripheral beam and connection adjustments which are required to utilize the tensile membrane action in the composite slab. Because both Design 2 and Design 3 have the same performance objectives, the cost study determines the best economical solution.

Typical design for fire does not consider structural response or calculate the capacity, and thus has an indeterminate margin of safety. Structural fire engineering increases the safety and understanding of the structural behavior. Real fire scenarios and structural responses to such fires are evaluated explicitly through performance-based structural fire design. The project goals and stakeholder design objectives need to be set at an early stage of the design to result in more efficient and economical design processes.

REFERENCES

Agarwal, A., and A. H. Varma. 2011. “Design of steel columns at elevated temperatures due to fire: effects of rotational restraints.” *Eng. J.* 48 (4): 297−314.

CEN (Commission of European Communities). 2001. EN 1991-1-2 *Eurocode 1. Basis of design and actions on structures, Part 1.2: Actions on structures- actions on structures exposed to fire.* Brussels: CEN.

Elhami-Khorasani, N., C. Fang, and T. Gernay. 2017. “Comparative fire analysis of steel-concrete composite buildings designed following performance-based and U.S. prescriptive approaches.” In *Proc., Applications of Structural Fire Engineering Conference*. Boca Raton, FL: CRC Press.

Franssen, J.-M., and T. Gernay. 2017. “Modelling structures in fire with SAFIR®: Theoretical background and capabilities.” *J. Struct. Fire Eng.* 8 (3): 300–323.

Proulx, G. 2002. “The movement of people: The evacuation timing.” In *SFPE handbook of fire protection engineering*, 3rd ed. Gaithersburg, MD: SFPE.

Sarraj, M. 2007. “The behavior of steel fin-plate connections in fire.” Ph.D. thesis, Univ. of Sheffield.

Strand7. 2010. *Using Strand7: Introduction to the Strand7 finite element analysis system, release 2.4.6.* Sydney, AU: Strand7.

Vassart, O., and B. Zhao. 2012. *MACS+ for membrane action of composite structures in case of fire. Design guide*. Luxembourg: ArcelorMittal.

Vassart, O., B. Zhao, L. G. Cajot, F. Robert, U. Meyer, and A. Frangi. 2014. *Eurocodes: background and applications structural fire design*. JRC Science and Policy Report EUR 26698 EN. Ispra, IT: Joint Research Centre.